

ABDALA, AHMED A. Solution rheology and microstructure of associative polymers
(under the direction of Dr. Saad Khan and Dr. Alan Tonelli)

Water-soluble associative polymers are widely used in a variety of applications because of their ability to modulate rheology and material microstructures. This study focuses on understanding the structure-property relationship for hydrophobically modified alkali soluble emulsion (HASE) polymers with emphasis on their microstructure and rheological properties. These polymers have a complex comb-like structure that is a polyelectrolyte backbone, a copolymer of acrylic or methacrylic acid and alkyl acrylate, with a few hydrophobic macromonomers randomly grafted to this backbone. The hydrophobic macromonomer consists of hydrophobic groups that are separated from the polymer chains by polyethylene oxide (PEO) spacers. Upon neutralization, the polymer backbone adopts a more extended conformation allowing the hydrophobic groups to associate forming a transient network structure that enhances the solution rheological properties.

In the first part of this study, we investigate the effect of the polymer composition on their microstructures and rheological properties. In particular, the effects of the concentrations of methacrylic acid (MAA) and macromonomers on the solution rheology are examined. We find that polymers with low MAA content have smaller hydrodynamic size and weaker network structures compared to larger hydrodynamic size and stronger network structure for polymers with high MAA content. However, due to chain increased stiffness at higher MAA and the lower contribution from the aggregation of ethyl-acrylate groups, a broad maximum in the viscoelastic properties of the polymer solution is observed at about 40

mole% MAA. Moreover, the material functions of polymers with different MAA content show different concentration dependences.

In the second part of this study, co-solvents of water and propylene glycol (PG) in different proportions are used to investigate the effect of the solvent quality on the solution rheology of these polymers. The steady and dynamic properties show the presence of two regimes with respect to the solvent composition. In “water-rich” solvents, the hydrophobic association dominates the solution rheology. In contrast, in “PG-rich” solvents, the hydrophobic association is suppressed due to the lower tendency of the hydrophobes to aggregate, the smaller coil size of the polymer chains and changes in the PEO spacer conformations. These two different types of behavior are discussed and confirmed by the different concentration dependences in each regime.

In the third part of the study, the ability of using diffusing wave spectroscopy (DWS) to probe the dynamics of HASE polymers is examined. We find that DWS accurately probes the structural changes induced by the change in the solvent quality or the polymer concentration. Moreover, comparison with conventional mechanical rheometry data reveals excellent qualitative agreement between the data obtained from the two techniques. Quantitatively, however, there is a discrepancy between the data obtained from each technique. Several reasons for the discrepancy are discussed, including the possibility that the dynamics at the micro-level could be different from the bulk properties. The scaling of the creep compliance, high-frequency elastic modulus and relaxation time with polymer concentration show power-law dependences. The power-law exponents are discussed in light of theoretical predictions and available experimental data.

An approach to modulate the hydrophobic association is presented in the last part of the study. The first step in this approach involves the addition of inclusion compound forming hosts (α - or β - cyclodextrin) to the polymer solution. The encapsulation of the hydrophobic groups leads to significant reduction in the solution viscosity and viscoelastic properties. The second step requires the addition of surfactants to reactivate the hydrophobic groups and thus recover the solution rheological properties. We are able to recover the solution properties using different nonionic surfactants.

**SOLUTION RHEOLOGY AND MICROSTRUCTURE
OF ASSOCIATIVE POLYMERS**

Ahmed A. Abdala

A dissertation submitted to the Graduate Faculty of North Carolina State University
in partial fulfillment of the requirements for the degree of Doctor of Philosophy

December 2002

**Department of Chemical Engineering
&
Fiber and Polymer Science Program**
North Carolina State University
Raleigh, NC 27695-7905

APPROVED BY:

Dr. Richard J. Spontak

Dr. Sam S. Hudson

Dr. John van Zanten

Dr. Alan E. Tonelli
Co-chairman of Advisory Committee

Dr. Saad A. Khan
Chairman of Advisory Committee

Dedication

This work is entirely dedicated to my parents, my brothers, my sisters, my wife and my son for their sacrifices, never-ending support and encouragement during the course of my educational endeavors and pursuit of life.

Personal Biography

Ahmed Abdel-Hay Ahmed Abdala was born in Albehara, Egypt on March 31st, 1968. A few years later, he moved with his family to a small town near Alexandria, Egypt. In May 1990, he received his undergraduate degree with honors in Petroleum Refining Engineering from Suez Canal University, Egypt. In August 1995, he received an MS degree in Petrochemistry from the same university.

In 1998, he joined North Carolina State University to start his Ph. D. from a scholarship provided by the Egyptian government. Initially, he started in the Fiber and Polymer science program of the College of Textiles and later switched his Ph. D. to a co-major Ph. D. in Chemical Engineering and Fiber & Polymer Science. His Ph. D. research is focused on the rheology of associative polymers. In December 2001, he was awarded his second MS degree from the Department of Chemical Engineering, NCSU.

Upon completion of all education in the USA, Ahmed will return to Egypt as a faculty member in the Department of Petroleum and Chemical Engineering, Suez Canal University.

Acknowledgments

I would like to express my deepest gratitude to all of those people, without whose help, this manuscript would not have been completed. First, I am very grateful to my advisors, Dr. Saad Khan for his guidance and mentorship during the course of the study and Dr. Alan Tonelli for his assistance and helpful discussions with my project. I would also like to thank Dr. John van Zanten for his assistance and valuable discussion with the tracer microrheology part of the project and for taking the time to serve on my committee. In addition, I would like to thank Dr. Richard Spontak and Dr. Sam Hudson for their contribution to my project. I would also like to acknowledge the financial support I received from the Egyptian government.

I also would like to acknowledge the assistance of those who provided me with help during the course of the study. In particular, thanks are due to Dr. Hanna Gracz, NMR facilities at North Carolina State University, for her assistance with NMR work, Dr. Srinivasa Raghavan, University of Maryland, and Dr. Robert English, Northeast Wales Institute, for their very valuable discussions and encouragement throughout the course of the study.

Lastly, but certainly not the least, thanks to the people whom I enjoyed working with and sharing light moments for the past five years. I have indeed enjoyed working with the past and current members of the Rheology Group, including Jenny Shay, Bor-Sen Chiou, Vandita Pai, Mathew Burke, Jeremy Walls, Jeff Yarian, Deola Ali, Ahmed Eissa, Collins Apaw, Shamsheer, and Angelica Sanchez. Thanks also to Dr. Samiul Amin, Chris Kloxin, and Francis Probeni. I am especially indebted to my family for their love and support and I could not have completed this dissertation without their encouragement through the years.

TABLE OF CONTENTS

List of Tables	ix
List of Figures	x
CHAPTER 1. INTRODUCTION & OVERVIEW	1
Abstract	2
1.1 Introduction	3
1.2 Project Goals	5
1.3 Thesis Overview	8
1.4 References	10
CHAPTER 2. BACKGROUND AND LITERATURE REVIEW	13
Abstract	14
2.1 Introduction	15
2.2 Hydrophobically Modified Polymers	16
2.3 Applications of HASE Polymers	16
2.4 Structure of HASE Polymers	17
2.5 Thickening Mechanisms of HASE Polymers	18
2.6 Structural and Environmental Factors Affecting the Rheology of HASE Polymers	19
2.6.1. Effect of the Solution pH	19
2.6.2 Effect of the Solution Ionic strength	20
2.6.3 Effect of the Size of Hydrophobic Groups	21
2.6.4 Effect of the PEO Spacer Length	21
2.7 Cyclodextrin	22
2.8 References	25
CHAPTER 3. EXPERIMENTAL TECHNIQUES	37
Abstract	38
3. 1 Rheological Characterization	39

3.1. 1 Dilute Solution Measurement	39
3. 1. 2. Steady-State or Simple Shear Flow	40
3. 1. 3. Dynamic or Small Amplitude Oscillatory Shear Flow	40
3. 1. 4. Transient Shear Flow	42
3.2 Diffusing Wave Spectroscopy	43
3.3 Nuclear Magnetic Resonance	45
3.4 Differential Scanning Calorimetry	46
3. 5 Thermal Gravimetric Analysis	47
3.6 References	48

CHAPTER 4. EFFECT OF POLYMER COMPOSITION ON MICROSTRUCTURE AND

SOLUTION RHEOLOGY	52
Abstract	53
4.1 Introduction	55
4.2 Experimental Materials and Method	56
4.2.1 Polymers	56
4.2.2 Solution Preparation	57
4.2.3 Rheological measurements	57
4.2.4. Glass transition temperature (T _g) measurements	58
4.3 Results and Discussion	59
4.3.1 Effects of MAA content	59
4.3.2 Concentration Effects	62
4.3.4 Effects of macromonomer concentration	65
4.4 Summary	67
4.5 References	69

CHAPTER 5. SOLUTION RHEOLOGY OF HYDROPHOBICALLY MODIFIED

ASSOCIATIVE POLYMERS: SOLVENT QUALITY AND HYDROPHOBIC	
INTERACTIONS	83
Abstract	84

5.1 Introduction	86
5.2 Experimental Materials and Method	88
5.3 Results and Discussion	90
5.3.1 Effects of solvent quality	90
5.3.2 Concentration effects	94
5.3.3 Solvent quality and polymer interaction modes	96
5.4 Conclusions	98
5.5 Acknowledgment	99
5.6 References	100

CHAPTER 6. A TRACER MICRORHEOLOGY STUDY OF ASSOCIATIVE POLYMER

SOLUTIONS	113
Abstract	114
6.1 Introduction	115
6.2 Materials and Methods	116
6.3 Results and Discussion	119
6.3.1 Solvent quality effects	119
6.3.2 Concentration effects	124
6.3.2.1 Scaling behavior	126
6.3.2.2 Time dependent Diffusion Coefficient	128
6.4 Conclusions	130
6.5 References	131

CHAPTER 7. MODULATION OF HYDROPHOBIC INTERACTIONS IN ASSOCIATIVE

POLYMERS WITH INCLUSION COMPOUNDS AND SURFACTANTS	152
Abstract	153
7.1 Introduction	154
7.2 Experimental	157
7.2.1 Materials	157
7.2.2 Methods	158

7.3 Results and Discussion	159
7.3.1 Effect of CDs on solution rheology	159
7.3.2 Macromonomer-cyclodextrin complexation	161
7.3.2.1 Characterization and interaction modes of CD- macromonomer ICs	163
7.3.4 Recovery of solution rheology	166
7.4 Conclusions	168
7.6 References	170
CHAPTER 8. CONCLUSIONS AND RECOMMENDATIONS FOR FUTURE WORK	187
8.1 Concluions	188
8.2 Future work Recommendations	191
8.2.1 Tracer microrheology measurements	191
8.2.2 Recovery of solution rheology after deactivation of the hydrophobic groups.....	192
8.3 References	195

LIST OF TABLES

CHAPTER 5

Table 1. Solvent's composition, solubility parameter components and solubility parameter.....	104
Table 2: Intrinsic viscosity ($[\eta]$), Huggins coefficient (k_H) and the difference between Huggins and Kramer Coefficient (k_H-k_K) for modified and unmodified polymers in water/propylene glycol (PG) co-solvent, with different compositions.....	105

CHAPTER 6

Table 1. Solvent's composition, solubility parameter components and solubility parameter.	138
--	-----

LIST OF FIGURES

CHAPTER 1

- Figure 1. Schematic for the architecture of a typical HASE polymer and molecular constitution of the HASE polymers used in this study..... 11
- Figure 2: Schematic representation of possible hydrophobic interaction modes..... 12

CHAPTER 2

- Figure 1. Molecular structure of a hydrophobically modified associative polymer. The structure shown is for a hydrophobically modified alkali-soluble emulsion (HASE) polymer 32
- Figure 2. Effect of solution pH on the network structure, radius of gyration and viscosity of a HASE polymer solution 33
- Figure 3. Effect of salt (NaCl) concentration on the steady shear viscosity of a 1% polymer solution. 34
- Figure 4. Schematic representation of HASE polymer aggregates for (a) short PEO spacer length and (b) long PEO spacer length 35

CHAPTER 3

- Figure 1. Viscosity as a function of shear rate showing different material response; Newtonian, shear thinning and shear thickening 49
- Figure 2. Elastic (G') and viscous (G'') moduli as functions of angular frequency (ω) showing the typical behavior of polymer solutions (melts) and elastic gels. 50
- Figure 3. Time profile of shear creep and creep recovery experiments for (a) elastic solid, (b) Newtonian fluid, and (c) viscoelastic material. ... 51

CHAPTER 4

- Figure 1. Schematic representation of a typical HASE polymer together with its molecular constitution of the HASE polymers used in this study. R refers to the hydrophobic groups. x, y, z, p are structural parameters 70

Figure 2. Composition of the polymers used in this study. A total of 18 samples have been used, including 4 non-associative ASE samples that have no macromonomers.	71
Figure 3. Steady shear data for 3% solution of HASE polymers with different MAA concentration. Polymers have 0.22 mole% macromonomers with C18 hydrophobes and 40 EO units: Viscosity is shown as function of shear rate.....	72
Figure 4. Dynamic frequency spectrum of a) the elastic modulus (G') and b) dynamic frequency spectrum for 3% solution of HASE polymers with different MAA content and 0.22 mole% macromonomer.	73
Figure 5. Creep compliance, $J(t)$, as function of time for 3% solution of HASE polymers with different MAA content and 0.22 mole% macromonomer: compliance as function of time is shown	74
Figure 6. Intrinsic viscosity ($[\eta]$) and glass transition temperature (T_g) for polymers with different MAA content. All polymers have 0.22 mole% macromonomer with C ₁₈ hydrophobes and 40 EO units ..	75
Figure 7. Steady shear viscosity versus shear rate for the non-associative ASE polymers with different MAA acid. Inset shows the zero shear viscosity as a function of MAA mole%.	76
Figure 8. Effect of MAA content and polymer concentration on a) the steady shear viscosity at shear rate $=0.01 \text{ s}^{-1}$ b) the elastic modulus at angular frequency $=100 \text{ rad/s}$, and c) the creep compliance at $t=100 \text{ s}$. Macromonomer concentration = 0.22 mole%, C ₁₈ hydrophobes and 40 units EO.	77
Figure 9. Concentration dependence of steady shear viscosity (η) at 0.01 s^{-1} , elastic modulus (G') at 100 rad/s and the creep compliance $J(t)$ at $t=100 \text{ s}$ for polymer with .a) 43 mole% and b) 23 mole% MAA ..	78
Figure 10. Effect of MAA content on the transition concentrations (c_L and c_U) and the overlap concentration (c^*).	79
Figure 11. Possible hydrophobic interaction modes at difference concentration regimes.	80
Figure 12: Effect of MAA content on the steady shear viscosity of 3% solution of polymers with a) 0.3 mole%, b) 1.0 mole% and c) 1.9 mole% macromonomer.	81

CHAPTER 5

Figure 1: Chemical constitution of the HASE polymer. Here $p=40$ and R corresponds to $C_{22}H_{44}$; $x/y/z = 43.57/56.21/0.22$ by mole.	106
Figure 2. Effect of solvent composition on the relative viscosity of a 3% HASE polymer solution. The numbers after PG (propylene glycol) correspond to the weight percent of PG in the water-propylene glycol co-solvent.	107
Figure 3. Comparison of the steady (filled symbols) and complex (open symbol) viscosity of a 3% HASE polymer solution shown for different co-solvent compositions. The numbers after PG (propylene glycol) correspond to the weight percent of PG in the water-propylene glycol co-solvent	108
Figure 4. Effect of solvent composition on (a) the storage modulus G' , and, (b) the storage (G') and loss (G'') moduli of a 3% HASE polymer solution.	109
Figure 5. Effect of the solvent solubility parameter on the (a) relative viscosity, and, (b) elastic modulus G' at a fixed frequency (1 rad/sec) of HASE polymer solutions. The numbers (in %) correspond to different polymer concentrations. Lines are for guidance only and have no further justification	110
Figure 6. Concentration dependence of the relative viscosity of HASE polymer solutions in “water-rich” solvents. Results are shown for different compositions of the co-solvent.	111
Figure 7. Concentration dependence of the relative viscosity of HASE polymer solutions in “PG-rich” solvents. Results are depicted for different co-solvent compositions.	112
Figure 8. Effect of addition of β -cyclodextrin on the relative viscosity of a 1% HASE polymer solution. The numbers correspond to the moles of cyclodextrin added per mole of the hydrophobe. The unmodified polymer reflects the same polymer as the HASE polymer but without the hydrophobes.	113
Figure 9. Concentration dependence of the relative viscosity for unmodified polymer (without hydrophobe) in water and in PG, and the HASE polymer with the hydrophobes deactivated through the addition of 20 moles β -cyclodextrin/mole hydrophobe.	114

CHAPTER 6

Figure 1. Schematic representation of the architecture of a typical HASE polymer and its molecular structure. Here, $p=40$ and R correspond to $C_{22}H_{44}$; $x/y/z = 43.57/56.21/0.22$ by mole..	139
Figure 2. Diffusing wave spectroscopy (DWS) experimental setup in the transmission mode. The beam is focused and incident upon flat scattering cell containing the sample and spherical optical probes. The light is multiply scattered and collected by two photomultiplier tubes..	140
Figure 3. Evolution of the mean square displacement for water, PG/water 91/9 (w/w) mixture, and 0.9% HASE polymer in PG/water co-solvents at different PG ratios.	141
Figure 4. Comparison of the creep compliance obtained from mechanical rheometry (symbols) and tracer microrheology (lines) for 0.9% HASE polymer in PG/water co-solvents at different PG ratios. ...	142
Figure 5. Frequency dependence of a) the complex modulus, G^* , and b) the elastic (G') and viscous (G'') moduli obtained from tracer microrheology for 0.9% HASE polymer solutions in PG/water cosolvent with different PG ratios.	143
Figure 6. Frequency dependence of the elastic (G') and viscous (G'') moduli obtained from mechanical rheometry measurements for 0.9% HASE polymer solutions in PG/water co-solvent at different PG ratios.	144
Figure 7 Comparison of a) elastic (G') and b) viscous (G'') moduli obtained from mechanical rheometry (symbols) and tracer microrheology (lines) for 0.9% HASE polymer in PG/water co-solvent at different PG ratios.	145
Figure 8. Comparison of the creep compliance obtained from tracer microrheology using different sphere sizes embedded in 0.9% aqueous polymer solution. The line represents the creep compliance obtained from mechanical rheometry measurement. .	146
Figure 9. Evolution of the mean square displacement of 0.996 μ m PS spheres in aqueous solution of HASE polymer at different concentrations..	147

Figure 10. Comparison of the creep compliance obtained from mechanical rheometry (symbols) and tracer microrheology (lines) for aqueous solution of HASE polymer at different concentrations. ..	148
Figure 11. Comparison of a) the elastic (G') and b) the viscous (G'') moduli obtained from mechanical rheometry (symbols) and tracer microrheology (lines) for aqueous solution of HASE polymer at different concentrations.	149
Figure 42. Scaling of the elastic modulus (G'), the creep Compliance ($J(t)$), and the longest relaxation time (τ_L) with the polymer concentrations. G' is taken at a fixed frequency 10 rad/s and $J(t)$ at a fixed time 10 sec.	150
Figure 13. Time dependent diffusion coefficient of 0.966 μ m spheres embedded in HASE polymer solution at different concentrations as a function of (a) time and (b) the average sphere displacement.	151

CHAPTER 7

Figure 1. Schematic representation of the architecture of a typical HASE polymer and its molecular structure. Here, $p=40$ and R correspond to $C_{22}H_{44}$; $x/y/z = 43.57/56.21/0.22$ by mole.	175
Figure 2: Effects of addition of a) α -CD and b) β -CD on the steady shear viscosity of 3% HASE associative polymer solution. Numbers correspond to the moles of cyclodextrin per moles of hydrophobes	176
Figure 3: Effects of addition of a) α -CD and b) β -CD on the dynamic elastic (G') and viscous (G'') moduli of a 3% HASE associative polymer solution. Numbers correspond to moles of cyclodextrin per hydrophobes	177
Figure 4: Effect of addition of various amounts of β -CD amount on the a) steady shear viscosity and b) dynamic elastic (G') and viscous (G'') moduli of 1% unmodified polymer that is analogous to the HASE polymer in this study but with the hydrophobic groups replaced by CH_3 groups.	178
Figure 5. Yield of macromonomer-CD inclusion complexes as a function of the molar ratio of CD/macromonomers.	179

Figure 6. Effect of the CD/hydrophobe molar ratio on the % of active macromonomers present, calculated based on the yield data in Figure 2	180
Figure 7. DSC scans of a) α -CD, macromonomer, and their inclusion compound and b). β -CD, macromonomer, and their inclusion compound. The scans shown are the second heatings taken after heating the samples at 200° C for 3 minutes to erase any thermal history.	181
Figure 8. TGA scans for a) α -CD, macromonomer and their inclusion compound and b) β -CD, Macromonomer and their inclusion compound. Samples were heated at 20° C/min under nitrogen.	182
Figure 9. 500 MHz ^1H NMR spectra of a) macromonomer, α -CD and their inclusion compound and b) macromonomer, β -CD and their inclusion compound. All spectra were acquired in DMSO-d6. ...	183
Figure 10. Part of the 500 MHz ^1H NMR spectra showing a) the aliphatic CH_2 protons of the macromonomer and its inclusion compounds with α -CD and β -CD and b) the $\text{CH}_2\text{-CH}_2\text{-O}$ protons of the macromonomer and its inclusion compounds with α -CD and β -CD. All spectra were acquired in DMSO-d6.	184
Figure 11. Effect of adding macromonomer to a 3% HASE polymer solution that has the hydrophobic groups deactivated by 20 moles β CD on the (a) steady shear viscosity and (b) dynamic elastic (G') and viscous (G'') moduli of the polymer solution. Numbers in figure denote amounts of macromonomer added to solution in mM.	185
Figure 12. Effect of NP4 surfactant addition to a 3% HASE polymer solution that has the hydrophobic groups deactivated by 20 β CD/macromonomer on the (a) steady shear viscosity and (b) dynamic elastic (G') and viscous (G'') moduli of the polymer solution. Numbers in figure denotes amount of NP4 surfactant added to solution in mM.	186

CHAPTER 8

Figure 1. Effect of CDase enzyme on the (a) steady shear viscosity and (b) dynamic elastic (G') and viscous (G'') moduli of 3% polymer solution encapsulated with 20 moles α -CD/hydrophobes. pH 9, incubation temperature 50°C, incubation time 24 hrs.	198
--	-----

Figure 2. Effect of solution pH on the (a) steady shear viscosity and (b) dynamic elastic (G') and viscous (G'') moduli of 3% polymer solution.	199
Figure 3. Effect of CDase enzyme on the (a) steady shear viscosity and (b) dynamic elastic (G') and viscous (G'') moduli of a 3% polymer solution encapsulated with 20 moles α -CD/hydrophobes. pH 7.5, incubation temperature 50°C, incubation times 1 and 10 hr.	197
Figure 4. Effect of Clarase enzyme on the (a) steady shear viscosity and (b) dynamic elastic (G') and viscous (G'') moduli of a 3% polymer solution encapsulated with 20 moles α -CD/hydrophobes. pH 7.5, incubation temperature 50°C, incubation time 30 hrs Figure 4. Effect of Clarase enzyme on the (a) steady shear viscosity and (b) dynamic elastic (G') and viscous (G'') moduli of a 3% polymer solution encapsulated with 20 moles α -CD/hydrophobes. pH 7.5, incubation temperature 50°C, incubation time 30 hrs	200

CHAPTER 1

INTRODUCTION & OVERVIEW

Abstract

In this chapter, we introduce the reader to the complex and fascinating world of an interesting class of water-soluble associative polymers, that of the hydrophobically modified alkali soluble emulsion (HASE) polymers. These comb-like polymers consist of an alkyl hydrophobe attached to a hydrophilic backbone. We also motivate the topic of this dissertation –solution rheology and microstructures of associative polymers. HASE polymers are currently being used as rheology modifiers in a variety of applications, from coatings to anti-icing fluids. While many of these applications involve the use of polymers in aqueous medium, some also require the use of glycols as cosolvent. The efficient use of these polymers requires both an understanding of their structure-property relationship and the ability to tailor their rheological behavior. In this regard, we study the effects of the polymer structure and the use of cosolvent on solution rheology and other properties. We also discuss a way to tailor the rheological properties through interactions with inclusion compound forming hosts and surfactants.

1.1 Introduction

Associative polymers have recently drawn considerable interest due to their original and specific rheological properties that distinguish them from other polymers in terms of their viscosity enhancement and reversibility of their associative phenomena. Hydrophobically modified alkali soluble emulsion (HASE) polymers are one class of water-soluble associative polymers. These polymers have a comb-like structure with pendant hydrophobic groups randomly grafted to the polyelectrolyte backbone. HASE polymers have several advantages over other associative polymers in terms of cost and wide formulation latitude¹. They are currently being used as rheology modifiers in a wide range of applications, including paint formulations, paper coatings, personal and home care products, UV-photoprotecting and aerated emulsions, fabric softeners, and as glycol based aircraft anti-icing fluids.

The structure of HASE polymers can be thought of as a hybrid of the conventional alkali soluble emulsion (ASE) polymers and the hydrophobically modified ethoxylate urethane (HEUR). HEUR polymers have a simple structure composed of a PEO backbone capped with one hydrophobic group at each end. The polyelectrolyte backbone of HASE polymers has the structure of the nonassociative ASE polymers while the hydrophobic macromonomer has a structure similar to HEUR polymers. In fact, the earlier name of HASE polymers was HEURASE polymers². A typical structure of a HASE polymer is shown in Figure 1.

Similar to surfactants in aqueous media, these polymers are capable of non-specific hydrophobic interactions³. These hydrophobic interactions include inter- and intra-molecular

associations, giving rise to network structures assuming the concentration is sufficient, and a range of rheological behaviors. A schematic drawing for possible hydrophobic interactions are shown in Figure 2. Due to their complex structure, the rheological properties of this polymer system are expected to be very sensitive to both structural and environmental parameters. Examples of the structural parameters include the polymer molecular weight and molecular weight distribution, the polymer backbone composition, PEO spacer length, and the type and concentration of the hydrophobic groups. On the other hand, polymer concentration, temperature, medium pH and ionic strength, and the solvent quality are examples of the environmental parameters.

Although the associative nature of HASE polymers, which makes them attractive from a rheological standpoint, is the result of the hydrophobic interactions, the ability to control these interactions is often an advantageous feature. In this regard, the ability to deactivate and reactivate the hydrophobic groups is always desirable. Two reasons for the removal of hydrophobic interactions are ease of handling during solution preparation and prior to the end use stage, and, extraction of useful information from characterization of these polymers using techniques such as light scattering and gel permeation chromatography (GPC). In the latter case, the presence of hydrophobic association makes extraction of information from these techniques complicated and less accurate.

The dynamics of HASE polymers and their viscoelastic characteristics are in general usually characterized using traditional mechanical rheometry. Nevertheless, the information gained from rheological measurements is of macroscopic nature and one has to guess their structure at the micro-level. The use of light scattering is one approach to extract information

about the dynamics of such systems at the micro-level. However, traditional dynamic light scattering techniques limit the range of the polymer concentrations to very dilute concentration due to the limiting condition of single scattering. A recent light scattering technique known as diffusing wave spectroscopy (DWS), however, extends the concentration range by working at the multiple scattering limit⁴. This technique has advantages over both conventional rheometry and traditional dynamic light scattering in terms of the time scale, the strain applied on the material and the amount of the sample required. This technique has been used quite extensively to study the dynamics of simple polymeric and bio systems such as polyethylene oxide (PEO) and actin filaments. In spite of the success of this technique to study the dynamics of simple polymeric systems, its validity and the range of frequency over which it can apply for systems where local inhomogeneity is expected to be present are still debatable issues. In this research we test the applicability of this technique to a complex associative system. Direct comparison between the results obtained using the DWS technique with those from traditional mechanical rheometry would help in resolving this debate.

1.2 Projects Goals

The overarching objective of this research is to gain a fundamental understanding of the structure-property relationship of a complex class of associative polymers, namely HASE polymers, and develop an approach to modulate the rheological properties of these polymers. In particular, this research has the following specific goals:

1. Investigate the effects of polymer structure on the association behavior and solution rheology

The chemical composition and polymer architecture can have a profound influence on

the behavior of associative polymers. These architectural parameters include the (a) structure of the backbone that dictates the water solubility and flexibility of the polymer chain, (b) structure of the macromonomer including the type of hydrophobic groups and the length of polyethylene oxide spacer, and (c) concentration of the hydrophobic macromonomer. In our study, we specifically investigate the effects of the polymer backbone composition and the concentration of the macromonomer on the microstructure and rheology of the polymer solution. Based on the structure of the polymer used in this study, the polymer backbone is a copolymer of a water-soluble monomer, methyl metha-acrylic acid (MAA), and a water insoluble monomer, ethyl acrylate (EA). The concentration of each monomer will affect the polymer solubility and stability as well as the accessibility of the hydrophobic groups. We investigate the effect of MAA/EA ratio on the solution properties. We also examine the effects of the macromonomer concentration on the solution properties and the associative nature of these polymers. By comparing the behavior of these sets of samples we investigate the effect of the concentration of the hydrophobic macromonomer on the solution properties.

2. Understand the effects of solvent quality on hydrophobic interactions and solution rheology

The continuous phase in which the associative polymer is solvated plays a major role in the association behavior of these polymers. In this regard, the effects of the medium pH and ionic strength on the association mechanism of HASE polymers have been the focus of a number of previous studies⁵⁻⁹. However, almost all these studies were carried out in aqueous media and the effects of solvent quality or non-aqueous co-solvents on the solution behavior have been overlooked. This becomes particularly important in deciphering the modes of

hydrophobic associations and developing new applications involving non-aqueous media, such as anti-icing fluids. We study the effect of solvent quality on the hydrophobic interactions and rheology of HASE polymers by using cosolvents of water and propylene glycol in different proportions. In this regard, the solvent solubility parameter is used to quantify the solvent quality.

3. Examine the applicability of the diffusing wave spectroscopy (DWS) technique to associative polymers

The goal of this part of the study is to test the validity of a new light scattering technique, known as diffusing wave spectroscopy (DWS), in extracting the rheological properties of HASE polymers. DWS provides information about the properties of viscoelastic media by tracking the motion of microspheres embedded in this medium. It has been recently used extensively to extract the mechanical properties of polyethylene oxide and F-actin filaments. However, the ability of DWS to extract the viscoelastic properties of more complex systems has not been proven. We choose to test the validity of DWS because it has advantages over both conventional light scattering and mechanical rheometry. For example, it provides information over a very wide range of frequency, including very high frequencies that are not accessible with conventional mechanical rheometry. In addition, the viscoelastic properties of the material are extracted without disrupting the material as the strain applied to the material is of the order $k_B T$.

4. Develop approaches to modulate hydrophobic association

Our main focus during this portion of the research work is to uncover a method to modulate the hydrophobic interactions. The hydrophobic interactions can be removed by

deactivating the hydrophobic groups. One way to achieve that is to encapsulate the hydrophobic groups using inclusion compound forming hosts, such as cyclodextrins, which are cyclic oligoaccharides consisting of 6, 7, or 8 glucose units corresponding to α , β , and γ -CD joined by α -1,4-glycosidic linkages. Two scenarios for reactivation of the hydrophobic groups are considered. In the first scenario, the addition of a suitable surfactant would be expected to shift the equilibrium between the hydrophobic groups and the cyclodextrin away from complexation, thereby reactivating these groups. In the second scenario, the cyclodextrin is enzymatically degraded and the hydrophobic groups are re-exposed and reactivated.

1.3 Thesis Overview

At this point, we provide a brief summary of the contents of the following chapters. In Chapter 2, we provide a detailed literature review about the rheology of HASE associative polymers. Chapter 3 presents a summary of the experimental techniques utilized through the course of this research. Chapter 4 focuses on the effect of the polymer composition/architecture on the microstructure and rheology of their polymer solution. Chapter 5 provides a detailed rheological study of the effect of the solvent quality on the hydrophobic interactions and the behavior of the polymer solutions. Chapter 6 presents another approach to study the effect of the solvent quality and the polymer concentration on the microstructure and solution rheology of HASE polymers using a tracer microrheology technique, diffusing wave spectroscopy. This chapter also presents a direct comparison between rheological data obtained from the tracer microrheology measurement and those

obtained using traditional mechanical rheometry. Chapter 7 provides an approach to tailor the rheological properties of the polymer solution by deactivation/reactivation of the hydrophobic groups. Encapsulation of the hydrophobic groups by forming inclusion compounds using cyclodextrins hosts deactivates the hydrophobic groups while addition of nonionic surfactants or possibly enzymatic degradation of cyclodextrins, can reversibly activate these groups. This approach provides ease of handling of concentrated solution and provides a way to decouple the hydrophobic interactions from the polymer backbone effects. Finally, research conclusions and our recommendations for future research are presented in Chapter 8.

1.4 References

1. Tirtaatmadja, V.T.; Tam, K. C.; Jenkins, R. D.; Bassett, D. R. Stability of a Model Alkali-Soluble Associative Polymer in The Presence of a Weak and a Strong Base, *Colloid and Polymer Science* **1999**, 277, 276-281.
2. Shay, G.D.; Rich, A. F. Urethan-Functional Alkali-Soluble Associative Latex Thickeners, *J. Coat. Tech.* **1986**, 58, 43-53.
3. Ng, W.K.; Tam., K. C.; Jenkins, R. D. Evaluation of Intrinsic Viscosity Measurements of Hydrophobically Modified Polyelectrolyte Solutions, *European Polymer Journal* **1999**, 35, 1245-1252.
4. Weitz, D.A.; Pine D.J. Diffusing-Wave Spectroscopy, In *Dynamic Light Scattering: The Method and Some Applications*, Vol. 60, 652-720, Oxford University Press, Oxford, 1993.
5. Wang, C.T.; Tam, K.C.; Jenkins, R.D.; Bassett, D.R. Potentiometric Titration and Dynamic Light Scattering of Hydrophobically Modified Alkali Soluble Emulsion (HASE) Polymer Solutions, *Phys. Chem. Chem. Phys.* **2000**, 2, 1967-1972.
6. Kumacheva, E.R.; Rharbi, Y.; Winnik, M A.; Guo, L.; Tam, K. C.; Jenkins, R. D. Fluorescence Studies of an Alkaline Swellable Associative Polymer in Aqueous Solution, *Langmuir* **1997**, 13, 182-186.
7. Horiuchi, K.R.; Rharbi, Y.; Yekta, A.; Winnik, M.A.; Jenkins, R.D.; Bassett, D.R. Dissolution Behavior in Water of a Model Hydrophobic Alkali- Swellable Emulsion (HASE) Polymer with C₂₀H₄₁ Groups, *Canadian Journal of Chemistry-Revue Canadienne De Chimie* **1998**, 76, 1779-1787.
8. Tirtaatmadja, V.; Tam, K.C.; Jenkins, R. D. Rheological Properties of Model Alkali-Soluble Associative (HASE) Polymers: Effect of Varying Hydrophobe Chain Length, *Macromolecules* **1997**, 30, 3271-3282.
9. Tan, H.; Tam, K.C.; Tirtaatmadja, V.; Jenkins, R. D.; Bassett, D. R. Extensional Properties of Model Hydrophobically Modified Alkali-Soluble Associative (HASE) Polymer Solutions, *J. Non-Newtonian Fluid Mech.* **2000.**, 92, 167-185.

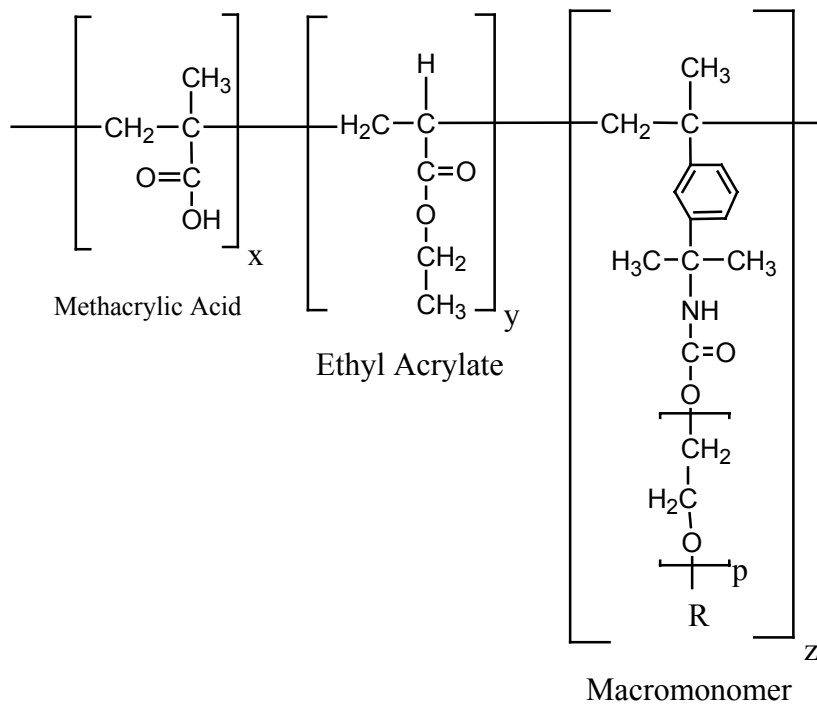


Figure 1. Schematic representative of a typical HASE polymer together with its molecular constitution of the HASE polymers used in this study. R refers to the hydrophobic groups. x, y, z, p are structural parameters.

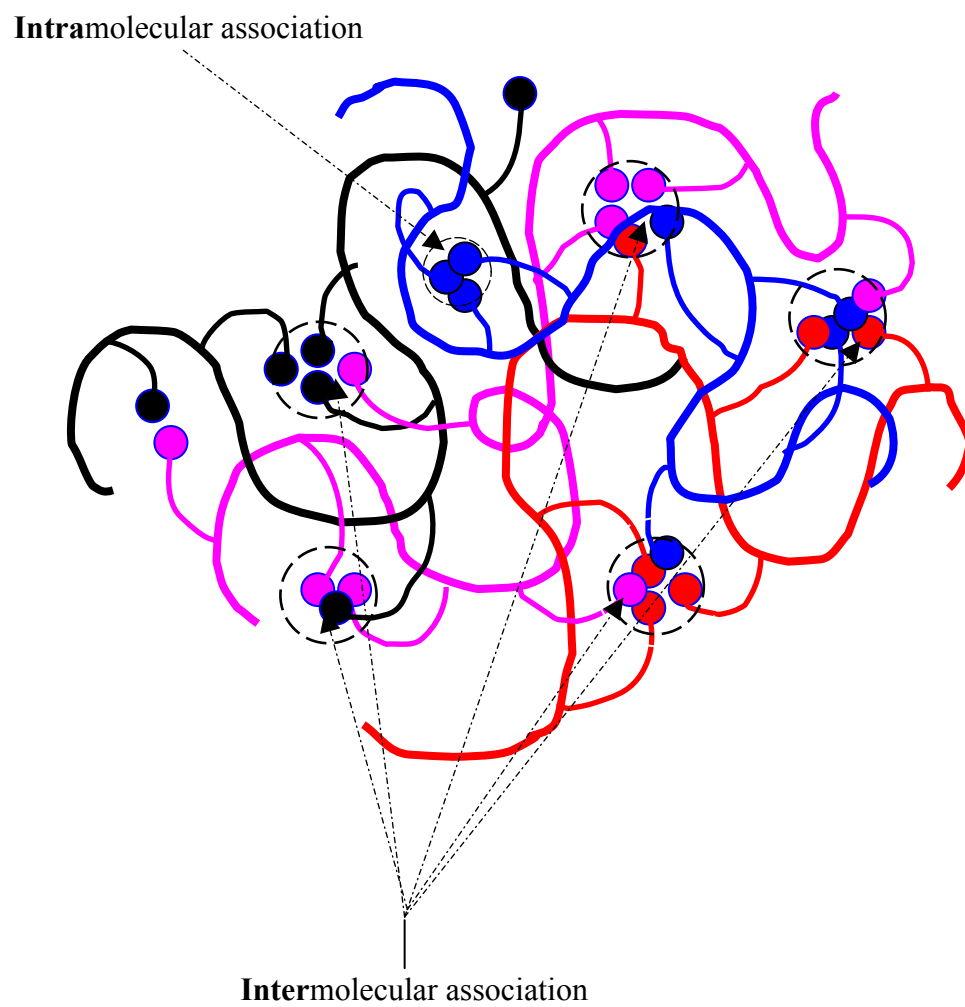


Figure 2: Schematic representation of possible hydrophobic interaction modes

CHAPTER 2

BACKGROUND AND LITERATURE REVIEW

Abstract

In this chapter, we provide the reader background information on the hydrophobically modified alkali soluble emulsion (HASE) associative polymers. Although these polymers are currently used in a variety of applications, there is a scarcity of scientific research that allows for a complete understanding of their fundamental structure-property relationships. We summarize the findings of previous research that deal with the structure of HASE polymers and the factors that affect their solution microstructures and solution rheology.

2.1 Introduction

Associative polymers are macromolecules with attractive groups that form an interesting class of polymeric systems with numerous applications. These applications include rheology modifiers, adhesives, adsorbents, coatings, surfactants and stabilizers for heterogenous polymerization, cosmetics, paper coatings, enhanced oil recovery, flocculants for waste-water treatment, biomedical implants, suspending agents for pharmaceutical delivery systems, and in aircraft anti-icing fluids. The association of their attractive groups leads to formation of physical bonds. The structures formed by these polymers in solutions depend on many factors including polymer concentration, number of attractive groups per chain and the strength of the physical bond. This class of polymers includes charged polymers, block copolymers in strongly selective solvents, and polymers with hydrogen bonding^{1,2}.

Block copolymers consist of either block(s) of one type of homopolymer attached sequentially to block(s) of another type or grafted onto the main chain of a different polymer³. Examples of block copolymers in selective solvents are amphiphilic copolymers, such as poly(ethylene-oxides) poly(propylene-oxides) poly(ethylene oxide) (PEO-PPO-PEO) copolymers, and hydrophobically modified polymers. Poly(acryloylglycinamide) copoly(acrylic acid)⁴ and blends of poly(4-vinylphenol) with poly(Bu acrylate), poly(Bu methacrylate), or poly(vinyl Bu ether)^{5,6} are examples for the hydrogen bonding polymers. Our interest in this research, however, lies with polymers with attached hydrophobes that form associations in aqueous solvents.

2.2 Hydrophobically Modified Polymers

Hydrophobically modified associative polymers are synthetically derived, water soluble polymers that contain a small numbers of hydrophobic groups⁷. These hydrophobic groups aggregate in order to minimize their exposure to water, in a fashion analogous to surfactants, above the critical micelle concentration. Several hydrophobically modified polymers are currently available commercially and utilized in a wide range of applications, as rheology modifiers. Examples of those polymers are: hydrophobically modified (hydroxyethyl) cellulose^{8, 9}, hydrophobically modified ethoxylate urethane (HEUR)¹⁰⁻¹², hydrophobically modified polyacrylamide (HMAM)^{13,14}, and hydrophobically modified alkali soluble emulsion (HASE) polymers.

These hydrophobically modified polymers have either a telechelic structure in which the chains are end-capped with the hydrophobic groups, or more complicated comb-like structures in which the hydrophobic groups are randomly grafted to the polymer backbone. HEUR polymers are one example of the telechelic polymers and HASE polymers are an example of the polymers with comb-like structures. HEUR polymer structure can be described as a polyethylene oxide backbone end capped with hydrophobic groups. On the other hand, HASE polymers have more complex structures. The ionic charges on the polymer backbone add more complexity to the structure.

2.3 Applications of HASE Polymers

HASE polymers have several advantages over other associative polymers in terms of cost and wide formulation latitude¹⁴. Compared to other hydrophobically modified polymers, HASE polymers have a unique ability to dramatically modify the solution properties.

In particular, a few percent of the polymer can increase the solution zero-shear viscosity up to several decades. On the other hand and due to their shear thinning property, the high shear rate viscosity is very low. A viscosity profile with a large zero-shear viscosity and a low high-shear viscosity is ideal for many applications. The superior rheological properties of HASE polymers make them attractive candidates as rheology modifiers in a multitude of applications, including paint formulations¹⁵⁻¹⁷, paper coatings¹⁸, personal and home care products¹⁹⁻²², UV-photoprotecting and aerated emulsions^{23, 24}, fabric softeners^{25, 26} and as glycol based aircraft anti-icing fluids²⁷⁻³¹.

2.4 Structure of HASE Polymers

The structure of HASE polymers can be thought of as a hybrid of the conventional alkali-soluble emulsion polymers (ASE), a polyelectrolyte backbone composed of a copolymer of one hydrophilic and one hydrophobic monomer, and low molecular weight HEUR polymer attached to such a backbone. Therefore, HASE polymers provide the performance of the HEUR systems and the pH sensitivity of ASE. However, the microstructure and rheological properties of these polymers are more complex and yet have to be fully understood.

Figure 1 represents the chemical structure of a typical HASE polymer. The polymer backbone has a polyelectrolyte nature and is composed of a copolymer of methacrylic acid, the water soluble segments of the backbone, and ethylacrylate, as the somewhat water insoluble segments. The acid monomer provides the solubility of the polymer and the slightly water insoluble monomer enhances the thickening performance and promotes adsorption of

the polymer to a hydrophobic latex, which is part of the solution formulation in many applications. The polymer is hydrophobically modified by randomly grafting a small number of hydrophobic macromonomers to the polymer backbone. The hydrophobic macromonomer is composed of hydrophobic groups, C₈-C₃₀ alkyl or alkyl aryl. These groups are separated from the polymer backbone by a polyethylene oxide (PEO) spacer, with 5-40 moles of ethoxylation. The macromonomer is usually attached to the polymer backbone via a urethane linkage.

2.5 Thickening Mechanisms of HASE Polymers

As discussed in the previous sections, HASE polymers are considered to be chemical hybrids of ASE and HEUR polymers of intermediate molecular weight. Because of their hybrid structure, HASE polymers enhance the solution properties via several thickening mechanisms. The main contribution comes from the hydrophobic interaction between either hydrophobic groups that are attached to the same polymer chain (intra-molecular association) or hydrophobic groups that are attached to different polymer chains (inter-molecular association). A moderate degree of hydrodynamic thickening is contributed by the relatively long polymer backbone. The hydrodynamic volume expansion is accentuated by their electrostatic repulsion of the carboxylic anions along the backbone upon the neutralization with a base at pH above 6. Below this pH, the polymer is assumed to have a compact conformation and show no thickening behavior. Theoretically, some hydrogen bonding between the PEO ether oxygen and the carboxylic groups of the backbone may also occur. The bulky backbone ethyl acrylate groups may also aggregate due to their hydrophobic nature. Among these different mechanisms, the hydrophobic association has been

established to be the dominant thickening mechanism for these polymers.

2.6 Structural and Environmental Factors Affecting the Rheology of HASE Polymers

With the complex architecture of HASE polymers, the association behavior of these polymers would be expected to be quite diverse and dependent on many factors such as, the structure of the backbone that dictates their water solubility and flexibility, the structure and concentration of the macromonomer, which include the type of the hydrophobic groups and the length of their polyethylene oxide spacers. The continuous phase in which the HASE polymer is solvated also plays a major role in the association behavior of these polymers. In this regard, the effects of the medium pH and ionic strength on the association mechanism of HASE polymers have been the focus of a number of studies^{15, 32-36}

In the next few section, we summarize the findings of the research work that deals with the factors that affect the microstructure and rheology of aqueous solution of HASE polymers. These factors include the solution pH and ionic strength, the hydrophobe size and the PEO spacer length. Other factors such as the composition of the backbone and the solvent quality are part of the current research and will be summarized in their relevant chapters.

2.6.1. Effect of the Solution pH

Due to the polyelectrolyte nature of the HASE polymer's backbone, the polymer microstructure and solution rheology is highly dependent on the pH. Therefore, the effects of solution pH on the behavior of HASE polymer have been studied using probe fluorescence, dynamic light scattering and potentiometric titration⁻³²⁻³⁵. The collective findings of these results can be summarized in the next paragraph.

The HASE polymers are usually prepared and supplied as an insoluble latex at low pH (~ 3); the hydrodynamic radius (R_H) of these polymer latexes is of the order of 75 nm. These latexes have water-like viscosity. The addition of a base ionizes the COOH backbone groups, the backbone extends, and the polymer swell to a larger size ($R_H \sim 225$ nm) due to the repulsion between the negative charges on the backbone. At a pH around 6.5, the polymer starts to dissolve and the solution viscosity increases rapidly. At this point both inter- and intra-molecular associations are possible and the polymer forms aggregates in a manner similar to the micellization of a surfactant. With further addition of base, the particles dissociate into several smaller clusters, $R_H \sim 100$ nm, and the solution viscosity continues to increase. As the solution reaches a pH ~ 7.5 , the polymer is completely neutralized and the solution viscosity remains constant at a maximum level. Figure 2 summarizes the effect of the solution pH on the polymer microstructure, solution viscosity, and the polymer hydrodynamic size.

2.6.2 Effect of the Solution Ionic strength

The neutralization of the polymer solution at high pH expands and solubilizes the polymer chains due to the repulsion of the negative charges distributed along the backbone. In the extended conformation, the hydrophobic groups associate to form both inter- and intra-molecular association. This association makes the polymer backbone stiff. The addition of a salt would shield the electrostatic charges and reduce the stiffness of the backbone and transform some of the inter-molecular associations to intra-molecular association. Tan *et al.*³⁶ report that increasing the salt (NaCl) concentration reduces the shear viscosity; however, the shear-induced structure becomes more pronounced with an increase of the salt

concentration up to a specific level. The appearance of the shear-induced structure is also shifted to higher shear rates (Figure 3). At large salt concentrations (>0.6 M), the polymer backbone collapses due to the shielding of the electrostatic charges and the disruption of the hydrophobic interaction; thus, both viscosity and the degree of the shear-induced structure are reduced.

2.6.3 Effect of the Size of Hydrophobic Groups

The effect of the hydrophobic group type and size has been the focus of several publications. Tirtaatmadja *et al.* used alkyl hydrophobes with varied size, C_{12} , C_{16} and C_{20} ³⁵. They reported an increase in the hydrophobic association strength with the increase of the hydrophobe size. Both the association number, the number of hydrophobes that form a network junction, and the junction density were increased with the hydrophobe size. In another study³⁷ in which the hydrophobe size was increased from C_1 to C_{20} , dynamic light scattering data also showed an increase in the association number. These findings were also confirmed using pulsed-gradient spin-echo (PGSE) nuclear magnetic resonance (NMR) measurements³⁸. Extensional flow measurements also revealed similar findings; the network strength was proportional to the hydrophobe length³⁵. The hydrophobe length has an impact on the network strength, not only through association number or density, but also through the difference in the molecular associations. Shorter hydrophobes will tend to form intra-molecular association rather than inter-molecular association.

2.6.4 Effect of the PEO Spacer Length

The viscoelastic properties of HASE polymer are highly dependent on the

chemical structures of the hydrophobic macromonomer. The spacer length that extends the hydrophobic moiety from the polymer backbone dictates the accessibility of the hydrophobic group. Dai, et al used dynamic light scattering to examine the effect of the PEO spacer length on the microstructure of dilute HASE polymer solutions³⁷. They found that increasing the PEO length results in a decrease in the hydrophobicity of the macromonomer. Thus, the number of junctions will decrease, but the aggregation number will increase. This conclusion is supported by the results of another study from the same group³⁹. In this latter study, increasing the length of PEO spacer was associated with an increase of the activation energy, extracted from the temperature dependence of the viscosity based on the Arrhenius equation. This implies that with longer PEO spacers, the network structure becomes stronger which may be attributed to the increase of the aggregation number as suggested by Dai's study. The microstructures of the HASE polymer with shorter and longer PEO spacer as described by those studies are shown in Figure 4.

2.7 Cyclodextrin

Cyclodextrins are seminatural products that are produced enzymatically from a renewable natural material, starch. They are torus-like macrorings that are cyclic oligosaccharides consisting of 6, 7, or 8 glucose units (corresponding to α , β , and γ -CD) joined by α -1,4-glycosidic linkages. The structure and dimension of different cyclodextrins is shown in Figure 5. Their torus-like structure enables them to include a variety of substances in their annular gap in different arrangements. Through their inclusion complex forming ability, the properties of the complexed substances can be modified significantly⁴⁰.

Cyclodextrins have shown superior tendencies to interact with the hydrophobic segments of different hydrophobically modified water soluble associative polymers, including: hydrophobically end capped polyethylene oxide⁴¹⁻⁴⁶, poly(ethylene glycol)s (PEGs) bearing hydrophobic ends (naphthyl and phenyladamantyl)⁴⁷, N,N-dimethylacrylamide-hydroxyethyl methacrylate copolymer hydrophobically modified with adamantyl groups⁴⁸⁻⁵⁰, hydrophobically modified ethyl(hydroxy ethyl) cellulose⁵¹, hydrophobically modified, degradable, poly(malic acid)⁵², isobutene maleate polymer with pendant hydrophobic 4-tert-butylanilide^{53,54}, hydrophobically modified ethoxylated urethanes⁵⁵, hydrophobically modified alkali soluble emulsion polymers^{56,57}, and hydrophobically modified Dextran⁵⁸. Cyclodextrins has also been reported to form inclusion compounds with many nonionic surfactants⁵⁹⁻⁷⁵. The interaction between cyclodextrins and the hydrophobically modified polymers usually leads to the deactivation of the hydrophobic nature of these polymers.

Gupta *et al*⁵⁶ used methylated β -cyclodextrin (m- β CD) to encapsulate the hydrophobic moiety of HASE polymers. The addition of up to 3% m- β CD to polymer with short hydrophobes, C₁-C₈ showed no change in the solution viscosity. On the other hand, a reduction in the solution viscosity was observed when longer hydrophobes, C₁₂-C₂₀, were used. However, no details about possible stoichiometric ratio for the interaction between the polymer and m- β CD were given. In another study⁵⁷, Islam *et al* also used m- β CD to deactivate the hydrophobic moiety of dilute HASE solution. Due to light scattering measurements the polymer concentration used in the study was limited to very dilute concentrations, $\sim 5 \times 10^{-4}$ g/ml. The amount of m- β CD required to completely remove the

hydrophobic association was about 1500 moles/ hydrophobes.

In spite of the successful use of cyclodextrins in the deactivation of the hydrophobic groups of HASE polymers, detailed studies on the mechanism of deactivation and its effect on the solution rheology is needed. Other techniques are also needed to understand the nature of the interaction at the molecular level. Some of these techniques are nuclear magnetic resonance (NMR), differential scanning calorimetry (DSC) and thermal gravimetric analysis (TGA). Moreover, no approach has been presented for the reversible recovery of the activity of hydrophobic groups. These issues are part of this current study and will be fully addressed in Chapter 7.

2.8 References

1. Rubinstein, M.; Dobrynin, A. V. Association Leading to the Formation of Reversible Network and Gels, *Current Opinion in Colloid & Interface Science*. **1999**, 4, 83-87.
2. Rubinstein, M.; Dobrynin, A. V., Solution of Associative Polymers. *TRIP* **1997**, 5(6), 181-186.
3. Alexandridis, P. Amphiphilic Copolymers and Their Applications. *Current Opinion in Colloid & Interface Science* **1996**, 1, 490-501.
4. Sasase, H.; Aoki, T.; Katono, H.; Sanui, K.; Ogata, N.; Ohta, R.; Kondo, T.; Okano, T.; Sakurai, Y. Regulation of Temperature-Response Swelling Behavior of Interpenetrating Polymer Networks Composed Of Hydrogen Bonding Polymers. *Makromolekulare Chemie, Rapid Communications* **1992**, 13, 577-581.
5. French, R. N.; Walsh, J. M.; Machado, J. M. Relating The Heat-of-Mixing of Analog Mixtures to the Miscibility of Hydrogen-Bonding Polymers. *Polymer Engineering and Science* **1994**, 34, 42-58.
6. Graf, J. F.; Painter, P. C.; Coleman, M. M. Free Volume in Hydrogen Bonding Polymer Blends. *Polymer Preprints* (American Chemical Society, Division Of Polymer Chemistry) **1990**, 31, 537-538.
7. Bock, J.; Siano, D. B.; Valint, P. L. (Jr.); Pace, S. J. Structure and Properties of Hydrophobically Modified Associating Polymers. In *Polymers in Aqueous Media Performance Through Association*. Glass, J. E., ed.; *Advances in Chemistry Series 223*; American Chemical Society: Washington, DC, 1989.
8. Sau, A. C.; Landoll, L.M. Synthesis and Properties of Hydrophobically Modified (Hydroxyethyl)cellulose. In *Polymers in Aqueous Media Performance Through Association*. Glass, J. E., ed.; *Advances in Chemistry Series 223*; American Chemical Society: Washington, DC, 1989.
9. Goodwin, J.W.; Hughes, R.W.; Lam, C.K.; Miles, J.A.; Warren, B. C. H. The Rheological Properties of Hydrophobically Modified Cellulose. In *Polymers in Aqueous Media Performance Through Association*. Glass, J. E., ed.; *Advances in Chemistry Series 223*; American Chemical Society: Washington, DC, 1989.
10. Kraunasena, A.; Brown, R.G.; Glass, J.E. Hydrophobically Modified Ethoxylate Urethane Architecture: Importance of Aqueou-and Dispersed-Phase Properties. In *Polymers in Aqueous Media Performance Through Association*. Glass, J. E., ed.; *Advances in Chemistry Series 223*; American Chemical Society: Washington, DC, 1989.

11. Jenkins, R.D.; Silebi, C.A.; El-Aasser, M.S. Steady-Shear and Linear-Viscoelastic Material Properties of Model Associative Polymer Solutions. *In Polymers as Rheology Modifiers*. Schultz, D.N.; Glass, J. E., eds.; ASC Symposium Series 462; American Chemical Society: Washington, DC, 1991.
12. Jenkins, R.D.; Bassett, D.R.; Silebi, C.A.; El-Aasser, M.S. Synthesis and Characterization of Model Associative Polymers. *Journal of Applied Polymer Science* **1995**, 58(2), 209-230.
13. Miffleton, J.C. Cummins, D.F.; McCormick, C.L. Rheological Properties of Hydrophobically Modified Acrylamide-Based Polyelectrolytes. *In Water-Soluble Polymers Synthesis, Solution Properties and Applications*; Shalaby, S. W.; McCormick, C.L. and Butler, G.B., eds.; ASC Symposium Series 467; American Chemical Society: Washington, DC, 1991.
14. Regalado, E.; Selb, J.; Candau, F. Viscoelastic Behavior of Semidilute Solutions of MultiSticker Polymer Chains. *Macromolecules* **1999**, 32, 8580-8588.
15. Tirtaatmadja, V. T., K. C. Jenkins, R. D. Bassett, D. R. Stability of a Model Alkali-Soluble Associative Polymer in the Presence of a Weak and a Strong Base. *Colloid and Polymer Science* **1999**, 277, 276-281.
16. Rich, A. F.; Benes, P. C.; Adams, L. E. Combinations of Polymeric Associative Thickeners for Aqueous Latex Paints. US Patent 4735981, 1988.
17. Jones, C. E.; Reeve, P. F. D. Mixed Surfactant and Hydrophobically-Modified Polymer Compositions for Thickeners for Aqueous Systems. EP Patent 875557, 1998.
18. Jenkins, R. D.; Bassett, D. R.; Shay, G. D. Water-Soluble Polymers Containing Complex Hydrophobic Groups. US Patent 5292828, 1994.
19. Harrington, J. C.; Zhang, H. T. Using Hydrophobically Associative Polymers in Preparing Cellulosic Fiber Compositions. WO Patent 0140578, 2001.
20. Marchant, N. S.; Yu, S. Rheology Modifying Copolymer Composition. US Patent 06433061, 2002.
21. Brooks, A.; Du Reau, C. M. A. Cleansing Compositions Containing Polar Oils and Skin Conditioners. WO Patent 9800495, 1998.
22. Herd, H. E.; Williams, R. Preparation and Properties of Shear-Thinning, Thickened Cleaning Composition. GB Patent 2346891, 2000.

23. Alan, B.; Du Reau, C. M. A. Cleansing Compositions. US Patent 6191083, 2001.
24. Veronique, R.; Therese, D. Aerated Composition, Process for its Manufacture and its Use. US Patent 6251954, 2001.
25. Didier, C.; Serge, F.; Anne-Marie, P. UV-photoprotecting Emulsions Comprising Micronized Insoluble Screening Agents and Associative Polymers. US Patent 6409998, 2002.
26. Ewbank, E.; Collard, C.; Tummers, D.; Breuer, E.; Thibert, E. Liquid Fabric Softening Compositions Containing a Fatty Alcohol Ethoxylate Diurethane Polymer as a Thickener. US Patent 6001797, 1999.
27. Alfons, C. R. A.; Madeleine, D. B. F. J.; Jean, H. B. A. Fabric Softener Compositions. US Patent 6020304, 1999.
28. Jenkins, R. D.; Bassett, D. R.; Lightfoot, R. H.; Boluk, M. Y. Glycol-Based Aircraft Anti-Icing Fluids Thickened by Associative Polymers Containing Hydrophobe-Bearing Macromonomers. US Patent 5681882, 1997.
29. Jenkins, R. D.; Bassett, D. R.; Lightfoot, R. H.; Boluk, M. Y. Aircraft Anti-icing Fluids Thickened by Associative Polymers. WO Patent 9324543, 1993.
30. Carder, C. H.; Garska, D. C.; Jenkins, R. D.; McGuinness, M. J. Aircraft Deicing/Anti-icing Fluids Thickened by Associative Polymers. US Patent 5708068, 1998.
31. Carder, C. H.; Garska, D. C.; Jenkins, R. D.; McGuinness, M. J. Aircraft Deicing/anti-icing Universal Fluids. JP Patent 10237428, 1998.
32. Wang, C.; Tam, K.C.; Jenkins, R.D.; Bassett, D.R. Potentiometric Titration and Dynamic Light Scattering of Hydrophobically Modified Alkali Soluble Emulsion (HASE) Polymer Solutions. *Phys. Chem. Chem. Phys.* **2000**, 2, 1967-1972.
33. Kumacheva, E.; Rharbi, Y.; Winnik, M A.; Guo, L.; Tam, K. C.; Jenkins, R. D. Fluorescence Studies of an Alkaline Swellable Associative Polymer in Aqueous Solution. *Langmuir* **1997**, 13, 182-186.
34. Horiuchi, K.; Rharbi, Y.; Yekta, A.; Winnik, M.A.; Jenkins, R.D.; Bassett, D.R. Dissolution Behavior in Water of a Model Hydrophobic Alkali- Swellable Emulsion (HASE) Polymer with C₂₀H₄₁ Groups. *Canadian Journal of Chemistry-Revue Canadienne De Chimie* **1998**, 76, 1779-1787.

35. Tirtaatmadja, V.; Tam, K.C.; Jenkins, R.D. Rheological Properties of Model Alkali-Soluble Associative (HASE) Polymers: Effect of Varying Hydrophobe Chain Length. *Macromolecules* **1997**, *30*, 3271-3282.
36. Tan, H.; Tam, K.C.; Tirtaatmadja, V.; Jenkins, R.D.; Bassett, D.R. Extensional Properties of Model Hydrophobically Modified Alkali-Soluble Associative (HASE) Polymer Solutions. *J. Non-Newtonian Fluid Mech.* **2000**, *92*, 167-185.
37. Dai, S. T., Tam, K.C.; Jenkins, R.D.; Bassett, D.R. Light Scattering of Dilute Hydrophobically Modified Alkali-Soluble Emulsion Solutions: Effect of Hydrophobicity and Spacer Length of Macromonomer. *Macromolecules* **2000**, *33*, 7021-7028.
38. Nagashima, K.; Strashko, V.; Macdonald, P.M.; Jenkins, R.D.; Bassett, D.R. Diffusion of Model Hydrophobic Alkali-Swellable Emulsion Associative Thickeners. *Macromolecules* **2000**, *33*(25), 9329-9339.
39. Tam, K.C.; NG, W.K.; Jenkins, R.D.; Bassett, D.R. Viscoelastic Behavior of Model HASE Associative Polymer Solutions. Proceedings of the XIIIth International Congress on Rheology, Cambridge, UK, **2000**. 329-331.
40. Szejtli, J. Introduction and General Overview of Cyclodextrin Chemistry. *Chem. Rev.* **1998**, *98*, 1743-1753.
41. Amiel, C.; David, C.; Renard, E.; Sebille, B. Macromolecular Assemblies Generated by Inclusion Complexes between Amphipathic Polymers and β -Cyclodextrin Polymers in Aqueous Media, *Polymer Preprints (American Chemical Society, Division of Polymer Chemistry)* **1999**, *40*, 207-208.
42. Amiel, C.; Moine, L.; Brown, W.; Renard, E.; Guerin, P.; Sebille, B. Associations of Amphiphilic Degradable Polymers with B-Cyclodextrin Polymers: pH-Dependent Network, *Proceedings of the International Symposium on Cyclodextrins, 9th, Santiago de Comostela, Spain, May 31-June 3, 1998*, 1999, 81-84.
43. Amiel, C.; Sebille, B. New Associating Polymer Systems Involving Water-Soluble β -Cyclodextrin Polymers, *Rev. Inst. Fr. Pet.* **1997**, *52*(2), 248-250.
44. Amiel, C.; Sebille, B. New Associating Polymer Systems Involving Water-Soluble β -Cyclodextrin Polymers, *J. Inclusion Phenom. Mol. Recognit. Chem.* **1996**, *25*, 61-67.
45. Amiel, C.; Sandier, A; Sebille, B.; Valvvat, P.; Wintagens, V. Association Between Hydrophobically End-Capped Polyethylene Oxide and Water Soluble β -Cyclodextrin Polymers, *int. J. Polymers Analysis & Characterization* **1995**, *1*, 289-300.

46. Sandier, A.; Brown, W.; Mays, H.; Amiel, C. Interaction between an Adamantane End-Capped Poly(ethylene oxide) and a β -Cyclodextrin Polymer, *Langmuir* **2000**, *16*, 1634-1642.
47. Amiel, C.; Moine, L.; Sandier, A.; Brown, W.; David, C.; Hauss, F.; Renard, E.; Gosselet, M.; Sebille, B. Macromolecular Assemblies Generated by Inclusion Complexes between Amphipathic Polymers and β -Cyclodextrin Polymers in aqueous media, *ACS Symposium Series* **2001**, 780, 58-81.
48. Gosselet, N. M.; Naranjo, H.; Renard, E. Amiel, C.; Sebille, B. Association of Poly-N-[tris(hydroxymethyl)methyl] Acrylamide with a Water Soluble β -Cyclodextrin Polymer, *European Polymer Journal* **2002**, *38*, 649-654.
49. Gosselet, N. M.; Borie, C.; Amiel, C.; Sebille, B. Aqueous Two Phase Systems from Cyclodextrin Polymers and Hydrophobically Modified Acrylic Polymers, *J. Dispersion Sci. Technol.* **1998**, *19*, 805-820.
50. Gosselet, N. M.; Beucler, F.; Renard, E.; Amiel, C.; Sebille, B. Association of Hydrophobically Modified Poly (N,N-dimethylacrylamide hydroxyethyl methacrylate) with Water Soluble β -Cyclodextrin Polymers, *Colloids and Surfaces, A: Physicochemical and Engineering Aspects* **1999**, *155*, 177-188.
51. Karlson, L.; Thuresson, K. and Lindman, B. Investigation of the Complex Formation between Hydrophobically Modified Ethyl(hydroxy ethy) Cellulose and Cyclodextrin. *Carbohydrate Polymers* **2002**, *50*(3), 219-226.
52. Moine, L.; Amiel, C.; Brown, W.; Guerin, P. Associations between a hydrophobically modified, degradable, poly(malic acid) and a β -cyclodextrin polymer in solution, *Polymer International* **2001**, *50*, 663-676.
53. Wenz, G.; Weickenmeier, M.; Huff, J. Association thickener by host-guest interaction of β -cyclodextrin polymers and guest polymers, *ACS Symposium Series* **2000**, *765*, 271-283.
54. Weickenmeier, M.; Wenz, G.; Huff, J. Association Thickener by Host Guest Interaction of a β -Cyclodextrin Polymer and Polymer with Hydrophobic Side-Groups., *Macromol. Rapid Commun.*, **1997**, *18*(12), 1117-1123.
55. Ma, Z.; Glass, J. E. Complexations of β -Cyclodextrin with Surfactants and Hydrophobically Modified Ethoxylated Urethanes. In *Analytical application in adsorption measurements*. ACS Symposium Series, 2000. **765**(Associative Polymers in Aqueous Media): p. 254-270.

56. Gupta, R.K.; Tam, K. C.; Ong, S. H.; Jenkins, R. D. Interactions of Methylated β -Cyclodextrin with Hydrophobically Modified Alkali-Soluble Associative Polymers (HASE): Effect of Varying Carbon Chain Length. In *Proc. Int. Congr. Rheol.*, 13th. 2000.
57. Islam, M. F.; Jenkins, R. D.; Bassett, D. R.; Lau, W.; Ou-Yang, H. D. Single Chain Characterization of Hydrophobically Modified Polyelectrolytes Using Cyclodextrin/Hydrophobe Complexes, *Macromolecules*, **2000**, 2480-2485.
58. Amiel, C., Renard, E.; Sandier, A.; Moine, L.; Gosselet, M.; Sebille, B. Macromolecular assemblies generated by inclusion complexes between amphipathic polymers and β -cyclodextrin polymers in aqueous media. Book of Abstracts, 218th ACS National Meeting, New Orleans, Aug. 22-26, 1999.
59. Ahmed, M.O. Comparison of Impact of the Different Hydrophilic Carriers on the Properties of Piperazine-Containing Drug. *European Journal of Pharmaceutics and Biopharmaceutics*, **2001**, 51(3), 221-225.
60. Alexandridis, Paschalis; Tsianou, M.; Ahn, S. Effect of Cyclodextrins on Polymer-Surfactant Interactions in Aqueous Solution. *Proceedings of the International Symposium on Controlled Release of Bioactive Materials*, 2000, 1134-1135.
61. Alvarez, A. R.; Garcia-Rio, L.; Herves, P.; Leis, J. R.; Mejuto, J. C.; Perez-Juste, J. Basic Hydrolysis of Substituted Nitrophenyl Acetates in β -Cyclodextrin/Surfactant Mixed Systems. Evidence of Free Cyclodextrin in Equilibrium with Micellized Surfactant. *Langmuir*, **1999**, 15(24), 8368-8375.
62. Buschmann, H. J.; Cleve, E.; Schollmeyer, E. The Interactions between Nonionic Surfactants and Cyclodextrins Studied by Fluorescence Measurements. *Journal of Inclusion Phenomena and Macrocyclic Chemistry*, **1999**, 33(2), 233-241.
63. Cserhati, T.; Oros, G.; Szejtli, J. Effect of Cyclodextrins of Nonionic Surfactants: Reduction of Surface Activity and Phytotoxicity, *Tenside, Surfactants, Deterg.*, **1992**, **29**(1), 52-57.
64. Cserhati, T.; Forgacs, E. Charge-Transfer Chromatographic Study of the Interaction of Non-ionic Surfactants with Hydroxypropyl- β -Cyclodextrin. *J. Chromatogr., A*, **1994**, **665**(1), 17-25.
65. Eli, W.; Chen, W.; Xue, Q. Determination of Association Constants of Cyclodextrin-Nonionic Surfactant Inclusion Complexes by a Partition Coefficient Method, *Journal of Inclusion Phenomena and Macrocyclic Chemistry*, **2000**, 38(1-4), 37-43.

66. Hodul, P.; Duris, M.; Kralik, M. Inclusion Complexes of β -Cyclodextrin with Non-ionic Surfactants in Textile Preparation Processes., *Vlakna Text.*, **1996**, 3(1), 15-19.
67. Katougi, Y.; Saito, Y.; Hashizaki, K.; Taguchi, H.; Ogawa, N. Comparison of the Solubilizing Ability of Cyclodextrins and Surfactants for (+)- α -pinene. *Journal of Dispersion Science and Technology*, **2001**, 22(2 & 3), 185-190.
68. Oros, G.; Cserhati, T.; Szejtli, J. Cyclodextrins Decrease the Phytotoxicity of Nonionic Tensides. *Acta Agron. Hung.*, **1989**, 38(3-4), 211-17.
69. Rohrbach, R. P.; Allenza, P.; Schollmeyer, J.; Oltmann, H. D. Biodegradable Polymeric Materials and Articles Fabricated Therefrom, US Patent 9106601, 1991.
70. Saito, Y.; Katougi, Y.; Hashizaki, K.; Taguchi, H.; Ogawa, N. Solubilization of (+)- α -Pinene by Cyclodextrin/Surfactant Mixed Systems. *Journal of Dispersion Science and Technology*, **2001**, 22(2 & 3), 191-195.
71. Saket, M. Improvement of Solubility and Dissolution Rate of Meclozine Hydrochloride Utilizing Cyclodextrins and Non-ionic Surfactant Solutions Containing Cosolvents and Additives. *Acta Technol. Legis Med.*, **1997**, 8(1), 33-48.
72. Topchieva, I. N.; Karezin, K. I. Molecular Self-assembly in Nonionic Surfactant-Cyclodextrin Systems. *Colloid Journal (Translation of Kolloidnyi Zhurnal)*, **1999**, 61(4), 514-519.
73. Topchieva, I.; Karezin, K. Self-Assembled Supramolecular Micellar Structures Based on Non-ionic Surfactants and Cyclodextrins. *Journal of Colloid and Interface Science*, **1999**, 213(1), 29-35.
74. Wilson, L. D.; Verral, R. E. ¹H NMR Study of Cyclodextrin-Hydrocarbon Surfactant Inclusion Complexes in Aqueous Solutions. *Canadian Journal of Chemistry*, **1998**, 76(1), 25-34.
75. Woo, R. A.; Trinh, T.; Cobb, D. S.; Schneiderman, E.; Wolff, A. M.; Ward, T. E.; Chung, A. H.; Reece, S.; Rosenbalm, E. L. Uncomplexed Cyclodextrin Compositions for Odor Control and Refreshening of Garments. US Patent 9,856,888, 1998.

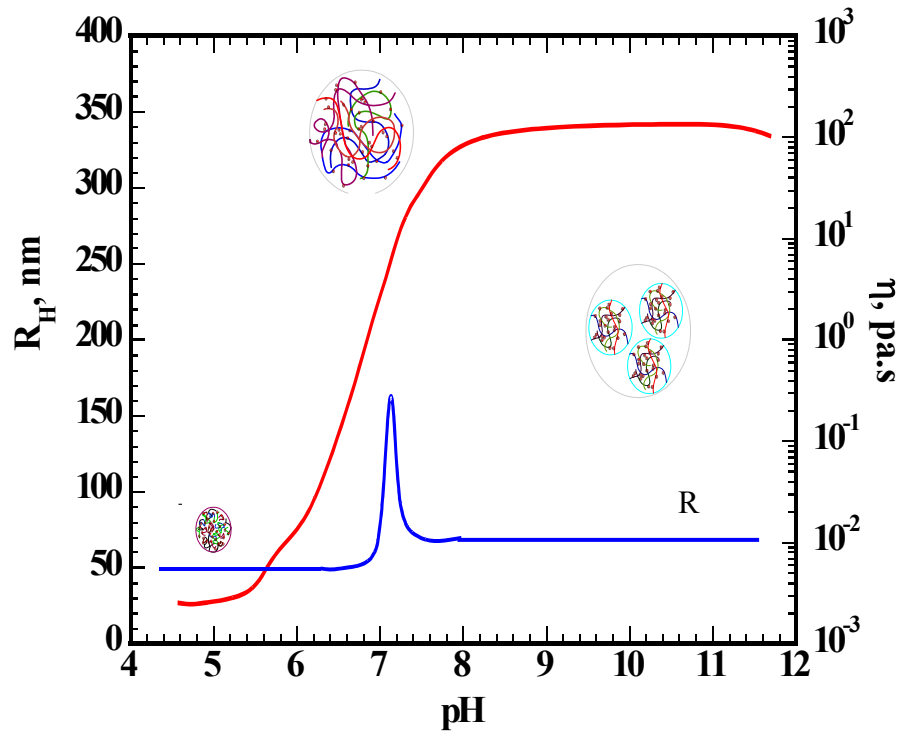
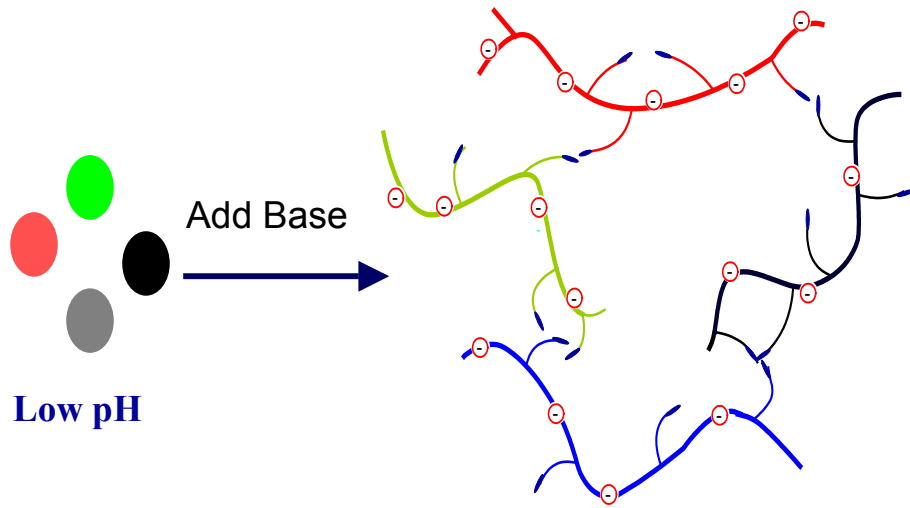


Figure 2. Effect of solution pH on the network structures, radius of gyration and viscosity of HASE polymer solution

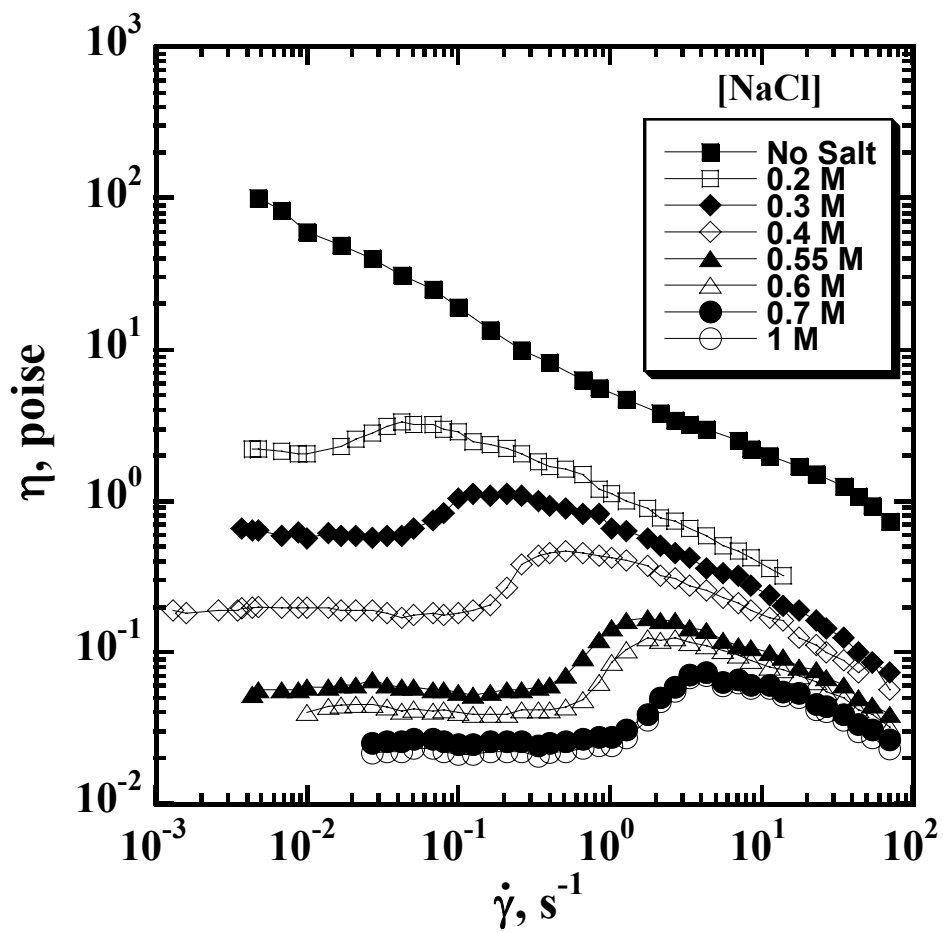


Figure 3. Effect of salt (NaCl) concentration on the steady shear viscosity of a 1% polymer solution³³.

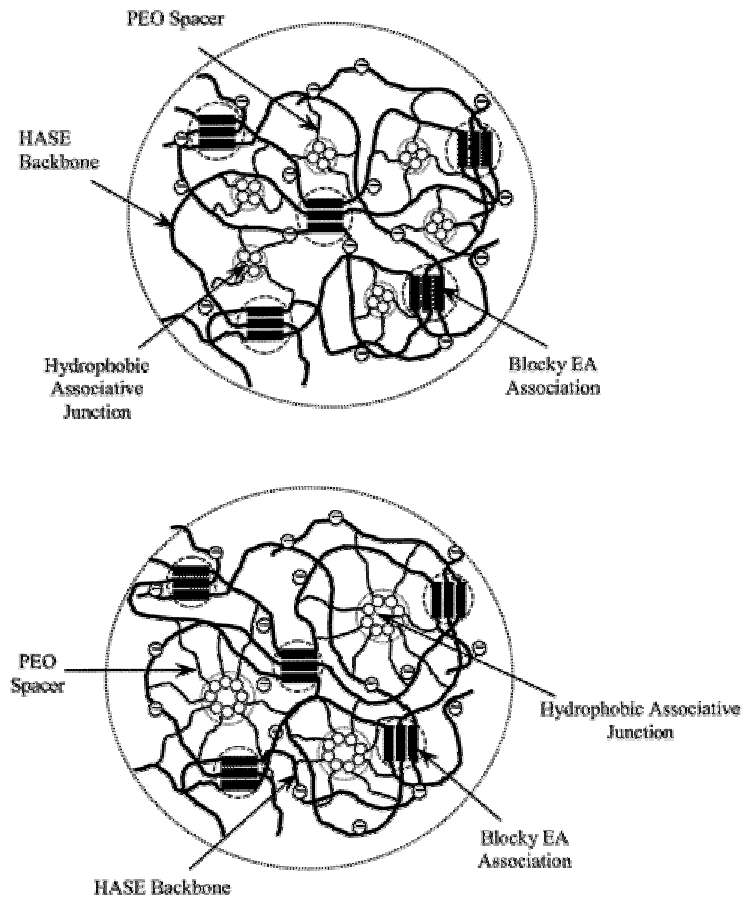


Figure 4. Schematic representation of HASE polymer aggregates for (a) short PEO spacer length and (b) long PEO spacer length³⁴.

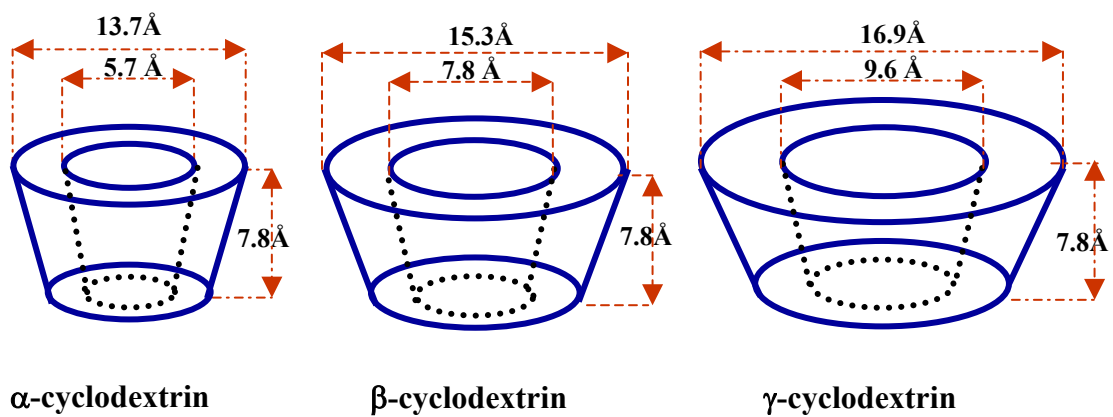
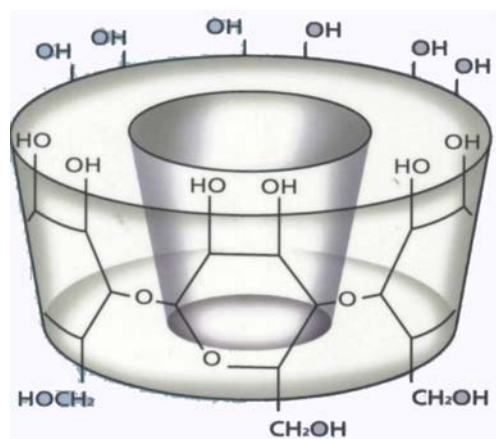


Figure 5. Structure of β-cyclodextrin and approximate geometric dimension of α-, β- and γ-cyclodextrin molecules

CHAPTER 3

EXPERIMENTAL TECHNIQUES

Abstract

Many experimental techniques can be used to characterize the structure and rheological properties of hydrophobically modified associative polymers. This chapter summarizes the theoretical principles behind the techniques that are utilized during the course of this study. These techniques include rheology, diffusing wave spectroscopy (DWS), nuclear magnetic resonance (NMR), differential scanning calorimetry (DSC), and thermal gravimetric analysis (TGA).

3. 1 Rheological Characterization:

Rheology is defined as the science that deals with the deformation of materials as a result of an applied stress¹. It is a powerful tool that is capable of characterizing the properties and microstructure of many polymeric and non-polymeric systems. Rheology provides information that is important in designing and optimizing material properties². In the next few sections, we give a brief summary to different rheological techniques that have been used in this study.

3.1. 1 Dilute Solution Measurement

The rheology of dilute solution is one of the widely used techniques for characterizing polymers². In dilute solution experiments, the viscosity of very dilute solutions is measured and the intrinsic viscosity, $[\eta]$, is determined by extrapolating to zero concentration. The mathematical definition of $[\eta]$ is:

$$[\eta] = \lim_{c \rightarrow 0} \left(\frac{\eta - \eta_o}{\eta_o c} \right) \quad (1)$$

where η is the viscosity of solution of concentration c and η_o is the viscosity of the solvent. Dilute solution experiments also gives information about the polymer dimension, the polymer-solvent interactions and the crossover concentration (c^*). c^* is defined as the concentration at which the polymer coils begin to overlap and span the entire solution volume, and is usually taken as the reciprocal of $[\eta]$.

In our study, the viscosities of the solvent and dilute polymer solutions wer measured with Ubbelohde dilution viscometers situated in a thermostated water bath at 25°C. The efflux times of the polymer solutions were converted to reduced and inherent

viscosities. Using the familiar Huggins and Kraemer equations, the intrinsic viscosity was obtained by plotting the resulting reduced and inherent viscosities against concentration and extrapolating to zero concentration¹.

3. 1. 2. Steady-State or Simple Shear Flow

In a steady shear experiment, a steady shear stress is applied on the sample and the resultant shear rate is measured. The apparent viscosity is defined as the ratio of the shear stress to the shear and reported as a function of the shear rate (or shear stress):

$$\eta(\dot{\gamma}) = \frac{\tau}{\dot{\gamma}} \quad (2)$$

According to the behavior of η as function of $\dot{\gamma}$, the fluid can be classified as Newtonian (constant viscosity), pseudoplastic/shear thinning (viscosity decreases with shear rate), or dilatants/shear thickening (viscosity increases with shear rate). The different material responses are shown in Figure 1.

3. 1. 3. Dynamic or Small Amplitude Oscillatory Shear Flow

The dynamic rheological technique is a useful tool in probing microstructures of materials without disrupting these structures. In dynamic (oscillatory) shear flow, a sinusoidally varying strain of amplitude γ_0 is applied to the sample:

$$\gamma = \gamma_0 \sin(\omega t) \quad (3)$$

where ω is the frequency of oscillation. The dynamic experiment is usually carried out using very small strain amplitude and the sample is said to be within the linear viscoelastic (LVE) region. In the LVE region the sample response is independent of the applied strain amplitude

and the stress generated due to the sinusoidal shear will again be sinusoidal:

$$\tau = \tau_0 \sin(\omega t + \delta) \quad (4)$$

Here, δ is the phase angle. For elastic solids both stress and strain will be in phase ($\delta=0^\circ$) while for Newtonian fluids, the stress and strain will be completely out of phase ($\delta=90^\circ$). Correspondingly, viscoelastic materials exhibit a phase angle between 0 and 90° . Using trigonometric identities, the stress wave can be decomposed into an in-phase and out-of-phase component.

$$\tau = \tau_0 \cos(\delta) \sin(\omega t) + \tau_0 \sin(\delta) \cos(\omega t) \quad (5)$$

The in-phase component corresponds to the ability of the material to elastically store energy and the out-of-phase component corresponds to its ability to dissipate energy. Moreover, the shear storage (elastic) modulus (G') and the shear loss (viscous) modulus (G'') is defined as the ratio of the corresponding stress component to the strain amplitude, as follows:

$$G' = \tau_0 \cos(\delta) / \gamma_0 \quad (6)$$

$$G'' = \tau_0 \sin(\delta) / \gamma_0 \quad (7)$$

The complex viscosity (η^*) can be defined as the ratio of the complex modulus ($G^* = (G'^2 + G''^2)^{1/2}$) to the frequency of deformation:

$$\eta^*(\omega) = \frac{G^*}{\omega} = \sqrt{\left(\frac{G'}{\omega}\right)^2 + \left(\frac{G''}{\omega}\right)^2} \quad (8)$$

The frequency dependence of G' and G'' , the dynamic mechanical spectrum, provides the most important information about the microstructure of a material. For example, gels exhibit G' that is larger than G'' with both moduli independent of frequency. Polymer melts show G' and G'' at low frequencies that are dependent on ω^2 and ω , respectively. For viscoelastic

materials, the overlap frequency (the frequency at which G' and G'' curves intersect) gives information about the relaxation time of the system. The plateau modulus, the value of G' at high frequency, gives information about the strength of the structures formed in the material. Typical dynamic spectra for gels and common polymer solution or melts are shown in Figure 2.

3. 1. 1. Transient Shear Flow

In our study, we consider only one type of transient shear flow experiments, the creep recovery experiment. In a creep experiment, the material that is initially at rest is subjected to a sudden constant stress and the deformation is measured as a function of time¹. The creep experiment is composed of creep step(s) followed by a recovery step where the applied stress is removed. The behavior of elastic, viscoelastic and Newtonian materials during a creep and creep recovery experiment is shown in Figure 3. The creep compliance, $J(t)$ is often used to describe the deformation during a creep experiment and is defined as the ratio between the strain and the constant stress; it has dimensions of reciprocal modulus³.

The steady, dynamic and transient rheological properties of the polymer solutions were measured using a stress-controlled rheometer (Rheometrics DSR II) fitted with appropriate cone and plate, parallel plates or couette geometries. The linear viscoelastic region (LVE) was determined for each sample by running a dynamic sweep experiment. Both the dynamic frequency sweep and the stress creep experiments were conducted by applying stresses within the LVE.

3. 2 Diffusing Wave Spectroscopy

Diffusing Wave Spectroscopy (DWS) is a dynamic light scattering technique that extends dynamic light scattering to very highly multiple scattering media. DWS is very similar to conventional dynamic light scattering. Both techniques measure the temporal fluctuation of the intensity of a single speckle spot of the scattered light. These intensity fluctuations in turn reflect the dynamics of the scattering medium⁴. Using DWS, the viscoelastic properties of complex fluids and polymeric systems can be extracted from the measurements of the means square displacement of microspheres embedded in the viscoelastic medium⁵. The measured electric field autocorrelation function can be related to the mean square displacement of the scattering particles through⁴:

$$g_1(t) = \int_0^{\infty} P(s) \exp\left[-\frac{1}{3} k_o^2 \langle \Delta r^2(t) \rangle \frac{s}{l^*}\right] ds \quad (9)$$

where $g_1(t)$ is the electric field autocorrelation function, $P(s)$ is the path length distribution function, k_o is the wave vector, $\langle \Delta r^2(t) \rangle$ is the particle mean squared displacement and l^* is the distance over which light becomes completely randomized.

The viscoelastic properties of the media can be extracted using one of two approaches. The first approach uses the Stokes-Einstein equation ($D = \frac{k_B T}{6\pi a \eta}$) then generalizes it using the mean field assumption to a frequency dependent form⁶:

$$\tilde{G}(s) \approx \frac{k_B T}{6\pi a s \langle \Delta \tilde{r}^2(s) \rangle} \quad (10)$$

where $\tilde{G}(s)$ is the viscoelastic modulus in the frequency domain, s is the Laplace frequency.

$\tilde{G}(s)$ can be transformed to the more familiar complex shear modulus, $G^*(\omega)$, using analytical continuation and the substitution $s = i\omega$. The storage $G'(\omega)$ and loss $G''(\omega)$ moduli are taken as the real and imaginary parts of $G^*(\omega)$ ⁷.

The second approach is simpler and does not require any transformation from the time to the frequency domain. Instead, it involves direct transformation of the mean square displacement, $\langle \Delta r^2(t) \rangle$, to the creep compliance $J(t)$ through the following relation⁸:

$$\langle \Delta r^2(t) \rangle = \frac{k_B T}{\pi a} J(t) \quad (11)$$

The loss and storage moduli can be calculated using the retardation spectrum $L(\tau)$ determined by regularized fit of the creep compliance using a set of impartial basis⁹:

$$J(t) = J_e + \frac{t}{\eta} - \sum_{n=1}^N L_n \exp\left(-\frac{t}{\tau_n}\right) \quad (12)$$

where N is the number of terms and τ_n are fixed to be logarithmically spaced.

$$G^*(\omega) = \left(\sum_{n=1}^N \frac{L_n \tau_n}{1 + i\omega \tau_n} \right)^{-1} \quad (13)$$

The last equation is an exact equation; thus, the uncertainty in the transformation from the time to frequency domain lies only in the compromise between the degree of smoothing of L_n and the quality of the fit⁹.

A **DWS** setup operating in the transmission mode was utilized in carrying out all measurements. In this setup, the beam from a diode pumped solid state (DPSS) Nd-YAG laser operating at a wavelength of 532 nm *in vacuo* was incident upon a 2 or 3 mm width flat scattering cell, containing the HASE polymer solution with spherical optical probes (1%

monodispersed polystyrene (PS) spheres added to insure a highly scattering medium). The size of the PS spheres was varied from 0.195 μm to 1.55 μm to check for presence of heterogeneity. The multiply scattered light was collected by an ALV SI/SIPD photon detector via a single mode optical fiber. The output from the ALV SI/SIPD photon detector was fed into a correlator working in the cross correlation mode. The measured intensity auto correlation function was converted into the electric field autocorrelation function using the Siegert relationship.

3. 3 Nuclear Magnetic Resonance

Nuclear Magnetic Resonance is a phenomenon that occurs when the nuclei of certain atoms are immersed in a static magnetic field B_0 and exposed to a second transverse rotating magnetic field B_1 . Some nuclei experience this phenomenon, and others do not, depending upon whether they possess a property called spin. When the spin of the protons and the neutrons comprising the nuclei are not paired, the overall spin of the charged nuclei generates a magnetic dipole along the spin axis. The magnitude of this dipole is known as the nuclear magnetic moment, μ . For atoms with spherically symmetric charge distribution, the nucleus is said to have a spin number (I) of $\frac{1}{2}$. Examples are nuclei of ^1H , ^{13}C , ^{15}N , ^{19}F , ^{31}P .

In the presence of an external magnetic field of strength B_0 , the nuclear magnetic moment can align with this external field in $2I+1$ ways, reinforcing or opposing B_0 . Nuclei with $I=\frac{1}{2}$ have 2 ways to align with the external field either parallel, energetically favored, or anti-parallel to the external field and the spinning nucleus will precess about the magnetic field with a frequency ω_0 (Larmor frequency $\omega_0 = \gamma B_0$). γ is called the magnetogyric ratio and it relates the spin number I to the magnetic momentum ($\gamma = 2\pi\mu/h I$), h is

Planck's constant. At a specific rotating frequency of the transverse magnetic field B_1 , the nucleus will resonate or flip from parallel to anti-parallel or vice-versa. The exact frequency of the spin flip identifies the kind of atom that is involved and the other atoms to which it is connected in the molecule. By measuring all of the frequencies, the molecular structure can be determined. The NMR spectrometer identifies spin-flip transitions by detecting the energy change that is associated with the transition process, $\Delta E = h\gamma B_0/2\pi$. The NMR spectrometer detects, amplifies, and displays this magnetic interaction to identify the structure of the molecule¹⁰.

All ^1H NMR spectra in this study were obtained using a 500 MHz Bruker DRX NMR spectrometer. All spectra were acquired in DMSO- d_6 as solvent at 298°K using Tetramethylsilane (TMS) as internal standard. The instrumental parameters for acquisition of the one-dimensional proton spectra are as follow: tuning frequency 500.128 MHz, Spectral Width 13.2 ppm, number of data points 32K, relaxation and acquisition times 1 and 2.47 sec (respectively), pulse width 10.5 μs , tip angle 90° and number of transients 16.

3. 4 Differential Scanning Calorimetry

Differential Scanning Calorimetry (DSC) is a thermal analysis technique that is concerned with the energy changes in a substance¹¹. Each DSC instrument has two separate heating circuits- the average temperature controller and the differential heating circuit. The sample and a reference are heated in separate well-isolated chambers and the temperature of both these chambers are measured and averaged. The heat output of the heater is automatically adjusted so that the average temperature of the sample and the reference is changed in a predefined manner. The temperature between the sample and the

reference adjusts the power to either the reference or the sample chamber to keep both at the same temperature. The power supplied to the two differential heaters is plotted versus the sample temperature. DSC gives information about both first and second order energy transitions, such as glass transition temperature, crystallization, recrystallization, melting, and thermal degradation¹².

The DSC experiments in this study were carried out on 3-8 mg samples with a Perkin-Elmer DSC-7 thermal analyzer equipped with a cooler system. A heating rate of 10°C/min was used and an indium standard was used for calibration. Before each scan, samples were annealed at 200°C for 3 minutes to erase thermal history, followed by a flash quenching to -100°C at 500°C/min.

3. 5 Thermal Gravimetric Analysis

Thermal Gravimetric Analysis (TGA) is a thermal analysis technique that examines the mass changes of a sample as a function of temperature or time. It is used to characterize decomposition and thermal stability of materials under a variety of condition and to examine the kinetics of the physicochemical processes occurring within a sample¹².

TGA measurements in this study were carried out on Perkin-Elmer Pyris1 Thermogravimetric Analyzer. Approximately 20 mg samples were heated from 25-600°C at rate of 20°C/min and the sample weight was recorded as a function of sample temperature.

III.6 References:

1. Carreau, P.J.; De Kee, D.C.R.; Chhabra, R.P. *Rheology of Polymeric Systems Principles and Applications*; Hanser Gardner Publications, Inc.: Cincinnati, 1997.
2. Rohn, C. L. *Analytical Polymer Rheology: Structure-Processing-Property Relationships*, Hanser Gardner Publications, Inc.: Cincinnati, 1995.
3. Ferry, J. D. *Viscoelastic Properties of Polymers*, 3rd ed.; John Wiley and Sons, Inc.: New York, 1980.
4. Weitz, D.A.; Pine, D. J. Diffusing-Wave Spectroscopy. In *Dynamic Light Scattering*, B. Wyn, ed.; Oxford University Press: Oxford, 1993.
5. Rufener, K.; Almer, A.; Xu, J.; Wirtz, D. High Frequency Dynamic and Microrheology of Macromolecular Solution Probed by Diffusing Wave Spectroscopy: the Case of Concentrated Solutions of F-actin. *J. Non-Newtonian Fluid Mech.* **1999**, 82, 303-314.
6. Mason, T.G.; Gang, H.; Weitz, D.A. Diffusing-wave-spectroscopy Measurement of Visco-elasticity of Complex Fluids. *Journal of Optical Society of America* **1997**, 14(1), 139-149.
7. Mason, T.G. Estimation the Viscoelastic Moduli of Complex Fluid using the Generalized Stokes-Einstein Equation. *Rheol. Acta* **2000**, 39, 371-378.
8. Xu, J.; Viasnoff, V.; Wirtz, D. Compliance of Actin Filament Networks Measured by Particle Tracking Microrheology and Diffusing Wave Spectroscopy. *Rheol. Acta* **1998**, 37, 387-398.
9. Mason, T.G.; Gisler, T. ; Kroy, K.; Frey, E.; Weitz, D.A. Rheology of F-actin Solution Determined from Thermally Driven Tracer Motion. *J. Rheol.* **2000**, 44(4), 917-928.
10. Abraham, R.J.; Fisher, D.A.; Loftus, P. *Introduction to NMR spectroscopy*; Wiley: New York, 1988.
11. Griffin, V. J.; Laye, P. G. Differential Thermal Analysis and Differential Scanning Calorimetry. In *Thermal Analysis-Techniques & Applications*; Charsley, E.L.; Warrington, S.B., eds.; Hartnolls Ltd.: Bodmin, 1992.
12. Hatakeyama, T.; Quinn, F.X. *Thermal Analysis Fundamentals and Applications to Polymer Science*, 2nd ed.; Wiley: New York, 1999.

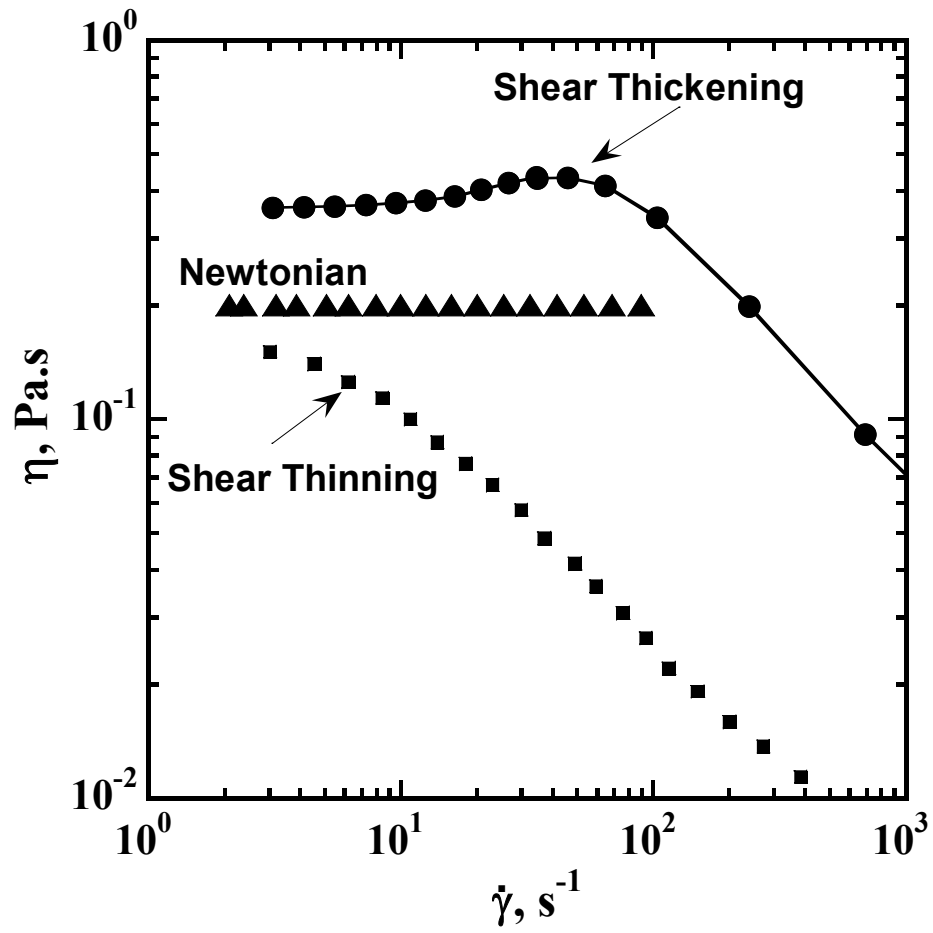


Figure 1: Viscosity as a function of shear rate showing different material response; Newtonian, shear thinning and shear thickening.

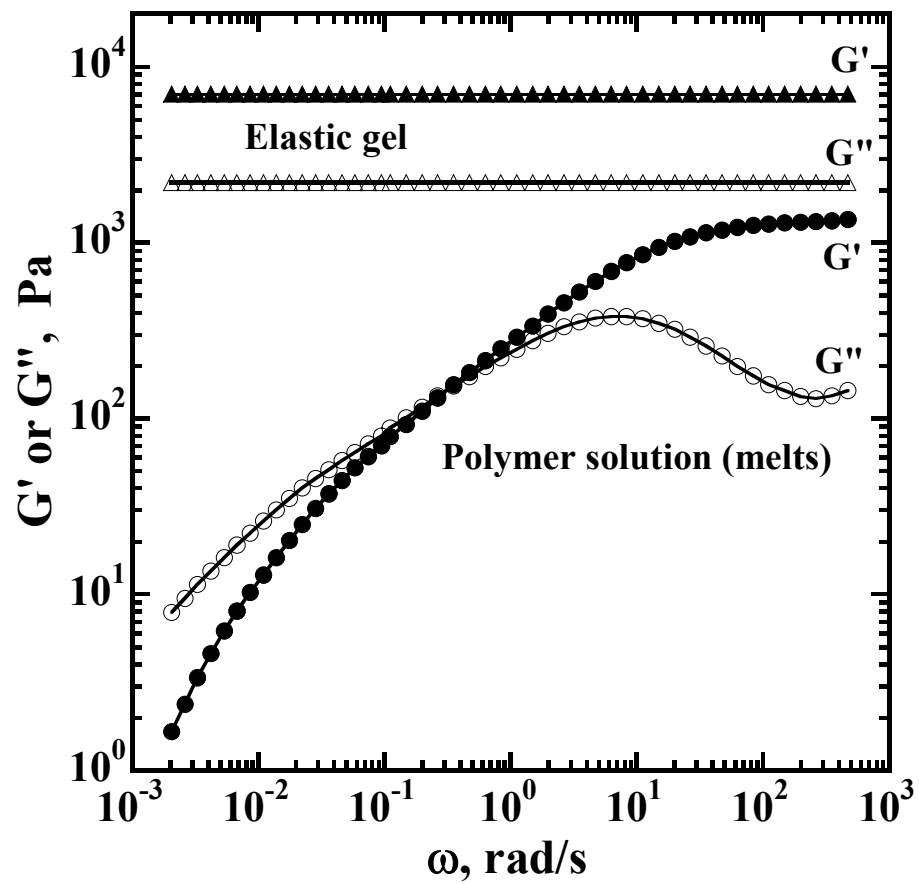


Figure 2: Elastic (G') and viscous (G'') moduli as function of angular frequency (ω) showing the typical behavior of polymer solutions (melts) and elastic gels

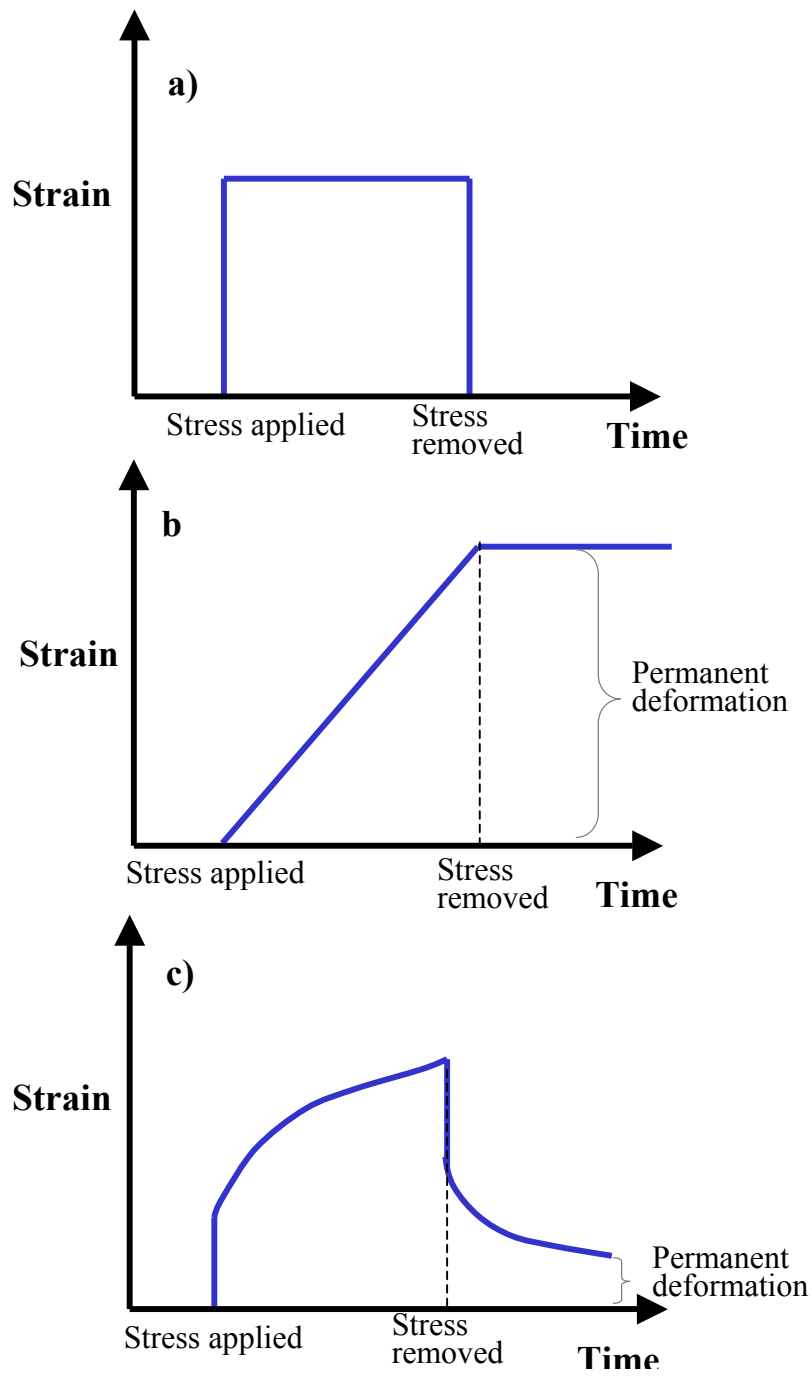


Figure 3: Time profile of shear creep and creep recovery experiments for (a) elastic solid, (b) Newtonian fluid, and (c) viscoelastic material.

CHAPTER 4

**EFFECT OF POLYMER COMPOSITION ON MICROSTRUCTURE AND
SOLUTION RHEOLOGY**

Chapter 4 is essentially a manuscript by Ahmed Abdala, Keith Olesen, Wenjun Wu and Saad Khan prepared for submission to Journal of Rheology.

Effect of Polymer Composition on Microstructure and Solution Rheology

Ahmed A. Abdala¹, Keith Olesen², Wenjun Wu², and Saad A. Khan^{1*}

¹Department of Chemical Engineering, North Carolina State University, Raleigh NC 27695-7905

²The Dow Chemical Company, UCAR Emulsion Systems, 410 Gregson Drive, Cary, NC 27511

Abstract

We investigate the effects of polymer molecular structure on the solution rheology of a hydrophobically modified associative polymer comprised of macromonomers with alkyl hydrophobes attached to a poly(ethyl acrylate-co-methacrylic acid) backbone. In particular, the effects of polymer backbone composition of varying proportions of methylacrylic acid (MAA) and ethyl acrylate (EA) are examined. We find that the concentration of the MAA monomer has a large impact on polymer viscoelasticity. Polymers with low MAA content have smaller chain size that results in lower viscosity and dynamic elastic modulus compared to polymers with high MAA content. Moreover, the balance between the polymer chain size, the chain flexibility and the aggregation of the bulky EA groups yields a maximum in all these material functions with respect to the MAA concentration. The scaling of the shear viscosity, the high frequency elastic modulus and the creep compliance with polymer concentration exhibit a power-law behavior with different exponents. In all cases, three power-law regimes are observed, regardless of the MAA content. However, the transitions shift to lower concentrations as the MAA content increases. The scaling behavior in the three regions can be attributed to the presence of different hydrophobic interaction modes and are compared to theoretical predictions based on the sticky Rouse and sticky reptation models. Variation in the macromonomer concentration reveals a substantial increase in viscosity at

* corresponding author; phone: 919-515-4519; fax: 919-515-3465; email: khan@eos.ncsu.edu

intermediate macromonomer concentration (1 mole%) possibly due to an increase in the number of intermolecular junctions as the number of hydrophobes per chain increases. This is in contrast to low macromonomer concentration (0.3 mole%) behavior that reveals low viscosity due to weak hydrophobic associations, and, high macromonomer concentration (1.9 mole%) behavior that favors more intramolecular association resulting in lower viscoelastic properties compared to intermediate macromonomer concentration.

4.1 Introduction

Alkali soluble emulsion (ASE) polymers are carboxylic functional copolymers produced by free-radical emulsion polymerization of ethylenically unsaturated monomers. These ASE polymers are insoluble in water at low pH but exhibit thickening upon dissolution in aqueous media at higher degree of ionization, usually at pH greater than 6¹. These non-associative polymers can be hydrophobically modified by incorporation of small number of hydrophobic macromonomers, usually nonionic surfactants that have been end-capped with an unsaturated double bond². The hydrophobically modified alkali-soluble emulsion (HASE) polymers exhibit the nature of both the ASE polymers, swelling upon neutralization, and the associative nature of hydrophobically modified ethoxylate urethane (HEUR) polymers, forming transient networks through molecular associations. Due to their hybrid nature, HASE polymers have been increasingly used as rheology modifiers in a variety of applications including cosmetic and personal care products, painting, paper coatings and anti-icing fluids. However, optimal use of these polymers requires controlling the structure and composition of these polymers.

The structure of a typical HASE polymer is shown in Figure 1. This structure can be described as a polyelectrolyte backbone with number of hydrophobic macromonomers randomly grafted to the backbone. The backbone is composed of a copolymer of a hydrophilic segment that provides solubility of the polymer and a slightly water insoluble segment that enhances the thickening performance and promotes adsorption of the polymer to hydrophobic latex in many applications. The hydrophilic polymer is usually an acrylic acid or alkyl acrylic acid polymer while the water insoluble polymer is an acrylate or alkyl acrylate polymer. In most studies of HASE polymers including this, the hydrophilic

segment is methacrylic acid (MAA) whereas the other segment is ethyl acrylate. The hydrophobic macromonomers are attached to the polymer backbone through urethane linkage and end capped with alkyl or alkyl aryl groups that are separated from the backbone by 5-100 polyethylene oxide (PEO) units. The complexity of the HASE polymer structures can be seen in Figure 1, which shows the chemical structure of the polymers used in this study. With such a complex architecture, the association behavior of these polymers would be expected to be quite diverse and dependent on many factors such as, the structure of the backbone that dictates their water solubility and flexibility, the structure and concentration of the macromonomer that include the type of the hydrophobic groups and the length of polyethylene oxide spacer².

The effects of polymer-architectural parameters such as the PEO spacer length, and the type and concentration of the hydrophobic groups on the solution behavior have thus been the subject of many recent studies²⁻¹². However, the effects of the composition of the polymer backbone have received little attention^{2, 13}. An understanding of how the polymer backbone composition affects polymer flexibility, hydrophobic associations and the rheological properties is important not only from a fundamental standpoint but also in tailoring polymers with controlled bulk properties. In this study, we examine this issue using polymers that contain different proportions of MAA and EA in its backbone.

4.2 Experimental Materials and Method

4.2.1 Polymers

Two sets of model HASE polymers (DOW Chemical Company, Cary, NC) were used in this study. The macromonomer on the first set of polymers have C₂₀ hydrophobes

with PEO spacers of 32-35 units. The second set of samples has macromonomers with C₁₈ hydrophobes and 40 units of EO spacers. The composition of these polymers is shown in Figure 2. As seen from the figure, the MAA acid content was varied between 18 and 73 mole%. The lower limit of MAA, 18%, is bounded by the solubility of the polymer. On the other hand, the upper limit, 73%, was chosen to maintain the colloidal stability of the polymer in the latex form. The macromonomer level was varied between 0.2 to 1.9 mole% and was chosen based on the colloidal stability and the polymer performance as a thickener.

4.2.2 Solution Preparation

The polymer latexes were dialyzed against de-ionized water using cellulosic tubular membranes for at least three weeks with daily change of water. After dialysis, the polymer was freeze-dried and 5% solutions were prepared and neutralized to pH of 9.0 ± 0.1 with NaOH, with the ionic strength adjusted to 10^{-4} M with KCl. Other concentrations were subsequently prepared by the dilution of the 5% solution with both the pH and the ionic strength kept at the same level.

4.2.3 Rheological measurements

The rheological properties of the polymer solution were measured using stress-controlled rheometers (Rheometrics DSR II or TA Advanced rheometer RA2000) fitted with appropriate cone and plate or couette geometries. The rheological properties of HASE polymers have been shown to be dependent on their previous shear history; therefore, a pre-shear regime was necessary to be considered. Prior to any measurement, the sample was subjected to a shear rate of 1 s^{-1} for 5 min followed by a 10 minute-rest period. This protocol

was found to be sufficient for structure recovery in the sample as noticed from dynamic time sweep experiments. In this study we employed three rheological techniques, steady shear, dynamic oscillatory, and transient creep techniques. Both the dynamic frequency oscillation and the transient creep experiments were carried out using small stresses, so that the sample was within the linear viscoelastic region, where the dynamic properties are independent of the applied stress.

The intrinsic viscosity of the polymer solutions was measured with Ubbelohde dilution viscometers situated in a thermostated water bath. The efflux times of the polymer solutions were converted to reduced and inherent viscosities from the following definitions:

$$\eta_{reduced} = \frac{\eta_{specific}}{c} = \frac{t - t_s}{ct_s}; \quad (1)$$

$$\eta_{inherent} = \frac{\ln(\eta_{relative})}{c} = \frac{\ln(t / t_s)}{c} \quad (2)$$

where t_s is the solvent efflux time. Using the familiar Huggins and Kraemer equations,

$$\eta_{reduced} = [\eta] + K_H [\eta]^2 c \quad (3)$$

$$\eta_{inherent} = [\eta] + K_K [\eta]^2 c \quad (4)$$

the intrinsic viscosity was obtained by plotting the resulting reduced and inherent viscosities against concentration and extrapolating to zero concentration.

4.2.4. Glass Transition Temperature (T_g) Measurements

The second order transition temperature, T_g , was measured using a Perkin-Elmer DSC-7 thermal analyzer equipped with a cooler system. Measurements were carried out on 3-8 mg samples at a heating rate of 10° C/min and an indium standard was used for calibration. Before each scan, samples were annealed at 200° C for 3 minutes to erase thermal history, followed by a flash quenching to -100° C at 500° C/min. T_g was taken as the midpoint of the glass transition.

4.3 Results and Discussion

4.3.1 Effect of MAA content

The steady shear viscosity profiles of polymers with different MAA mole% at a fixed level of macromonomer are shown in Figure 3. We find all samples to exhibit strong shear thinning with a small or nominal zero shear plateau indicating that all samples maintain their associative behavior. One of the functions of the MAA group is to render the polymer soluble (and not be a latex) and we find that even at a low MAA content of 18 mole% the polymer is sufficiently soluble and expanded to allow hydrophobic associations. This implies that even the lower MAA content, 18mole %, was high enough to render the polymer solubility . The figure also reveals a large increase in the steady shear viscosity as the MAA content is increased from 18 to 35 mole%, with a substantial jump observed between 24 and 35 mole%. Further increase of the MAA content to 46% shows a moderate increase in viscosity. With MAA molar% higher than 46%, the viscosity shows a slight decrease. A maximum in Brookfield viscosity has been reported previously for an analogous polymer system at a MAA composition of 40-mole%².

Similar behavior is observed when we examine the dynamic behavior of these samples as probed by an oscillatory shear experiment. In Figure 4a, which shows the elastic modulus (G') as function of frequency, we observe a significant increase in G' as the MAA increases up to 35% followed by a slight increase as the MAA content is increased to 46%. Further increase in the MAA acid content to 54% leads to a slight decrease in G' . In addition, a jump in G' is observed when the MAA concentration is increased from 25 to 35%. All these characteristics are reminiscent of the steady shear behavior. Moreover, there is a

change in the dependence of G' on frequency as the MAA content increase. With low MAA, $G' \sim \omega^{1.3}$ in the terminal region followed by a less dependence at high frequencies as $G' \sim \omega^{0.4}$. In contrast, at high MAA content, there is less dependence on frequency as $G' \sim \omega^{0.6}$ in the terminal region and reaches a plateau at higher frequency. It is very interesting that the slope at the terminal region for the sample with 54% MAA increases to 0.7 which suggests the presence of an optimum MAA concentration that yield the lowest dependence on frequency. Another interesting behavior is the change in the longest relaxation time (taken as the reciprocal of the angular frequency where G' and G'' are equal) with MAA content. Figure 4-b shows the dynamic frequency spectrum for one sample with low MAA (23%) and another sample with high MAA (46%). G' , G'' crossover shifts to higher frequency as the MAA increases. The slower dynamics for the samples with low MAA is unexpected because of their weaker network structures. However, the only possible explanation seems to be that polymers with low and high MAA acid may have different relaxation mechanisms.

We have probed the effect of increasing MMA content further through transient creep experiments. Figure 5 shows the time evolution of the creep compliance ($J(t)$) for samples with different MAA content. We observe $J(t)$ to decrease with increasing MAA content and show a minimum, consistent with the behavior observed in steady and dynamic experiments. The fact that $J(t)$ decreases with MAA concentration, and not increases, is because increased hydrophobic interactions impede creep in opposition to the what they do to viscosity or modulus.

The large increase in the viscosity and moduli as well as the large decrease in the creep compliance as the MAA content increases in the range of 18 to 34 mole% may be

attributed to the increase in the hydrodynamic size of the polymer chain as the MAA content increases. This increase in the hydrodynamic size would be the result of an increase in the hydrophilicity of the polymer backbone. To verify this hypothesis, experiments were conducted to measure the intrinsic viscosity $[\eta]$ of various samples. Figure 6 shows a representative plot of polymers with different MAA proportion for a fixed macromonomer content. This change in the hydrodynamic size is evident from the observed increase in the intrinsic viscosity $[\eta]$. To further examine how changes in hydrodynamic size alone would affect viscosity, we measured the viscosity of a 5% solution of the non-associative ASE polymers which are copolymers of MAA and EA. We find the viscosity of such polymers, shown in Figure 7, to increase with MAA content and plateau out at large MAA concentration, similar to the behavior observed in the associative polymers.

For associative polymers, we envision other factors to play a role, as well, in dictating rheology as the MAA content is increased. At low MAA concentrations, the smaller chain size will limit the hydrophobic interaction to only intramolecular association. As the MAA content is increased, the polymer hydrophilicity increases and the chains become more extended, and the solution viscosity and viscoelastic properties could be further enhanced by the ability of the hydrophobes to form intermolecular association. On the other hand, increasing the MAA content would increase the inherent chain stiffness and hinder accessibility of the hydrophobic groups. The loss of chain flexibility as a result of increasing the MAA is corroborated from the increase in the glass temperature (T_g) values as MAA content increases, as seen in Figure 6. Another factor that would contribute to the rheology would be the EA groups. The contribution from the aggregation of the bulky EA groups

would decrease due to the relative decrease of the EA content. The balance among these three factors (hydrodynamic size, the chain flexibility and the aggregation of EA groups) possibly leads to a maximum in G' and η , and a minimum in $J(t)$ behavior as a function of increased MAA content.

4.3.2 Concentration Effects

To determine if the observed trends in viscosity, modulus and creep compliance with increasing MAA content carries over to other polymer concentrations, we examine in Figure 8 the viscoelastic characteristics of polymers at four different concentrations (1, 2, 3 and 5%). Figure 8a shows the steady shear viscosity at a fixed shear rate of 0.01 s^{-1} as function of MAA mole% for the different polymer concentrations. We find all four polymer concentrations to show the same dependence on MAA content with a broad maximum around 40 mole% MAA. Similar results are obtained when the high frequency elastic modulus (G' at $\omega=100 \text{ rad/s}$) is plotted versus MAA content for the different polymer concentrations, as shown in Figure 8b. On the other hand, a broad minimum is observed when the creep compliance at $t=100$ is plotted versus the MAA content for different concentrations (Figure 8c). It is interesting to point out that all three material functions are consistent in that the maximum or minimum occur approximately at the same MAA content of 40 mole%.

The change in the polymer behavior and $[\eta]$ values at low and high MAA should manifest themselves in different concentration dependence of the rheological material functions. Figure 9 shows the concentration dependence of the low shear viscosity (shear rate = 0.01 s^{-1}), the high-frequency elastic modulus (at 100 rad/s), and the creep

compliance (at $t=100$ s) for two representative polymers of different MAA content. In both cases we find η , G' and $J(t)$ to exhibit power-law behavior, albeit with different exponents. In fact, we observe three distinct power-law regimes for all three material functions regardless of the MAA content. However, the concentration at which these transition occur shifts to lower values as the MAA acid content increases. Interestingly, three concentration regimes have been observed recently for similar HASE polymer¹⁴ and other hydrophobically modified polymers¹⁵. It also has been predicted by the sticky Rouse model¹⁶.

For unmodified polymers, concentration transitions are typically attributed to a change from dilute, to unentangled and entangled semidilute regimes and occur at concentrations relative to the overlap concentration, c^* . For associative polymers, on the contrary, the parameter c^* is not the relevant variable. This can be demonstrated by comparing the concentration at which the transitions occur. For simplicity we denote the lower transition concentration as c_L and the upper transition concentration c_U . Figure 10 shows the transition concentrations c_L and c_U for samples with different MAA content. To compare the transition concentration with the overlap concentration (c^*), the figure includes data for 10 times c^* . As shown in this figure, the transition concentration shifts to lower values as the MAA content increases. Moreover, the lower transition concentration changes from about 20 times c^* at low MAA to less than 10 times c^* at high MAA. This confirms the irrelevance of c^* as the parameter for any concentration transitions.

We believe that the three concentration regimes in Figure 9 can be explained in terms of different modes of hydrophobic associations. Figure 11 shows schematically the expected hydrophobic associations possible in these different regions. In Regime 1 in which $c < c_L$, the

polymer chains are isolated and as a result only intramolecular associations are possible. The solution viscosity in this region is similar to that of unmodified polymer analogs. In this regime, the scaling exponent for each material function varied with MAA. At low MAA content (18 mole%), scaling exponents of 1.2, 2.0, and -1.3 are observed for η , G and $J(t)$, respectively. These exponents decrease with MAA content and reach values of 0.60 and -0.65 corresponding to viscosity and creep compliance, respectively. The change in the scaling exponent can be attributed to the change in the polymer solvent interactions. There is an increase in the polymer hydrophilicity as the MAA content increases which leads to a relative change in solvent quality towards being a good solvent. The scaling exponent for η is in full agreement with an exponent of 1.3 for unentangled un-associative polymers in good solvents.

In Regime 2 in which $c_L < c < c_U$, the polymer chains become overlapped and the hydrophobes are engaged in intra and inter-molecular association. Therefore, this region is characterized by a very rapid increase in viscosity due to the transformation from intra- to inter-molecular association and a strong dependence on concentration is expected. In fact, η , G' and $J(t)$ exhibit very large dependence on concentration for all samples. The scaling exponents, however, changes as the MAA content changes. For samples with low MAA content (18 mole%), exponent factors as high as 9.0 for η , 4.6 for G' and -8.9 for $J(t)$ are obtained, as compared to 4.3 for η and -4.3 for $J(t)$ for sample with 54% MAA. Regaldo *et al.* also obtained varied scaling exponents in this region for a solution of hydrophobically modified polyacrylamide polymers¹⁵. Scaling exponents varied below and above 4.3 based on the number of stickers (hydrophobes) per chain. Our result of a viscosity exponent (4.3) at

high MAA is in excellent agreement with the theoretical value of 4.2 based on the sticky Rouse model for an associative polymer in a good solvent¹⁶. On the other hand, the higher value (9.0) at low MAA content is in good agreement with the theoretical values (8.5) based on the sticky reptation Model¹⁶ and with the reported exponent (7.9) for similar HASE polymer¹⁷. The change in the polymer behavior from sticky Rouse to sticky reptation implies that in this regime the polymer chains are unentangled at high MAA content and become entangled at low MAA. This can be supported by the fact that the transition starts at concentrations more than 20 times c^* for low MAA samples compared to less than 10 times for samples with high MAA.

In Regime 3 for $c > c_U$, the hydrophobes are engaged in mostly intermolecular interactions. Thus, a weaker dependence on concentration is expected. We obtained scaling exponents of 2.6, 1.8 and -2.4 for η , G' and $J(t)$, respectively. The viscosity scaling exponent is in full agreement with the reported value of 2.7 for similar HASE polymers¹⁷. However, it is lower than the 3.75 predicted by the sticky reptation model¹⁶ and observed experimentally for hydrophobically modified polyacrylamide¹⁵.

4.3.4 Effect of macromonomer concentration

To examine the effect of macromonomer concentration on rheology, we used a set of 9 polymers each having macromonomers with C_{20} hydrophobe and a degree of ethoxylation of 33 EO units. Every 3 polymers in this set have the same macromonomer concentration and varied MAA and EA content, as shown in Figure 2. Figure 12 compares the viscosity versus shear rate profiles for 3% polymer solutions using samples with different MAA content. Regardless of the concentration of the macromonomers, there is an optimum MAA

concentration that leads to a maximum in steady shear viscosity, similar to what has we have discussed for Figures 3 and 8. This optimum concentration lies between 43 to 60 mole% MAA. However, the viscosity increase for these samples is much weaker than the samples of the other polymer set (with C₁₈ hydrophobes and 40 EO units) in Figure 2 that had been used in the previous sections. This difference could be attributed to different molecular weight and/or molecular weight distribution. Currently, there is no confirmed data about the Mw and Mw distribution of the samples used in this study. It also worth mentioning that the two set of samples, although both prepared by Dow Chemical Company, were prepared at 2 different locations.

The effect of the concentration of the macromonomers on the steady shear data can also be observed from Figure 12. At a low macromonomer concentration (0.3%), we observe the viscosity to be low and almost Newtonian indicating the presence of weak hydrophobic associations (Fig. 12a). It is clear that the highest viscosity in this set of samples is obtained with 1.0 mole% macromonomers, Figure 12b. The steady shear viscosity of a 3% solution of samples with 1.0% macromonomers and low or moderate content of MAA is about 2 orders of magnitude higher than that of any of the other samples. This indicates that there is also an optimum macromonomer concentration that yields the highest enhancement in viscosity. Such a result can be explained in the light of the similarity between our polymer system and surfactants. The optimum concentration of the macromonomer is analogous to the concentration of surfactant between the lower and higher critical micelle concentration. The higher steady shear viscosity of the samples with 1% macromonomer concentration compared to those with 0.3% macromonomer can be attributed to the increase in the number

of intermolecular junctions as the number of hydrophobes per chain increases. On the other hand, if there are too many hydrophobes per chain such that the distance between every 2 hydrophobes is less than polyethylene oxide spacer, larger numbers of the hydrophobes will engage in intramolecular association rather than form active junction through intermolecular association. This would lead to a decrease in viscosity as is observed in Figure 12c for the sample with 1.9% macromonomer.

The steady shear viscosity and the viscoelastic properties of this polymer system are largely dependent on the number of active intermolecular association. The transient network theory¹⁷ predicts that the plateau modulus is proportional to number of active junctions and the steady shear viscosity is the product of the plateau modulus and the microscopic relaxation time corresponding to the reciprocal of bond breaking and reformation rate. Thus increasing the number of active junctions will increase the steady shear viscosity through both increasing the plateau modulus and slowing the relaxation process.

4.4 Summary

This study provides a comprehensive analysis of the effects of polymer composition on the rheology of associative polymers. The effect of the polymer backbone composition is elucidated by varying the relative proportion of methyl acrylic acid (MAA) and ethyl acrylic (EA) while that of the macromonomer is examined by varying its concentration. An increase in the proportion of MAA in the backbone reveals a higher viscosity and enhancement in viscoelastic characteristics (G' , J) consistent with a concomitant increase in chain size. At higher MAA concentration, a maxima in viscosity and viscoelastic properties are observed. Such a behavior can be attributed to the combined effects of increased chain dimension, loss

of chain flexibility and reduced contribution from the aggregation of EA bulky groups that occurs with increased MAA content. The scaling of viscosity, elastic modulus and creep compliance with polymer concentration revealed the presence of three transitional regimes, each with a power-law dependence. These regimes were attributed to changes in the hydrophobic interactions with concentration.

The macromonomer concentration also has a strong influence on polymer behavior with a maximum in viscosity observed at intermediate macromonomer concentrations. At low macromonomer concentration, low viscosity resulting from weak associative behavior was observed. On the other hand, high concentration favors the formation of intra over inter molecular association leading to a reduction in solution viscosity from that observed at intermediate macromonomer concentrations.

4.5 References

1. Shay, G. D., "Alkali-Swellable and Alkali-Soluble Thickeners: A Review," *In Water Soluble Polymers*, Edited by J. E. Glass (ACS Advances in Chemistry Series No 223 American Chemical Society, Washington, DC, 457-494 (1989)).
2. Jenkins, R. D., L. M. DeLong, and D. R. Bassett, "Influence of Alkali-Soluble Associative Emulsion Polymer Architecture on Rheology," in *Hydrophilic Polymers: Performance with Environmental Acceptance*, edited by J. E. Glass (ACS Advances in Chemistry Series No 248 American Chemical Society, Washington, DC, 425-447 (1996)).
3. Lau, A. K., C. Tiu, C. and K. C. Tam, "Rheology of Hydrophobically-Alkali-Soluble-Emulsions (HASE)," In *6th World Congress of Chemical Engineering*: Melbourne, Australia (2001).
4. Seng, W. P., K. C. Tam, R. D. Jenkins and D. R. Bassett, "Calorimetric Studies of a Model Hydrophobically Alkali-Soluble Emulsion Polymers with Varying Spacer Chain Length," *Macromolecules*, 33, 1727-1733 (2000).
5. Tan, H. T., K. C. Tam, and R. D. Jenkins, "Network Structures of a Model HASE Polymer in Semidilute Salt Solutions," *Journal of applied polymer science*, 79, 1486-1496 (2001).
6. Tan, H., K. C. Tam, V. Tirtaatmadja, R. D. Jenkins, R. D. and D. R. Bassett, "Extensional Properties of Model Hydrophobically Modified Alkali-Soluble Associative (HASE) Polymer Solutions," *J. Non-Newtonian Fluid Mech.*, 92, 167-185 (2000).
7. English, R. J., S. R. Raghavan, R. D. Jenkins and S. A. Khan, "Associative Polymers Bearing n-Alkyl Hydrophobes: Rheological Evidence for Microgel-Like Behavior?," *J. Rheol.*, 43, 1175-1194 (1999).
8. English, R. J., H. S. Gulati, R. D. Jenkins and Khan, S. A., "Solution Rheology of a Hydrophobically Modified Alkali-Soluble Associative Polymer," *J. Rheol.*, 41, 427-444 (1997).
9. Olesen, K. R., D. R. Bassett, D. R. and C. L. Wilkerson, "Surfactant co-Thickening in Model Associative Polymers," In *Proc. - Int. Conf. Org. Coat.: Waterborne, High Solids, Powder Coat.*, 24th307-322 (1998).
10. Tirtaatmadja, V., K. C. Tam, and R. D. Jenkins, "Rheological Properties of Model Alkali-Soluble Associative (HASE) Polymers: Effect of Varying Hydrophobe Chain Length," In *Macromolecules* 30, 3271-3282 (1997).

11. Tam, K. C., M. L. Farmer, R. D. Jenkins and D. R. Bassett, "Rheological Properties of Hydrophobically Modified Alkali-Soluble Polymers-Effects of Ethylene-Oxide Chain Length," *J. Polym. Sci., Part B: Polym. Phys.*, *36*, 2275-2290 (1998).
12. Tam, K. C., W. K. Ng, R. D. Jenkins and D. R. Bassett, "Viscoelastic Behavior of Model HASE Associative Polymer Solutions," In *Proc. Int. Congr. Rheol., 13th*, 329-331 (2000).
13. Gupta, R. K., K. C. Tam and R. D. Jenkins, "Rheological Properties of Model Alkali-Soluble Associative (HASE) Polymers: Effect of Varying Acid Monomer and Macromonomer Composition," In *Proc. Int. Congr. Rheol., 13th*, 340-342 (2000).
14. Knaebel, A., R., Skouri, J. P. Munch and S. J. Candau, "Structural and Rheological Properties of Hydrophobically Modified Alkali-Soluble Emulsion Solutions," *Journal of Applied Polymer Science: Part B: Polymer Physics*, *40*, 1985-1994 (2002).
15. Regalado, E. J., J. Selb and F. Candau, "Viscoelastic Behavior of Semidilute Solutions of Multisticker Polymer Chains," *Macromolecules*, *32*, 8580-8588 (1999).
16. Rubinstein, M., A. N. Semenov, "Dynamic of Entangled Solution of Associating Polymers," *Macromolecules*, *34*, 1058-1068 (2001).
17. English, R. J., J. H. Laurer , R. J. Spontak and S. A., "Hydrophobically Modified Associative Polymer Solutions: Rheology and Microstructure in the Presence of Nonionic Surfactant," *Ind. Eng. Chem. Res, ASAP article* (2002).
18. Tanaka, F. and S. F. Edwards, "Viscoelastic Properties of Physically Crosslinked Networks. 1. Transient Network Theory," *Macromolecules*, *25*, 1516-1523 (1992).

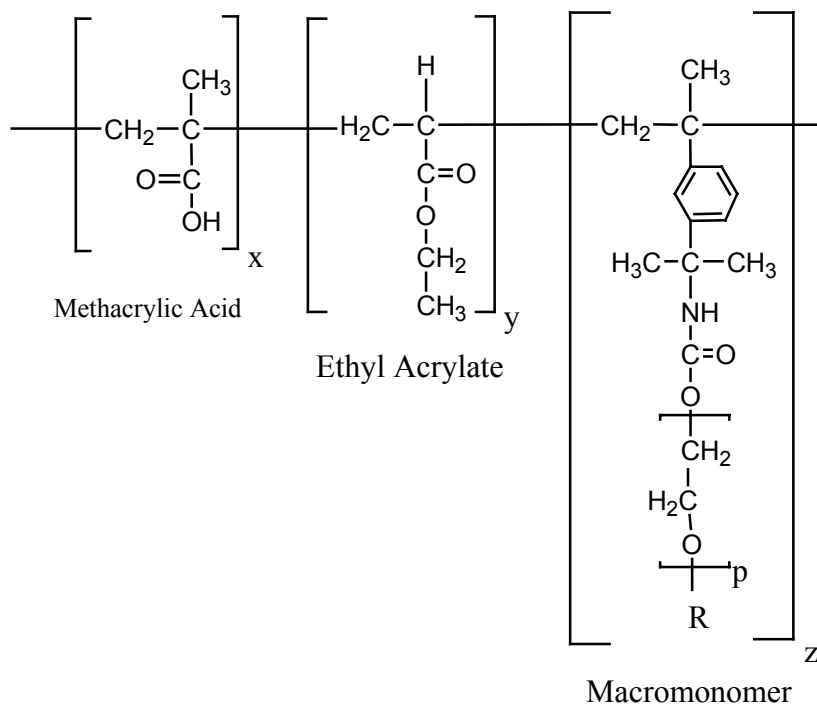
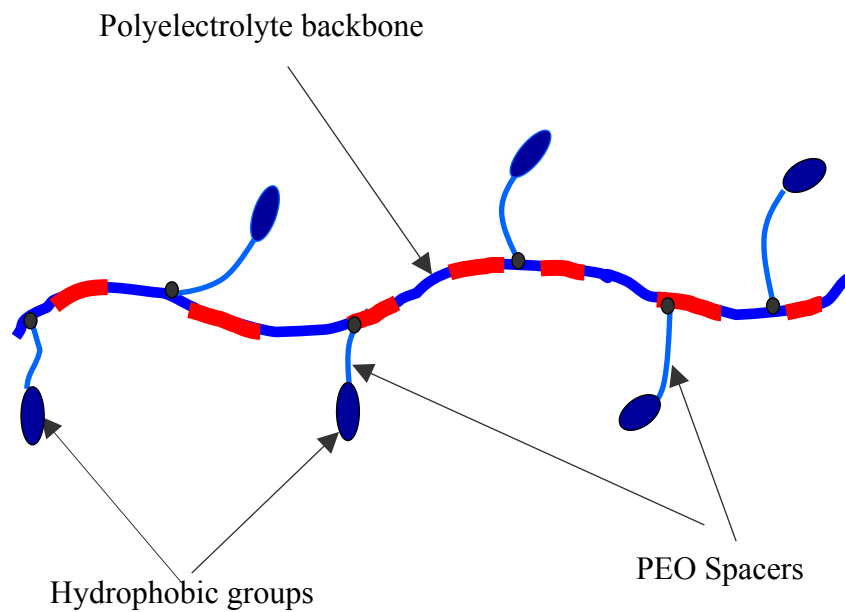


Figure 1. Schematic representation of a typical HASE polymer together with its molecular constitution of the HASE polymers used in this study. R refers to the hydrophobic groups. x, y, z, p are structural parameters.

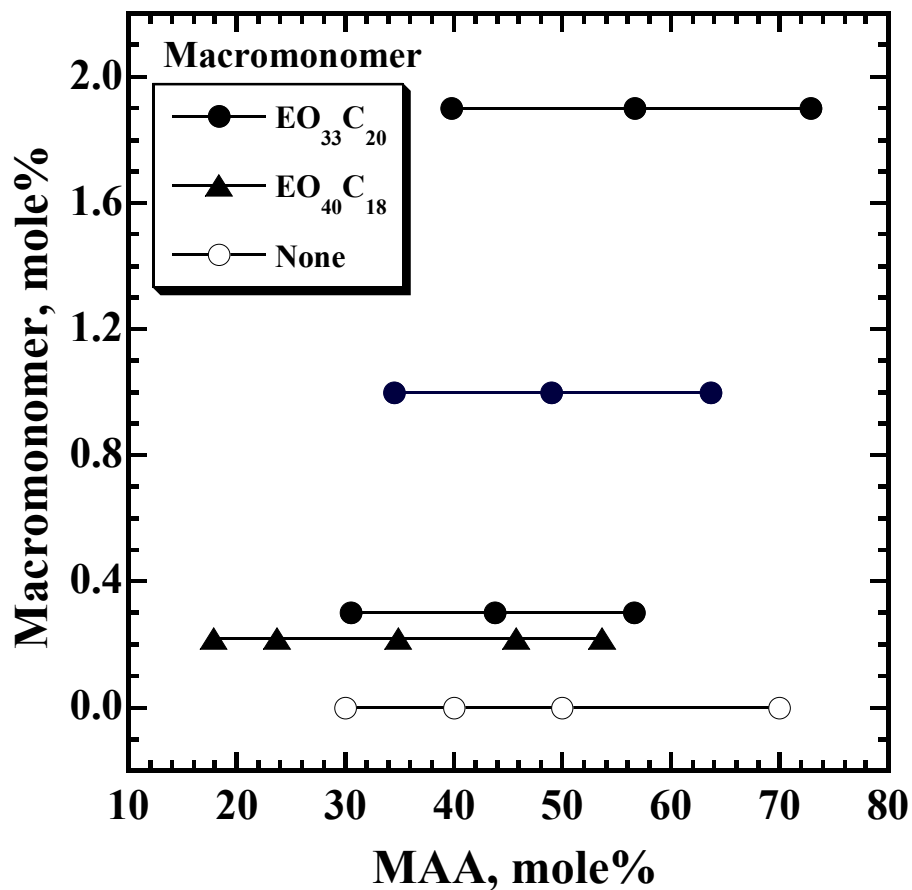


Figure 2. Composition of the polymers used in this study. A total of 18 samples have been used, including 4 non-associative ASE samples that have no macromonomers.

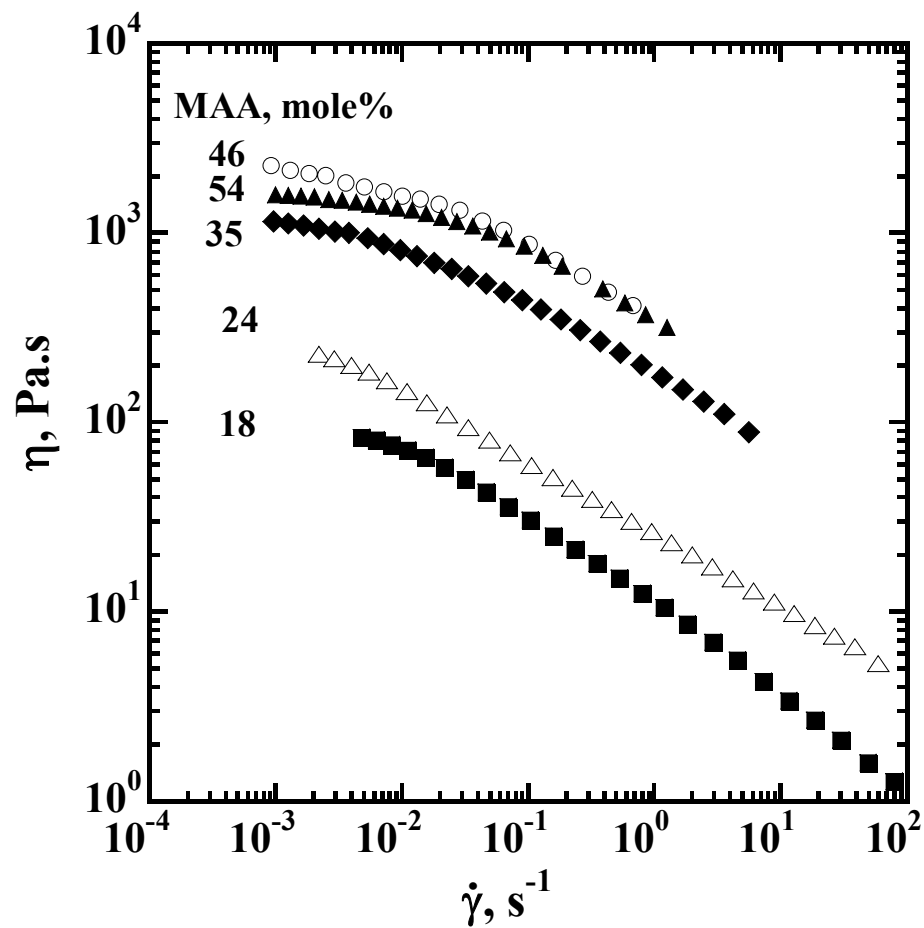


Figure 3. Steady shear data for 3% solution of HASE polymers with different MAA concentration. Polymers have 0.22 mole% macromonomers with C18 hydrophobes and 40 EO units: Viscosity is shown as function of shear rate.

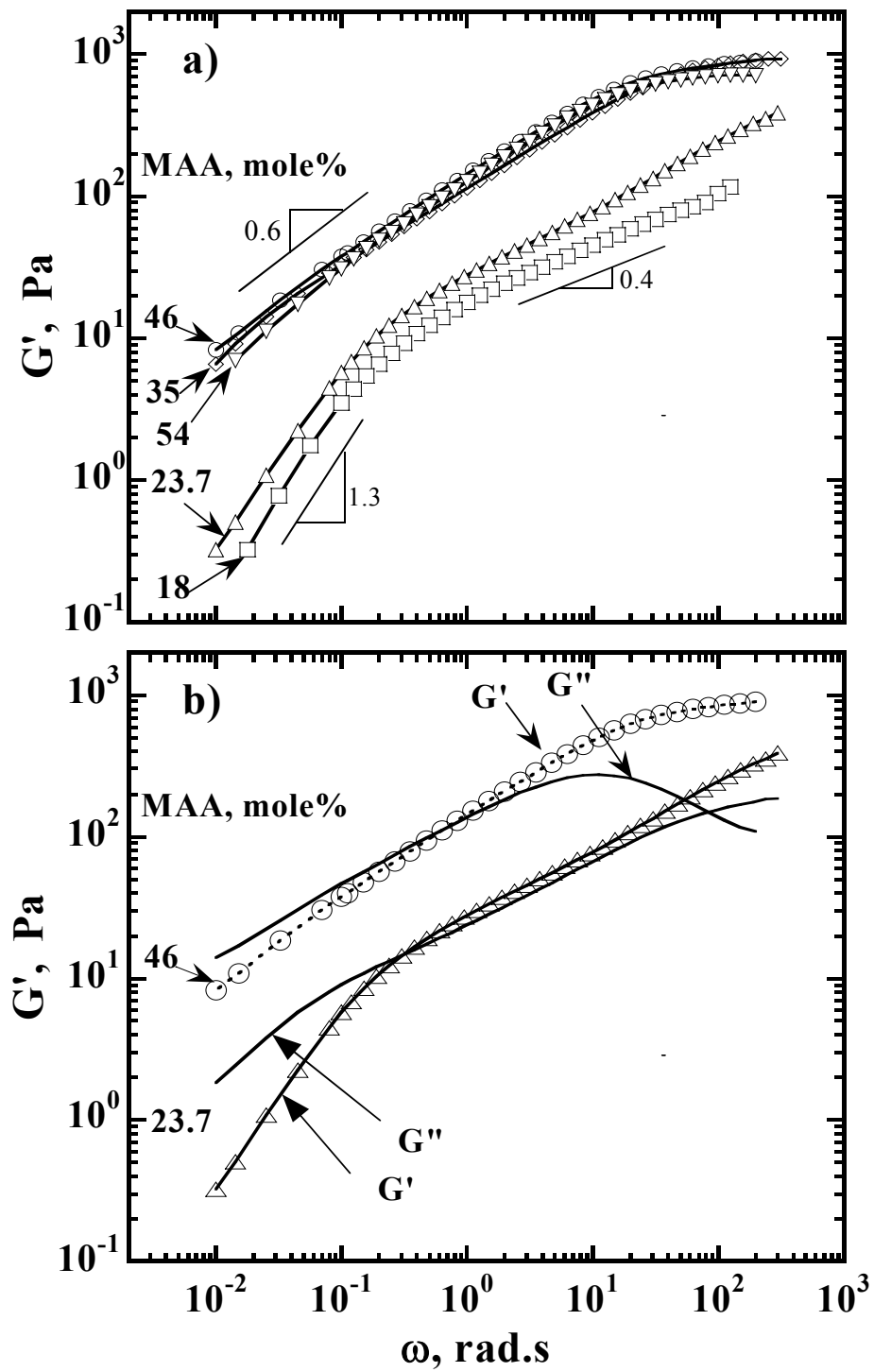


Figure 4. Dynamic frequency spectrum of a) the elastic modulus (G') and b) dynamic frequency spectrum for 3% solution of HASE polymers with different MAA content and 0.22 mole% macromonomer.

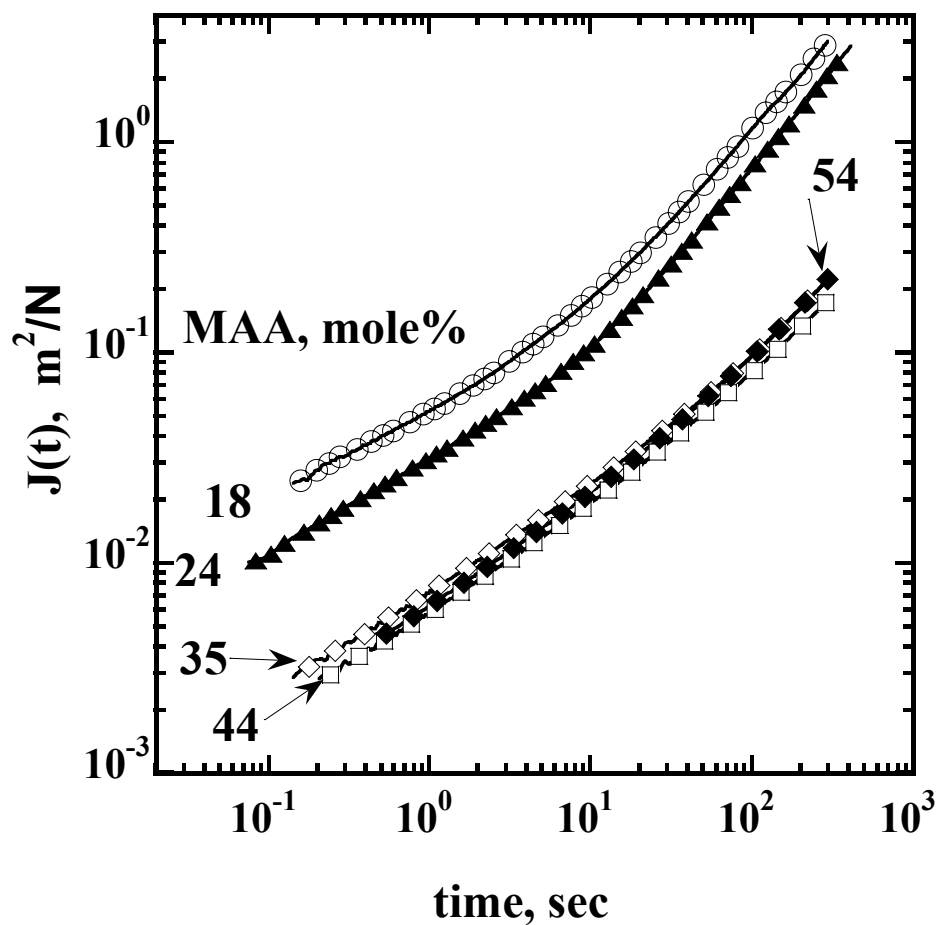


Figure 5. Creep compliance, $J(t)$, as function of time for 3% solution of HASE polymers with different MAA and 0.22 mole% macromonomer: compliance as function of time is shown

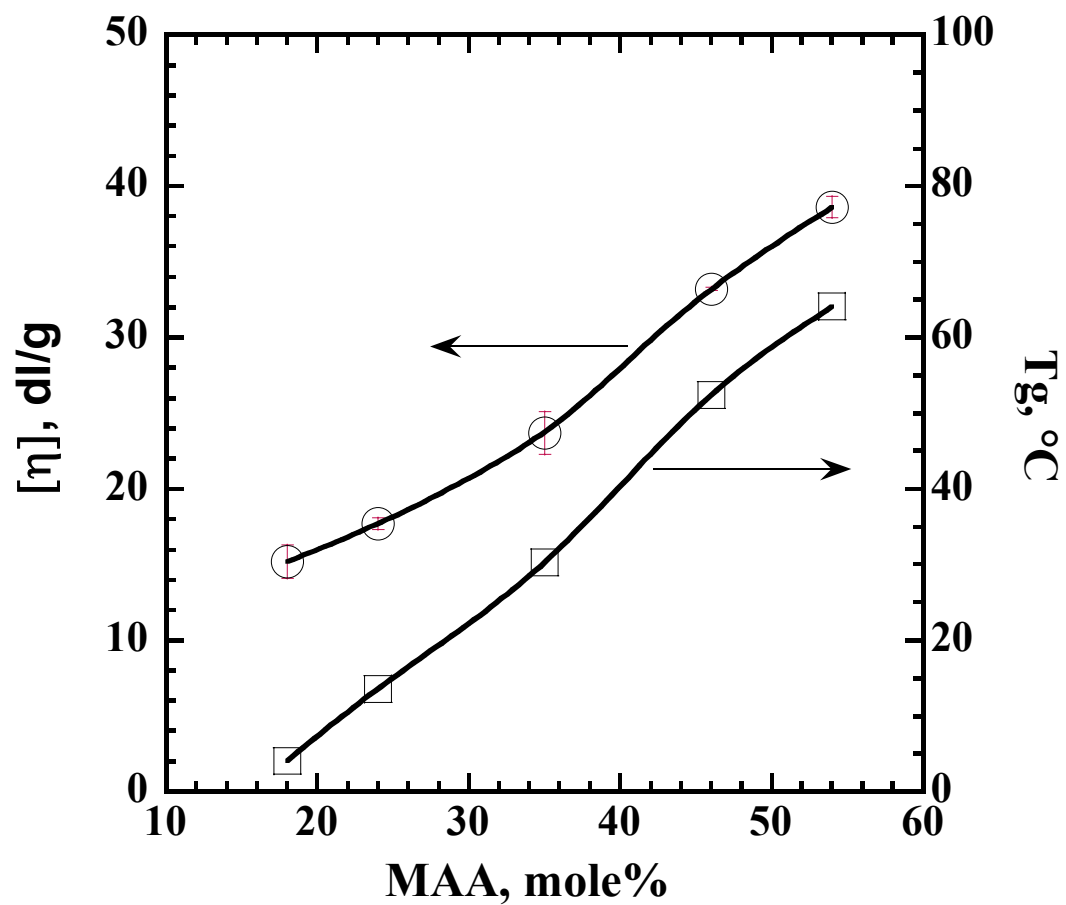


Figure 6. Intrinsic viscosity ($[\eta]$) and glass transition temperature (T_g) for polymers with different MAA content. All polymers have 0.22 mole% macromonomer with C_{18} hydrophobes and 40 EO units

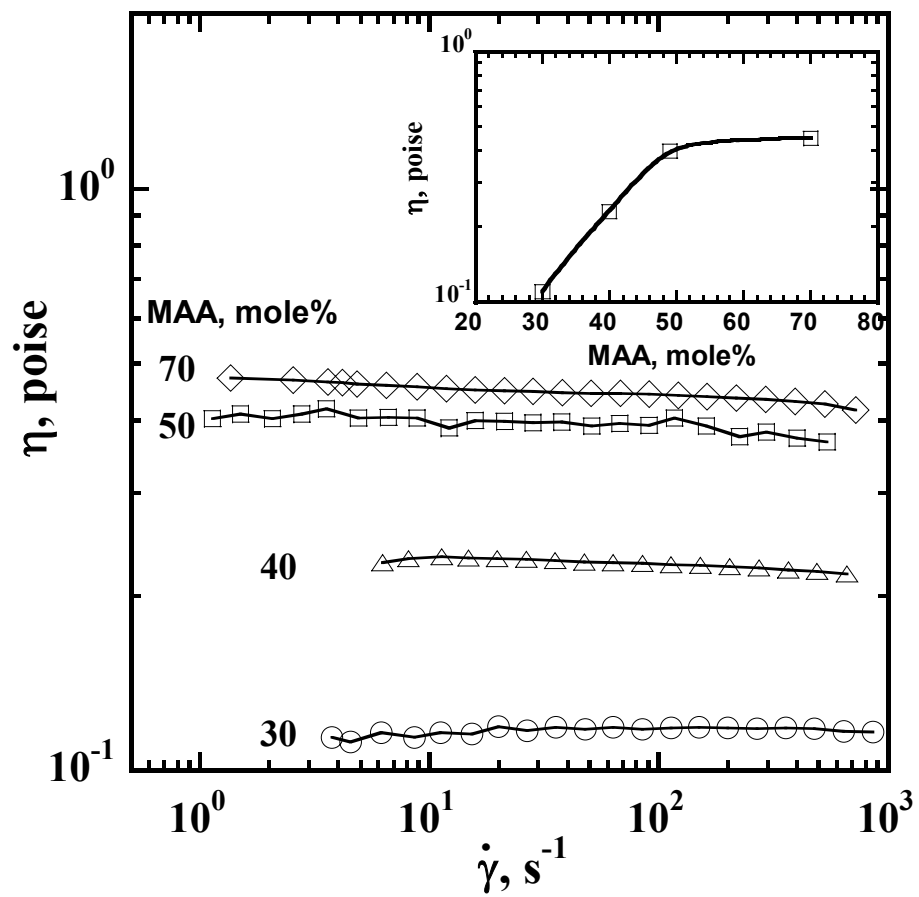


Figure 7. Steady shear viscosity versus shear rate for the non-associative ASE polymers with different MAA acid. Inset shows the zero shear viscosity as function of MAA mole%.

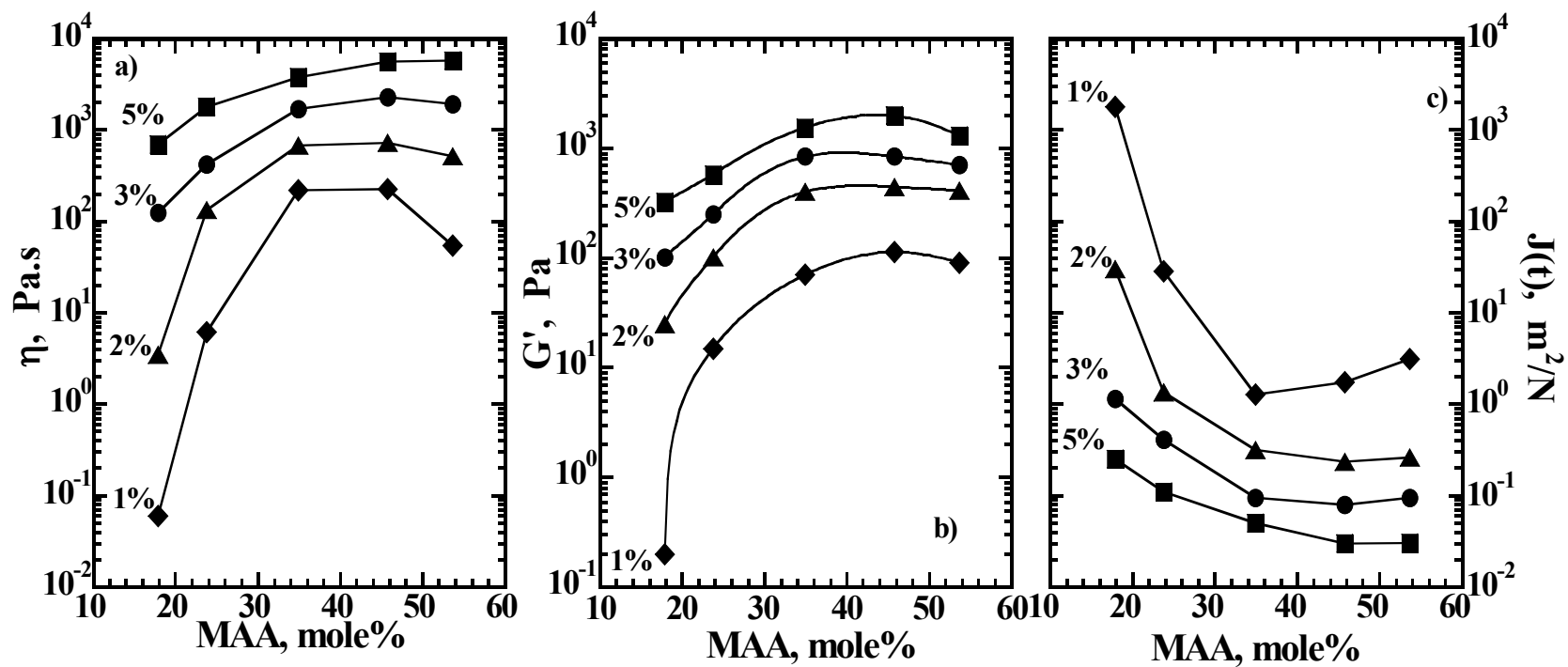


Figure 8. Effect of MAA content and polymer concentration on a) the steady shear viscosity at shear rate = 0.01 s^{-1} b) the elastic modulus at angular frequency = 100 rad/s , and c) the creep compliance at $t=100 \text{ s}$. Macromonomer concentration = 0.22 mole\% , C_{18} hydrophobes and 40 units EO.

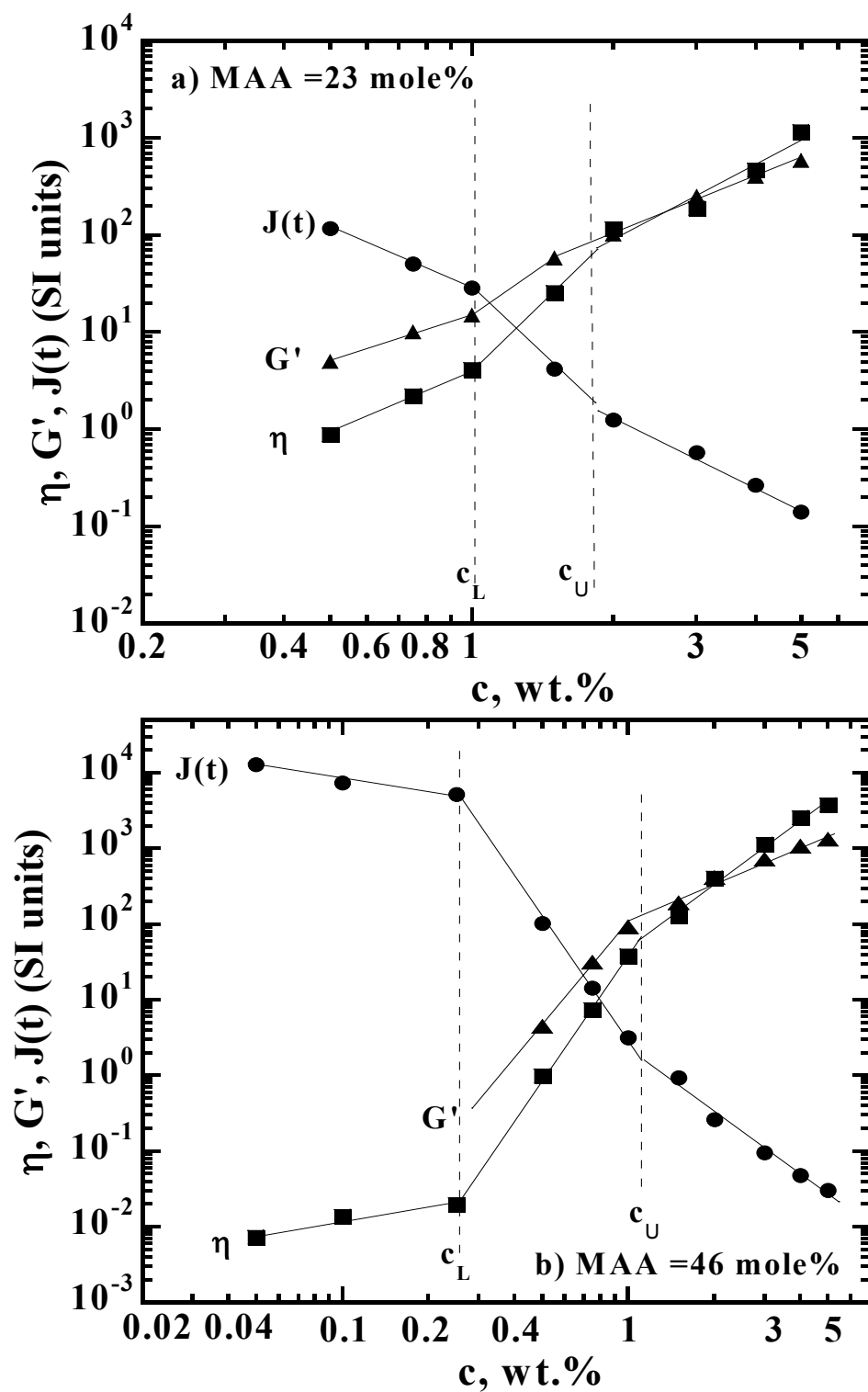


Figure 9. Concentration dependence of steady shear viscosity (η) at 0.01 s^{-1} , elastic modulus (G') at 100 rad/s and the creep compliance $J(t)$ at $t=100 \text{ s}$ for polymer with .a) 43 mole% and b) 23 mole% MAA.

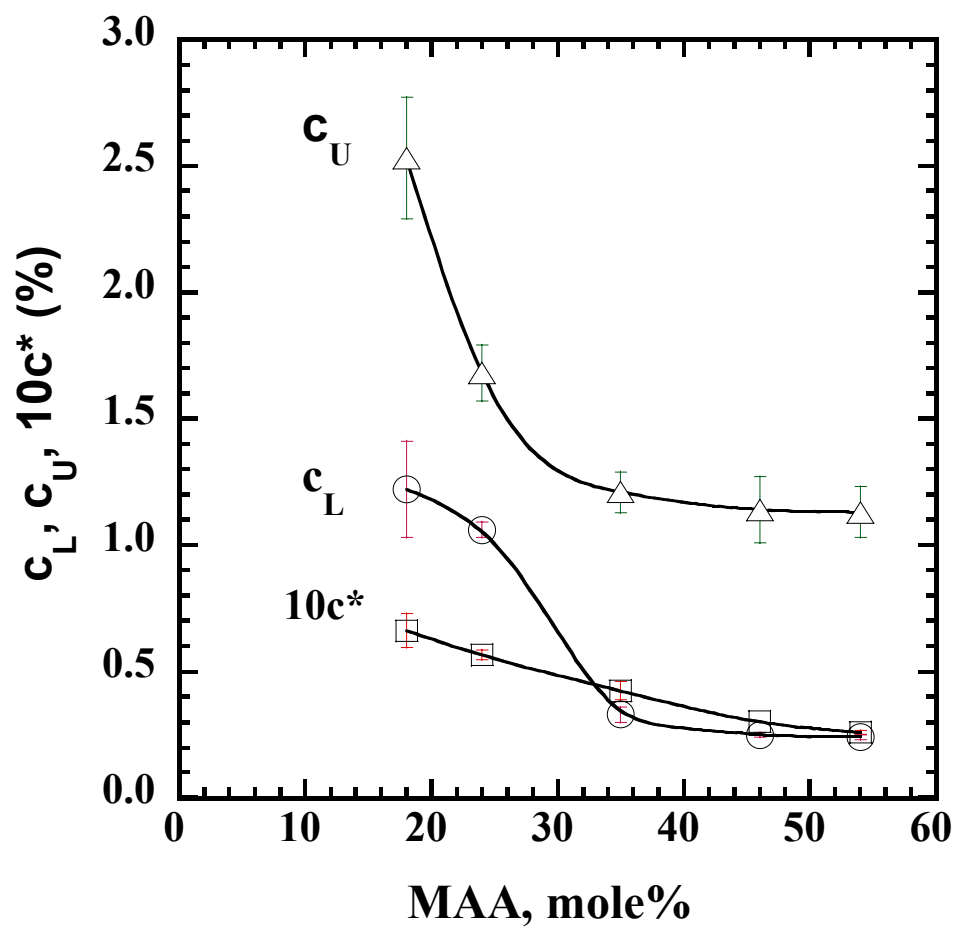


Figure 10. Effect of MAA content on the transition concentrations (c_L and c_U) and the overlap concentration (c^*).

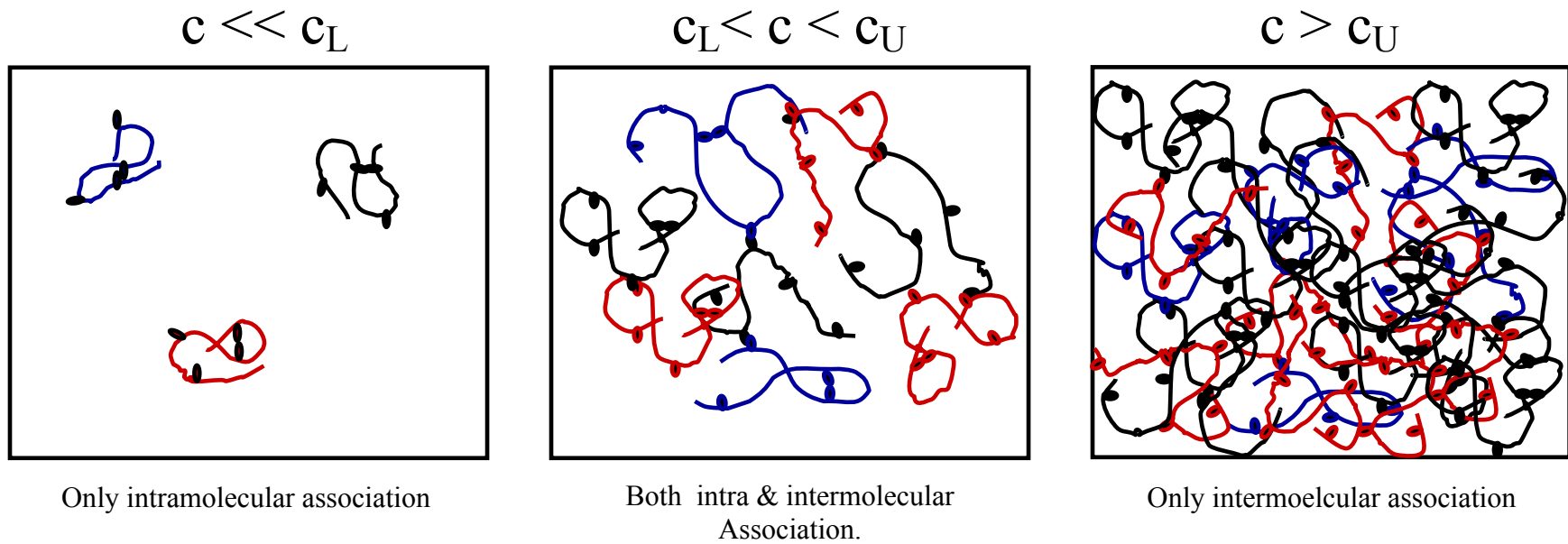


Figure 11. Possible hydrophobic interaction modes at different concentration regimes.

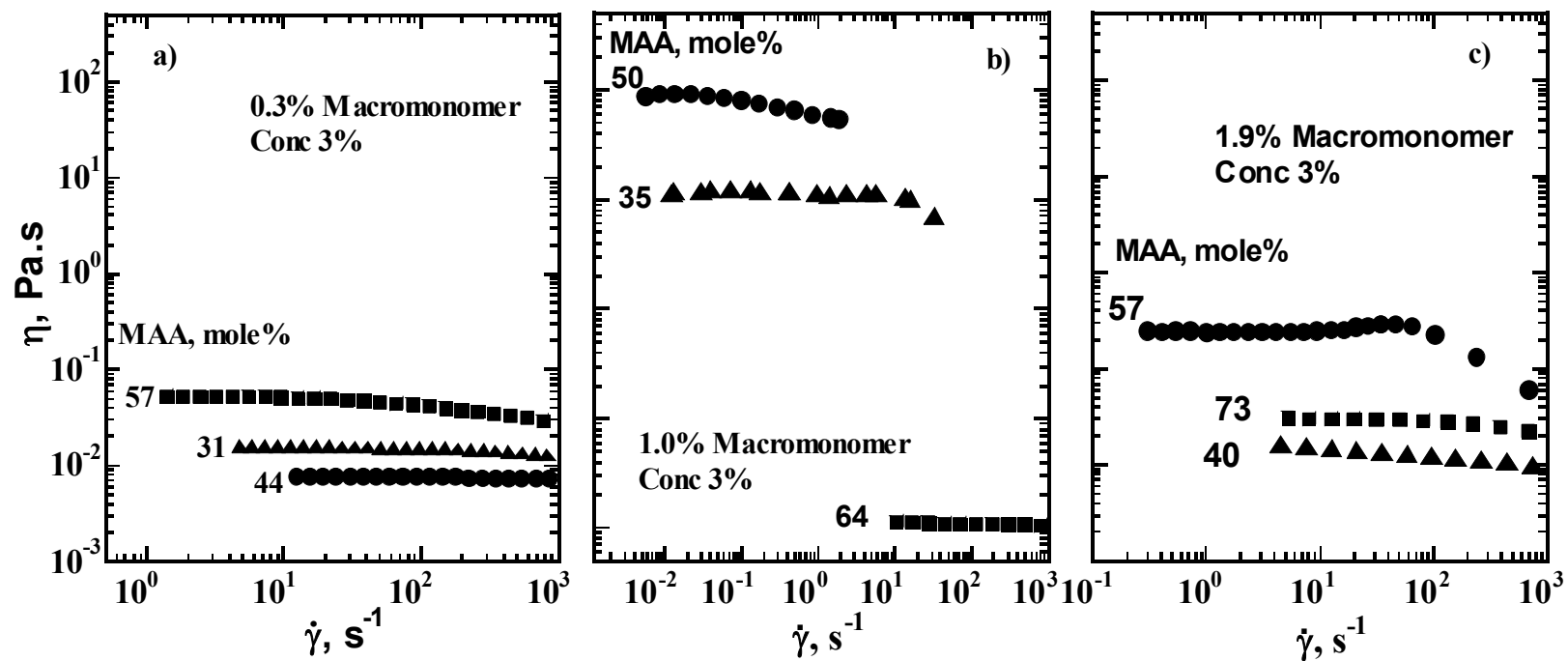


Figure 12: Effect of MAA content on the steady shear viscosity of 3% solution of polymers with a) 0.3 mole%, b) 1.0 mole% and c) 1.9 mole% macromonomer.

CHAPTER 5

SOLUTION RHEOLOGY OF HYDROPHOBICALLY MODIFIED ASSOCIATIVE POLYMERS: SOLVENT QUALITY AND HYDROPHOBIC INTERACTIONS

Chapter 5 is essentially a manuscript by Ahmed A. Abdala, Keith Olesen and Saad Khan submitted to the Journal of Rheology.

Solution Rheology of Hydrophobically modified Associative Polymers: Solvent Quality and Hydrophobic Interactions

Ahmed A. Abdala¹, Keith Olesen² and Saad A. Khan^{1*}

¹Department of Chemical Engineering, North Carolina State University, Raleigh NC 27695-7905

²The Dow Chemical Company, UCAR Emulsion Systems, 410 Gregson Drive, Cary, NC 27511

Abstract

The rheological behavior of a model hydrophobically modified alkali soluble emulsion (HASE) polymer, comprising a random copolymer backbone of methacrylic acid (MAA) and ethylacrylate (EA) with grafted pendant hydrophobic macromonomers is examined in co-solvents of water and propylene glycol (PG) of different proportions. We find the solvent solubility parameter to have a direct impact on both the steady and dynamic behavior of the polymer solutions. In particular, scaling of the relative viscosity (η_{rel}) and the elastic modulus at a fixed frequency (G') with the solvent solubility parameter (δ_s) reveal the presence of two distinct regimes with different dependences on δ_s . In “water-rich” solvents, both η_{rel} and G' show a strong dependence on δ_s in contrast to “PG-rich” solvents, in which there is slight or no dependence on δ_s . The concentration dependences of both η_{rel} and G' are also found to be different in “water-rich” solvents from that in “PG-rich” solvents. In “water-rich” solvents, η_{rel} and G' reveal power-law dependences with exponents of 2.5 and 3.2 respectively compared to exponents of 1.4 and 2.3 in “PG-rich” solvents. The different behavior in “PG-rich” solvents is ascribed to the presence of minimal hydrophobic associations, with the polymer behavior analogous to that of unmodified polymers without

* corresponding author; phone: 919-515-4519; fax: 919-515-3465; email: khan@eos.ncsu.edu

hydrophobes. This hypothesis is supported by the similarity in η_{rel} scaling with concentration observed for both the HASE polymer in “PG-rich” solvents and a similar polymer without the hydrophobes in both solvents. The lack of hydrophobic interactions in the “PG-rich” solvents may be attributed to the observed decrease in polymer coil dimension together with a lower tendency of the hydrophobes to form micelles in less polar media.

5.1 Introduction

Associative polymers are macromolecules with attractive groups either attached to the ends or randomly distributed along the backbone [Rubinstein and Dobrynin (1997)]. Hydrophobically modified alkali soluble emulsion (HASE) polymers are one class of the water-soluble associative polymers. These polymers have a comb-like structure with pendant hydrophobic groups randomly grafted to the polyelectrolyte backbone. HASE polymers have several advantages over other associative polymers in terms of cost and wide formulation latitude [Tirtaatmadja *et al.* (1999)]. They are currently being used in a range of applications, including paint formulations, paper coatings, and recently as glycol based aircraft anti-icing fluids [Carder *et al.* (1998; 1999); Jenkins *et al.* (1993; 1997)] and have potential for use in enhanced oil recovery and personal care products.

Similar to surfactants in aqueous media, these polymers are capable of non-specific hydrophobic interactions [Ng *et al.* (1999)]. These hydrophobic interactions include both inter- and intra-molecular associations, giving rise to network structures, and a range of rheological behavior [English *et al.* (1997; 1999); Tirtaamadja *et al.* (1997)] and morphologies [English *et al.* (2002)]. With such a complex architecture, the association behavior of these polymers would be expected to be quite diverse and dependent on many factors such as, the structure of the backbone that dictates their water solubility and flexibility, the structure and concentration of the macromonomer which include the type of hydrophobic groups and the length of polyethylene oxide spacers [Jenkins *et al.* (1996)]. The effects of these polymer-architectural parameters, including the backbone composition, the PEO spacer length and the type and concentration of the hydrophobic groups, on the solution

behavior has thus been the subject of many recent studies [Lau *et al.* (2001); Dai *et al.* (2000); Gupta *et al.* (2000a, b); Seng *et al.* (2000); Tan *et al.* (2000); English *et al.* (1999); Olesen *et al.* (1998); Tam *et al.* (1998); English *et al.* (1997); Tirtaatmadja *et al.* (1997); Jenkins *et al.* (1996)].

The continuous phase in which the HASE polymer is solvated also plays a major role in the association behavior of these polymers. In this regard, the effects of the medium pH and ionic strength on the association mechanism of HASE polymers have been the focus of a number of studies [Dai *et al.* (2001); Tan *et al.* (2001); Kaczmariski *et al.* (1999); Tirtaatmadja *et al.* (1999); Horiuchi *et al.* (1998); Shay *et al.* (1998)]. Nevertheless, almost all these studies were carried out in aqueous media and the effect of the solvent quality or non-aqueous co-solvents on the solution behavior has been rarely studied [Olesen *et al.* (1998); Schaller (1985); Thibeault *et al.* (1986)]. This becomes particularly important in deciphering the modes of hydrophobic associations and developing new applications involving non-aqueous media, such as anti-icing fluids.

In this study, we investigate the steady and dynamic rheological behavior of a model HASE polymer in a co-solvent of water and propylene glycol. We quantify solvent quality in terms of the solubility parameter and examine the dependence of the relative viscosity and the plateau modulus on both the solvent solubility parameter and the polymer concentration. The role of the hydrophobic interactions are further ferreted by comparing the results of the HASE polymer with (i) an analogous polymer but without the hydrophobe and with (ii) the HASE polymer in which the hydrophobes are encapsulated using an inclusion compound forming host, β -cyclodextrin [Szejti (1998)]. The results of this study should help better

understand the mechanism of rheology modification by this class of associative polymers and their behavior in the presence of co-solvents.

5.2 Experimental Materials and Method

The model associative polymer used in this study is a hydrophobically modified alkali-soluble (HASE) polymer synthesized by UCAR Emulsion Systems (Dow Chemical, NC) via emulsion polymerization of methacrylic acid (MAA), ethylacrylate (EA) and a hydrophobic macromonomer (Figure 1). This macromonomer is end capped with a C₂₂H₄₅ alkyl hydrophobe that is separated from the backbone by 40 units of polyethylene oxide (PEO). Details of the preparation method can be found in a previous publication [Shay *et al.* (1985)]. In addition to the hydrophobically modified polymer, an unmodified polymer that has the same structure as the modified polymer with the C₂₂H₄₅ hydrophobes replaced by equivalent amount of methyl groups was also used. Both the modified and the unmodified polymers were prepared in an identical manner and are believed to have the same molecular weight. The polymer latexes were dialyzed against de-ionized water using cellulosic tubular membrane for at least three weeks with daily change of water. After dialysis, the polymer was freeze-dried and 5% solutions were prepared and neutralized to pH of 9.0 ±0.1 using 28% NH₄OH with the ionic strength adjusted to 10⁻⁴ M KCl. Other concentrations were subsequently prepared by the dilution of the 5% solution with the appropriate solvent composition, while maintaining the pH and ionic strength constant.

In this study, eight different mixtures of water and propylene glycol (PG) were used as co-solvents. The composition of these mixtures expressed as weight% of PG in the solvent

mixture is shown in Table 1. Throughout this manuscript, these solvent mixtures will be called PGXX, with XX corresponding to the wt.% of PG in the mixture. The solubility parameter of these mixtures was calculated using the Hansen three-dimensional solubility parameter approach [Hansen (1999); Hansen and Beerbower (1971); Hansen (1967)]. In this method, the solubility parameter (δ) is given by the sum of the dispersion (δ_d), polar (δ_p) and hydrogen bonding (δ_h) contribution as follows:

$$\delta^2 = \delta_d^2 + \delta_p^2 + \delta_h^2 \quad (1)$$

Here δ_d , δ_p and δ_h for each mixture were calculated as volume average, $\delta_x = \sum (\delta_x)_i \phi_i$; with x standing for d, p or h, i referring to PG or water and ϕ_i to the volume fraction of component i in the solvent mixture. The solubility parameter as well as the dispersion, polar and hydrogen bonding contribution for each solvent mixture are also shown in Table 1.

The intrinsic viscosities of the polymer solutions were measured with Ubbelohde dilution viscometers situated in a thermostated water bath at 25°C. The efflux times of the polymer solutions were converted to reduced and inherent viscosities from the following definitions:

$$\eta_{reduced} = \frac{\eta_{specific}}{c} = \frac{t - t_s}{ct_s}; \quad (2)$$

$$\eta_{inherent} = \frac{\ln(\eta_{relative})}{c} = \frac{\ln(t/t_s)}{c} \quad (3)$$

where t_s is the solvent efflux time. Using the familiar Huggins and Kraemer equations,

$$\eta_{reduced} = [\eta] + K_H [\eta]^2 c \quad (4)$$

$$\eta_{inherent} = [\eta] + K_K [\eta]^2 c \quad (5)$$

the intrinsic viscosity was obtained by plotting the resulting reduced and inherent viscosities against concentration and extrapolating to zero concentration.

The rheological properties of the polymer solution were measured using a stress-controlled rheometer (Rheometrics DSR II) fitted with appropriate cone and plate or couette geometries. The rheological properties of HASE polymers have been shown to be dependent on their previous shear history [English *et al.* (1997)]; therefore, it was necessary to consider a pre-shear regime. Prior to any measurement, the sample was subjected to a shear rate of 1 s^{-1} for 5 min followed by a 10 minute-rest period. This protocol was found to be sufficient for structure recovery in the sample as noticed from dynamic time sweep experiments. Experiments were run using the two geometries, when possible, to check for wall slip effects and the data were found to be in good agreement eliminating the presence of such effects.

5.3 Results and Discussion

5.3.1 Effects of solvent quality

The steady shear behavior of a 3% polymer in a mixture of water and propylene glycol (PG) with different PG proportions is shown in Figure 2. In general, the steady shear profile shows a weak shear thinning behavior at low shear rates followed by a stronger shear thinning region at higher shear rates. There is also a decrease in the relative viscosity η_{rel} (defined as the steady shear viscosity divided by the solvent viscosity) as the PG content increases. In addition, the shear thinning behavior seems to be more pronounced in “water-rich” solvents. The reduction in the relative viscosity with PG content reflects changes in the polymer solution microstructure, possibly a weakening of the hydrophobic associations, as

the solvent quality changes.

Figure 3 compares the complex and steady shear viscosities of a 3% polymer solution with different proportions of the co-solvents. There is a decrease in the magnitude of the complex viscosity as the solvent PG content increases, consistent with the steady shear results. In addition for the “PG-rich” solvents, both steady and complex viscosity overlay well obeying the Cox-Merz rule [Cox *et al.* (1958)]. However, for “water rich” solvents there is deviation from the Cox-Merz rule with the complex viscosity lower than the steady viscosity especially at intermediate and high shear rates. This deviation from the Cox-Merz rule in “water-rich” solvents has previously been observed with HASE polymer in aqueous medium and can be attributed to the formation of shear-induced structures [English *et al.* (1997); English *et al.* (1999)]. Please note that the viscosity of the PG sample is higher than that of PG70 in Figure 3. The reverse trend is observed because PG has a higher viscosity than PG70, and the solution viscosity is dominated by the solvent for these compositions. If the data are plotted in terms of relative viscosity, the expected trend is observed (e.g., Figure 2).

Figure 4a shows the storage modulus (G') of a 3% polymer solution as a function of co-solvent composition. We find the magnitude of G' to decrease as the PG content of the solvent increases while the slope of the terminal region shows an opposite trend, increasing as PG content increases. These results also suggest changes in the sample microstructure with changing solvent composition. As PG content increases, the behavior changes from a relatively elastic-like behavior to a solution-like behavior, with $G' \sim \omega^{0.5}$ in water and $G' \sim \omega^{1.5}$ in PG. This transition could be related to the changes in the solvent-hydrophobe interactions

and thus the network structures. Similar findings are observed when we examine the composite dynamic elastic and loss moduli of representative samples in Figure 4b. The G'' decreases and the slope of the terminal region increases as PG content increases. A shift in the crossover point is also observed (or suggested) as the solvent quality changes. For the case of water, we observe a crossover frequency of approximately 10^{-2} s^{-1} followed by a plateau region. The crossover frequency increases by more than two orders of magnitude reflecting a decrease in the longest relaxation time, $\tau = 1/\omega_{\text{cross over}}$, as the PG content of the solvent increases. In fact, in the case of the sample containing 85% PG, the crossover frequency is not even accessible within the experimental frequency limit.

Both steady and dynamic data suggest a change in the network structure as the solvent changes from being “water-rich” to “PG-rich”. To further probe the effects of solvent quality on rheology, we plot in Figure 5 the relative viscosity (η_{rel}) and the plateau modulus as a function of the solvent solubility parameter (δ_s) for different polymer concentrations. Figure 5a reveals that the relative viscosity increases with increasing polymer concentration or solubility parameter. More importantly, we observe the presence of two distinct regimes with different dependence of η_{rel} on δ_s . Referring to these regimes as regime 1 corresponding to “water rich” solvents with higher solubility parameter and regime 2 corresponding to “PG-rich” solvents with lower solubility parameter, we observe the relative viscosity to show a much stronger dependence on δ_s in regime 1. In addition, the dependence of the relative viscosity on the solubility parameter seems to be independent of concentration for either regime. This behavior is observed for all concentrations above 0.5%, which shows only regime 2-type dependence. The point where the two regions meet shifts towards a lower δ_s

3rd concentration. A plot of the elastic modulus at a fixed frequency (1 rad/s) versus the solvent solubility parameter (Figure 5b) also shows the presence of two regimes, indicating that this behavior is not material-function specific. The plateau modulus for samples in “PG-rich” solvents is almost independent of the solvent composition, while in “water-rich” solvents the plateau modulus increases sharply with the solvent solubility parameter. These data are consistent with the results of the scaling of η_{rel} with the solvent solubility parameter δ_s .

It is interesting to note that the inflection point occurs at a lower δ_s for the elastic modulus compared to the relative viscosity. The difference can be attributed to the fact that we do not reach the plateau regime for the dynamic experiments. Had we been able to access that, the “PG-rich” samples would have had a higher G' ; this would have shifted the transition point to a higher δ_s , consistent with the steady data. The two-regime behavior is also observed when either η_{rel} or the elastic modulus at fixed frequency is plotted versus the individual components of the solubility parameter (data not shown). The same trend is observed when the polar or hydrogen bonding components are used. On the other hand, an opposite trend is observed when the dispersion component is used instead, as the PG has a higher dispersion component than water.

The two-regime behavior could be explained based on changes in solution microstructure as the solvent quality changes. In regime 1 at high solubility parameters, the dominant mode of interaction is hydrophobic associations. With increases in PG content of the solution in this regime, there is a reduction in the hydrophobic interactions due to the reduced tendencies of the hydrophobes to associate and this leads to lower η_{rel} and G'_p . In

regime 2, there may be a lack of hydrophobic association and the polymers are behaving as regular entangled polymer chains. At the inflection point, we are assuming that the hydrophobic interactions are suppressed. Such an explanation is supported by the work of Jenkins et al [1995] who reported that a 40/60 mixture of Butyl Carbitol and water suppressed the formation of an association network for 2.5% linear water-soluble poly(oxyethylene) end capped with the hexadecyl alkyl group.

5.3.2 Concentration effects

The different modes of interaction in the “water-rich” and “PG-rich” solvents should manifest themselves in different concentration dependences of rheological material functions in these regimes. We probe this effect by plotting the concentration dependence of the relative viscosity for “water-rich” solvents at different co-solvent compositions in Figures 6. For the concentration range studied, we observe a power-law behavior for the relative viscosity ($\eta_{\text{rel}} \sim c^n$) with a scaling exponent n of about 2.5, independent of the solvent composition. This value of n is consistent with the reported value of 2.68 for HASE polymer with C_{16} hydrophobes [Tan *et al.* (2000)]. However, this value is lower than the theoretically predicted values of 3.75 in the entangled semi-dilute regime using the Sticky-Reptation model of associative polymers [Rubinstein and Semenov (2001)]. The value of the scaling exponent is dependent on the transition from intra- to inter-molecular association as the polymer concentration increases. With very few hydrophobes per polymer chain (the macromonomer concentration is only 0.22 mole%), we expect a low value for the scaling exponent as there is a lower chance for the hydrophobes to form intra-molecular association

and thus a very low fraction of the hydrophobes will undergo transition from intra- to inter-molecular association.

Figure 7 shows scaling of the relative viscosity with concentration for “PG-rich” solvents. A scaling factor of 1.4 independent of the solvent is obtained. The lower value of the scaling factor in “PG-rich” solvents should be the result of the absence of hydrophobic association. Similar scaling of the elastic modulus at fixed frequency (1 rad/s) with concentration (data not shown) also revealed two different dependencies. In "water-rich" solvent, a scaling factor of 3.2 was observed while in “PG-rich” solvents a lower scaling factor of 2.3 was observed. The scaling factor within each region was independent of the solvent.

To support our hypothesis that the behavior in regime 2 is due to the lack of hydrophobic association, we investigated the dependence of the relative viscosity on concentration for solutions where no hydrophobic association is possible. This was done using two approaches. First, an unmodified polymer with the same structure and molecular weight as the HASE polymer, but with no hydrophobic groups at the end of the macromonomer, was used in our study. With this unmodified polymer, no hydrophobic association is possible. The second approach entailed using the same HASE polymer in our study but after deactivating the hydrophobic groups. We deactivated the hydrophobic groups using an inclusion compound forming host(β -cyclodextrin). Cyclodextrins have a unique ring shaped structure with a hydrophobic annular core and a hydrophilic exterior. Because of the hydrophobicity of the annular core of cyclodextrin, it can encapsulate the hydrophobic part of a HASE polymer resulting in deactivation of the hydrophobes. In this regard, cyclodextrins

have been used for the removal of hydrophobic association of HASE solutions [Islam *et al.* (2000), Gupta *et al.* (2002a, 2002c)]. The effect of adding β -cyclodextrin on the viscosity of a 1% polymer solution is shown in Figure 8. With the addition of β -cyclodextrin more hydrophobes are deactivated resulting in reduction in the solution viscosity. At about 15 moles β -cyclodextrin/hydrophobe, the addition of more β -cyclodextrin seems to have no effect on the solution viscosity.

Figure 9 shows the dependence of the relative viscosity on the concentration for unmodified polymer (without hydrophobe) in water and PG as well as for the HASE polymer after encapsulation of the hydrophobes with 20 moles β -cyclodextrin/hydrophobe. A constant exponent factor of 1.4 is observed for the unmodified polymer (without hydrophobes) in both water and PG consistent with results of the HASE polymer in “PG-rich” solvents (Figure 7). These results prove the lack of association in “PG-rich” solvents. For the HASE polymer with the hydrophobic groups deactivated with β -cyclodextrin, an exponent of 1.2 is obtained, which again supports the lack of hydrophobic association in regime 2.

5.3.3 Solvent quality and polymer interaction modes

The lower viscosity and moduli of the polymer solution as the PG content of the co-solvent increases as well as the display of two-regime behavior can be attributed to reduced hydrophobic associations. Several factors contribute to this phenomenon. First, the hydrophobic groups have a lower tendency to associate as the solvent become less polar. The hydrophobes are not forced out of the solvent media as strongly as in the case of the aqueous solution. The lower affinity of the hydrophobes to form micelles would result in weaker or

negligible network structure and therefore lower viscosity and viscoelastic properties. Secondly, the effective length of the PEO spacer becomes shorter due to the dehydration of the PEO by the glycol, as reported for nonionic surfactants [Penfold *et al.* (1997); Aramaki *et al.* (1999)]. Shorter PEO spacer length will also reduce intermolecular associations [Dai *et al.* (2000)]; the possibility of intra-molecular association is always low because our polymer has very few hydrophobes (~ 3) per chain. Finally, the polymer coil dimensions decrease as the solvent becomes “PG-rich”, as shown by a decrease in $[\eta]$ values (Table 2). The less expanded chains will hinder the formation of any intermolecular associations. At some solvent composition, these factors together will completely prevent the hydrophobic association. In summary, we contribute the 2-regime behavior to the absence of the hydrophobic association in regime-2.

The change in $[\eta]$ may imply change in the concentration regime from entangled to un-entangled semi-dilute regime. However, contrary to regular polymer solutions this is not an issue here. For associative polymers, at concentrations below c^* only intramolecular association is possible [Candau *et al.* (1998); Regalado *et al.* (1999)]. At concentrations higher than c^* both inter and intramolecular association contribute to the solution rheology. At higher concentrations, entanglement occurs in addition to hydrophobic association. However, the physical entanglement of the polymer chains does not affect the rheological properties of the semi-dilute solutions [Ng, *et al.* (2001)]. Thus, a distinct change in the dependence of viscosity on concentration only occurs at c^* when intermolecular associations appear, and not with the addition of entanglements. Since the overlap concentration, c^* calculated as $1/[\eta]$, for this polymer solution is about 0.02% in water and 0.45% in PG, all

samples examined in this study are above c^* . This information, together with the similarity in behavior observed among the unmodified polymer (without hydrophobes), the HASE polymers encapsulated with β -cyclodextrin and the HASE polymer in “PG-rich” solvents, all lend credence to the fact that the *two-regime behavior* is due to changes in hydrophobic associations. This is also supported by the values of k_H - k_K shown in Table 2. In “PG-rich” solvents, this value approaches the theoretical value of 0.5 similar to the unmodified polymer. In contrast, the k_H - k_K values deviate substantially from the theoretical value in “water-rich” solvents, suggestive of the presence of strong hydrophobic interactions.

5.4 Conclusions

The effect of solvent quality on the rheological behavior of a hydrophobically modified associative polymer has been examined using co-solvents of water and propylene glycol (PG) with different proportions. Two distinct modes of behavior are observed depending on whether the co-solvent is “water rich” or “PG rich”. In both regimes, the relative viscosity and plateau modulus reveal power-law dependences with the solvent solubility parameter; however, the dependence is much stronger in the “water rich” regime. In addition, the concentration dependence of the viscosity is very different for the two regimes with the “water rich” regime revealing stronger power-law dependence consistent with that observed in associative systems. In the “PG-rich” solvents, on the other hand, the polymer shows behavior akin to that of the same polymer without the hydrophobe or to polymers with the hydrophobes deactivated by inclusion compound formation with β -cyclodextrin. This leads us to attribute the dual-mode behavior to a lessening in the ability of

the hydrophobic groups for micellization as the solvent quality changes. This lack or reduction of hydrophobic interactions in the “PG-rich” solvents is possibly induced by less expanded polymer chains and conformational changes in PEO spacers, together with a lower tendency of the hydrophobes to form micelles in less polar medium.

5.5 Acknowledgements

The authors gratefully acknowledge the comments and suggestions of Srinivasa R. Raghavan (U. Maryland) and Robert J. English (Northeast Wales Institute) during the preparation of the manuscript.

5.6 References

- Aramaki, K., U. Olson, Y. Yamaguchi and H. Kunieda, "Effect of Water Soluble Alcohols on Surfactant Aggregation in The C₁₂EO₈ System," *Langmuir* 15, 6226-6232 (1999).
- Candau, F., J. R. Regalado and J. Selb, "Scaling Behavior of the Zero Shear Viscosity of Hydrophobically Modified Poly(acrylamide)s," *Macromolecules* 31, 5550-5552 (1998).
- Carder, C. H., D. C. Garska, R. D. Jenkins and M. J. McGuiness, "Aircraft Deicing/Anti-Icing Fluids Thickened By Associative Polymers," US 5708068 (1998).
- Carder, C. H., D. C. Garska, R. D. Jenkins and M. J. McGuiness, "Process of Making Aircraft Deicing/anti-icing Fluids Thickened by Associative Polymers" US 5,863,973 (1999).
- Cox, W. P. and E. H. Merz, "Correlation of Dynamic and Steady State flow Viscosity," *Journal of polymer Science* 28, 619-622 (1958).
- Dai, S. T., K. C. Tam, R. D. Jenkins and D. R. Bassett, "Light Scattering of Dilute Hydrophobically Modified Alkali-Soluble Emulsion Solutions: Effect of Hydrophobicity and Spacer Length of Macromonomer," *Macromolecules* 33, 7021-7028 (2000).
- English, R. J., H. S. Gulati, R. D. Jenkins and S. A. Khan, "Solution rheology of a hydrophobically modified alkali-soluble associative polymer," *J. Rheol.*, 41, 427-444 (1997).
- English, R. J., S. R. Raghavan, R. D. Jenkins and S. A. Khan, "Associative Polymers Bearing N-Alkyl Hydrophobes: Rheological Evidence for Microgel-Like Behavior," *J. Rheol. of Rheology* 43, 1175-1194 (1999).
- English, R. J., J.H. Laurer, R.J. Spontak and S. A. Khan, "Hydrophobically Modified Associative Polymer Solutions: Rheology and Microstructure in the Presence of Nonionic Surfactants" *Industrial and Engineering Chemistry Research*, Nov. web release (2002).
- Gupta, R. K., K. C. Tam, S. H. Ong, and R. D. Jenkins "Interactions of Methylated β -cyclodextrin with Hydrophobically Modified Alkali-Soluble Associative Polymers (HASE): Effect of Varying Carbon Chain Length," *Proc. 13th Int. Congr. Rheol.*, Cambridge, UK, Vol 1, 335-337 (2000a).
- Gupta, R. K., K. C. Tam, and R. D. Jenkins "Rheological Properties of Model Alkali Soluble Associative (HASE) Polymers: Effect of Varying Acid Monomer and Macromonomer Composition," *Proc. 13th Int. Congr. Rheol.*, Cambridge, UK, Vol 1, 340-342 (2000b).
- Gupta, R. K., K. C. Tam, S. H. Ong, and R. D. Jenkins, "Interactions of Methylated β -cyclodextrin and Hydrophobically Modified Alkali-Soluble Associative Polymers

- (HASE): a Rheological Study,” *Korea-Australia Rheology Journal*, 12, 93-100, (2000c).
- Hansen, C. M., “ The Three Dimensional Solubility Parameter- Key to Paint Component Affinities: I. Solvents Plasticizers, Polymers, and Resins,” *Journal of Paint Technology* 39, 104-117 (1967).
- Hansen, C. M. and A. Beerbower, “ Solubility Parameters,” *Encyclopedia of Chemical Technology*, Wiley: New York, 889-909 (1971).
- Hansen, C. M., “ Hansen Solubility Parameters: a user’s Handbook,” CRC Press: Boca Raton (1999).
- Horiuchi, K., Y. Rharbi, A. Yekta, M. A. Winnik, R. D. Jenkins and D. R. Bassett, “Dissolution Behavior in Water of a Model Hydrophobically Alkali- Swellable Emulsion (HASE) Polymer With C₂₀H₄₁ Groups,” *Canadian Journal of Chemistry* 76, 1779-1787 (1998).
- Islam, M. F., R. D. Jenkins, D. R. Bassett, W. Lau and H. D. Ou-Yang, “Single Chain Characterization of Hydrophobically Modified Polyelectrolytes Using Cyclo-dextrin/ Hydrophobe Complexes,” *Macromolecules* 33(7), 2480-2485 (2000).
- Jenkins, R. D., D. R. Bassett, R. H. Lightfoot and M. Y. Boluk, “Aircraft Anti-icing Fluids Thickened by Associative Polymers,” WO Patent 9,324,543 (1993).
- Jenkins, R. D., D. R. Bassett, C. A. Silebi and M. S. El-Aasser, “Synthesis and Characterization of Model Associative Polymers,” *Journal of Applied Polymer Science* 58, 209-230 (1995).
- Jenkins, R. D., L. M. Delong and D. R. Bassett, “Influence of alkali-soluble associative emulsion polymer architecture on Rheology,” in *Hydrophilic Polymers: Performance with Environmental Acceptance*, edited by J. E. Glass (ACS Advances in Chemistry Series No 248 American Chemical Society, Washington, DC, 425-447 (1996)
- Jenkins, R. D., D. R. Bassett, R. H. Lightfoot and M. Y. Boluk, “Glycol-Based Aircraft Anti-icing Fluids Thickened by Associative Polymers Containing Hydrophobe-Bearing Macromonomers,” US Patent 5,681,882 (1997).
- Kaczmariski, J. P., M. R. Tarng, Z. Y. Ma and J. E. Glass, “Surfactant and Salinity Influences on Associative Thickener Aqueous Solution Rheology,” *Colloids and Surfaces A- Physicochemical and Engineering Aspects* 147, 39-53 (1999).
- Lau, A. K. M., C. Tiu and K. C. Tam, ”Rheology of hydrophobically-alkali-soluble-emulsions (HASE),” 6th World Congress of Chemical Engineering, Melbourne, Australia (2001).

- Ng, W. K., K. C. Tam and R. D. Jenkins, "Evaluation of Intrinsic Viscosity Measurements of Hydrophobically Modified Polyelectrolyte Solutions," *European Polymer Journal* 35, 1245-1252 (1999).
- Ng, W. K., K. C. Tam and R. D. Jenkins, "Rheological Properties of Methacrylic Acid/Ethyl Acrylate Co-Polymer: Comparison Between Unmodified and Hydrophobically Modified System," *Polymer* 42, 249-259 (2001).
- Olesen, K. R., D. R. Bassett and C. L. Wilkerson, "Surfactant co-thickening in model associative polymers," *Progress in Organic Coatings* 35, 165-170 (1999)
- Penfold, J. S., E. I. Tucker and P. Cummins, "The Structure of Non-Ionic Micelles in Less Polar Solvents," *Journal of Colloid and Interface Science* 185, 424-431 (1997).
- Rubinstein, M. and A. N. Semenov, "Dynamic of Entangled Solution of Associating Polymers," *Macromolecules* 34, 1058-1068 (2001).
- Regalado, E. J., J. Selb and F. Canadu, "Viscoelastic Behavior of Semidilute Solutions of Multisticker Polymer Chains," *Macromolecules* 32, 8580-8588 (1999).
- Rubinstein, M. and A. V. Dobrynin, "Solutions of Associative Polymers," *Trends Polym. Sci.* 5, 181-186 (1997)
- Schaller, E. J. "Rheology Modifiers for Water-Borne Paints." *Surf. Coat. Aust.* **22**(10): 6-10, 12-13, 1985.
- Seng, W. P., K. C. Tam, R. D. Jenkins and D. R. Bassett, "Calorimetric Studies of Model Hydrophobically Modified Alkali-Soluble Emulsion Polymers with Varying Spacer Chain Length in Ionic Surfactant Solutions," *Macromolecules*, 33, 1727-1733 (2000)
- Shay, G. D., E. Eldridge and J. E. Kail, "Alkali-Soluble Latex Thickener," US Patent 4,514,552 (1985)
- Shay, G. D., K. R. Olesen and C. M. Miller, "Observance and Characterization of the Viscosity Spike Exhibited at Lower Degrees of Neutralization in HASE Polymers," 216th ACS National Meeting, Boston, August 23-27 (1998)
- Szejtli, J, "Introduction and General Overview of Cyclodextrin Chemistry," *Chemical Reviews* 98, 1743-1753, (1998)
- Tam, K. C., M. L. Farmer, R. D. Jenkins and D. R. Bassett, "Rheological Properties of Hydrophobically Modified Alkali-soluble Polymers: Effects of Ethylene-Oxide Chain Length," *J. Polym. Sci., Part B: Polym. Phys.* 36, 2275-2290 (1998)

- Tan, H., K.C. Tam, V. Tirtaatmadja, R. D. Jenkins and D. R. Bassett, "Extensional Properties of Model Hydrophobically Modified Alkali-Soluble Associative (HASE) Polymer Solutions," *J. Non-Newtonian Fluid Mech.* 92, 167-185 (2000)
- Tan, H. T., K. C. Tam and R. D. Jenkins, "Network Structures of a Model HASE Polymer in Semidilute Salt Solutions," *Journal of Applied Polymer Science* 79, 1486-1496 (2001)
- Thibeault, J. C., P. R. Sperry and E. J. Schaller, "Effect of surfactants and Cosolvents on the Behavior of Associative Thickeners in Latex Systems," *In Water-Soluble Polymers: Beauty with Performance* Edited by J. E. Glass (ACS Advances Chemistry . Series No. 213, American Chemical Society, Washington, D. C., 375-89, (1986).
- Tirtaatmadja, V., K. C. Tam and R. D. Jenkins, "Rheological Properties of Model Alkali-Soluble Associative (HASE) Polymers: Effect of Varying Hydrophobe Chain Length," *Macromolecules* 30, 3271-3282 (1997)
- Tirtaatmadja, V. T., K. C. Tam, R. D. Jenkins and D. R. Bassett, "Stability of a Model Alkali-Soluble Associative Polymer in The Presence of a Weak and a Strong Base," *Colloid and Polymer Science* 277, 276-281 (1999)

Table 1. Solvent's composition, solubility parameter components and solubility parameter.

Solvent	PG, wt. %	δ_d MP ^{1/2}	δ_p MP ^{1/2}	δ_h MP ^{1/2}	δ MP ^{1/2}
Water	0	12.3	31.3	34.1	47.8
PG15	15	12.9	28.0	32.5	44.8
PG25	25	13.3	26.0	31.5	42.7
PG35	35	13.9	22.9	30.7	40.7
PG50	50	14.5	20.4	28.8	38.2
PG70	70	15.3	16.2	26.6	34.8
PG85	85	16.2	12.9	24.9	32.1
PG	100	16.8	9.4	23.3	30.3

* Hansen (1967)

Table 2: Intrinsic viscosity ($[\eta]$), Huggins coefficient (k_H) and the difference between Huggins and Kramer coefficient ($k_H - k_K$) for modified and unmodified polymers in water/propylene glycol (PG) co-solvent with different compositions.

Solvent	δ_s Mpa ^{1/2}	Modified Polymer			Unmodified Polymer		
		$[\eta]$ dl/g	k_H	$k_H - k_K$	$[\eta]$	k_H	$k_H - k_K$
Water	47.9	42.2	3.22	2.11	55.8	0.37	0.50
PG25	43.0	14.4	3.26	3.03			
PG50	38.3	4.1	2.73	2.21	13.5	0.41	0.52
PG70	34.8	3.1	0.61	0.63			
PG85	32.4	2.7	0.34	0.51	4.1	0.38	0.52
PG	30.3	2.3	0.41	0.51	1.4	0.36	0.51

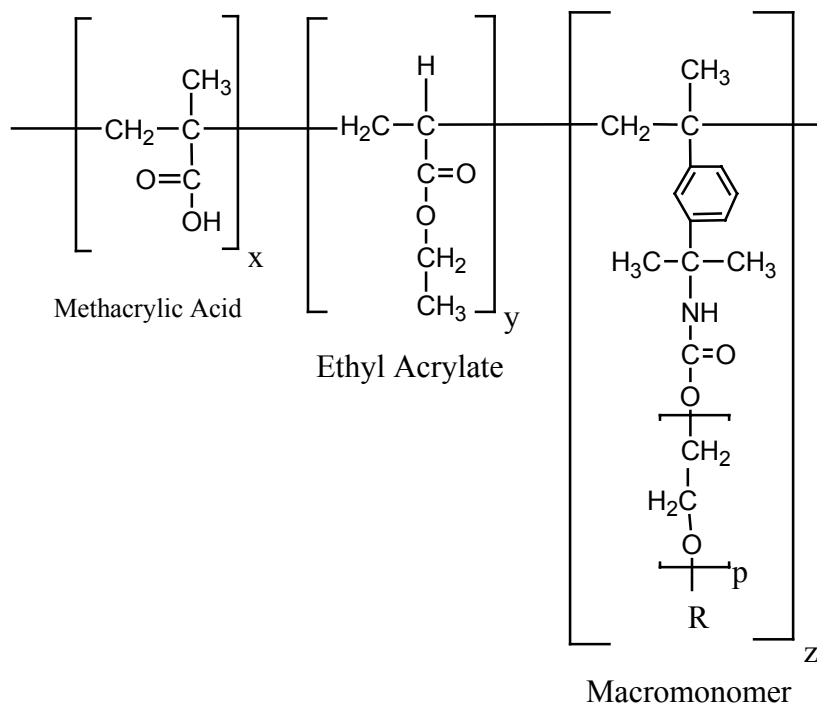


Figure 1: Chemical constitution of the HASE polymer. Here $p=40$ and R corresponds to $\text{C}_{22}\text{H}_{44}$; $x/y/z = 43.57/56.21/0.22$ by mole.

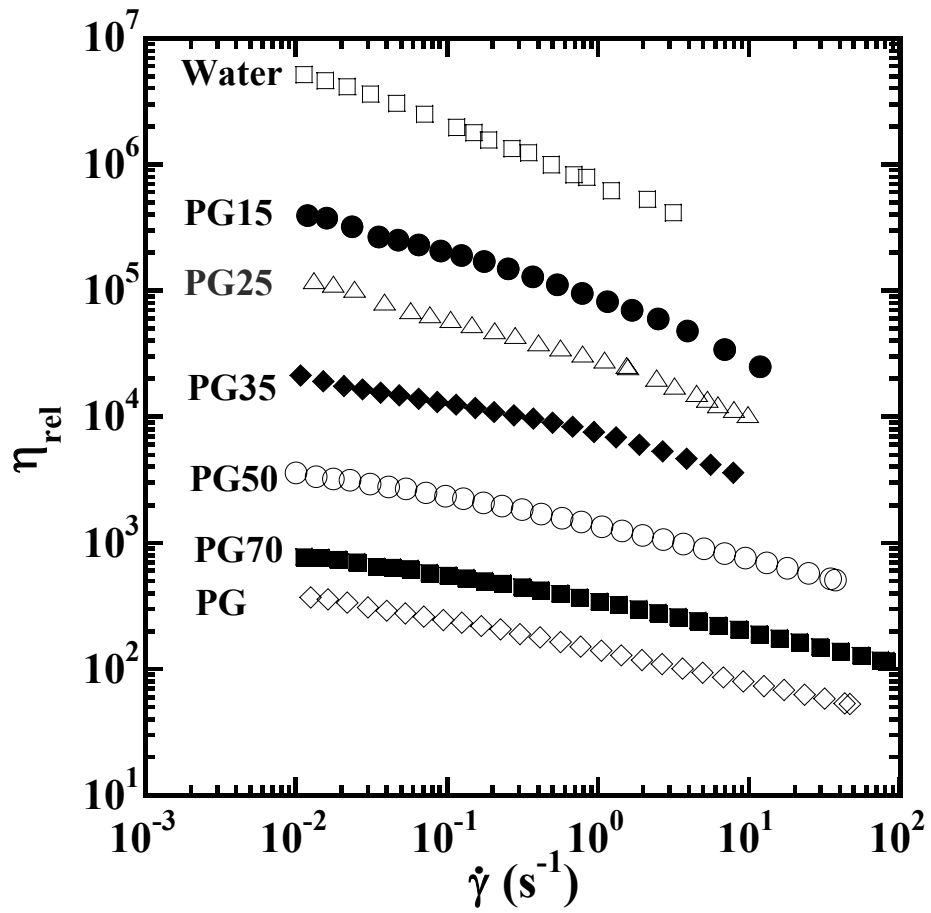


Figure 2. Effect of solvent composition on the relative viscosity of a 3% HASE polymer solution. The numbers after PG (propylene glycol) correspond to the weight percent of PG in the water-propylene glycol co-solvent.

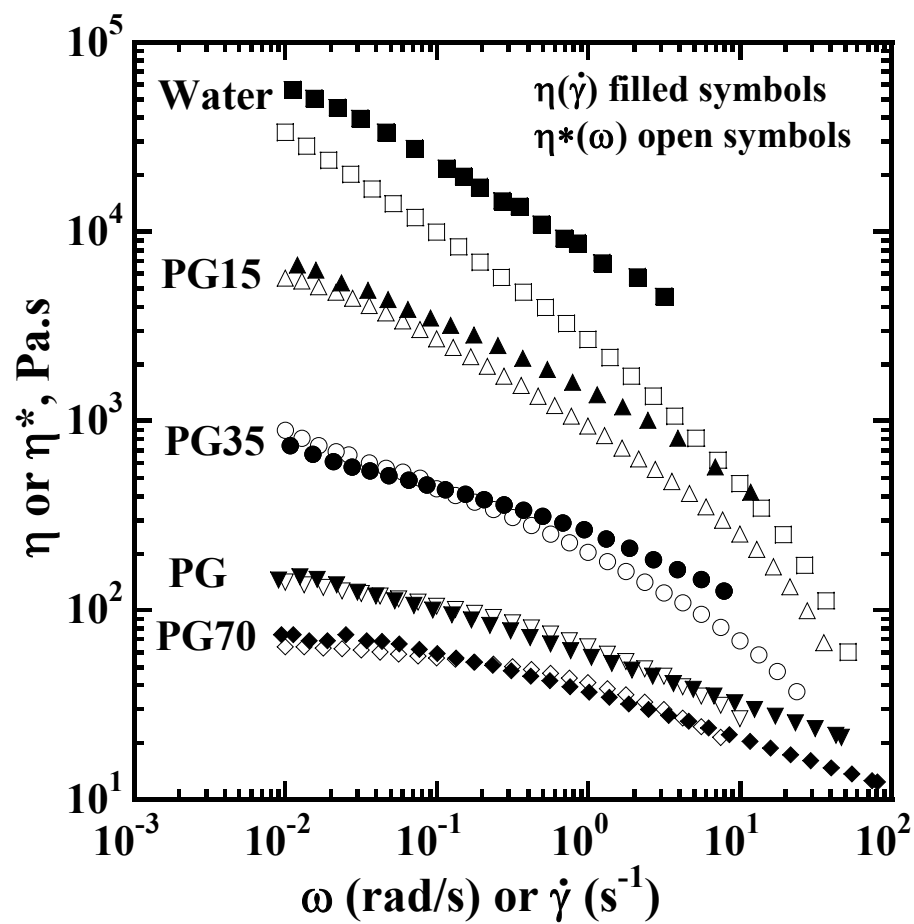


Figure 3. Comparison of the steady (filled symbols) and complex (open symbol) viscosity of a 3% HASE polymer solution shown for different co-solvent compositions. The numbers after PG (propylene glycol) correspond to the weight percent of PG in the water-propylene glycol co-solvent.

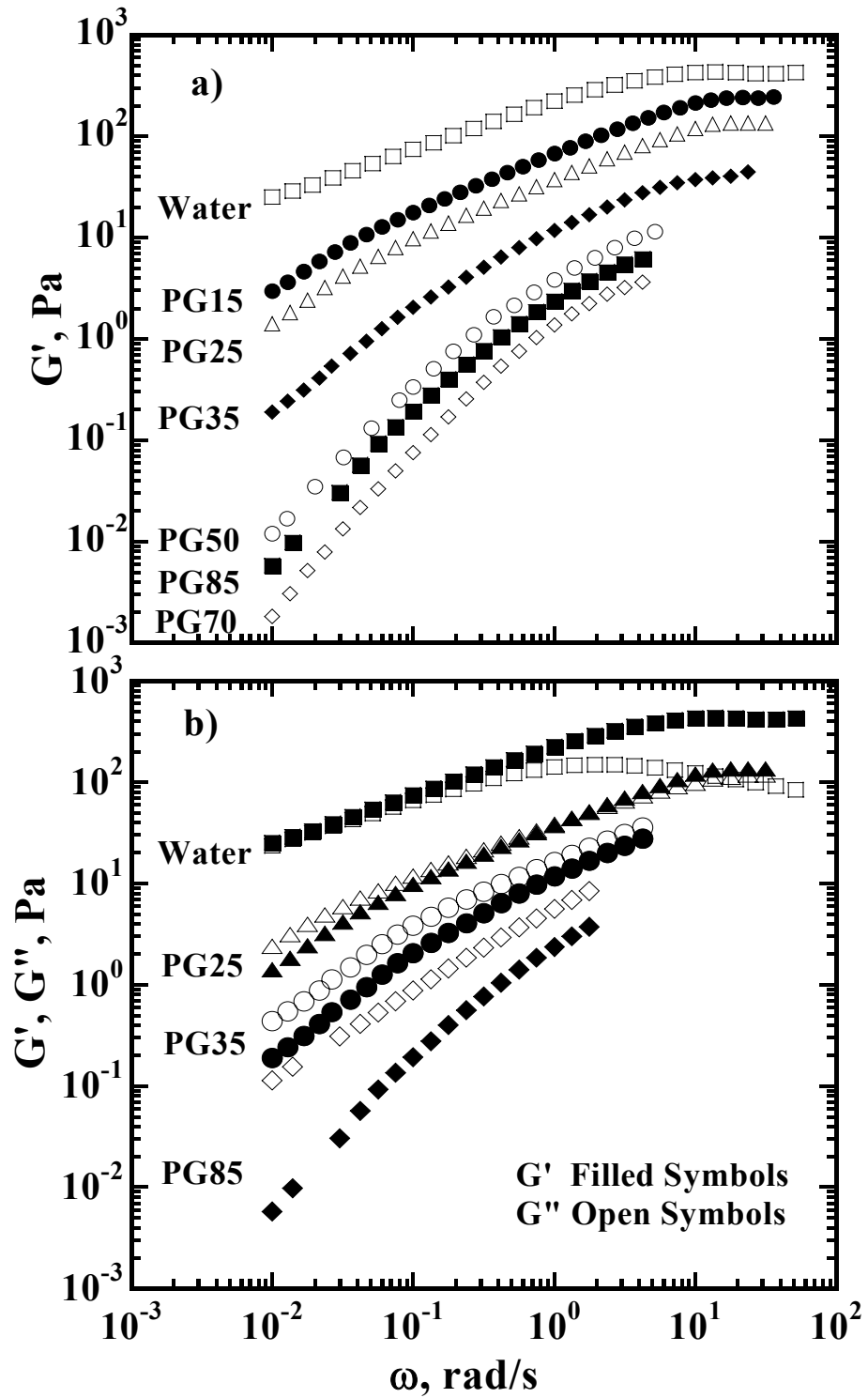


Figure 4. Effect of solvent composition on (a) the storage modulus G' , and, (b) the storage (G') and loss (G'') moduli of a 3% HASE polymer solution.

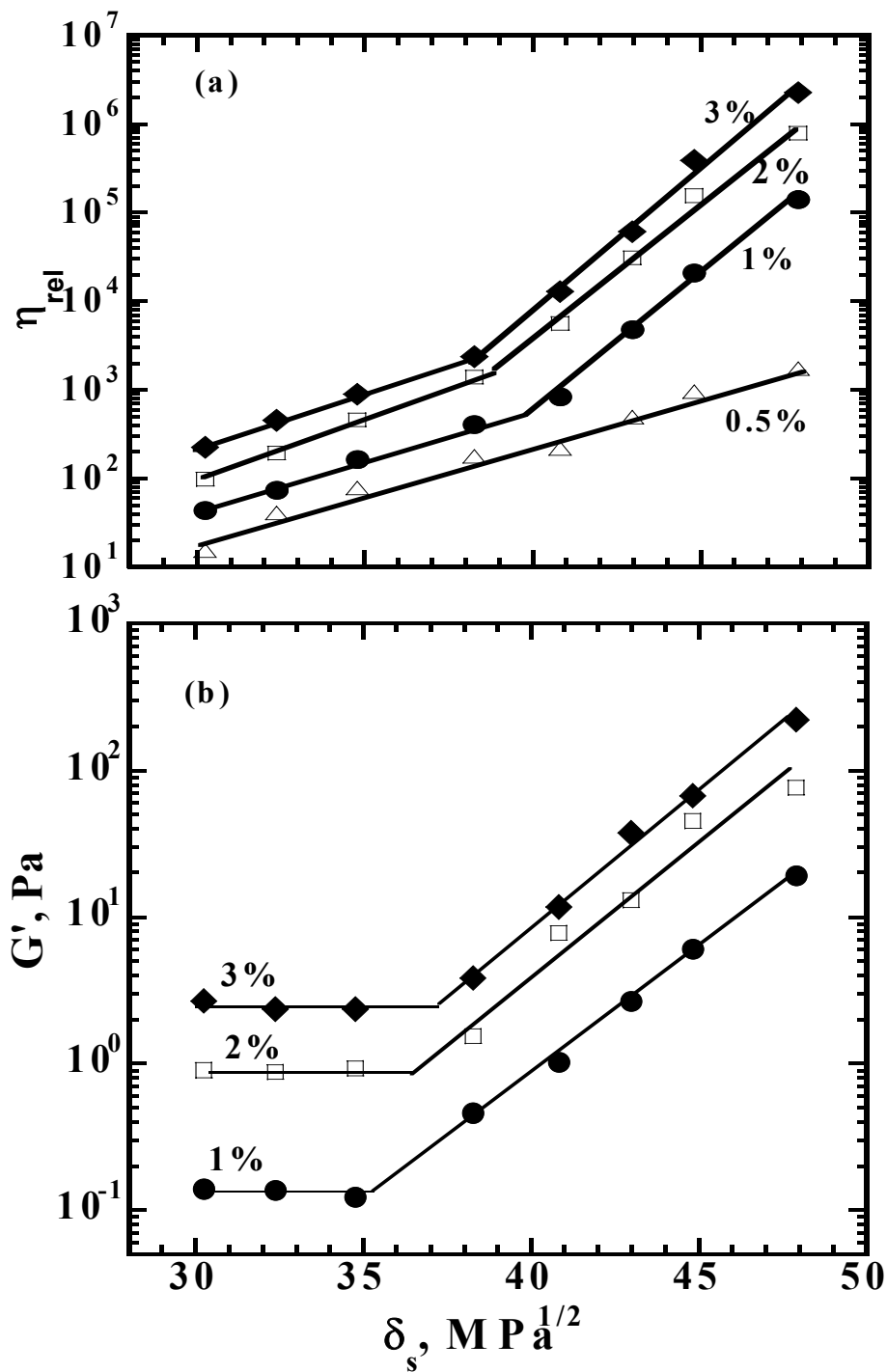


Figure 5. Effect of the solvent solubility parameter on the (a) relative viscosity, and, (b) elastic modulus G' at a fixed frequency (1 rad/sec) of HASE polymer solutions. The numbers (in %) correspond to different polymer concentrations. Lines are for guidance only and have no further justification.

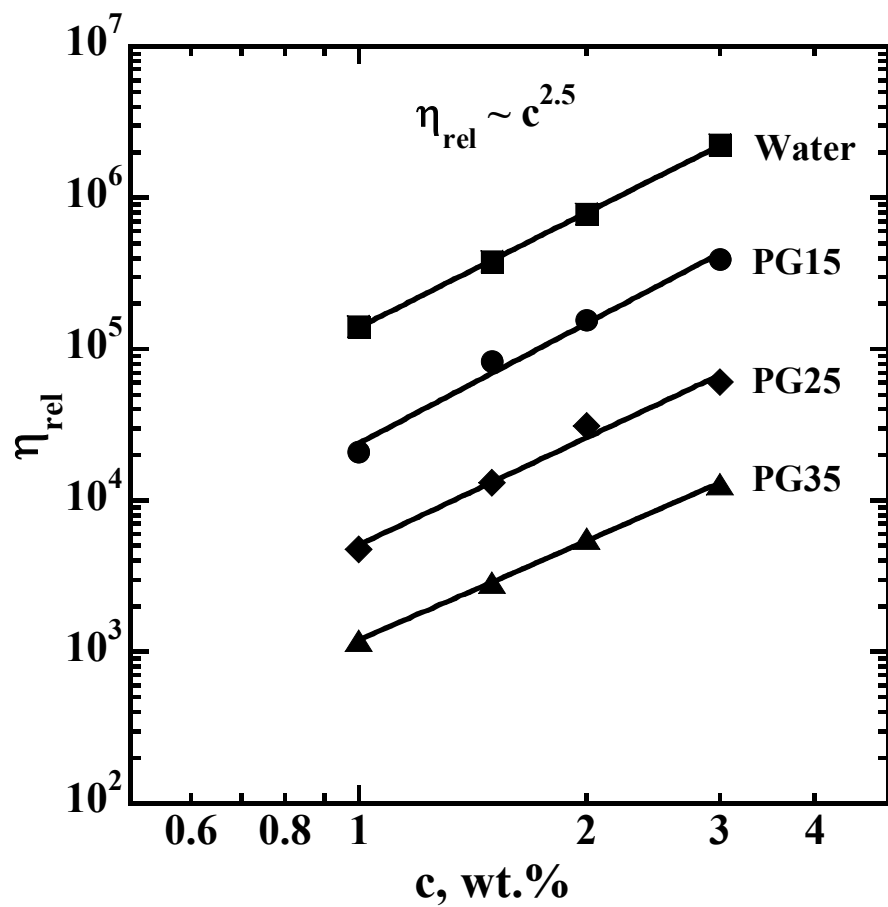


Figure 6. Concentration dependence of the relative viscosity of HASE polymer solutions in “water-rich” solvents. Results are shown for different compositions of the co-solvent.

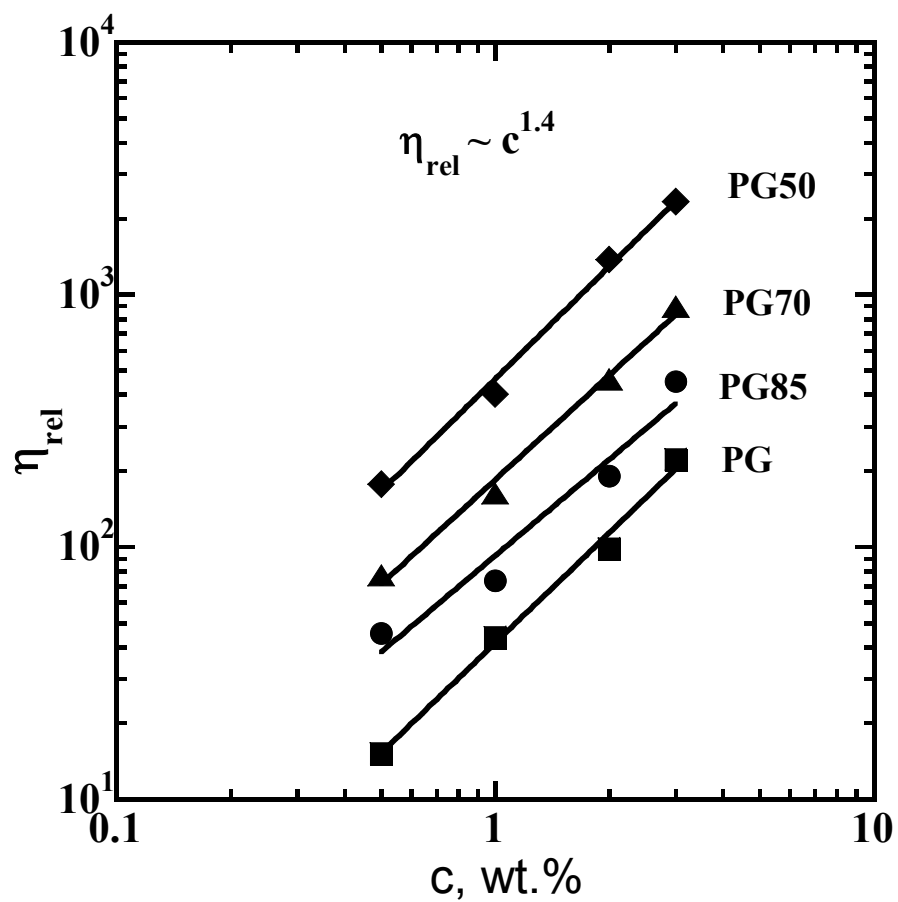


Figure 7. Concentration dependence of the relative viscosity of HASE polymer solutions in "PG-rich" solvents. Results are depicted for different co-solvent compositions.

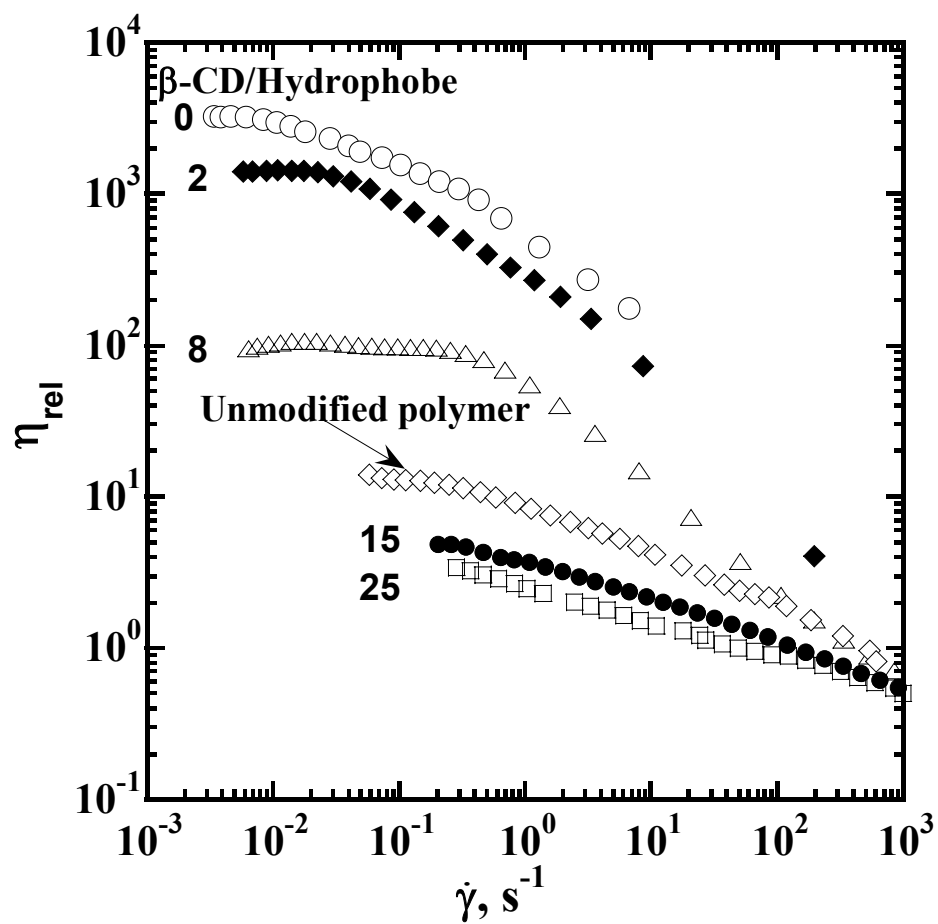


Figure 8. Effect of addition of β -cyclodextrin on the relative viscosity of a 1% HASE polymer solution. The numbers correspond to the moles of cyclodextrin added per mole of the hydrophobe. The unmodified polymer reflects the same polymer as the HASE polymer but without the hydrophobes.

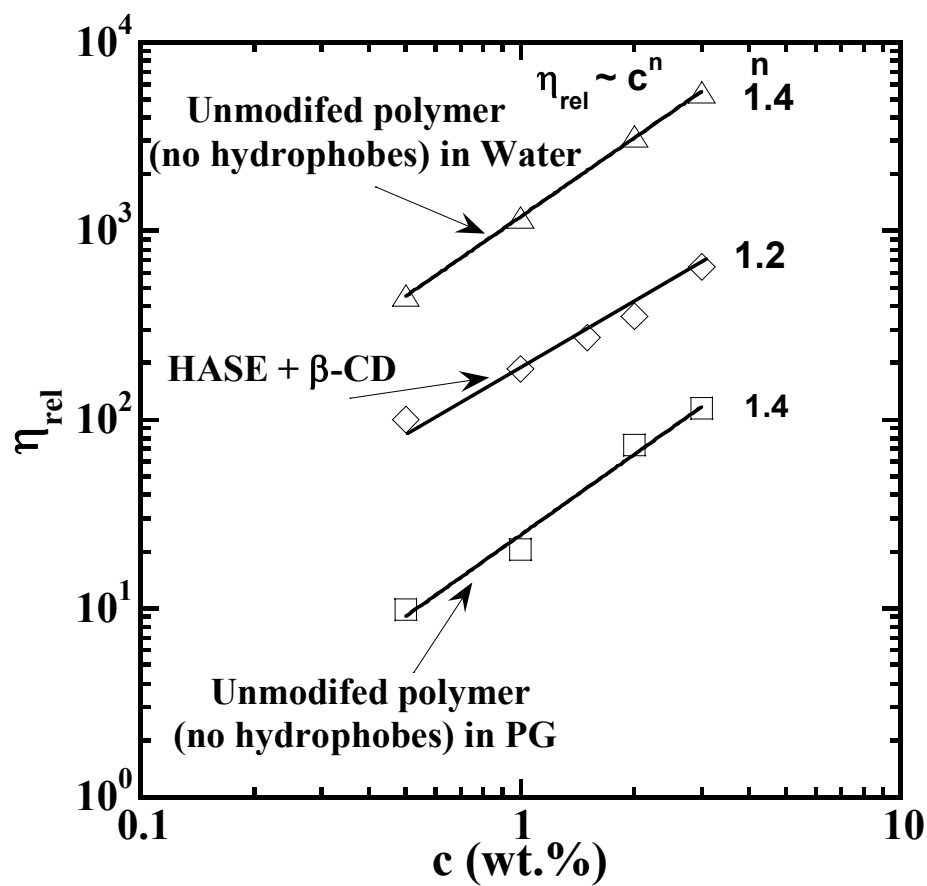


Figure 9. Concentration dependence of the relative viscosity for unmodified polymer (without hydrophobe) in water and in PG, and the HASE polymer with the hydrophobes deactivated through the addition of 20 moles β -cyclodextrin/mole hydrophobe.

CHAPTER 6

A TRACER MICRORHEOLOGY STUDY OF ASSOCIATIVE POLYMER SOLUTIONS

A revised version of Chapter 6 by Ahmed A. Abdala, Samiul Amin, John van Zanten, and Saad Khan is being prepared for submission to Macromolecules

Abstract

In this study, we investigate the ability of diffusing wave spectroscopy (DWS) to probe the dynamics of comb-like hydrophobically modified associative polymers. The effect of both solvent quality and polymer concentration on the dynamics of the polymer solution are examined. The creep compliance and dynamic moduli data extracted from DWS are compared to those measured using conventional rheometry. We find that DWS accurately probes the structural changes induced by the change in the solvent quality or the polymer concentration. The comparison with conventional mechanical rheometry data reveals excellent qualitative agreement between the data obtained from the two techniques. Quantitatively, however, the dynamic moduli extracted from DWS measurements are consistently higher than those obtained using conventional rheology. Several reasons for the discrepancy are discussed including the possibility that the dynamics at the micro-level could be different from the bulk properties. The scaling of the creep compliance, high-frequency elastic modulus and relaxation time with polymer concentration show power-law dependence. The power-law exponents are discussed in light of theoretical predictions and available experimental data. Finally, the time dependent diffusion coefficient have been obtained using DWS and reveal information about the length scales associated with changes from elastic to glassy behavior of the polymer.

6.1 Introduction

Hydrophobically modified alkali soluble emulsion (HASE) polymers are water-soluble associative polymers that have a comb-like structure with pendant hydrophobic groups randomly grafted to a polyelectrolyte backbone. They have several advantages over other associative polymers in terms of cost and wide formulation latitude¹. They are currently being used as rheology modifiers in a wide range of applications, including paint formulations²⁻⁴, paper coatings⁵, personal and home care products⁶⁻⁹, UV-photoprotecting and aerated emulsions^{10, 11}, fabric softeners^{12, 13} and as glycol based aircraft anti-icing fluids¹⁴⁻¹⁷.

The dynamics of HASE polymers, and associative polymers in general, is usually characterized using traditional mechanical rheometry measurements. However, a multiple light scattering technique was introduced recently by Pine et. al.¹⁹ as a method to study the dynamical processes in turbid media and has since been used to study collective dynamic properties in a wide variety of materials, including polymer solutions and gels¹⁹⁻²², biopolymers^{23,24}, colloidal suspensions and gels²⁵⁻²⁷, concentrated emulsions^{28,29}, associative polymers^{22, 30}, foams³¹⁻³⁵, nematic liquid crystals³⁶, actin filaments³⁷⁻⁴², magnetorheological suspensions⁴³, surfactants⁴⁴⁻⁴⁶, and proteins^{46,47}.

Compared to conventional rheology, DWS has several advantages. First, the dynamic properties are measured by applying a very small strain. Secondly, it requires very small amounts of sample. Thirdly, it provides dynamic data over a very wide range of frequency. Finally, and most importantly, owing to the multiple scattering nature of DWS, this technique is capable of resolving *angstrom*-scale particle motions and thereby short-time dynamics.

Because the use of DWS to probe the dynamics of polymers requires the addition of

optical probes that insure highly scattering medium, polystyrene spheres are usually used as the optical probes. This resembles a practical application of HASE associative polymers well, because these polymers are used in paints and coatings in conjunction with colloidal particles.

In this study, we explore the ability of DWS to examine the behavior of associative polymers. We investigate the effect of the solvent quality on the behavior of a HASE polymer through using a co-solvent of water and propylene glycol (PG). The solution dynamics in water-rich and “PG-rich” solvents is extracted by tracking the Brownian motion of polystyrene spheres embedded in the polymer solution. The data obtained using the DWS technique are compared to those obtained using conventional rheometry. In addition, we examine the behavior of the polymer solution at very high frequencies that is not accessible using conventional rheometry, which is of industrial relevance.

6.2 Materials and Methods

The associative polymer used in this study is a model hydrophobically modified alkali-soluble (HASE) polymer synthesized by Dow Chemicals, via emulsion polymerization of methacrylic acid (MAA), ethylacrylate (EA) and a hydrophobic macromonomer. Figure 1 shows a schematic representation of its structure together with its molecular constituents.. The macromonomers in Figure 1 is end capped with $C_{22}H_{45}$ alkyl hydrophobes that are separated from the polymer backbone by 40 units of polyethylene oxide (PEO). Details of the preparation method can be found in a previous publication⁴⁸.

The polymer latexes were dialyzed against de-ionized water using cellulosic tubular

membranes for at least three weeks with daily change of water. After dialysis, the polymer was freeze-dried and 0.9% solutions were prepared and neutralized to pH of 9 ± 0.1 using 1N NaOH with the ionic strength adjusted to 10^{-4} M KCl. In this study, mixtures of water and propylene glycol were used as co-solvents. The composition of these mixtures expressed as weight% of PG in the solvent mixture is shown in Table 1. Throughout the article, these solvent mixtures will be called PGXX, with XX corresponding to the wt.% of PG in the mixture.

The steady and dynamic properties of the HASE polymer solutions were measured using a stress-controlled rheometer (Rheometrics DSR II). A 40-mm cone and plate geometry with 0.04 radians cone angle was utilized for all the reported measurements. The linear viscoelastic region (LVE), the region where both G' and G'' are independent of the applied stress, was determined by carrying out a dynamic stress sweep experiment. Both the creep and the frequency sweep experiments were carried out using a stress within the LVE.

A DWS setup operating in the transmission mode was utilized in carrying out all measurements. A schematic diagram for the setup used in the DWS experiments is shown in Figure 2. In this setup, the beam from a diode pumped solid state (DPSS) Nd-YAG laser operating at a wavelength of 532 nm *in vacuo* was incident upon a flat scattering cell containing the polymer solutions with polystyrene spheres as the optical probes. The multiply scattered light was collected using an ALV SI/SIPD photon detector via a single mode optical fiber. In order to ensure point-to-point geometry, the single mode optical fiber has a Gradient Refractive Index (GRIN) lens with a very narrow angle of acceptance, attached to it. The output from the ALV SI/SIPD photon detector is fed into a correlator

working in the cross correlation mode. The measured intensity auto correlation function was converted into the electric field autocorrelation function using the Siegert relationship.

The electric field autocorrelation function obtained from a DWS measurement can be related to the mean square displacement through⁴⁹:

$$g_1(t) = \int_0^{\infty} P(s) \exp\left[-\frac{1}{3} k_o^2 \langle \Delta r^2(t) \rangle \frac{s}{l^*}\right] ds \quad (1)$$

where $g_1(t)$ is the electric field autocorrelation function, $P(s)$ is the path length distribution function, k_o is the wave vector, $\langle \Delta r^2(t) \rangle$ is the particle mean squared displacement and l^* is the distance over which light becomes completely randomized. The mean square displacement of the probing spheres was extracted pointwise from the electric field autocorrelation function through a bisection root-searching program. It is to be noted that in contrast to dynamic light scattering (DLS) in which the length scale over which particle motion is probed can be adjusted by varying the scattering angle and/or the wavevector the length scale over which the motion is probed in DWS is adjusted by varying the cell thickness L . In this study we used 2 mm and 10 mm cells.

The viscoelastic properties of a medium can be extracted from the mean square displacement data obtained from tracer microrheology either through direct comparison of the complex viscoelastic modulus (G^*) or through comparison of the creep compliance. The complex viscoelastic modulus is obtained from tracer microrheology experiments through application of the generalized Stokes-Einstein relation²⁹:

$$\tilde{G}(s) \approx \frac{k_B T}{6\pi a s \langle \Delta \tilde{r}^2(s) \rangle} \quad (2)$$

However, this expression involves a transformation of the data from the time domain to the frequency domain. A more direct method and one that has been shown to give better results is the use of the creep compliance. The time domain creep compliance, $J(t)$, is directly proportional to the mean square displacement and is given by^{41,42}:

$$J(t) = \frac{\pi a}{k_B T} \langle \Delta r^2(t) \rangle \quad (3)$$

The linear frequency-dependent storage and loss moduli can be obtained from the creep compliance using various methods⁵⁰. However, it is difficult to implement some of these methods, in particular the direct transformation methods, due to the very large temporal dynamic range and logarithmic spacing of the measured mean square displacement. Moreover, the accuracy of estimation methods can be reduced by the noise in the mean square displacement and rapid changes in the logarithmic slope of the mean square⁴². To avoid these potential problems, the storage and loss moduli are calculated using the retardation spectrum $L(\tau)$ as determined by a regularized fit of the creep compliance using a set of impartial basis function, following the method described by Mason et al.⁴².

6.3 Results and Discussion

6.3.1 Solvent Quality Effects

Our initial efforts focused on extracting information about the effects of the solvent quality on the behavior of HASE polymers from DWS by tracking the motion of 0.966- μm polystyrene spheres in 0.9 wt.% polymer solutions in different solvents. In this regard, Figure 3 compares the mean square displacement of the 0.966 μm spheres in pure water and that in a mixture of 91% PG and 10% with that of 0.9 wt.% HASE polymer solutions in co-

solvents of water and PG of different proportions. The observed Brownian motion of the spheres intimately reflects the dynamics of the suspending medium. In the purely viscous solvents of PG/water mixture and/or water, the behavior is diffusive as expected; this is confirmed by the linear dependence of the mean square displacement with time. In the viscoelastic medium (with polymer), the behavior becomes sub-diffusive, $\langle \Delta r^2(t) \rangle \sim t^n$ with $n < 1$ as shown for the polymer solutions in all solvent composition. The effect of the co-solvent on the mean square displacement at shorter times seems to be very different from that at longer times. At longer times, the behavior of the polymer solution is controlled by the viscoelastic nature of the polymer. In this limit, the solution exhibits more elastic character as the water content of the solvent increases as evident from the lower $\langle \Delta r^2(t) \rangle$ in water-rich solvents as well as the lower dependence of $\langle \Delta r^2(t) \rangle$ on time. On the other hand, at short times, the behavior is controlled by the viscous nature of the medium and approaches that of the solvent. This can be noticed from the lower $\langle \Delta r^2(t) \rangle$ for polymer solutions in “PG-rich” solvent which can be attributed to the high viscosity of “PG-rich” solvents compared to that of water-rich solvents, (PG viscosity is about 40 times the viscosity of water). It should be pointed out that this very short time behavior can never be probed by conventional rheometers.

The behavior of the polymer solutions, as obtained from DWS, can be directly compared to that obtained by conventional mechanical rheometry through the transformation of $\langle \Delta r^2(t) \rangle$ to the creep compliance, $J(t)$, using equation 3. Figure 4 compares the creep compliance of 0.9wt.% HASE polymer solutions in different solvents obtained using tracer microrheology and mechanical rheometry. The effect of the solvent on the behavior of the

polymer solution can be seen from the lower compliance (in both mechanical rheometry and DWS measurements) for the polymer in water-rich than in “PG-rich” solvents. Figure 4 also reveals excellent qualitative agreement between the mechanical and DWS compliance. However, quantitatively the compliance obtained from the DWS measurements is always lower than that obtained from mechanical measurement using stress values in the linear viscoelastic region (LVE).

By decomposing the creep data using the Voigt model, the complex modulus (G^*) and thus the elastic (G') and viscous moduli can be obtained. This is illustrated in Figures 5 which reflects the advantage of DWS; data over a very wide frequency range (6 decades) is obtained. Figure 5b shows both G' and G'' for 0.9% HASE solution in PG14 and PG77 solvents. From the figure, we observe the difference in the behavior of the solution rheology in water-rich and “PG-rich” solvents. In the “PG-rich” solvent (PG77), the behavior corresponds to that of a viscous fluid with G'' dominating G' over the entire frequency range. On the other hand, in the water-rich solvent (PG14), the G' and G'' response is that of a typical viscoelastic material; at short times the material response is relatively elastic compared to the viscous response at longer times. These same features are obtained using mechanical rheometry as well. This is illustrated in Figure 6 which shows G' and G'' for a 0.9% HASE solution in PG14 and PG77 solvents.. These similar qualitative features seen in Figures 5 and 6 are a testament to the feasibility of DWS for probing the behavior of our complex associative polymers. These findings are in full accordance with the results of our previous study where hydrophobic interaction played a major role in the solution behavior in “water-rich” solvents. In contrast, the lack of hydrophobic association in “PG-rich” solvents

was evident from the similarity of the polymer dynamics in “PG-rich” solvent to the behavior of unmodified polymer analog with no hydrophobes⁵¹.

A systematic comparison of the data obtained using both DWS and mechanical rheometry is illustrated in Figures 7 which shows the frequency spectrum of both G' and G'' for a 0.9 wt.% polymer in PG14 and PG 77 solvents. We observe excellent qualitative agreement between the data obtained using DWS and that obtained from mechanical rheometry. Quantitatively, the moduli obtained from DWS measurements are consistently higher than those measured using traditional rheometry. This discrepancy between DWS and mechanical rheometry could arise from different factors including the range of validity of the Generalized Stokes-Einstein relation (GSER), the presence of structural inhomogeneity, and possible interactions between the probe particles and the viscoelastic medium, which may include absorption or depletion effects. The range of validity of the GSER has been the focus of recent publications^{39, 52-55}. Levine and Lubensky found that there is a large frequency range over which the GSER is valid in many systems. The upper frequency range is bounded by the inertial effects that typically become significant at frequencies higher than 1 MHz. and thus may be safely ignored. On the other hand, the lower frequency range is bounded by a characteristic frequency, ω_c , below which the effective decoupling of network and fluid dynamics becomes significant. An order of magnitude estimate of ω_c can be determined from the following relation³⁹:

$$\omega_c \simeq \frac{G \xi^2}{\eta R^2} \quad (4)$$

where G is the shear modulus and can be taken as $G^*(\omega=0)$, η is the solvent viscosity, ξ is the network mesh size and R is the probe particle radius. There is no good estimate

for the mesh size of our system, yet. The decoupling between the solvent and the network would be highly dependent on the solvent quality and is expected to be enhanced with “water-rich” solvents compared to “PG-rich” solvents.

To approximate the lower frequency limit, we consider the worst-case scenario, i.e., when the solvent is pure water. Since the G/η ratio is on the order of 100 s^{-1} , $G^*(\omega=0.01)=0.2 \text{ Pa}$ and $\eta=1 \text{ mPa}\cdot\text{s}$, a sphere radius that is 10 times larger than the mesh size gives an estimate for ω_c of about 1 Hz. On the other hand an estimate of 0.001 Hz would result in the case of PG91 as the solvent. Thus, the discrepancy between DWS and mechanical rheometry measurements cannot be fully attributed to the validity range of the GSER.

Another factor that may be responsible for the deviation between the DWS and the mechanical rheology measurements is the presence of local inhomogeneity in the system. This can be examined by changing the probe size and comparing the extracted rheological properties. In addition, changing the sphere size can provide information on the range of frequency over which the GSER is valid. Figure 8 shows the creep compliance obtained by DWS measurement of a 0.9% HASE polymer in water using PS spheres of different sizes. The data extracted using mid size spheres (0.511-0.966 μm) seem to collapse perfectly to a single master curve that is in an acceptable agreement with the data obtained from the mechanical rheology measurements. However, the data extracted using the smallest and the largest spheres show deviation. The agreement between the data obtained using mid size spheres illustrates both the validity of the GSER and the absence of any local inhomogeneity.

Close examination of Figure 8 shows that the data obtained using the smallest spheres

are still in good agreement with those obtained using the mid size sphere at times $<10^{-3}$ s. This would imply that the lower frequency limit where the GSER is valid for this size spheres is on the order of 100 Hz. By simple back calculation we would get an average mesh size on the order of 0.1 μm . The deviation in the case of the largest spheres may be attributed to inter-particle interactions or aggregation.

In general, the deviation between the data measured using DWS and mechanical rheometry could be attributed to the perturbation of the polymer matrix by the probe spheres or to measurement errors. For example, DWS requires independent measurement of ℓ^* (the distance at which the light becomes completely randomized); any error in the value of ℓ^* will affect the calculated mean square displacement. Based on these discussion, we can surmise that the GSER is valid when spheres of suitable sizes are used,; the microstructure of the polymer solution is insensitive to the probe size, and the decoupling between the solvent and the network does not play any significant role on the dynamics of the system. It is therefore possible that the discrepancy could be a result of actual difference between the micro- versus macro rheological properties.

6.3.2 Concentration Effects

Here, we change the polymer concentration and examine the effect of the polymer concentration on the dynamics of the polymer solution. The microstructure and thus the dynamics of HASE polymer solutions are known to be highly dependent on the polymer concentration and their behavior can go through many transitions within a limited range of concentrations⁵⁵. In this regard, we examine the effects of the polymer concentration on

the dynamics of the polymer solution using DWS. Figure 9 shows the mean square displacement of 0.966 μm sphere embedded in aqueous solutions of a HASE polymer with different concentrations. As observed from the figure, the motion of the spheres becomes slower with increasing polymer concentration. This behavior is expected since the medium viscosity and viscoelastic properties are enhanced by increasing the polymer concentration. Moreover, the same $\langle \Delta r^2(t) \rangle$ -time profile is observed for all polymer concentrations. This profile can be described as an initial subdiffusive behavior at short times followed by the development of a plateau at intermediate times and another subdiffusive behavior at very long times. The similarity in $\langle \Delta r^2(t) \rangle$ -time profiles, in spite of different polymer concentrations, indicates that the dynamics probed by the spheres are of the same origin. A similar $\langle \Delta r^2(t) \rangle$ -time profile has recently been observed in a micellar soft crystal structure of a triblock copolymer of polyethylene oxide-polypropylene oxide-polyethylene oxide (PEO-PPO-PEO) known as PluronicTM 56. In our figure, there are however two minor differences in the $\langle \Delta r^2(t) \rangle$ -time profile for different polymer concentrations. First, the onset of the plateau and the final subdiffusive regions shift to shorter times as the polymer concentration increase. Second, the slope of the short time subdiffusive region decreases with polymer concentration. These differences could be attributed to the change in relaxation time as the polymer concentration increases. Indeed solutions with higher polymer concentration would have slower relaxation processes, because of the enhancement in the system viscoelasticity.

The $\langle \Delta r^2(t) \rangle$ -time profile can be explained as follows. At short times, the spheres diffuse in the viscoelastic media (initial subdiffusive region) before they are entrapped inside the polymer network (the plateau region), and finally escape after the relaxation of the

network (final subdiffusive region). It should be noted that although our polymer and soft crystal PluronicTM copolymers exhibit similar $\langle \Delta r^2(t) \rangle$ -time profiles, the relaxation mechanism is very different for them. While the PluronicTM copolymers relax by the micellar rearrangement⁵⁶, our polymer system relaxes by disengagement of associating sequencing.

Figure 10 shows the creep compliance data obtained from DWS measurements for different polymer concentrations and the analogous data obtained from stress-controlled rheometry. The figure reveals one advantage of combining data from DWS and mechanical rheometry measurements, i.e., data over a very wide range of time scale (8 decades) can be obtained. Note also that while mechanical rheometry measurements can never probe the short time behavior, DWS can probe both the long time and short time behavior by using cells of variable width. Figure 10 reveals excellent qualitative and good quantitative agreement between the compliance data for various concentrations.

To further examine the feasibility of the DWS technique and its ability to correctly probe the dynamics of the viscoelastic medium, the creep compliance was converted to the corresponding dynamic moduli. Figure 11 shows the elastic and viscous moduli as functions of angular frequency for the aqueous polymer solutions at different concentrations. As seen from Figure 11, and as expected from the $J(t)$ comparison, there is excellent qualitative agreement between the moduli extracted from the DWS data with that from mechanical rheometry, regardless of the polymer concentration.

6.3.2.1 Scaling behavior

The concentration dependence of material functions often reveals valuable

structural information about a polymer. The rheology of associative polymers are usually strongly dependent on concentration such that they can undergo several structural transitions. At low concentrations, intramolecular associations are the dominant hydrophobic interaction mode; as the concentration increases some of the intramolecular associations are converted to intermolecular association. At high enough concentrations, the intermolecular associations are the dominant mode of interaction. In this regard, we examine the high frequency elastic modulus (G') and the creep compliance $J(t)$ as a function of concentration in Figure 12. We find both these material functions to exhibit power-law behavior within the concentration regime studied. In this figure, the high frequency elastic modulus is taken at a fixed angular frequency of 10 rad/s; this is bounded by the highest frequency accessible by the mechanical rheometer for the lowest concentration. $J(t)$, on the other hand, was taken at a time of 50 seconds as bounded by the longest time accessible by the DWS technique. The error bars in the figure represent the standard deviation for the DWS and mechanical rheometry data. As observed from Figure 12, G' and $J(t)$ scale as $G' \sim c^{1.7}$ and $J(t) \sim c^{-1.8}$. It is worth mentioning that while the scaling of the elastic modulus at various frequencies with concentration yield the same scaling exponent, scaling of the $J(t)$ at different times yield scaling exponents that vary from -1.4 at short times to -1.9 at long times. The observed dependence of G' on concentration is somewhat weaker than the theoretical prediction of the sticky reptation model⁵⁶. The sticky reptation model predicts a scaling exponent of 2.2 for good solvent that increases slightly to 2.3 in θ solvents. Nevertheless, different exponents have been reported for similar associative polymers. English *et al*⁵⁷ reported scaling exponents 1.4, 2.8 and 6.5 for HASE polymers with C_8 , C_{16} and C_{20} hydrophobes, respectively. In fact, we obtained a

scaling exponent of 1.8 for several HASE polymers that is in full agreement with the 1.7 obtained here⁵⁸. The scaling exponent 1.8 observed for $J(t)$ is similar to that observed by Ng et. al for Hydrophobically modified Ethoxylate Urethane (HEUR) polymers⁵⁹.

Figure 12 also shows the scaling of the longest relaxation time (τ_{long}), defined as the reciprocal of the frequency at which G' and G'' crossover, versus the polymer concentration. τ_{long} values in the plot are the average of τ_{long} obtained from DWS and mechanical rheometry measurements and the error bars represent the standard deviation. The small error bars demonstrate the ability of DWS to accurately probe the dynamics of HASE polymers. The scaling shows that $\tau_{\text{long}} \sim c^{0.84}$. This scaling along with G' scaling suggests a scaling exponent 2.6 for the steady shear viscosity (η) based on the transient network theory prediction⁶⁰, $\eta = G_{\infty} \tau$. This exponent is in full agreement with that obtained in our laboratory for similar polymers⁵⁸.

6.3.2.2 Time dependent Diffusion Coefficient

The mean square displacement data can be further analyzed in terms of a time dependent diffusion coefficient, $D(t)$, defined as:

$$D(t) = \frac{\langle \Delta r^2(t) \rangle}{6t} \quad (4)$$

Figure 13 shows the evolution of $D(t)$ for different polymer concentrations. Regardless of the concentration, the diffusion coefficient decreases continuously and the motion of the spheres cannot be described by a single diffusion coefficient. Higher polymer concentrations result in a lower diffusion coefficient, as expected, due to the increase in the solution viscoelasticity.

At very short times and small length scales, the spheres are subjected to small amplitude, high frequency lateral fluctuation of the polymer network⁴¹. In this limit, the medium behavior is dominated by the glassy nature of the polymer and the diffusion coefficient approaches that of the spheres in pure water (D_0), $0.46 \mu\text{m}^2/\text{s}$. At long times or long length scales, the medium behavior is dominated by its elastic nature and microspheres becomes elastically trapped by the network structures. Therefore, a very small diffusion coefficient is expected at long times and higher concentrations. The very small diffusion coefficient, up to 7 order of magnitude lower than the diffusion coefficient of the $0.966 \mu\text{m}$ spheres in water, correspond to near arrest of the sphere by the network⁴¹. Moreover, from the values of the diffusion coefficient as presented in Figure 13, one would expected the sphere size to be much larger compared to the network mesh. Hence, if the sphere size were smaller than the network mesh, a diffusion coefficient similar to D_0 would be expected.

Information about the dynamic of the medium at different length scales can be extracted from the behavior of the diffusion coefficient as function of the sphere displacement, $\sqrt{\langle \Delta r^2(t) \rangle}$ as shown in Figure 13b. This figure shows three distinct dynamical regions for all concentrations studied. In the first region at short displacements, the diffusion coefficient shows a near plateau behavior. This region is followed by a sharp downward transition and finally a near plateau region is established at longer displacements. The length scale for the sharp transition decreases from 10 to 2.5 nm as the concentration is increased from 1 to 5%. Similar behavior has been reported for an actin filaments network⁴¹. The dynamics in the early near plateau region corresponds to a behavior dominated by the hydrodynamic interactions. As the spheres approach the polymer network, they

experience the dynamics of the elastic medium and finally become entrapped in the elastic cage formed by the network.

6.4 Conclusions

In this study, we use diffusing wave spectroscopy to probe the structural changes induced by the change of solvent quality and polymer concentration on a HASE associative polymer. In addition, we compare DWS results to those obtained using conventional rheometry. We find that cosolvents of water and propylene glycol (PG) impart significant changes in rheology depending on the composition. In “water-rich” solvents, the polymer behavior is dominated by hydrophobic associations; in contrast, in “PG-rich” solvents, the solution behavior is similar to that of an unmodified polymer without hydrophobes. In addition, comparison of DWS results with those obtained using conventional rheometry reveals excellent qualitative agreement. Further, DWS provided information on the polymer dynamics over a very wide frequency range, including high frequencies that are not accessible by mechanical rheometry. Finally, the concentration dependence of the creep compliance, high-frequency elastic modulus and relaxation time obtained using DWS or rheometry reveal power-law dependence with the same exponents regardless of the technique. However, the power-law exponents were different for the different materials functions, and are discussed in light of theoretical predictions and other available experimental results. These results taken together suggest diffusing wave spectroscopy (DWS) as a viable technique to probe the dynamics of associative polymers.

6.5 References

1. Tirtaatmadja; V. T.; Tam, K. C.; Jenkins, R. D.; Bassett, D. R. Stability of a Model Alkali-Soluble Associative Polymer in the Presence of a Weak and a Strong Base, *Colloid and Polymer Science* **1999**, 277, 276-281.
2. Rich, A. F.; Benes, P. C.; Adams, L. E. Combinations of Polymeric Associative Thickeners for Aqueous Latex Paints. US Patent 4735981, 1988.
3. Jones, C. E.; Reeve, P. F. D. Mixed Surfactant and Hydrophobically-Modified Polymer Compositions for Thickeners for Aqueous Systems. EP Patent 875557, 1998.
4. Jenkins, R. D.; Bassett, D. R.; Shay, G. D. Water-soluble Polymers Containing Complex Hydrophobic Groups. US Patent 5292828, 1994.
5. Harrington, J. C.; Zhang, H. T. Using Hydrophobically Associative Polymers in Preparing Cellulosic Fiber Compositions. WO Patent 0140578, 2001.
6. Marchant, N. S.; Yu, S. Rheology Modifying Copolymer Composition. US Patent 06433061, 2002.
7. Brooks, A.; Du Reau, C. M. A. Cleansing Compositions Containing Polar Oils and Skin Conditioners. WO Patent 9800495, 1998.
8. Herd, H. E.; Williams, R. Preparation and Properties of Shear-thinning, Thickened Cleaning Composition. GB Patent 2346891, 2000.
9. Alan, B.; Du Reau, C. M. A. Cleansing Compositions. US Patent 6191083, 2001.
10. Vorobyova, O.; Winnik, M. A. Determination of Aggregation Numbers in Aqueous Solutions of Hydrophobically Modified Polymers by Fluorescent Probe Techniques. *In Associative Polymers in Aqueous Media; ACS*, **2000**; Vol. 765, pp 143-162.
11. Didier, C.; Serge, F.; Anne-Marie, P. UV-Photoprotecting Emulsions Comprising Micronized Insoluble Screening Agents and Associative Polymers. US Patent 6409998, 2002.
12. Ewbank, E.; Collard, C.; Tummers, D.; Breuer, E.; Thibert, E. Liquid Fabric Softening Compositions Containing a Fatty Alcohol Ethoxylate diurethane Polymer as a Thickener. US Patent 6001797, 1999.
13. Alfons, C. R. A.; Madeleine, D. B. F. J.; Jean, H. B. A. Fabric Softener Compositions. US Patent 6020304, 1999.

14. Jenkins, R. D. B., D. R.; Lightfoot, R. H.; Boluk, M. Y. Glycol-Based Aircraft Anti-Icing Fluids Thickened by Associative Polymers Containing Hydrophobe-Bearing Macromonomers. US Patent 5681882, 1997.
15. Jenkins, R. D. B., D. R.; Lightfoot, R. H.; Boluk, M. Y. Aircraft Anti-Icing Fluids Thickened by Associative Polymers. WO Patent 9324543, 1993.
16. Carder, C. H.; Garska, D. C.; Jenkins, R. D.; McGuinness, M. J. Aircraft Deicing/Anti-Icing Fluids Thickened by Associative Polymers. US Patent 5708068, 1998.
17. Carder, C. H.; Garska, D. C.; Jenkins, R. D.; McGuinness, M. J. Aircraft Deicing/Anti-Icing Universal Fluids. JP Patent 10237428, 1998.
18. Pine, D. J.; Weitz, D. A.; Chaikin, P. M.; Herbolzheimer, E. Diffusing-Wave Spectroscopy, *Phys. Rev. Lett.* **1988**, 60, 1134-1137.
19. Mason, T. G.; Ganesan, K.; van Zanten, J. H.; Wirtz, D.; Kuo, S. C. Particle Tracking Microrheology of Complex Fluids, *Physical Review Letters* **1997**, 79, 3282-3285.
20. Nisato, G.; Hebraud, P.; Munch, J. P.; Candau, S. J. Diffusing-Wave-Spectroscopy Investigation of Latex Particle Motion in Polymer Gels, *Phys. Rev. E: Stat. Phys., Plasmas, Fluids, Relat. Interdiscip. Top.* **2000**, 61, 2879-2887.
21. Dasgupta, B. R.; Tee, S. Y.; Crocker, J. C.; Frisken, B. J.; Weitz, D. A. Microrheology of Polyethylene Oxide using Diffusing Wave Spectroscopy and Single Scattering, *Physical Review E: Statistical, Nonlinear, and Soft Matter Physics* **2002**, 65, 051505/051501-051505/051510.
22. Solomon, M. J.; Lu, Q. Rheology and Dynamics of Particles in Viscoelastic Media, *Current Opinion in Colloid & Interface Science* **2001**, 6, 430-437.
23. Crocker, J. C.; Valentine, M. T.; Weeks, E. R.; Gisler, T.; Kaplan, P. D.; Yodh, A. G.; Weitz, D. A. Two-Point Microrheology of Inhomogeneous Soft Materials, *Physical Review Letters* **2000**, 85, 888-891.
24. Schmitt, C.; Sanchez, C.; Lamprecht, A.; Renard, D.; Lehr, C. M.; de Kruif, C. G.; Hardy, J. Study of .Beta.-lactoglobulin/acacia Gum Complex Coacervation by Diffusing-Wave Spectroscopy and Confocal Scanning Laser Microscopy, *Colloids Surf., B* **2001**, 20, 267-280.

25. Ladd, A. J. C.; Gang, H.; Zhu, J. X.; Weitz, D. A. Temporal and Spatial Dependence of Hydrodynamic Correlations: Simulation and Experiment, *Physical Review E: Statistical Physics, Plasmas, Fluids, and Related Interdisciplinary Topics* **1995**, *52*, 6550-6572.
26. Ladd, A. J. C.; Gang, H.; Zhu, J. X.; Weitz, D. A. Time-dependent Collective Diffusion of Colloidal Particles, *Physical Review Letters* **1995**, *74*, 318-321.
27. Rojas-Ochoa, L. F.; Romer, S.; Scheffold, F.; Schurtenberger, P. Diffusing Wave Spectroscopy and Small-angle Neutron Scattering from Concentrated Colloidal Suspensions, *Physical Review E: Statistical, Nonlinear, and Soft Matter Physics* **2002**, *65*, 051403/051401-051403/051408.
28. Mason, T. G. Estimating the Viscoelastic Moduli of Complex Fluids using the Generalized Stokes-Einstein equation, *Rheologica Acta* **2000**, *39*, 371-378.
29. Mason, T. G.; Gang, H.; Weitz, D. A. Diffusing-Wave-Spectroscopy Measurements of Viscoelasticity of Complex Fluids, *Journal of the Optical Society of America A: Optics, Image Science, and Vision* **1997**, *14*, 139-149.
30. Knaebel, A. S., R.; Munch, J. P.; Candau, S. J. Structural and Rheological Properties of Hydrophobically Modified Alkali-Soluble Emulsion Solutions, *Journal of Applied Polymer Science: Part B: Polymer Physics* **2002**, *40*, 1985-1994.
31. Maret, G. Diffusing-Wave Spectroscopy, *Curr. Opin. Colloid Interface Sci.* **1997**, *2*, 251-257.
32. Fawcett, A.; Uhomobhi, J. O. Diffuse Wave Spectroscopy Finds that PEG Delays the Aging of a Foam, *Polym. Prepr. (Am. Chem. Soc., Div. Polym. Chem.)* **2001**, *42*, 442-443.
33. Earnshaw, J. C.; Wilson, M. A Diffusing Wave Spectroscopy Study of Constrictive Flow of Foam, *J. Phys. II* **1996**, *6*, 713-722.
34. Earnshaw, J. C.; Jaafar, A. H. Diffusing-Wave Spectroscopy of a Flowing Foam, *Phys. Rev. E: Stat. Phys., Plasmas, Fluids, Relat. Interdiscip. Top.* **1994**, *49*, 5408-5411.
35. Cohen-Addad, S.; Hohler, R. Bubble Dynamics Relaxation in Aqueous Foam Probed by Multispeckle Diffusing-Wave Spectroscopy, *Phys. Rev. Lett.* **2001**, *86*, 4700-4703.
36. Stark, H.; Kao, M. H.; Jester, K. A.; Lubensky, T. C.; Yodh, A. G.; Collings, P. J. Light Diffusion and Diffusing-Wave Spectroscopy in Nematic Liquid Crystals, *J. Opt. Soc. Am. A* **1997**, *14*, 156-178.

37. Rufener, K.; Palmer, A.; Xu, J.; Wirtz, D. High-Frequency Dynamics and Microrheology of Macromolecular Solutions Probed by Diffusing Wave Spectroscopy: the Case of Concentrated Solutions of F-actin, *Journal of Non-Newtonian Fluid Mechanics* **1999**, 82, 303-314.
38. Schnurr, B. Semiflexible Biopolymers: Microrheology and Single Filament Condensation, Ph.D. Dissertation, Univ. of Michigan, Ann Arbor, MI, 2000.
39. Schnurr, B.; Gittes, F.; MacKintosh, F. C.; Schmidt, C. F. Determining Microscopic Viscoelasticity in Flexible and Semiflexible Polymer Networks from Thermal Fluctuations, *Macromolecules* **1997**, 30, 7781-7792.
40. Xu, J.; Viasnoff, V.; Wirtz, D. Compliance of Actin Filament Networks Measured by Particle-Tracking Microrheology and Diffusing Wave Spectroscopy, *Rheol. Acta* **1998**, 37, 387-398.
41. Xu, J.; Palmer, A.; Wirtz, D. Rheology and Microrheology of Semiflexible Polymer Solutions: Actin Filament Networks, *Macromolecules* **1998**, 31, 6486-6492.
42. Mason, T. G.; Gisler, T.; Kroy, K.; Frey, E.; Weitz, D. A. Rheology of F-actin Solutions Determined from Thermally Driven Tracer Motion, *J. Rheol.* **2000**, 44, 917-928.
43. Furst, E. M.; Gast, A. P. Particle Dynamics in Magnetorheological Suspensions using Diffusing-Wave Spectroscopy, *Phys. Rev. E: Stat. Phys., Plasmas, Fluids, Relat. Interdiscip. Top.* **1998**, 58, 3372-3376.
44. van Zanten, J. H.; Rufener, K. P. Brownian Motion in a Single Relaxation Time Maxwell Fluid, *Phys. Rev. E: Stat. Phys., Plasmas, Fluids, Relat. Interdiscip. Top.* **2000**, 62, 5389-5396.
45. Amin, S.; Kermis, T. W.; van Zanten, R. M.; Dees, S. J.; van Zanten, J. H. Concentration Fluctuations in CTAB/NaSal Solutions, *Langmuir* **2001**, 17, 8055-8061.
46. Vasbinder, A. J.; van Mil, P. J. J. M.; Bot, A.; de Kruif, K. G. Acid-Induced Gelation of Heat-Treated Milk Studied by Diffusing Wave Spectroscopy, *Colloids Surf., B* **2001**, 21, 245-250.
47. Dalgleish, D. G.; Horne, D. S. Different Coagulation and Gelation Modes of Casein Micelles Followed by Diffusing Wave Spectroscopy, *Protein Interact., Symp. 201st Annu. Meet. Am. Chem. Soc.* **1992**, 87-101.

48. Shay, G. D.; Kail, J. E. Alkali-Soluble Latex Thickener. US Patent 4514552, 1985.
49. Weitz, D. A.; Pine, D.J. Diffusing-Wave Spectroscopy. In *Dynamic Light Scattering: the Method and Some Applications*; Oxford University Press: Oxford, 1993; Vol. 60, 652-720. Ferry, J. D. Viscoelastic Properties of Polymers, Third ed.; John Wiley & Sons, Inc.: New York, 1980.
50. Abdala, A. A.; Olesen, K.; Khan, S. A. Solution Rheology of Hydrophobically Modified Associative Polymers: Solvent Quality and Hydrophobic Interactions, *submitted to J. Rheol.* **2002**.
51. Levine, A. J.; Lubensky, T. C. One- and Two-Particle Microrheology, *Phys. Rev. Lett.* **2000**, 85, 1774-1777.
52. Levine, A. J.; Lubensky, T. C. Response Function of a Sphere in a Viscoelastic Two-Fluid Medium, *Phys. Rev. E: Stat., Nonlinear, Soft Matter Phys.* **2001**, 63, 041510/041511-041510/041512.
53. Levine, A. J.; Lubensky, T. C. Two-Point Microrheology and the Electrostatic Analogy, *Physical Review E: Statistical, Nonlinear, and Soft Matter Physics* **2002**, 65, 011501/011501-011501/011513.
54. Rubinstein, M., Semenov, A. N.,. Dynamic of Entangled Solution of Associating Polymers, *Macromolecules* **2001**, 34, 1058-1068.
55. Amin, S. Brownian Motion in Viscoelastic Media, Ph. D. Dissertation, North Carolina State University, Raleigh, NC, 2002.
56. English, R. J.; Gulati, H. S.; Jenkins, R. D.; Khan, S. A. Solution Rheology of a Hydrophobically Modified Alkali-Soluble Associative Polymer, *Journal of Rheology* **1997**, 41, 427-444.
57. Abdala, A. A.; Olesen, K.; Wu, W.; Khan, S. A. Effect of Polymer Composition on Microstructure and solution Rheology of Associative Polymers, *to be published*.
58. Ng, W. K.; Tam, K. C.; Jenkins, R. D. Lifetime and Network Relaxation Time of a HEUR-C20 Associative Polymer System, *J. Rheol.* **2000**, 44, 137-147.

Table 1. Solvent's composition, solubility parameter components and solubility parameter.

Solvent	PG, wt.%	δ_d MPa ^{0.5}	δ_p MPa ^{0.5}	δ_H MPa ^{0.5}	δ MPa ^{0.5}
Water	0	12.3	31.3	34.2	47.9
PG14	14	12.9	28.0	32.7	45.0
PG23	23	13.3	26.0	31.9	43.2
PG32	32	13.7	23.7	31.1	41.5
PG46	46	14.3	20.5	29.7	38.7
PG64	64	15.1	16.2	27.8	35.6
PG77	77	15.7	12.9	26.6	33.3
PG91	91	16.4	9.4	25.2	31.5

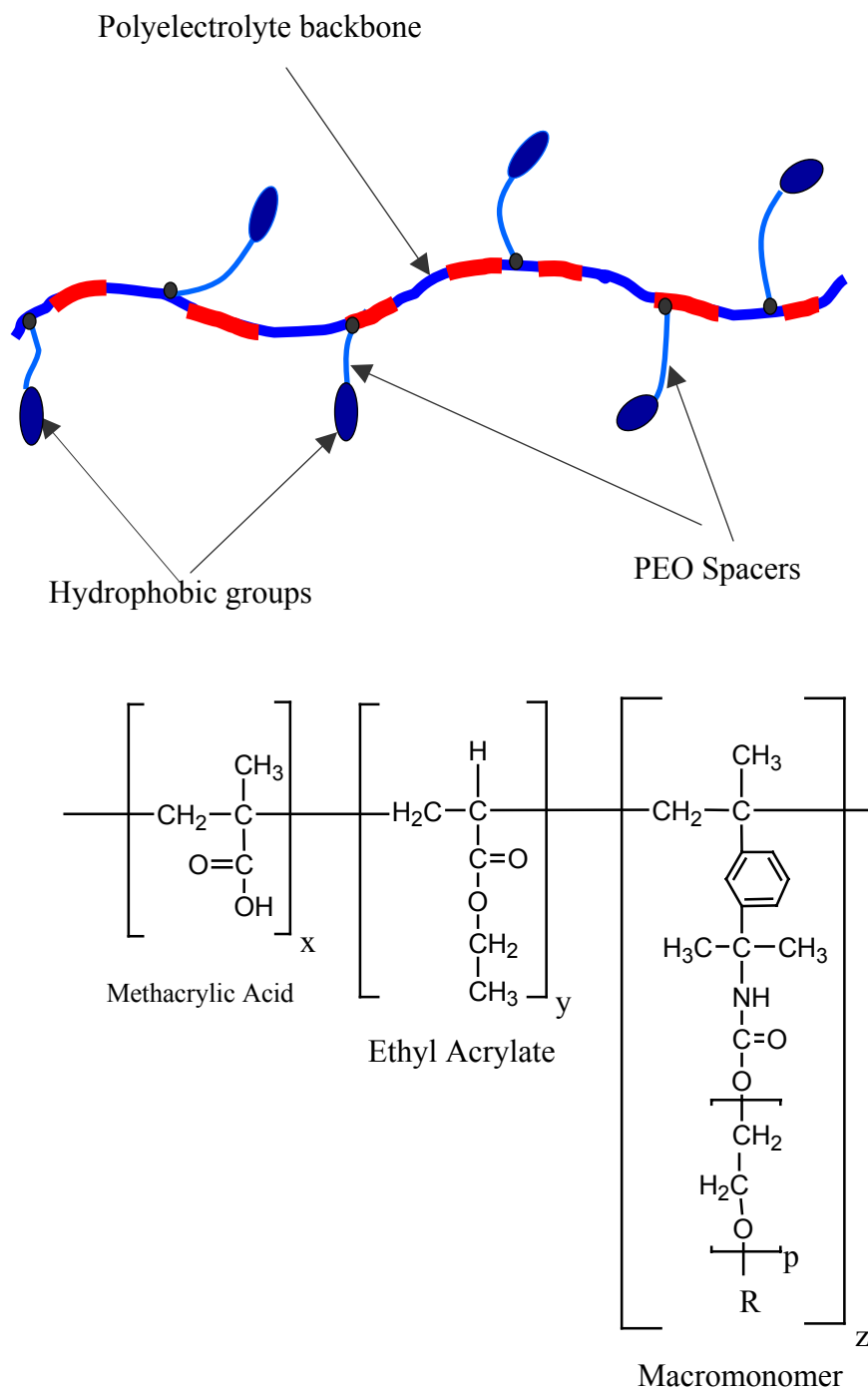


Figure 1. Schematic representation of the architecture of a typical HASE polymer and its molecular structure. Here, $p=40$ and R correspond to $C_{22}H_{44}$; $x/y/z = 43.57/56.21/0.22$ by mole.

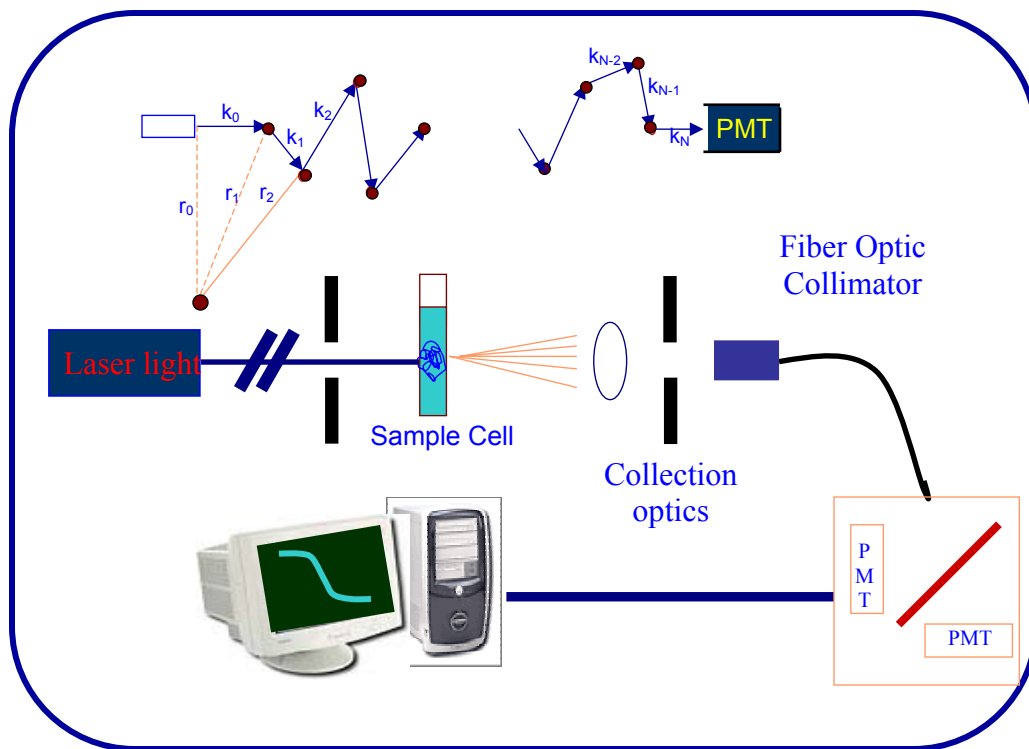


Figure 2. Diffusing wave spectroscopy (DWS) experimental setup in the transmission mode. The beam is focused and incident upon flat scattering cell containing the sample and spherical optical probes. The light is multiply scattered and collected by two photomultiplier tubes.

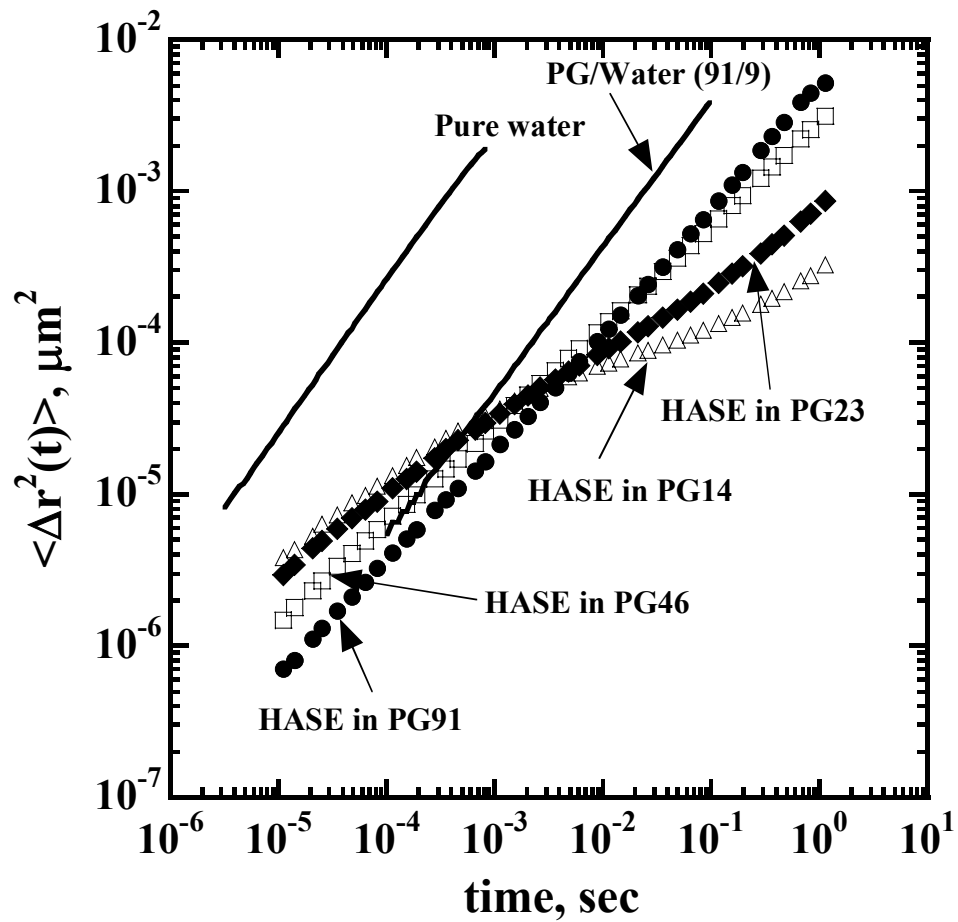


Figure 3. Evolution of the mean square displacement for water, PG/water 91/9 (w/w) mixture, and 0.9% HASE polymer in PG/water co-solvents at different PG ratios.

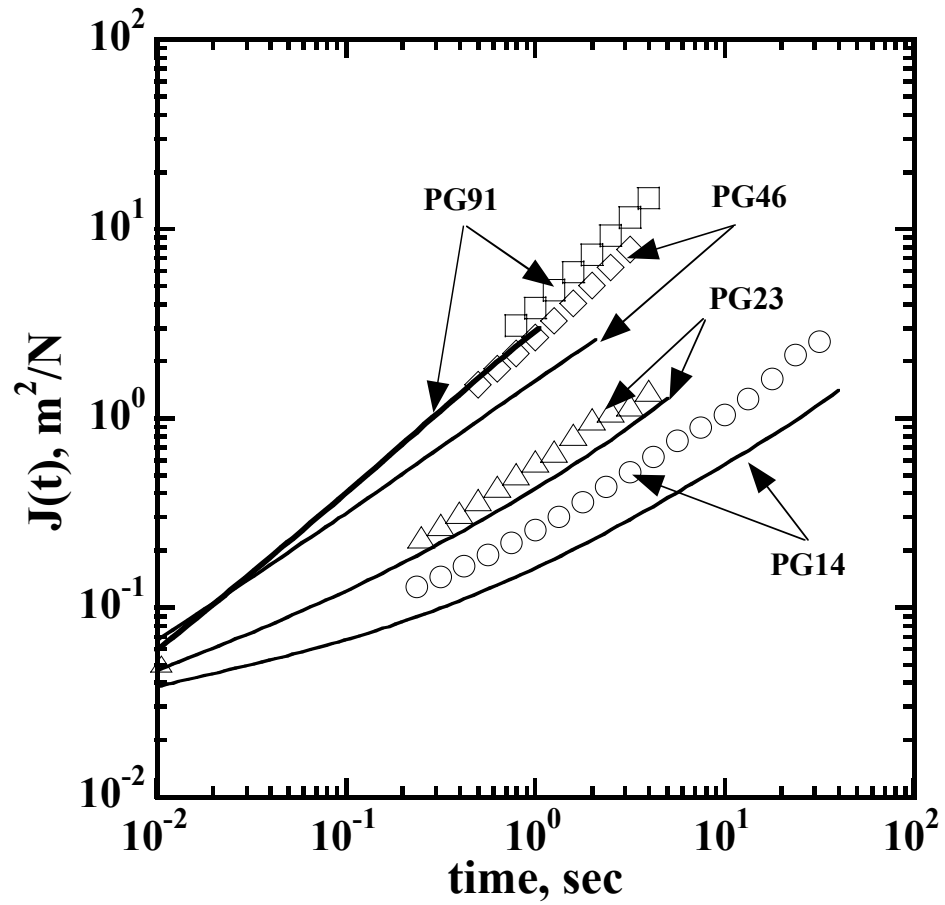


Figure 4. Comparison of the creep compliance obtained from mechanical rheometry (symbols) and tracer microrheology (lines) for 0.9% HASE polymer in PG/water co-solvents at different PG ratios.

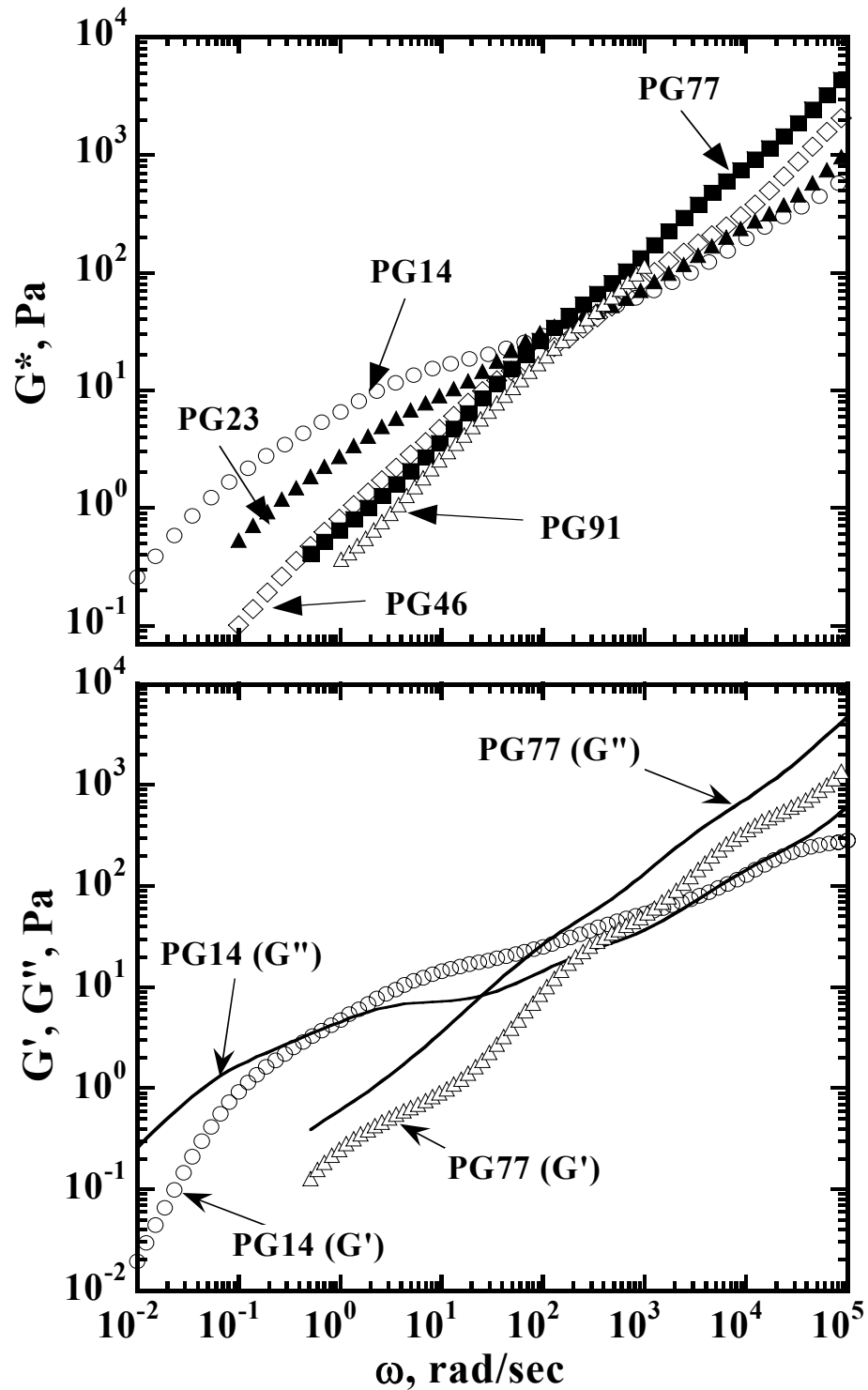


Figure 5. Frequency dependence of a) the complex modulus, G^* , and b) the elastic (G') and viscous (G'') moduli obtained from tracer microrheology for 0.9% HASE polymer solutions in PG/water cosolvent with different PG ratios.

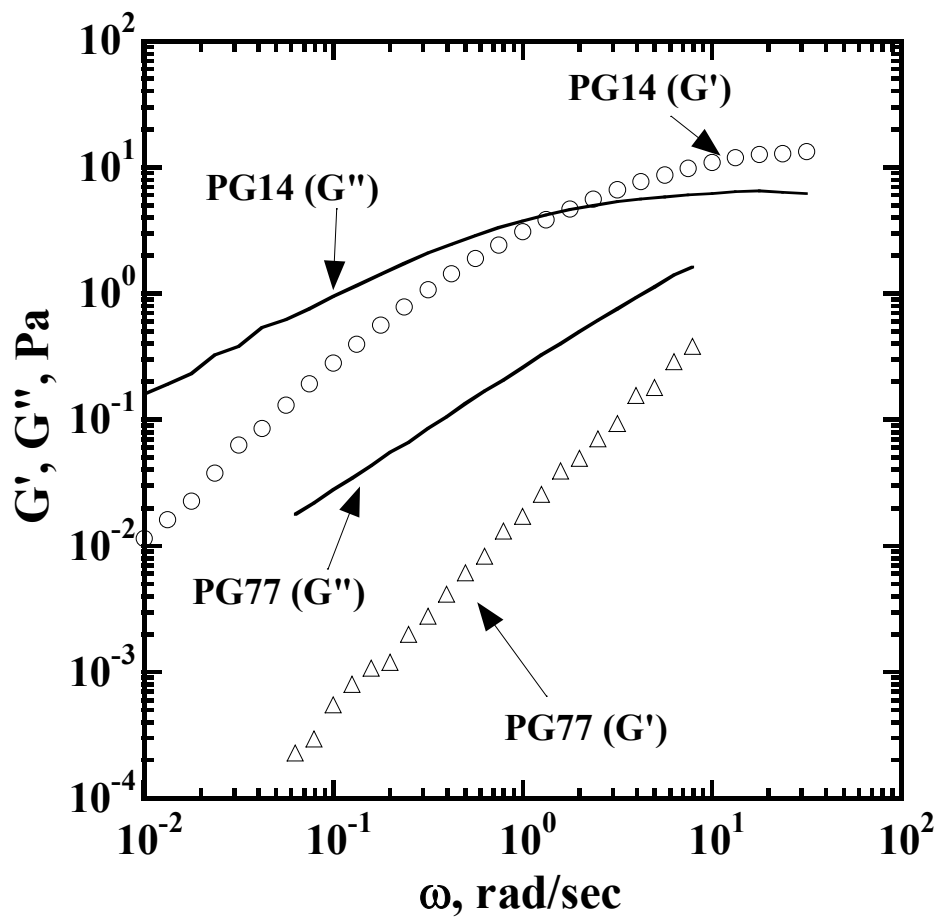


Figure 6. Frequency dependence of the elastic (G') and viscous (G'') moduli obtained from mechanical rheometry measurements for 0.9% HASE polymer solutions in PG/water co-solvent at different PG ratios.

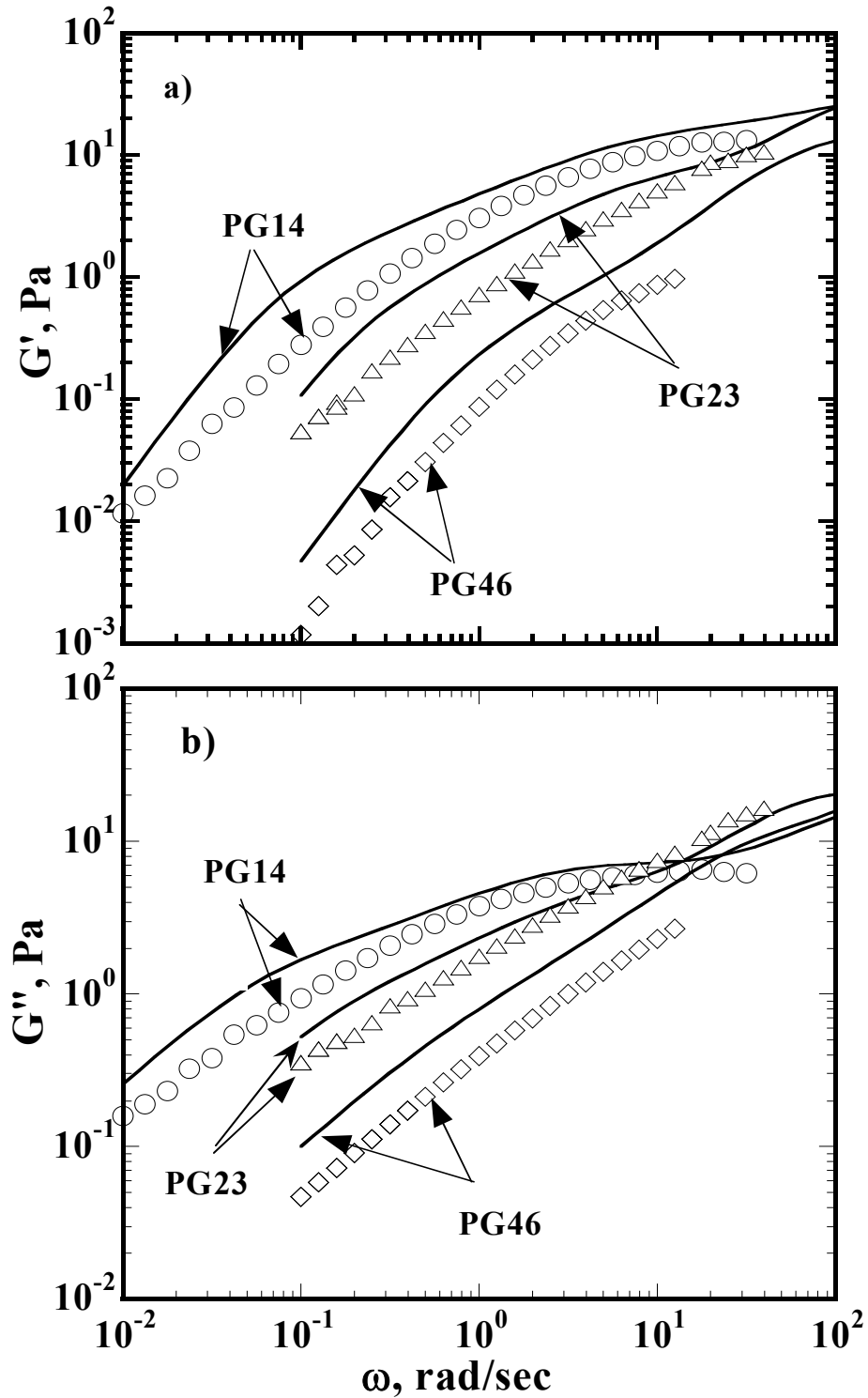


Figure 7 Comparison of a) elastic (G') and b) viscous (G'') moduli obtained from mechanical rheometry (symbols) and tracer microrheology (lines) for 0.9% HASE polymer in PG/water co-solvent at different PG ratios.

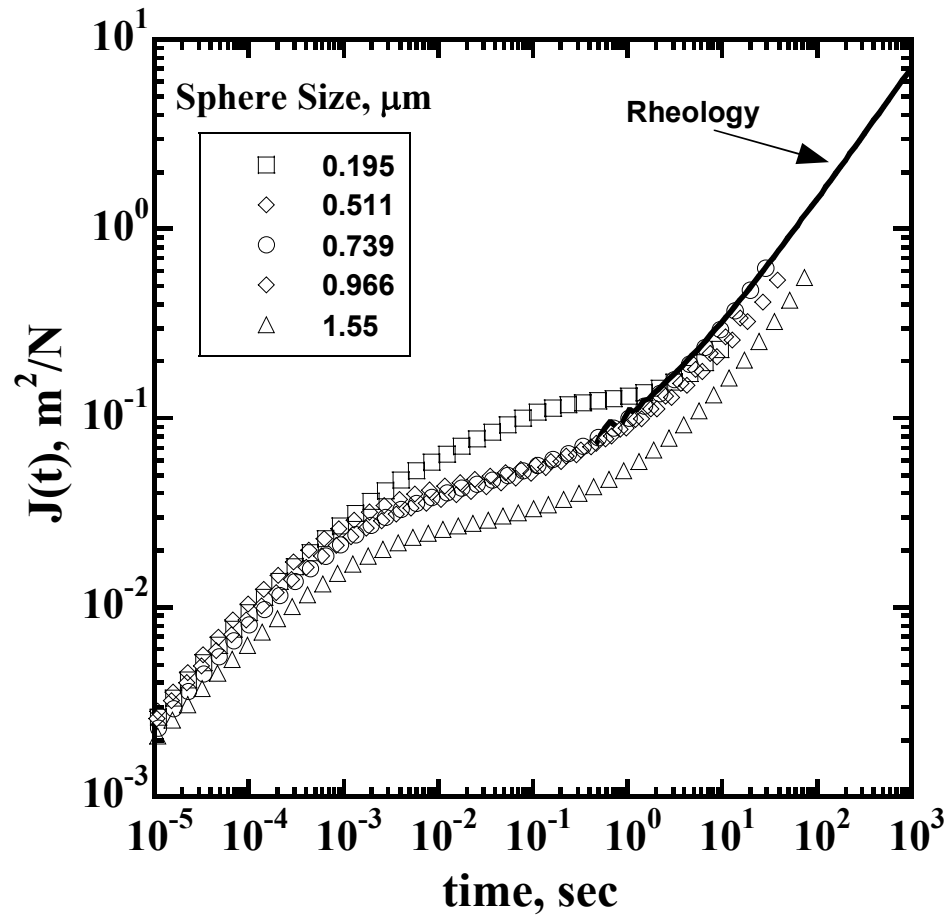


Figure 8. Comparison of the creep compliance obtained from tracer microrheology using different sphere sizes embedded in 0.9% aqueous polymer solution. The line represents the creep compliance obtained from mechanical rheometry measurement.

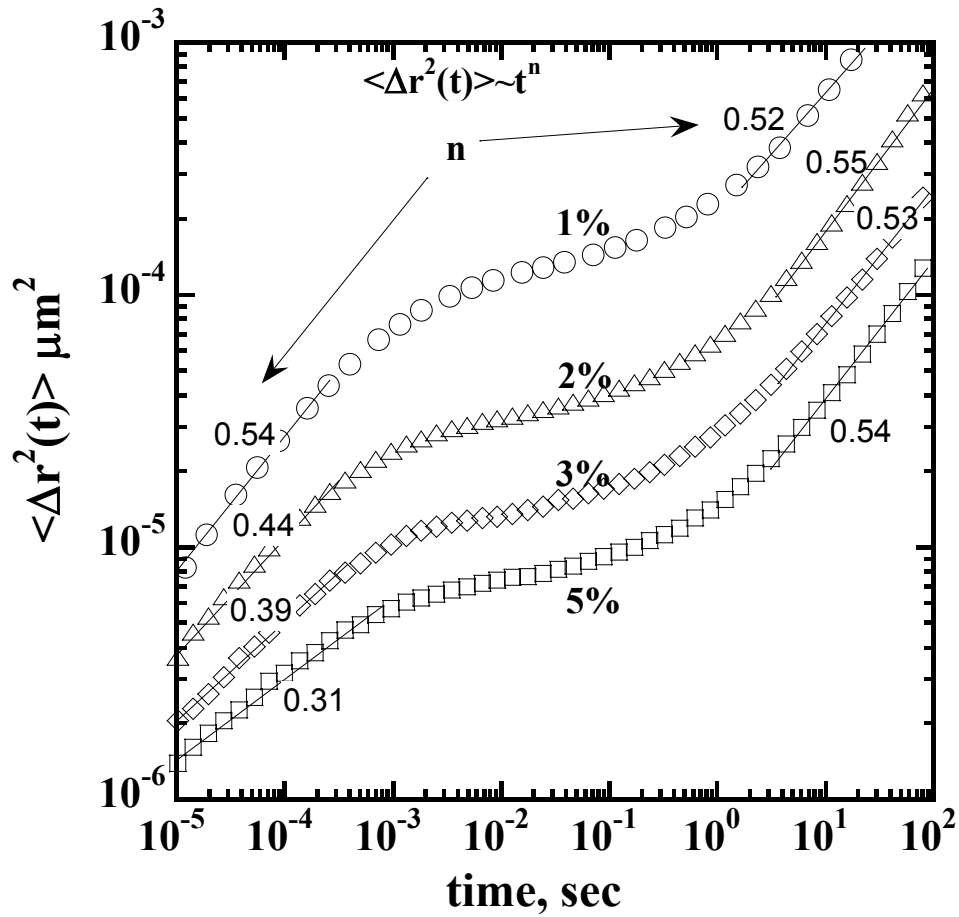


Figure 9. Evolution of the mean square displacement of 0.996 μm PS spheres in aqueous solution of HASE polymer at different concentrations.

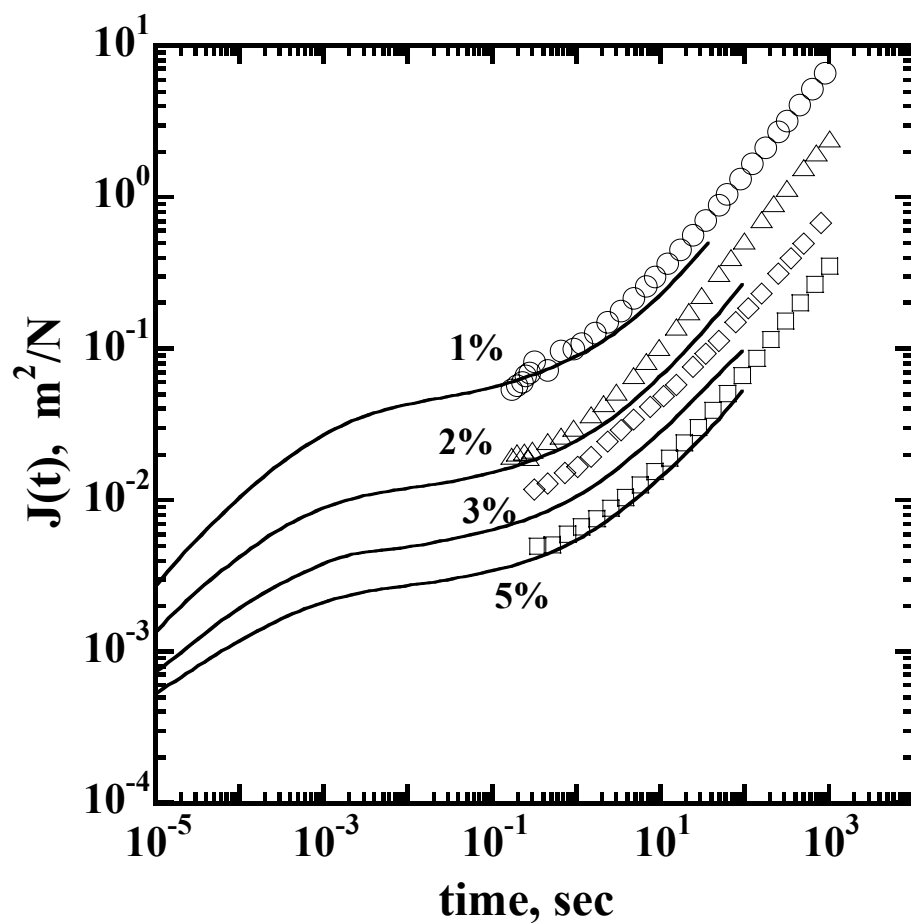


Figure 10. Comparison of the creep compliance obtained from mechanical rheometry (symbols) and tracer microrheology (lines) for aqueous solution of HASE polymer at different concentrations.

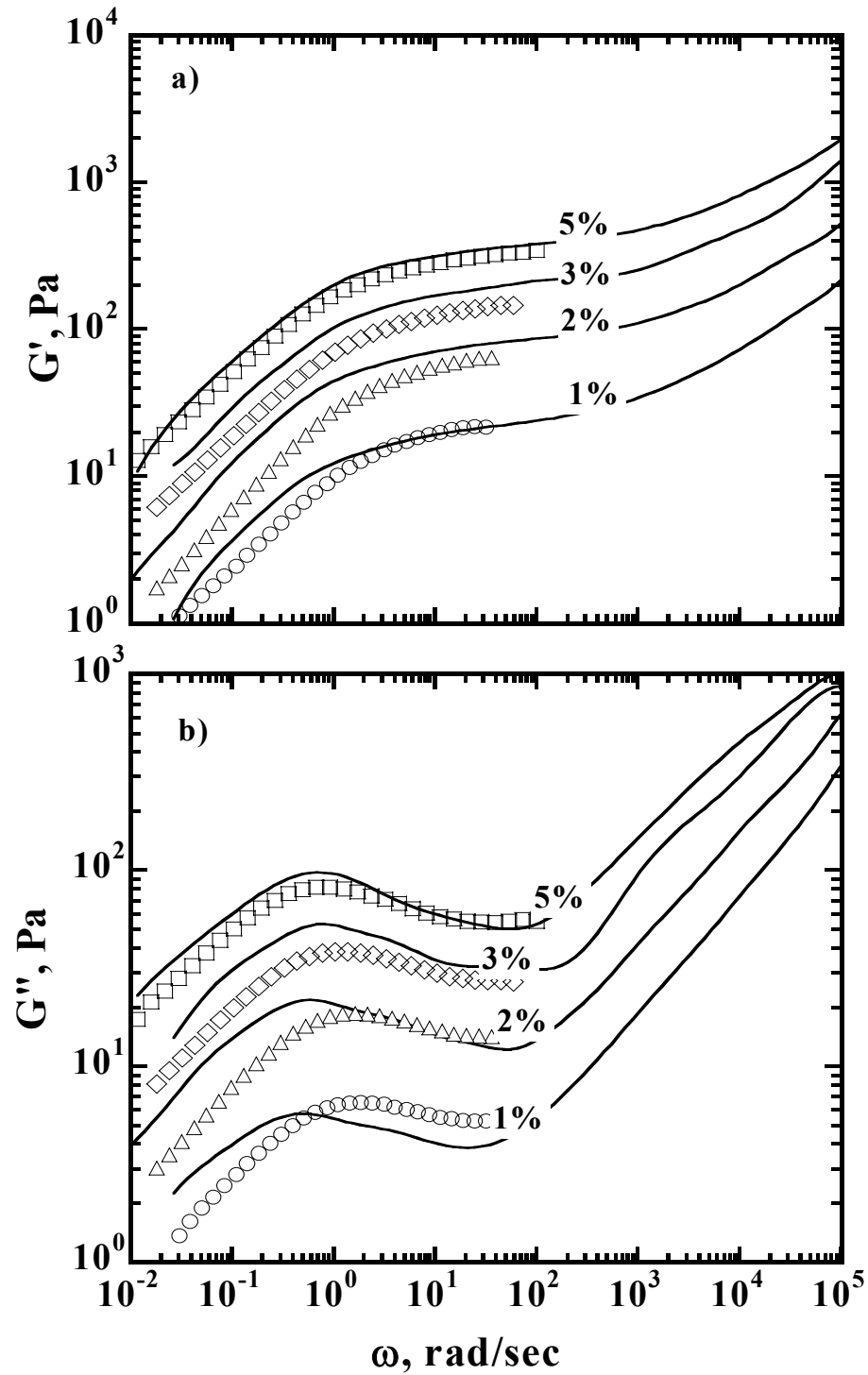


Figure 11. Comparison of a) the elastic (G') and b) the viscous (G'') moduli obtained from mechanical rheometry (symbols) and tracer microrheology (lines) for aqueous solution of HASE polymer at different concentrations.

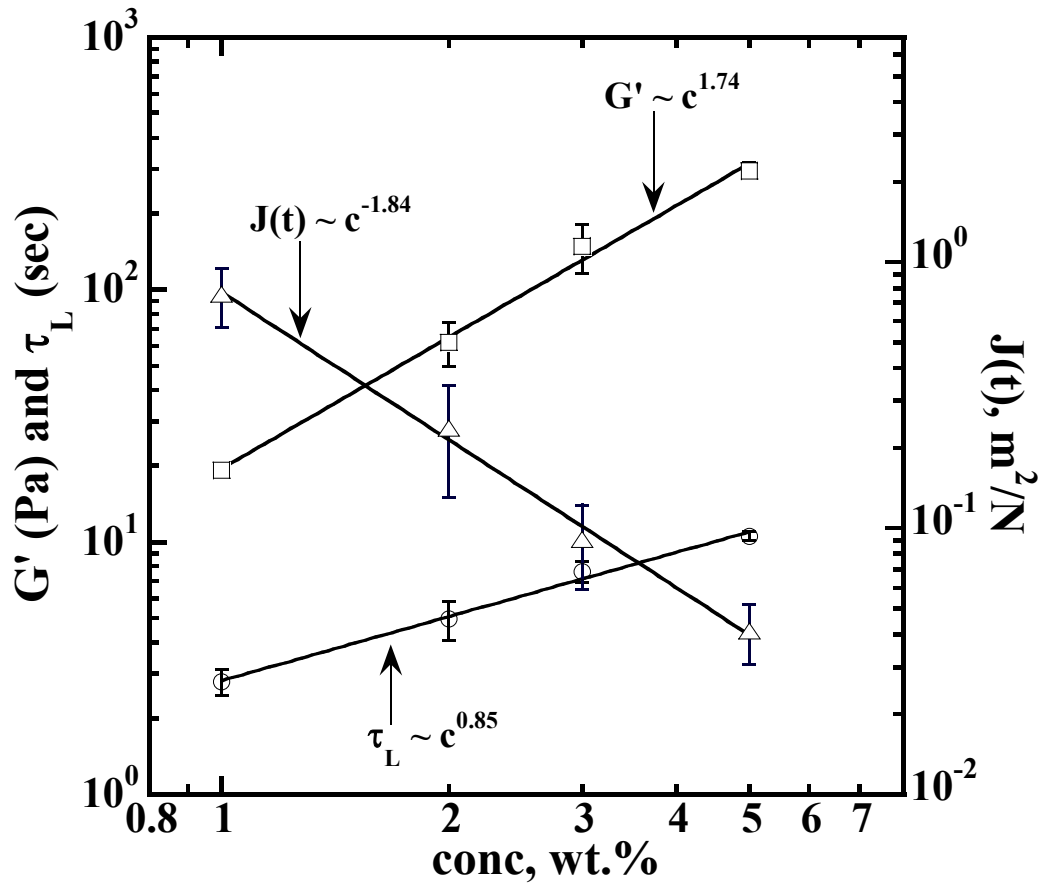


Figure 12. Scaling of the elastic modulus (G'), the creep Compliance ($J(t)$), and the longest relaxation time (τ_L) with the polymer concentrations. G' is taken at a fixed frequency 10 rad/s and $J(t)$ at a fixed time 10 sec..

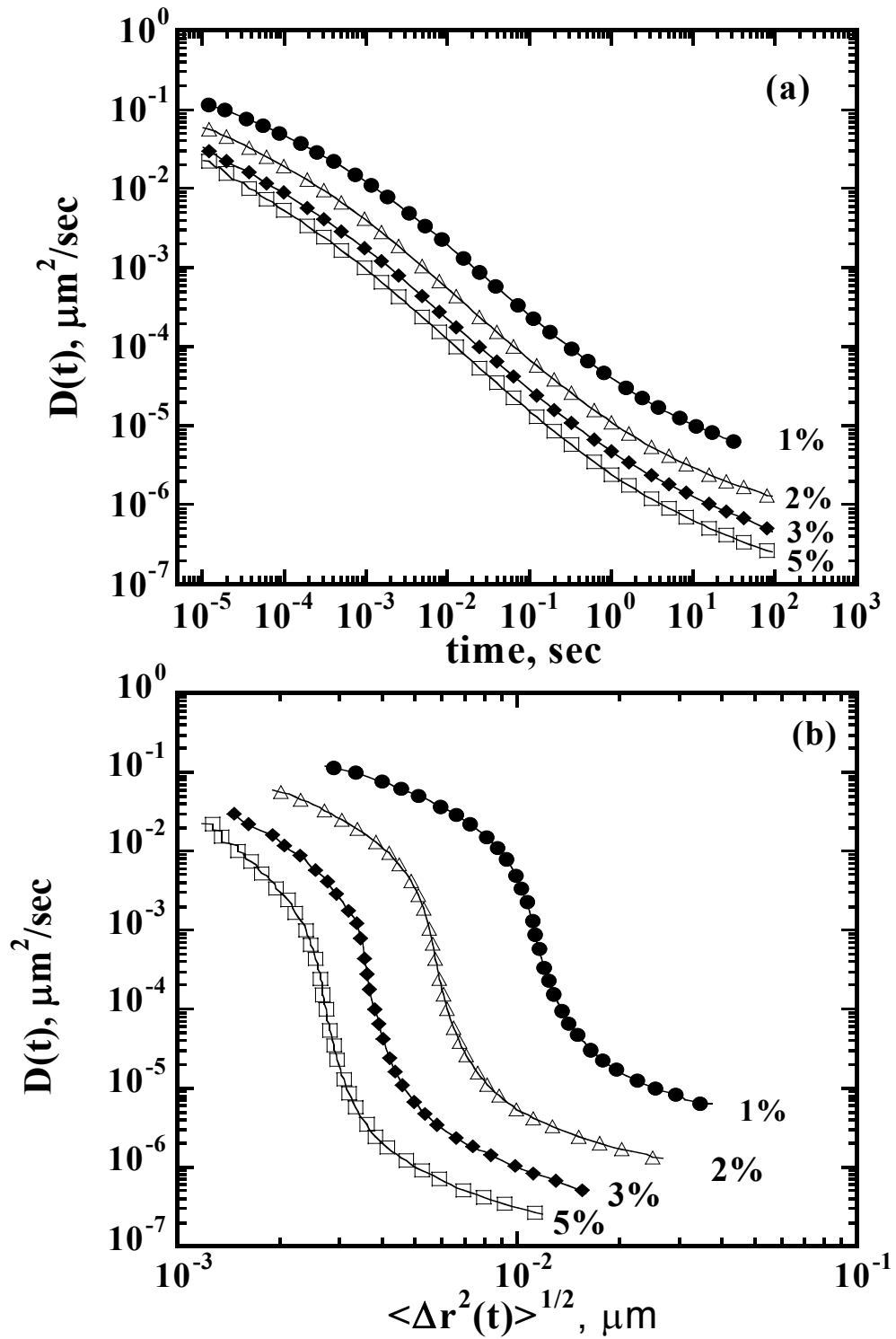


Figure 13. Time dependent diffusion coefficient of 0.966 mm spheres embedded in HASE polymer solution at different concentrations as a function of (a) time and (b) the average sphere displacement.

CHAPTER 7

MODULATION OF HYDROPHOBIC INTERACTIONS IN ASSOCIATIVE POLYMERS WITH THROUGH INCLUSION COMPOUNDS AND SURFACTANTS

Chapter 7 is essentially a manuscript by Ahmed A. Abdala, Alan E. Tonelli and Saad Khan prepared for submission to *Macromolecules*

Modulation of Hydrophobic Interactions in Associative Polymers with Inclusion Compounds and Surfactants

Ahmed A. Abdala¹, Alan E. Tonelli² and Saad A. Khan^{1*}

¹ Department of Chemical Engineering, North Carolina State University, Raleigh NC 27695, USA

² Fiber and Polymer Science Program, North Carolina State University, Raleigh NC 27695, USA

Abstract

In aqueous solution, the hydrophobic segments of a hydrophobically modified alkali-soluble emulsion (HASE) polymer usually associate forming physically cross-linked networks that enhance the solution viscosity and viscoelastic properties. While this enhancement attracts many technological applications, the ability to control the rheology is often desirable. In this study, we modulate the rheology of a model HASE polymer through the interaction of the hydrophobic groups with α - and β -cyclodextrin (CDs). The complexation between the hydrophobic segment (C₂₂-EO₄₀) and CDs are investigated using ¹H NMR, differential thermal analysis (DSC), and thermal gravimetric analysis (TGA). The stoichiometric ratio of complexation between CDs and the hydrophobic macromonomer is determined from NMR and the yield data and found to be 5 moles CD/mole hydrophobe. This interaction between the hydrophobic segment of the HASE polymer and the CD's reduced the polymer solution viscosity and dynamic moduli by several orders of magnitude. This reduction in viscoelasticity is reversibly recovered by the addition of different surfactants that have a higher propensity to complex with the CD than the hydrophobic segment of the polymer.

* corresponding author; phone: 919-515-4519; fax: 919-515-3465; email: khan@eos.ncsu.edu

7.1 Introduction

Associative polymers are macromolecules with attractive groups either attached to the ends or randomly distributed along the backbone¹. Hydrophobically modified alkali soluble emulsion (HASE) polymers are one class of water-soluble associative polymers that have a comb-like structure with pendant hydrophobic groups randomly grafted to a polyelectrolyte backbone. HASE polymers have several advantages over other associative polymers in terms of cost and wide formulation latitude². Consequently, they are currently being used in a range of applications, including paint formulations, paper coatings, and recently as glycol based aircraft anti-icing fluids³⁻⁵ and also have potential for use in enhanced oil recovery and personal care products. These polymers are usually added to either modify the rheology of aqueous solutions or increase the stability of dispersions. Because of their high thickening ability, a few percent of HASE polymers can increase the solution viscosity by several orders of magnitude. This thickening ability is predominantly the result of the molecular hydrophobic associations that occur to minimize contact between the aqueous media and the hydrophobic segments of the polymer; the hydrodynamic volume expansion upon neutralization of the carboxylic groups on the polymer backbone also plays a minor role in this regard.

Despite the importance of hydrophobic interactions to promote viscosity enhancement in this polymer system, there is also a need to remove these interactions in many instances. For example, the very high solution viscosity of a concentrated solution is always associated with difficulty in handling during solution preparation and prior to the end use stage. The hydrophobic interaction also makes extracting information from

characterization techniques, such as light scattering and gel permeation chromatography (GPC), cumbersome and less accurate. The removal of the hydrophobic interactions would simplify the information gained from these techniques and assist in understanding the behavior of these polymers. In addition, the properties of the hydrophobically modified polymers are usually compared to those of the unmodified parent polymer without hydrophobes to gain understanding about their microstructures and associating abilities. However, such an assessment may not be realistic, because modified and unmodified polymers may differ by more than just the hydrophobic modification⁶. The ability to compare modified polymers with that in which the hydrophobes are deactivated would provide a plausible basis for understanding their behavior.

In this study, we examine a powerful method to control the solution rheology of HASE polymers by means of removing the hydrophobic interactions using cyclodextrins to form inclusion compounds⁶ with the macromonomer part of the HASE polymer. Cyclodextrins (CDs) are ring-shaped oligosaccharides consisting of 6, 7, or 8 glucose units (corresponding to α , β , and γ -CD) joined by α -1,4-glycosidic linkages. They have a hydrophobic inner-core and a hydrophilic outer-shell thus making it possible for the hydrophobic segments of the polymer to reside inside them and form a complex referred to as an inclusion compound. Such a notion is supported from previous studies which reveal cyclodextrins to have superior tendencies to interact with the hydrophobic segments of different hydrophobically modified water soluble associative polymers, including: hydrophobically end capped polyethylene oxide⁷⁻¹², poly(ethylene glycol)s (PEGs) bearing hydrophobic ends (naphthyl and phenyladamantyl)¹³, N,N-dimethylacrylamide-hydroxyethyl

methacrylate copolymer hydrophobically modified with adamantyl groups¹⁴⁻¹⁶, hydrophobically modified ethyl(hydroxy ethyl) cellulose⁶, hydrophobically modified, degradable, poly(malic acid)¹⁷, isobutene maleate polymer with pendant hydrophobic 4-tert-butylanilide^{18,19}, hydrophobically modified ethoxylated urethanes²⁰, hydrophobically modified alkali soluble emulsion polymers^{21,22}, and hydrophobically modified Dextran²³. Cyclodextrins have also been reported to form inclusion compounds with many nonionic surfactants²⁴⁻⁴⁰.

In this work, we focus on investigating the effects of α - and β - cyclodextrin addition on rheology of HASE polymer solutions, understanding the mechanism of cyclodextrin polymer complexation and evaluating the reversibility of these interactions. As such, we examine initially the extent of rheology changes upon CD addition and the existence, if any, of quantitative relationship between the molar ratio of CDs to the polymer hydrophobes on solution rheology. In order to isolate whether the observed changes are due to interactions of the CD with the macromonomer containing the hydrophobes or with the polymer backbone, we take a two-prong approach. The interaction between the CDs and the polymer backbone is studied using the unmodified parent polymer without hydrophobes. On the other hand, a commercially available surfactant, RhodaSurf, was modified to resemble the macromonomer part and used to simulate the interaction between the macromonomer part of the HASE polymer with the CDs. A range of techniques including NMR, DSC and TGA are used to study the complexation and formation of an inclusion compound between the CDs and the hydrophobic macromonomer. Finally, the reversibility of the CD-polymer complexation and ability to recover the original solution rheology was investigated through addition of

nonionic surfactants. A higher affinity of the CD to form inclusion compound with the surfactant would lead to the release of the polymer from the CD and a concomitant reversal of rheology.

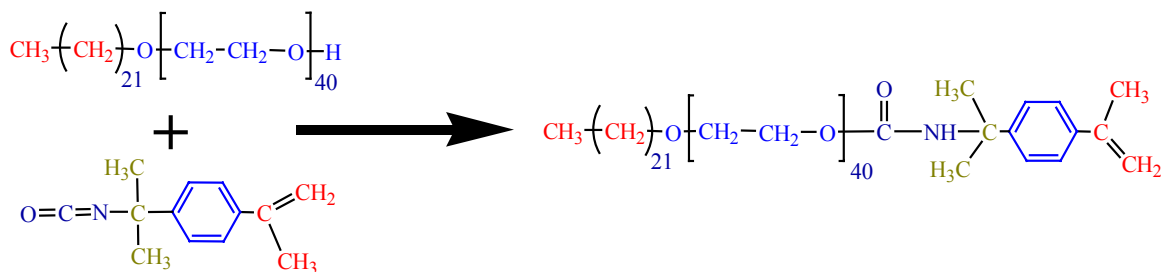
7.2 Experimental

7.2.1 Materials

The model associative polymer used in this study is a hydrophobically modified alkali-soluble (HASE) polymer synthesized by UCAR Emulsion Systems (Dow Chemical, NC) *via* emulsion polymerization of methacrylic acid (MAA), ethylacrylate (EA) and a hydrophobic macromonomer (Figure 1). This macromonomer is end capped with C₂₂H₄₅ alkyl hydrophobes that is separated from the backbone by 40 polyethylene oxide (PEO) units. Details of the preparation method can be found in a previous publication⁴¹. In addition to the hydrophobically modified polymer, an unmodified polymer that has the same structure as the modified polymer with the C₂₂H₄₅ hydrophobes replaced by an equivalent amount of methyl groups was also used. Both the modified and the unmodified polymers were prepared in an identical manner and are believed to have the same molecular weight. The polymer latexes were dialyzed against de-ionized water using a cellulosic tubular membrane for at least three weeks with daily change of water. After dialysis, the polymer was freeze-dried and 5% solutions were prepared and neutralized to pH of 9 ±0.1 using 1 N NaOH with the ionic strength adjusted to 0.1 M KCl.

C₂₂EO₄₀ surfactant under the commercial name of RhodaSurf was provided by DOW Chemical Company. The surfactant was modified to resemble the macromonomer part of the

HASE polymer through reaction with α, α , dimethyl meta-isopropenyl benzyl isocyanate (TMI[®] (meta), American Cyanamid) as follows:



Nonionic surfactant, Nonylophenol polyethylene glycol ether with degree of ethoxylation of 4 (NP4), was provided by DOW Chemical Company. Industrial grade α and β -cyclodextrins were supplied by Cerestar USA, and are used as received.

7.2.2 Methods

The steady-state and dynamic rheological behavior of the polymer solution were measured using a stress-controlled rheometer (Rheometrics DSR II) fitted with appropriate cone and plate, parallel plates, and couette geometries. Details on the rheological techniques are provided in previous publications (put here Rob's paper and yours)

¹H NMR data were obtained using a 500 MHz Bruker DRX NMR spectrometer. All spectra were acquired at 298 °K using Tetramethylsilane (TMS) as internal standard and all samples were prepared in DMSO-d⁶. The instrumental parameters for acquisition of the one-dimensional proton spectra are as follows: tuning frequency 500.128 MHz, Spectral Width 13.2 ppm, number of data points 32K, relaxation and acquisition times 1.0 and 2.47 sec (respectively), pulse width 10.5 μm , tip angle 90° and number of transients 16.

Differential scanning calorimetry (DSC) was carried out on 3-8 mg samples with a Perkin-

Elmer DSC-7 thermal analyzer equipped with a cooler system. A heating rate of 10° C/min was employed and an indium standard was used for calibration. Before each scan, samples were annealed at 200° C for 3 minutes to erase thermal history, followed by a flash quenching to -100° C at 500° C/min. Thermal gravimetric analysis (TGA) measurements were carried out on a Perkin-Elmer Pyris 1 Thermogravimetric Analyzer. Approximately 20 mg samples were heated from 25-600° C and the weight loss was recorded as function of sample temperature.

7.3 Results and Discussion

7.3.1 Effect of CDs on solution rheology

The effects of both α - and β -CD on the steady shear viscosities of a 3% HASE solution are shown in Figures 2a and b, respectively. With the addition of CDs, the steady shear viscosities of the polymer solutions decrease dramatically. Moreover, at about 15 moles of CD per hydrophobe, it seems that there is no further reduction in the solution viscosity for both α - and β -CD; however, the final viscosity obtained using α -CD is about one decade lower than that obtained using β -CD.

Similar findings are obtained from dynamic rheological measurements. Figures 3a and b demonstrate the effect of α and β -CD on the frequency spectrum of the elastic (G') and viscous (G'') loss moduli of 3% HASE polymer solutions. The addition of either α or β -CD reduces both the elastic and viscous moduli and increases their dependence on frequency. The decrease in the elastic modulus reflects a reduction in the number of active junctions between HASE polymer chains due to the deactivation of the hydrophobic groups; transient

network theory predicts that the elastic modulus is directly proportional to the number of active junctions⁴⁶. The higher dependence on the frequency is a sign of weaker network structures due to the reduction of the number of active hydrophobes. Additional CD above that of 15 moles of CD per mole of hydrophobe has no effect on either the level of the moduli or on their dependence on frequency. Moreover, the maximum reduction in the moduli, vis a vis the final moduli values, are about 2 decades lower with α -CD than those obtained with β -CD. These results are consistent with the steady shear findings.

The decrease in solution viscoelasticity upon addition of CD suggests that the CD interacts with either the polymer backbone, the hydrophobic macromonomer or both. To determine if any interactions occur between the CDs and the polymer backbone, an unmodified polymer with similar structure and molecular weight to those of the HASE polymer was used. The unmodified polymer was synthesized in the same manner that the HASE polymer was synthesized, but with the C₂₂ hydrophobes replaced with an equivalent amount of CH₃ groups. Figures 4a and b illustrate the effects of adding varying amounts of β -CD to an 1% unmodified polymer solution on both the steady shear viscosity and the dynamic moduli, respectively. We find that the addition of β -CD, regardless of the amount added, has no effect on the steady shear viscosity of the unmodified polymer solution nor on the frequency spectrum of the dynamic moduli. This suggests that there are no interactions between the β -CD and the polymer backbone, and any effect of CDs on the rheology of the HASE solution occurs primarily from the interaction between the CDs and the hydrophobic segments of the HASE polymer.

7.3.2 Macromonomer-cyclodextrin complexation

An extensive array of experiments were undertaken to decipher the interaction between α and β -CD and the macromonomer part of the polymer, the structure of which resembles that of a nonionic surfactant with the C₂₂ alkyl group as the hydrophobic segments and the 40 EO units as the hydrophilic segment of the surfactant. As a first step, a macromonomer-CD inclusion compound (IC) was formed by mixing 1% macromonomer aqueous solution with 1% α or β -CD aqueous solution to yield different CD/macromonomer molar ratios (0.5 to 50). Upon the addition of α -CD to the macromonomer solution, a cloudy solution was formed immediately. In contrast it took several hours after the addition of β -CD for the solution to become cloudy. The cloudiness of the solution is a sign of complexation between the CD and the hydrophobic macromolecule. Three days after mixing the two components, the complexes were isolated by centrifugation, filtration, washing with water, re-centrifugation, re-filtration, and freeze-drying.

Figure 5 shows the IC yield as function of the CD to macromonomer molar ratio for α -CD and β -CD. The IC yield was calculated as the weight of the dried IC divided by the total weight of the surfactant and the CD. As seen from the figure that the IC yield increases with increasing CD to macromonomer molar ratio reaching a maximum at a ratio of about 5 moles of CD to one mole of macromonomer before starting to decrease. This behavior is suggestive of the complexation process being stoichiometric. Figure 5 also reveals that α -CD gives a higher yield compared to β -CD. The difference in the yield between α and β -CD can be attributed to the difference in the annular size of the two. α -CD has a ring size of about 5.7 Å in which the hydrophobic segments of the macromonomer would have

a snug fit. On the other hand, the annular size of β -CD is larger ($\sim 7.8 \text{ \AA}$)⁴², giving the macromonomer sufficient room to move in and out. In fact, it has been reported by others as well that while α -CD was able to form inclusion compounds with polyethylene glycol and oligoethylene, β -CD was not⁴³.

A larger maximum yield value of the α -CD-macromonomer complex ($\sim 65\%$) compared to the β -CD-macromonomer complex ($\sim 54\%$) is consistent with the rheology data in Figures 2 and 3 which indicate that α -CD is more effective in deactivating the hydrophobic groups and reducing viscosity and modulus. However, the ratio of CD to hydrophobes where the maximum viscosity/modulus reduction occurs, 15 to 1, is different than the stoichiometric ratio, 5 to 1, where the maximum yield is obtained. This can nonetheless be easily explained if the yield is calculated based on the macromonomer weight rather than weight of both the macromonomer and the cyclodextrin. If we do this, the yield increases continuously rather than passing through a maximum.

In order to interpret the CD/hydrophobe ratio at which the maximum reduction in viscosity/moduli occurs, we can calculate the % of active hydrophobes (hydrophobes that are not complexed with CD) as function of the molar ratio of added CD/hydrophobes. This can be done following the scheme:



Using the initial molar ratio of CD/macromonomer (m) and the yield of their complex (y), the % active hydrophobes can be calculated by assuming a 5/1 stoichiometric complexation ratio as follows:

$$\begin{aligned}
 \text{Moles of macromonomer in 1 gram of feed, } (F) &= \frac{1}{(m * M_{CD} + M_{macro})} && \text{Moles} \\
 \text{Moles of complexed macromonomer, } (P) &= \frac{y}{(5 * M_{CD} + M_{macro})} && \text{Moles} \\
 \% \text{Active hydrophobes} &= \left(\frac{F - P}{F} \right) * 100
 \end{aligned}$$

where, M_{CD} is the molecular weight of the CD and M_{macro} is the macromonomer molecular weight. The % active hydrophobes based on the yield data and calculated according to the this scheme is shown in Figure 6. We observe a rapid initial decrease in the % active hydrophobes followed by a very slow decrease at CD/macromonomer molar ratios above 15. We also find that the % active hydrophobe at a CD/ hydrophobe molar ratio of about 15 is less than 10% for α -CD compared to about 20% for β -CD. These results explain the difference in the effects produced by α - and β -CD on the steady shear viscosity and dynamic moduli of the concentrated HASE solutions.

7.3.2.1 Characterization and interaction modes of CD-macromonomer ICs

The DSC technique was used to confirm complex formation and to determine whether the “inclusion compound” separated *via* centrifugation yielded a compound with no free macromonomer. Figures 7a and b show the DSC thermograms of the macromonomer, α -CD, β -CD and their ICs. The DSC thermograms of the macromonomer- α -CD and macromonomer- β -CD complexes show no endothermic peak where the melting point of the free macromonomer is expected. This confirms the absence of the free macromonomer in the ICs³⁸.

The complexation between CDs and the macromonomer also impacted the thermal stability of both CD's and the macromonomer. Figures 8a and b show the TGA data of α -CD, β -CD, macromonomer and their ICs. The TGA data for α - and β -CD show the onset of weight loss at about 315° C and 325° C, respectively. Both α and β -CD have a residue of about 20% at 500°C. On the other hand, the macromonomer has a higher temperature onset for weight loss of about 400° C and much lower residue, about 1% at 500° C. The macromonomer-CD ICs have an onset between that of the macromonomer and the CDs (about 340° C) and a residue of about 10% at 500° C. The improved thermal stability of the CDs due to the complexation as compared to the CDs by themselves has been observed in other cyclodextrin ICs^{44,45}.

Figure 8 also reveals that the macromonomer-CD ICs have a multistep decomposition profile. After the onset of weight loss, there is a rapid decomposition up to about 40% residue. This is followed by a very slow but small decomposition regime for a few weight % at about 400° C, and a final rapid decomposition until a final residue of about 10% is reached. Similar multistep profiles have been observed with 4-arm polyethylene glycol- α -CD IC, 4-arm polyethylene glycol- γ -CD IC⁴⁵ and C₄ π C₄EO₈- α -CD IC⁴⁴ and has been attributed to the dethreading of the guest (macromonomer) during the TGA run⁴⁴.

Further insights into the complexation between the CDs and the macromonomer has been obtained using ¹H NMR. Figures 9a and b show the ¹H NMR spectra for α -CD, β -CD the macromonomer and their IC recorded in DMSO-d⁶. Both the methylene protons in the alkyl C₂₂ and EO₄₀ in the ICs are shifted downfield as shown in Figures 9 and 10. The complexation stoichiometric ratio can be obtained by comparing the integral area under the

H₁ proton for the CD (4.80 - 4.82 ppm) with that of the methylene protons of the alkyl C₂₂ from the surfactant (1.20 ppm) in the IC spectrum. These peaks are fully resolved and free from any overlap with other peaks. The stoichiometric ratio obtained from the ¹H NMR data is about 5, which is consistent with that obtained from the yield data (Figure 5). Moreover, the formation of inclusion compounds is confirmed by the ¹H NMR spectra; a very significant shift is observed for cyclodextrin protons labeled as OH₂ and OH₃. A smaller shift is observed for the other cyclodextrin protons and both the aliphatic and the ethylene oxide protons on the macromonomer (Figure 10).

Two intriguing issues that remain to be resolved are how much of the macromonomer is encapsulated by the CD and whether such complexation is static or dynamic in nature. Because the height of each CD bracelet is $\sim 7.9 \text{ \AA}^{42}$, a fully extended macromonomer would require ~ 20 - 25 threaded CDs for complete coverage. However, as noted above we observe a CD-macromonomer complex stoichiometry of ~ 5 , so only roughly $\frac{1}{5} - \frac{1}{4}$ of the C₂₂-EO₄₀ chain is complexed by the CDs. Although tentative, we can offer further suggestions regarding the complexation of the macromonomer with CDs based on the ¹H NMR observations presented in Figures 9 and 10. Let us consider the following two scenarios: (i) all CDs are moving along and possibly threading onto and off of the C₂₂-EO₄₀ macromonomer chains rapidly on the NMR timescale (MHz), and (ii) some of the CDs are rapidly moving along and possibly threading and dethreading onto and off of the macromonomer as in (i), whereas the remaining CDs remain complexed with the macromonomer for longer times. If we reasonably suppose that CDs may only thread the macromonomer chain from the C₂₂ end, and not from the bulky TMI, (meta) end (see the

macromonomer structure in Figure 1)), then scenario (i) would be expected to evidence ^1H NMR spectra for the macromonomer-CD complexes with CH_2 protons from both the C_{22} and EO_{40} portions of the macromonomer chains resonating downfield from their positions in the free macromonomer. This appears to be the case for the C_{22} CH_2 protons as seen in Figure 10a. However, in Figure 10b we note that the CH_2 protons belonging to the EO_{40} portion of the complexed macromonomers, while also shifted downfield from their uncomplexed resonance frequencies, exhibit even higher field shoulders on their main resonance peaks. This is suggestive of two different populations of EO_{40} CH_2 protons, with the majority of EO units experiencing rapidly moving CDs, while the smaller remaining population are complexed and covered by the CDs for a longer period of time, as described in scenario (ii.).

We therefore suggest, that at any given time $\frac{1}{5} - \frac{1}{4}$ of the $\text{C}_{22}\text{EO}_{40}$ macromonomer chain is complexed and therefore covered by CDs, with CDs able to rapidly move along most of the $\text{C}_{22}\text{EO}_{40}$ chain and possibly thread/unthread onto/from the C_{22} end. In addition, a minor population of the EO_{40} macromonomer units, which are likely those closest to the bulky TMI, (meta) end, remain complexed and covered by CDs for longer times. Future NMR relaxation studies will be necessary to substantiate the suggestions we have tentatively offered here concerning the detailed characteristics of the macromonomer - and HASE-CD complexes.

7.3.3 Recovery of Solution Rheology

In the previous sections, we present an approach to reduce the viscoelasticity of HASE solutions through complexation with CDs to form inclusion compounds. This

complexation yields a solution with a final viscosity or dynamic modulus several orders of magnitude lower than the original solution. The question that needs to be resolved is whether the HASE solution can recover its viscoelastic characteristics and to what extent. Since the macromonomer part of the HASE polymer interacts with the CDs, the addition of more macromonomers to the HASE solution that is complexed with CD would shift the equilibrium between the polymer and the CDs away from their complexed state, as CD-macromonomer complexes are formed. This in turn would free some of the hydrophobic groups in the polymer and enhance solution viscoelasticity.

To test this hypothesis, we have added different amounts of macromonomer to a HASE solution complexed with CD. Figures 11a and b show the effect of macromonomer addition on the steady shear viscosity and dynamic moduli, respectively, of a 3% HASE that was complexed with 20 moles β -CD per hydrophobes. The addition of the macromonomer increases the solution viscosity and a complete recovery of the zero shear viscosity is reached with about 4.5 mM macromonomer. The macromonomer addition also increases both the elastic and loss modulus and reduced their dependence on frequency. In fact, with 4.5 mM macromonomer the plateau elastic modulus reaches that of the original solution. Further macromonomer addition yields a decrease in the steady and viscoelastic properties possibly because the free macromonomer concentration reached its upper critical limit.

The effect of a nonionic surfactant, nonylophenol surfactant with 4 EO units (NP4), on the steady shear viscosity and the dynamic moduli of 3% HASE solution complexed with 20 moles α -CD per hydrophobes was also examined and is illustrated in Figure 12. With about 40 mM surfactant the zero shear viscosity is fully recovered, but the viscosity profile is

different than that of the original solution. With added surfactant, the solution shows a higher degree of shear thinning compared to the original solution. Similar findings are also obtained from the dynamic measurements, with an increase in the level of the dynamic moduli and lower dependence on frequency with the addition of NP4 surfactant. A complete recovery of the plateau modulus has not been reached in this case.

Despite the recovery of the zero shear viscosity and the plateau modulus, there are, however, differences in the steady shear profile and dynamic spectrum of the recovered and the original solutions. The differences that are observed in either the macromonomer or NP4 surfactant case is a result of the fact that the added macromonomer or NP4 interacts with the HASE polymer⁴⁷.

7.4 Conclusions

The rheology of aqueous HASE solutions can be controlled by complexation of the normally associating hydrophobic macromonomer components with α - and β -cyclodextrins. The steady shear viscosity and dynamic moduli of the HASE solutions can be reduced by several orders of magnitude upon addition of the cyclodextrins. Furthermore, it is possible to reversibly recover the high viscoelastic characteristics of HASE solutions containing cyclodextrins by treatment with surfactants that compete with the hydrophobic portions of HASE for complexation with the cyclodextrins. As a consequence, cyclodextrins and surfactants in combination can be judiciously employed to lower the viscoelasticity of HASE solutions during processing, while subsequently recovering the high viscosity and viscoelastic properties that are sought in their applications.

Acknowledgement:

The authors gratefully acknowledge the support and help of Dow Chemical Company, UCAR Emulsions, for providing various samples for this study.

7.5 References:

1. Rubinstein, M.; Dobrynin, A. V. Solutions of Associative Polymers. *Trends in Polymer Science*, **1997**, *5*(6): p. 181-186.
2. Tirtaatmadja, V.; Tam, K. C.; Jenkins, R. D. Effects of Temperature on the Flow Dynamics of a Model HASE Associative Polymer in Nonionic Surfactant Solutions. *Langmuir*, **1999**. ASAP.
3. Jenkins, R. D. B., D. R.; Lightfoot, R. H.; Boluk, M. Y. Aircraft Anti-Icing Fluids Thickened by Associative Polymers. WO Patent 9324543, 1993.
4. Jenkins, R. D. B., D. R.; Lightfoot, R. H.; Boluk, M. Y. Glycol-Based Aircraft Anti-Icing Fluids Thickened by Associative Polymers Containing Hydrophobe-Bearing Macromonomers. US Patent 5681882, 1997.
5. Carder, C. H.; Garska, D. C.; Jenkins, R. D.; McGuinness, M. J. Aircraft Deicing/Anti-Icing Fluids Thickened by Associative Polymers. US Patent 5708068, 1998.
6. Karlson, L.; Thuresson, K. and Lindman, B. Investigation of the Complex Formation between Hydrophobically Modified Ethyl(hydroxy ethyl) Cellulose and Cyclodextrin. *Carbohydrate Polymers* **2002**, *50*(3), 219-226.
7. Amiel, C.; David, C.; Renard, E.; Sebille, B. Macromolecular Assemblies Generated by Inclusion Complexes between Amphiphilic Polymers and β -Cyclodextrin Polymers in Aqueous Media, *Polymer Preprints (American Chemical Society, Division of Polymer Chemistry)* **1999**, *40*, 207-208.
8. Amiel, C.; Moine, L.; Brown, W.; Renard, E.; Guerin, P.; Sebille, B. Associations of Amphiphilic Degradable Polymers with β -Cyclodextrin Polymers: pH-Dependent Network, *Proceedings of the International Symposium on Cyclodextrins, 9th, Santiago de Comostela, Spain, May 31-June 3, 1998* **1999**, 81-84.
9. Amiel, C.; Sebille, B. New Associating Polymer Systems Involving Water-Soluble β -Cyclodextrin Polymers, *J. Inclusion Phenom. Mol. Recognit. Chem.* **1996**, *25*, 61-67.
10. Amiel, C.; Sandier, A.; Sebille, B.; Valvat, P.; Wintagens, V. Association Between Hydrophobically End-Capped Polyethylene Oxide and Water Soluble β -Cyclodextrin Polymers, *int. J. Polymers Analysis & Characterization* **1995**, *1*, 289-300.
11. Sandier, A.; Brown, W.; Mays, H.; Amiel, C. Interaction between an Adamantane End-Capped Poly(ethylene oxide) and a β -Cyclodextrin Polymer, *Langmuir* **2000**, *16*, 1634-1642.

12. Amiel, C.; Moine, L.; Sandier, A.; Brown, W.; David, C.; Hauss, F.; Renard, E.; Gosselet, M.; Sebille, B. Macromolecular Assemblies Generated by Inclusion Complexes between Amphipathic Polymers and β -Cyclodextrin Polymers in aqueous media, *ACS Symposium Series* **2001**, 780, 58-81.
13. Gosselet, N. M.; Naranjo, H.; Renard, E. Amiel, C.; Sebille, B. Association of Poly-N-[tris(hydroxymethyl)methyl] Acrylamide with a Water Soluble β -Cyclodextrin Polymer, *European Polymer Journal* **2002**, 38, 649-654.
14. Gosselet, N. M.; Borie, C.; Amiel, C.; Sebille, B. Aqueous Two Phase Systems from Cyclodextrin Polymers and Hydrophobically Modified Acrylic Polymers, *J. Dispersion Sci. Technol.* **1998**, 19, 805-820.
15. Gosselet, N. M.; Beucler, F.; Renard, E.; Amiel, C.; Sebille, B. Association of Hydrophobically Modified Poly (N,N-dimethylacrylamide hydroxyethyl methacrylate) with Water Soluble β -Cyclodextrin Polymers, *Colloids and Surfaces, A: Physicochemical and Engineering Aspects* **1999**, 155, 177-188.
16. Moine, L.; Amiel, C.; Brown, W.; Guerin, P. Associations between a hydrophobically modified, degradable, poly(malic acid) and a β -cyclodextrin polymer in solution, *Polymer International* **2001**, 50, 663-676.
17. Wenz, G.; Weickenmeier, M.; Huff, J. Association thickener by host-guest interaction of β -cyclodextrin polymers and guest polymers, *ACS Symposium Series* **2000**, 765, 271-283
18. Weickenmeier, M.; Wenz, G.; Huff, J. Association Thickener by Host Guest Interaction of a β -Cyclodextrin Polymer and Polymer with Hydrophobic Side-Groups., *Macromol. Rapid Commun.*, **1997**, 18(12), 1117-1123.
19. Ma, Z.; Glass, J. E. Complexations of β -Cyclodextrin with Surfactants and Hydrophobically Modified Ethoxylated Urethanes. In *Analytical application in adsorption measurements*. ACS Symposium Series, 2000. **765**(Associative Polymers in Aqueous Media): p. 254-270.
20. Gupta, R.K.; Tam, K. C.; Ong, S. H.; Jenkins, R. D. Interactions of Methylated β -Cyclodextrin with Hydrophobically Modified Alkali-Soluble Associative Polymers (HASE): Effect of Varying Carbon Chain Length. In *Proc. Int. Congr. Rheol.*, 13th. **2000**.
21. Islam, M. F.; Jenkins, R. D.; Bassett, D. R; Lau, W.; Ou-Yang, H. D. Single Chain Characterization of Hydrophobically Modified Polyelectrolytes Using Cyclodextrin/Hydrophobe Complexes, *Macromolecules*, **2000**, 2480-2485.

22. Amiel, C., Renard, E.; Sandier, A.; Moine, L.; Gosselet, M.; Sebille, B. Macromolecular assemblies generated by inclusion complexes between amphipathic polymers and β -cyclodextrin polymers in aqueous media. Book of Abstracts, 218th ACS National Meeting, New Orleans, Aug. 22-26, 1999.
23. Ahmed, M.O. Comparison of Impact of the Different Hydrophilic Carriers on the Properties of Piperazine-Containing Drug. *European Journal of Pharmaceutics and Biopharmaceutics*, **2001**, 51(3), 221-225.
24. Alexandridis, Paschalis; Tsianou, M.; Ahn, S. Effect of Cyclodextrins on Polymer-Surfactant Interactions in Aqueous Solution. *Proceedings of the International Symposium on Controlled Release of Bioactive Materials*, 2000, 1134-1135.
25. Alvarez, A. R; Garcia-Rio, L.; Herves, P.; Leis, J. R.; Mejuto, J. C.; Perez-Juste, J. Basic Hydrolysis of Substituted Nitrophenyl Acetates in β -Cyclodextrin/Surfactant Mixed Systems. Evidence of Free Cyclodextrin in Equilibrium with Micellized Surfactant. *Langmuir*, **1999**, 15(24), 8368-8375.
26. Buschmann, H. J.; Cleve, E.; Schollmeyer, E. The Interactions between Nonionic Surfactants and Cyclodextrins Studied by Fluorescence Measurements. *Journal of Inclusion Phenomena and Macrocyclic Chemistry*, **1999**, 33(2), 233-241.
27. Cserhati, T.; Oros, G.; Szejtli, J. Effect of Cyclodextrins of Nonionic Surfactants: Reduction of Surface Activity and Phytotoxicity, *Tenside, Surfactants, Deterg.*, **1992**, 29(1), 52-57.
28. Cserhati, T.; Forgacs, E. Charge-Transfer Chromatographic Study of the Interaction of Non-ionic Surfactants with Hydroxypropyl- β -Cyclodextrin. *J. Chromatogr., A*, **1994**, 665(1), 17-25.
29. Eli, W.; Chen, W.; Xue, Q. Determination of Association Constants of Cyclodextrin-Nonionic Surfactant Inclusion Complexes by a Partition Coefficient Method, *Journal of Inclusion Phenomena and Macrocyclic Chemistry*, **2000**, 38(1-4), 37-43.
30. Hodul, P.; Duris, M.; Kralik, M. Inclusion Complexes of β -Cyclodextrin with Non-ionic Surfactants in Textile Preparation Processes., *Vlakna Text.*, **1996**, 3(1), 15-19.
31. Katougi, Y.; Saito, Y.; Hashizaki, K.; Taguchi, H.; Ogawa, N. Comparison of the Solubilizing Ability of Cyclodextrins and Surfactants for (+)- α -pinene. *Journal of Dispersion Science and Technology*, **2001**, 22(2 & 3), 185-190.
32. Oros, G.; Cserhati, T.; Szejtli, J. Cyclodextrins Decrease the Phytotoxicity of Nonionic Tensides. *Acta Agron. Hung.*, **1989**, 38(3-4), 211-17.

33. Rohrbach, R. P.; Allenza, P.; Schollmeyer, J.; Oltmann, H. D. Biodegradable Polymeric Materials and Articles Fabricated Therefrom, US Patent 9106601, 1991.
34. Saito, Y.; Katougi, Y.; Hashizaki, K.; Taguchi, H.; Ogawa, N. Solubilization of (+)- α -Pinene by Cyclodextrin/Surfactant Mixed Systems. *Journal of Dispersion Science and Technology*, **2001**, 22(2 & 3), 191-195.
35. Saket, M. Improvement of Solubility and Dissolution Rate of Meclozine Hydrochloride Utilizing Cyclodextrins and Non-ionic Surfactant Solutions Containing Cosolvents and Additives. *Acta Technol. Legis Med.*, **1997**, 8(1), 33-48.
36. Topchieva, I. N.; Karezin, K. I. Molecular Self-assembly in Nonionic Surfactant-Cyclodextrin Systems. *Colloid Journal (Translation of Kolloidnyi Zhurnal)*, **1999**, 61(4), 514-519.
37. Topchieva, I.; Karezin, K. Self-Assembled Supramolecular Micellar Structures Based on Non-ionic Surfactants and Cyclodextrins. *Journal of Colloid and Interface Science*, **1999**, 213(1), 29-35.
38. Wilson, L. D.; Verral, R. E. ¹H NMR Study of Cyclodextrin-Hydrocarbon Surfactant Inclusion Complexes in Aqueous Solutions. *Canadian Journal of Chemistry*, **1998**, 76(1), 25-34.
39. Woo, R. A.; Trinh, T.; Cobb, D. S.; Schneiderman, E.; Wolff, A. M.; Ward, T. E.; Chung, A. H.; Reece, S.; Rosenbalm, E. L. Uncomplexed Cyclodextrin Compositions for Odor Control and Refreshening of Garments. US Patent 9,856,888, 1998.
40. Shay, G. D.; Kail, J. E. Alkali-Soluble Latex Thickener. US Patent 4514552, 1985.
41. Szejtli, J. Introduction and General Overview of Cyclodextrin Chemistry. *Chem. Rev.*, **1998**, 98, 1743-1753.
42. Harada, A.; Suzuki, S.; Okada, M.; Kamachi, M. Preparation and Characterization of Inclusion Complexes of Polyisobutylene with Cyclodextrins. *Macromolecules*, **1996**, 29, 5611-5614.
43. Olosn, K.; Chen, Y.; Baker, G. L. Inclusion Complexes of α -Cyclodextrin and (AB)_n Block Copolymers. *Journal of Polymer Science, Part A: Polymer Chemistry*, **2001**, 39(16), 2731-2739.
44. Jia, H.; Goh, S. H.; Valiyaveetil, S. Inclusion Complexes of Multiarm Poly(ethylene glycol) with Cyclodextrins. *Macromolecules* **2002**, 35(5), 1980-1983.

45. Tanaka, F.; Edwards, S. F. Viscoelastic Properties of Physically Crosslinked Networks. 1. Transient Network Theory, *Macromolecules* **1992**, 25 (5), 1516-23.
46. English, R. J.; Laurer, J. H.; Spontak, R. J.; Khan, S. A. Hydrophobically Modified Associative Polymer Solutions: Rheology and Microstructure in the Presence of Nonionic Surfactant, *Ind. Eng. Chem. Res.* **2002**, ASAP article.

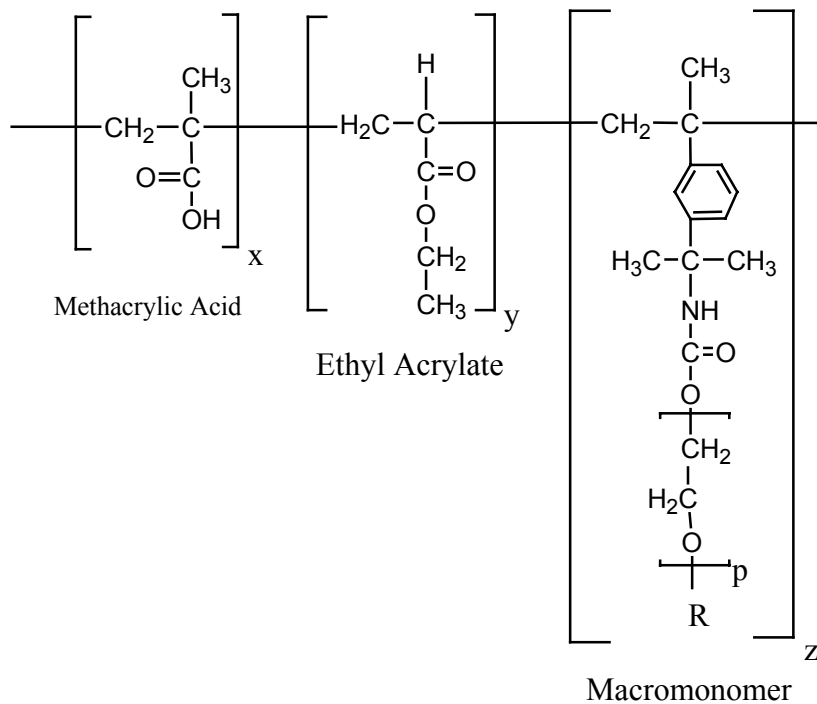


Figure 1. Schematic representation of a HASE associative polymer and the molecular constitution used in this study. R refers to the $\text{C}_{22}\text{H}_{45}$ hydrophobes, $p=40$, and. $x, y, z, p = x/y/z = 43.57/56.21/0.22$ by mole.

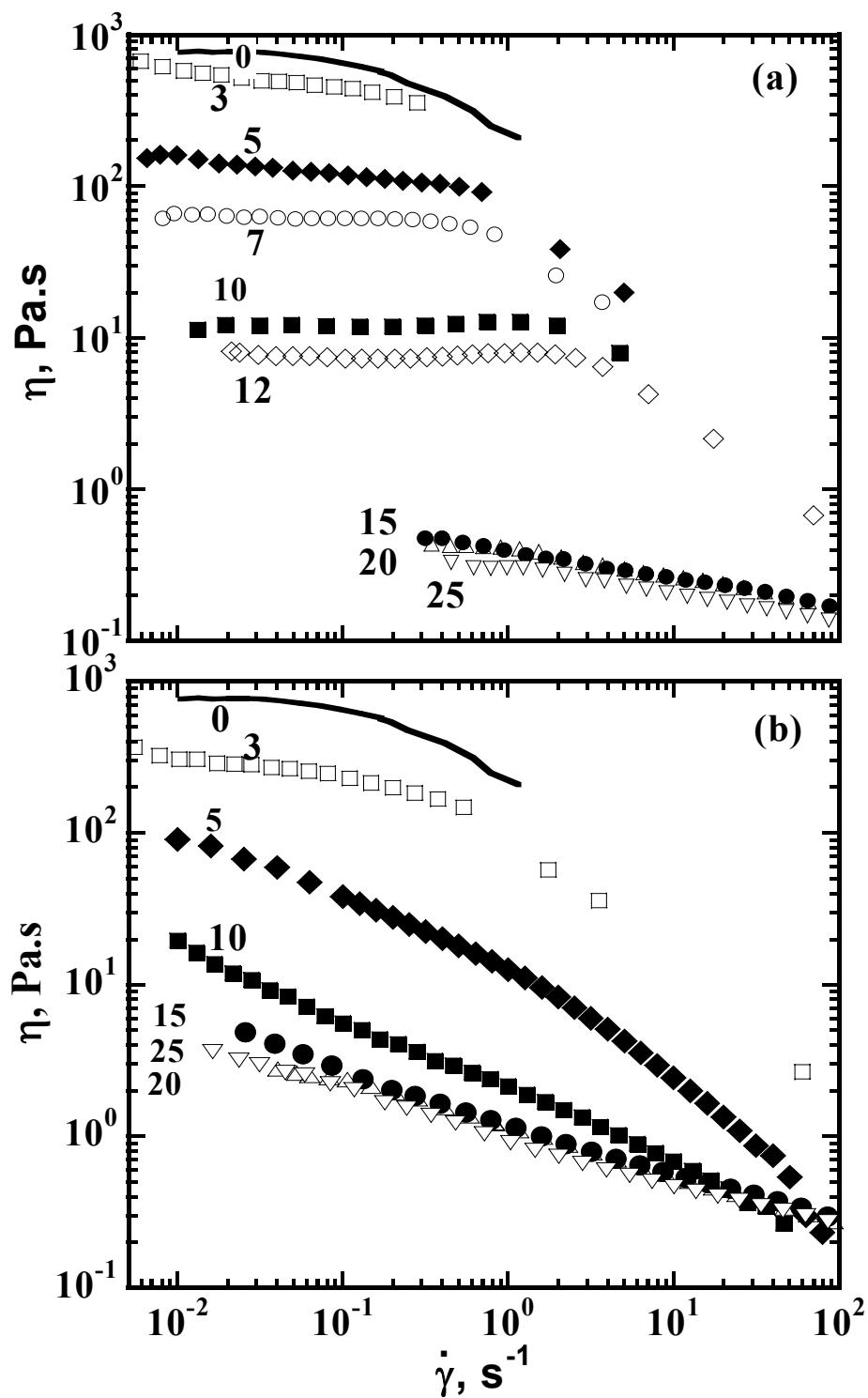


Figure 2: Effects of addition of a) α -CD and b) β -CD on the steady shear viscosity of 3% HASE associative polymer solution. Numbers correspond to the moles of cyclodextrin per moles of hydrophobes.

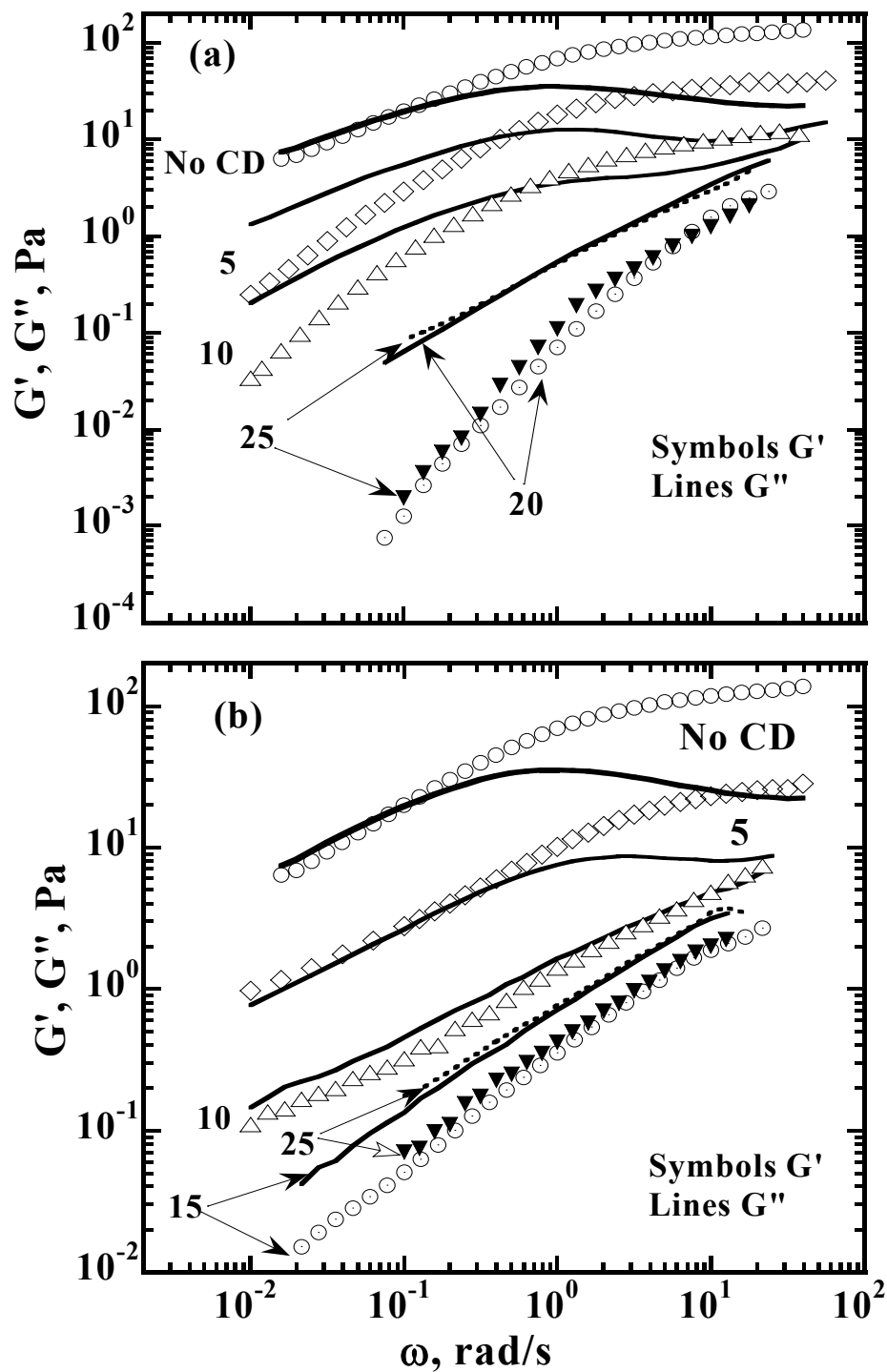


Figure 3: Effects of addition of a) α -CD and b) β -CD on the dynamic elastic (G') and viscous (G'') moduli of a 3% HASE associative polymer solution. Numbers correspond to moles of cyclodextrin per hydrophobes.

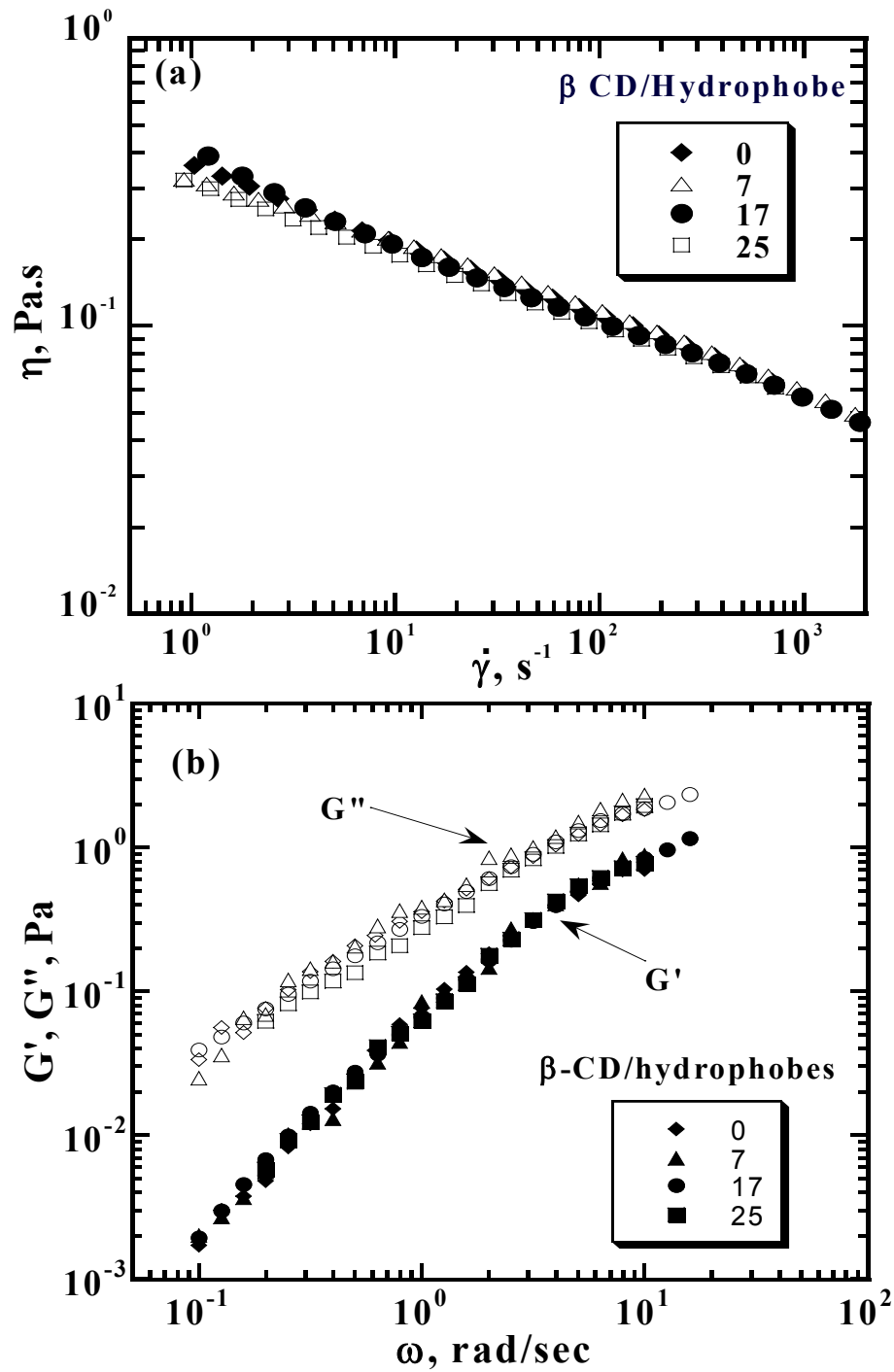


Figure 4: Effect of addition of various amounts of β -CD amount on the a) steady shear viscosity and b) dynamic elastic (G') and viscous (G'') moduli of 1% unmodified polymer that is analogous to the HASE polymer in this study but with the hydrophobic groups replaced by CH_3 groups.

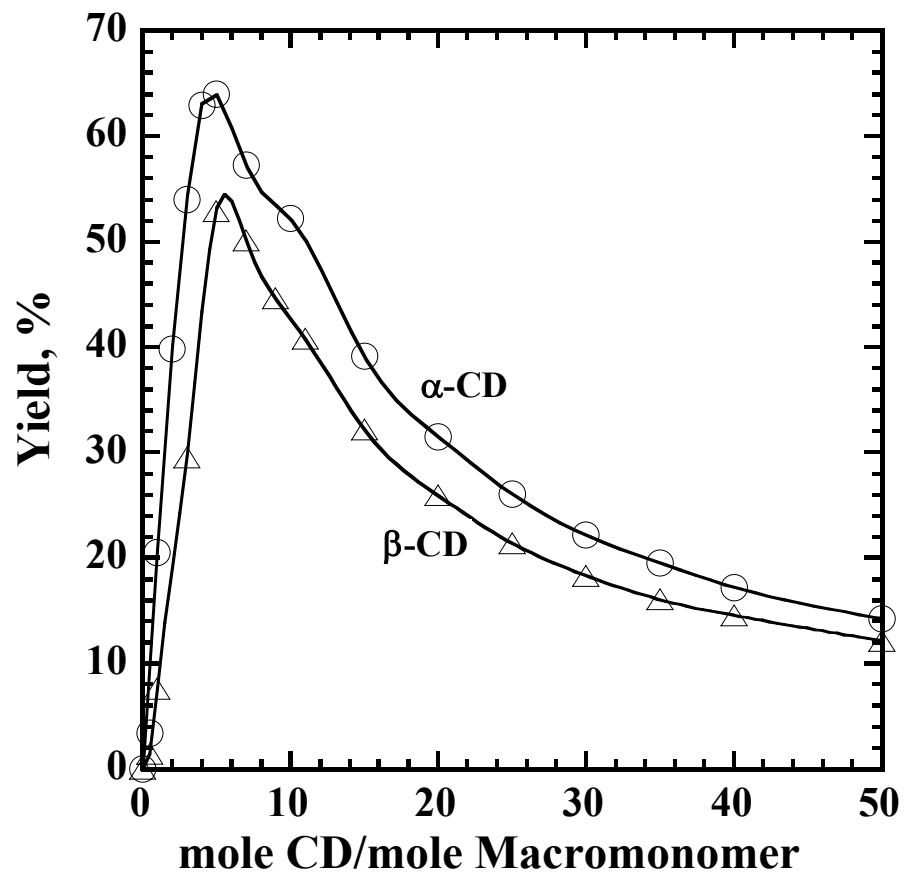


Figure 5. Yield of macromonomer-CD inclusion complexes as a function of the molar ratio of CD/macromonomers.

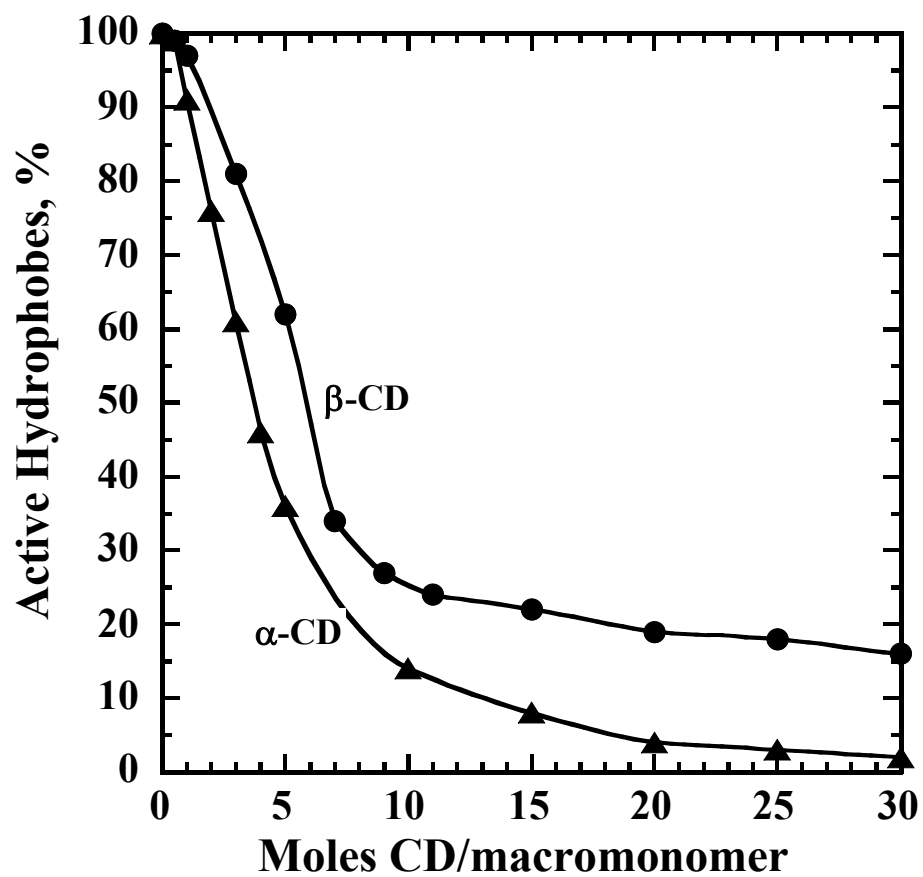


Figure 6. Effect of the CD/hydrophobe molar ratio on the % of active macromonomers present, calculated based on the yield data in Figure 2.

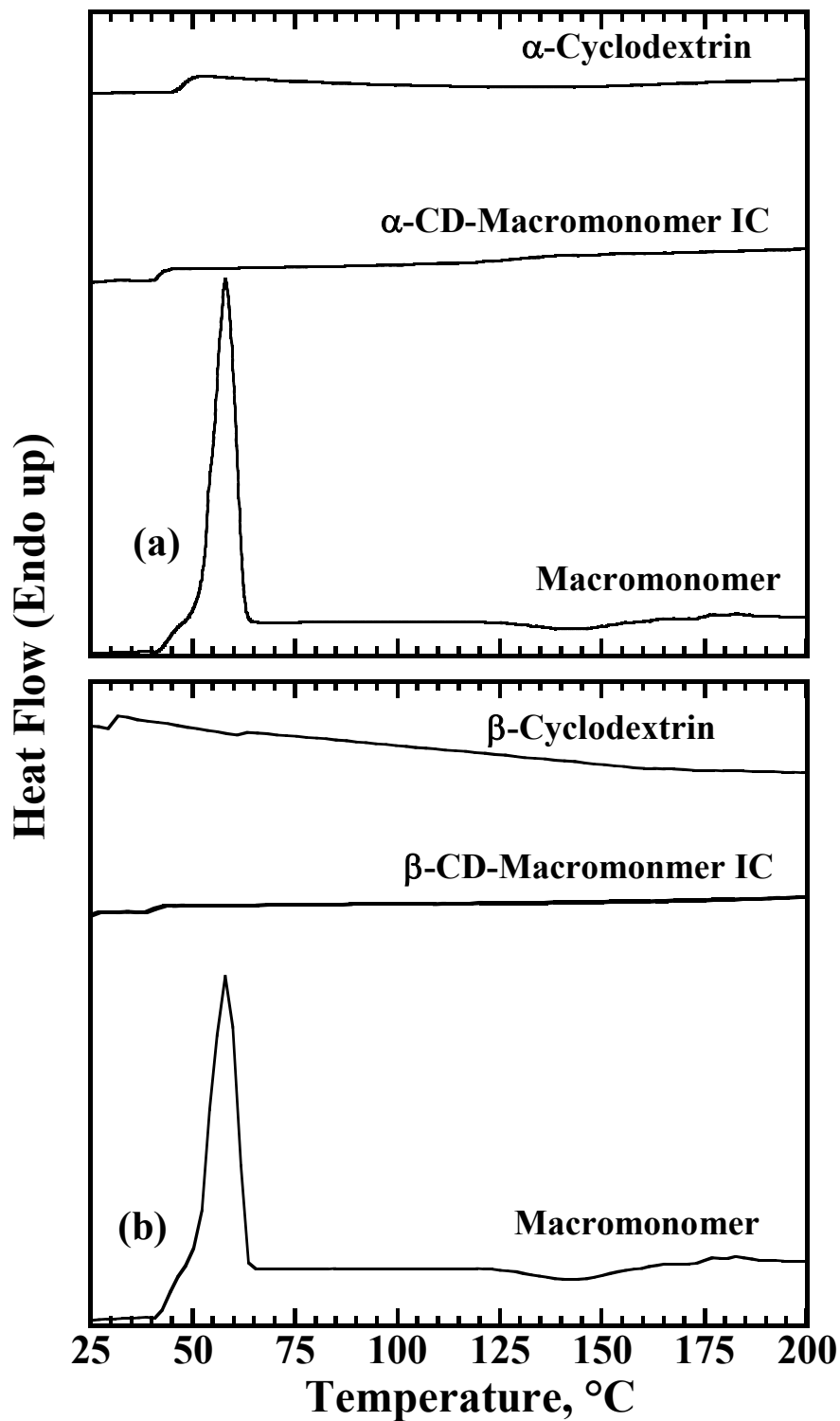


Figure 7. DSC scans of a) α -CD, macromonomer, and their inclusion compound and b). β -CD, macromonomer, and their inclusion compound. The scans shown are the second heatings taken after heating the samples at 200° C for 3 minutes to erase any thermal history.

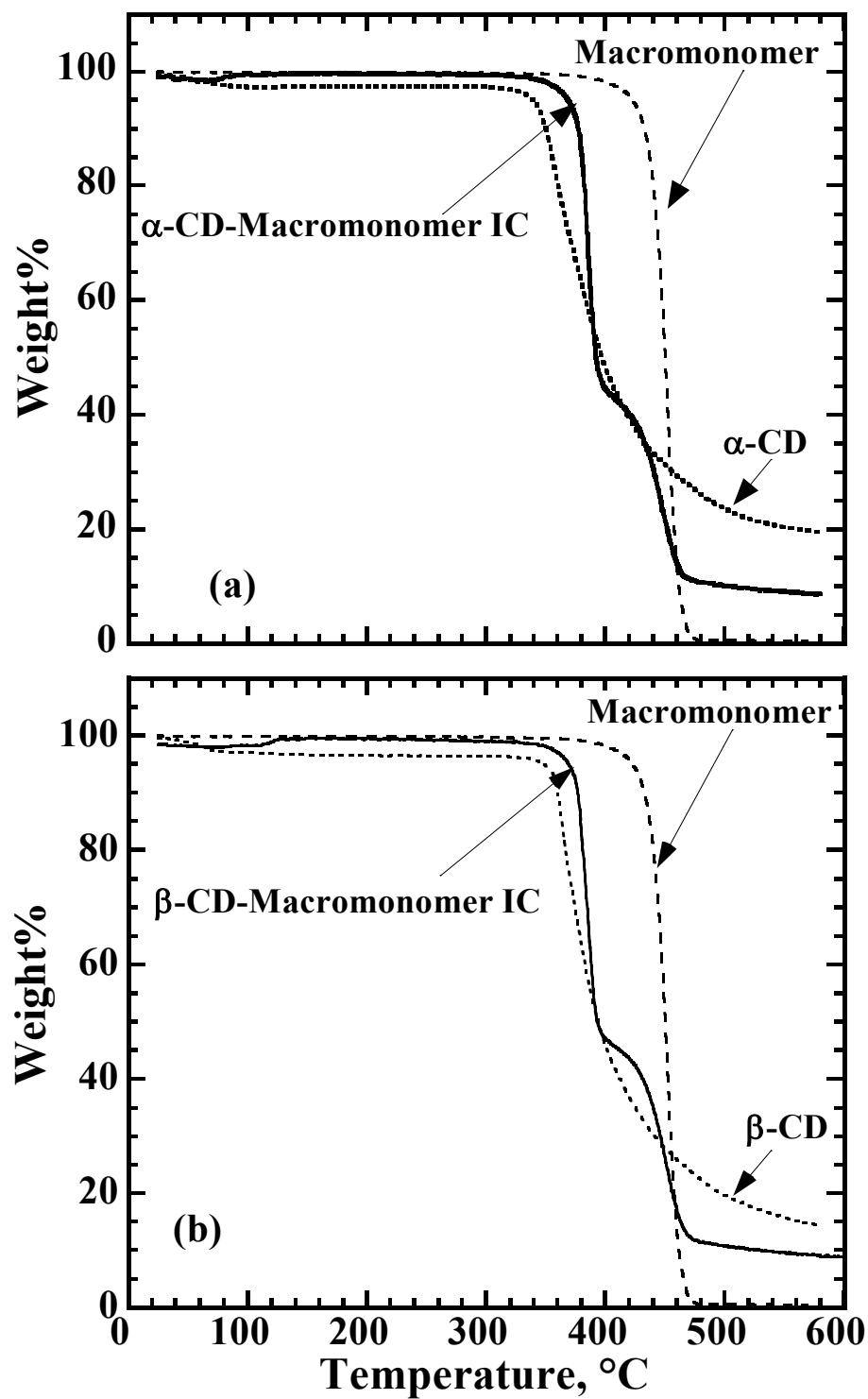


Figure 8. TGA scans for a) α -CD, macromonomer and their inclusion compounds and b) β -CD, Macromonomer and their inclusion compounds. Samples were heated at 20°C/min under nitrogen.

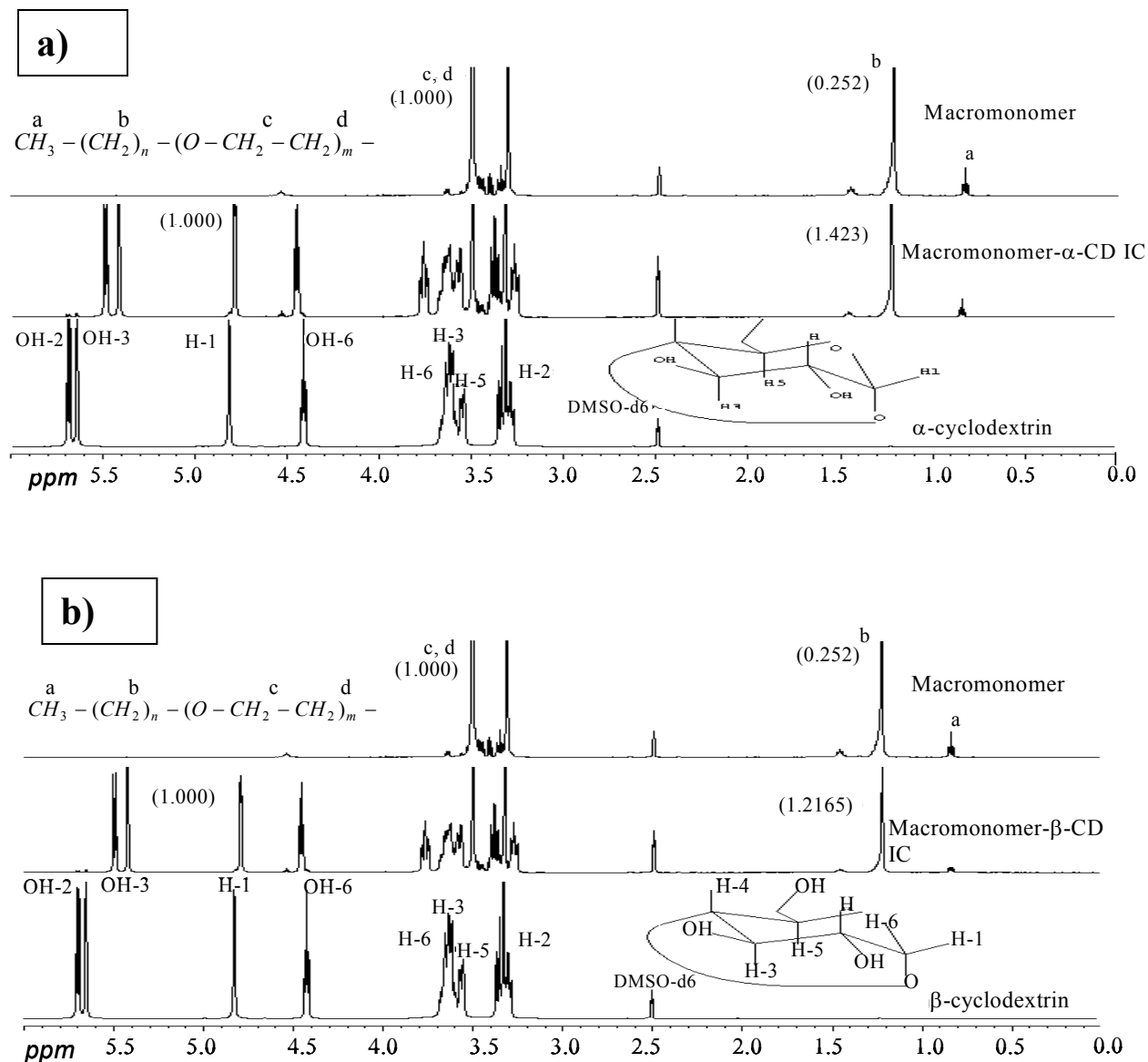


Figure 9. 500 MHz 1H NMR spectra of a) macromonomer, α -CD and their inclusion compound and b) macromonomer, β -CD and their inclusion compound. All spectra were acquired in DMSO-d₆.

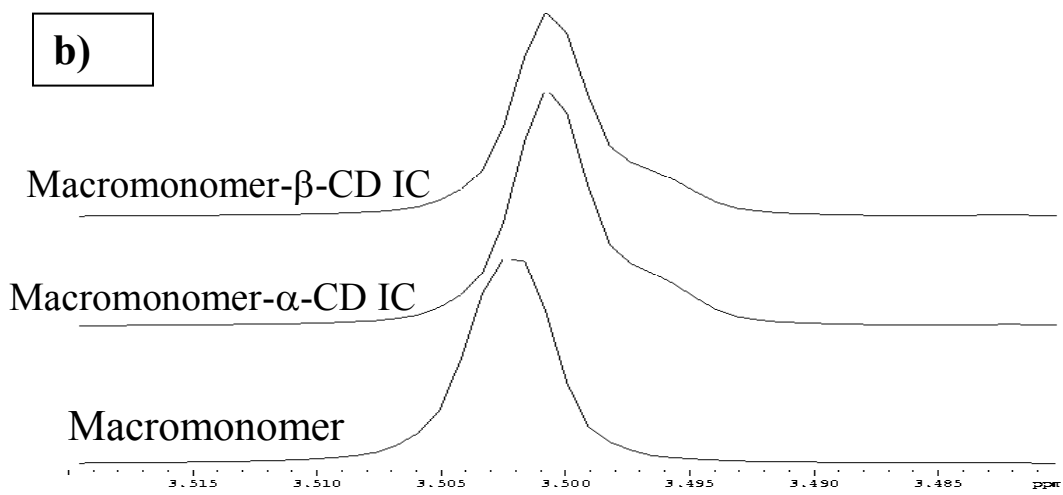
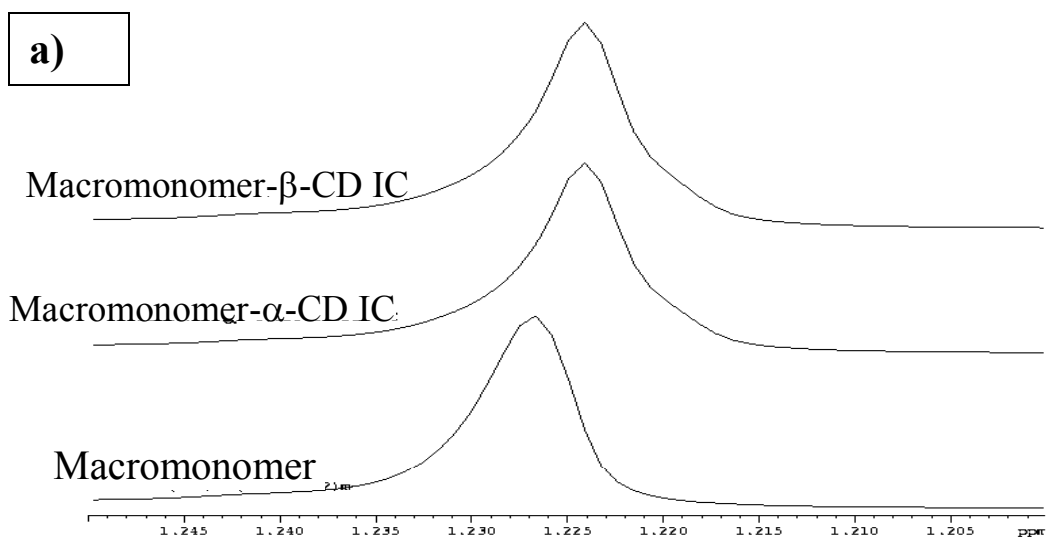


Figure 10. Part of the 500 MHz ^1H NMR spectra showing a) the aliphatic CH_2 protons of the macromonomer and its inclusion compounds with α -CD and β -CD and b) the $\text{CH}_2\text{-CH}_2\text{-O}$ protons of the macromonomer and its inclusion compounds with α -CD and β -CD. All spectra were acquired in DMSO-d_6 .

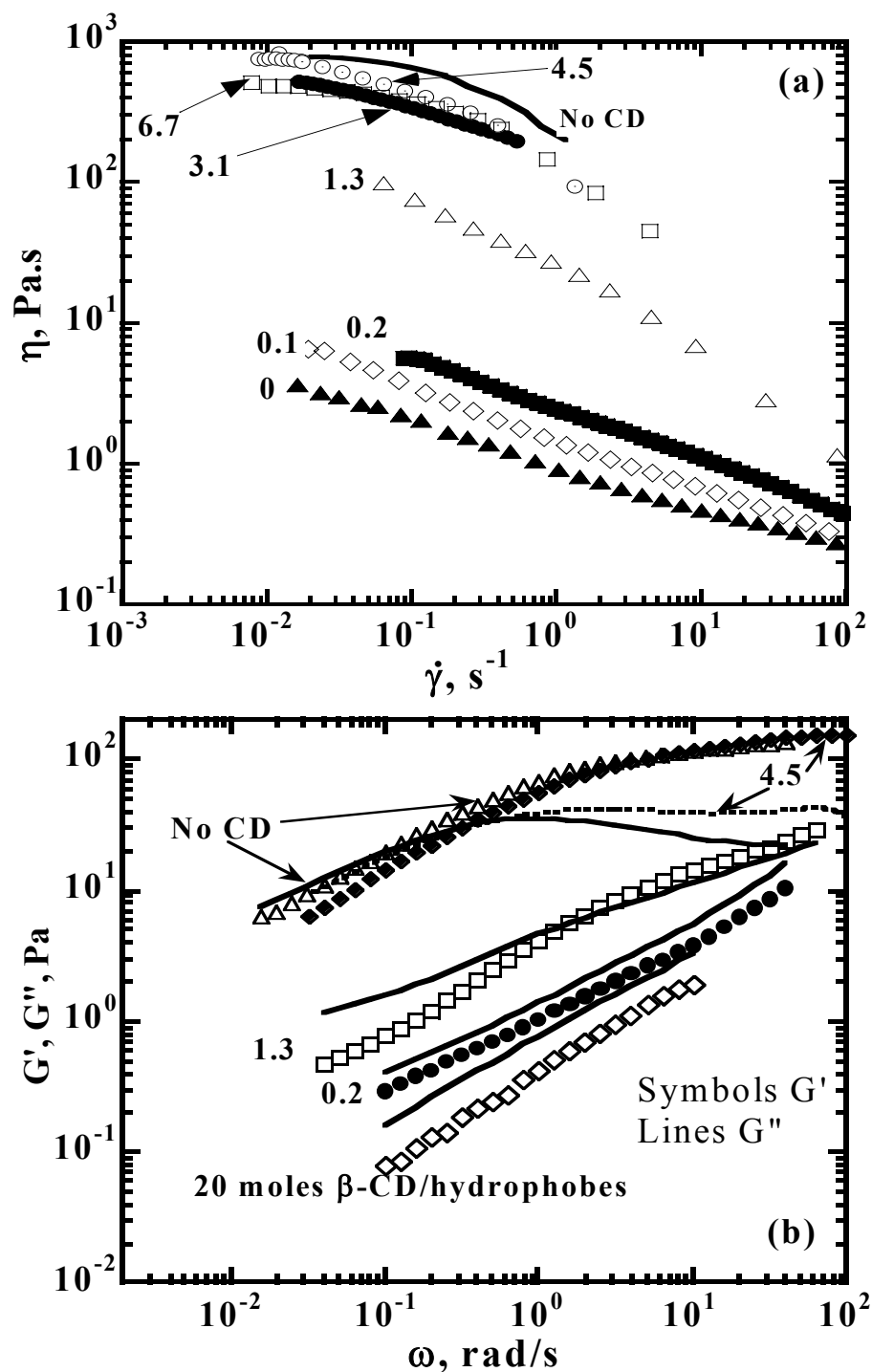


Figure 11. Effect of adding macromonomer to a 3% HASE polymer solution that has the hydrophobic groups deactivated by 20 moles β CD on the (a) steady shear viscosity and (b) dynamic elastic (G') and viscous (G'') moduli of the polymer solution. Numbers in figure denotes amount of macromonomer added to solution in mM

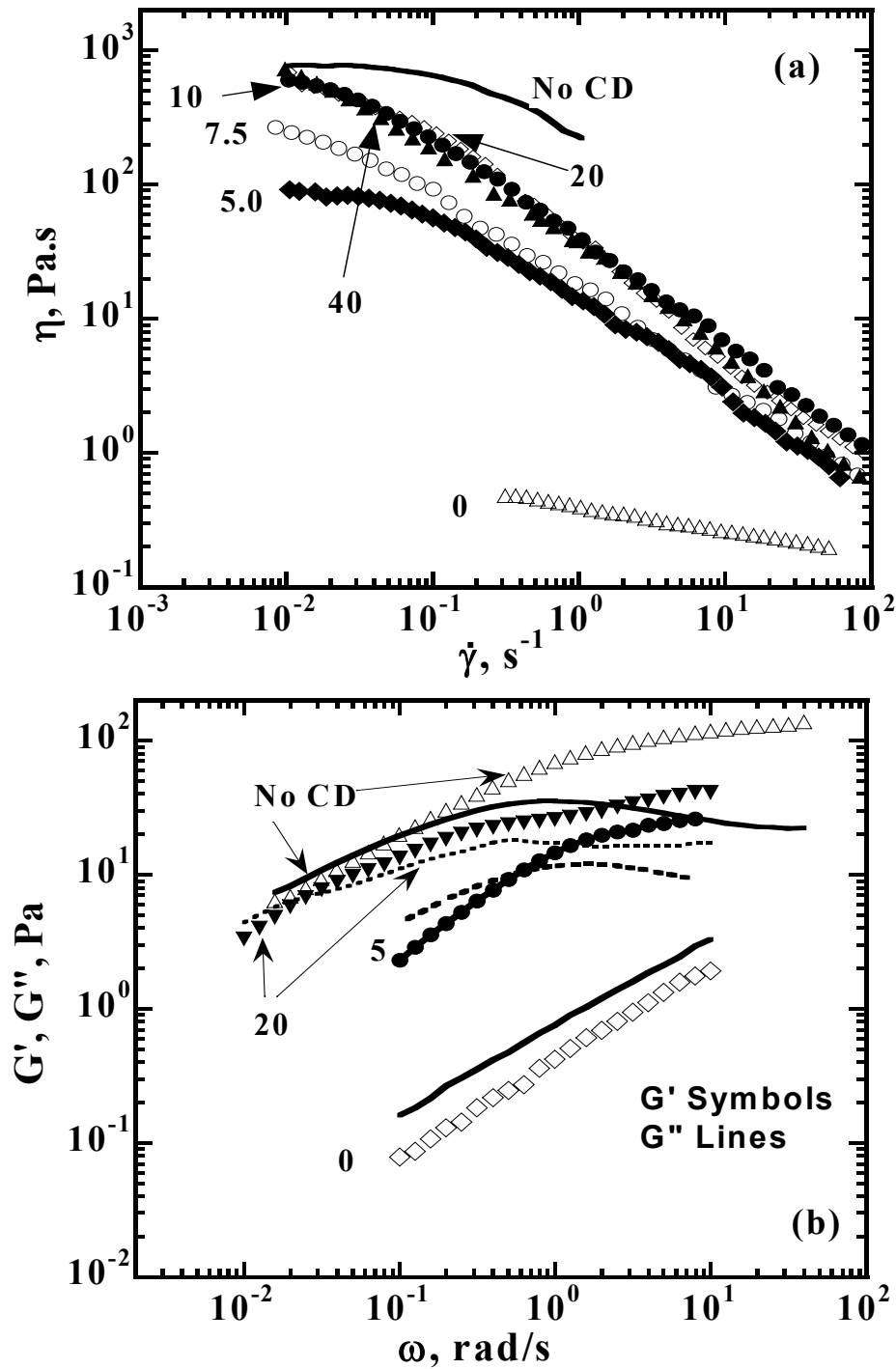


Figure 12. Effect of NP4 surfactant addition to a 3% HASE polymer solution that has the hydrophobic groups deactivated by 20 moles β CD on the (a) steady shear viscosity and (b) dynamic elastic (G') and viscous (G'') moduli of the polymer solution. Numbers in figure denotes amount of NP4 surfactant added to solution in mM.

CHAPTER 8

CONCLUSIONS AND RECOMMENDATIONS FOR FUTURE WORK

8.1 Conclusions

In this chapter we briefly summarize the key aspects of this dissertation. In the preceding chapters, we have shown that polymer composition and solvent quality have a large impact on the polymer solution microstructure and rheology. We also investigated the ability of diffusing wave spectroscopy to probe the dynamic of complex associative polymers. Moreover, we provided an approach to modulate the hydrophobic interactions through using inclusion compounds and surfactants. Some of the major findings of the study are summarized in the following paragraphs.

- Both the polymer backbone composition and the macromonomer concentration have profound impacts on the solution viscosity and viscoelastic properties. Increasing the MAA concentration in the polymer backbone increased the chains' hydrodynamic size but reduced its flexibility. A small increase in the macromonomer concentration, up to 1 mole%, enhances the intermolecular hydrophobic association and thus the solution viscosity and viscoelastic properties. However, further increase in the macromonomer concentration yield hydrophobic junctions with mostly intramolecular associations which reduce the solution viscosity and viscoelastic properties. The presence of competing mechanisms, i.e., increasing MAA concentration or macromonomer concentration, therefore result in a maximum in various material functions. Scaling various material functions with the polymer concentration yielded three transitional regimes. These transition regimes correspond to changes in the hydrophobic association modes. The concentrations at which these

transitions were observed were dependent on the polymer composition and shifted to lower concentration with increasing MAA content.

- The solvent quality exerted a strong influence on the polymer solution microstructure and rheology. In particular, two distinct modes of behavior were observed depending on whether the co-solvent was “water rich” or “glycol rich”. In both regimes, the relative viscosity and plateau modulus reveal power-law dependences with the solvent solubility parameter; however, the dependence is much stronger in the “water rich” regime. We attribute this dual-mode behavior to a lessening in the ability of the hydrophobic groups for micellization as the solvent changes from being “water-rich” to “ glycol-rich”. This lack or reduction of hydrophobic interactions in the “PG-rich” solvents is possibly induced by less expanded polymer chains and conformational changes in PEO spacers together with a lower tendency of the hydrophobes to form micelles in less polar media. This hypothesis was supported by examining the concentration dependence of viscosity and elastic modulus in each regime and comparing them to those of associative and nonassociative polymers.
- Using diffusing wave spectroscopy (DWS) to probe the structural changes induced by the change of solvent quality and polymer concentration on a HASE associative polymer has proved to be a viable approach. In particular, comparison of DWS results with those obtained using conventional rheometry reveals excellent qualitative agreement. Further, DWS provided information on the polymer dynamics over a very

wide frequency range, including high frequencies that are not accessible by mechanical rheometry. Finally, the concentration dependence of the creep compliance, high-frequency elastic modulus and relaxation time obtained using DWS or rheometry reveal power-law dependences with the same exponents regardless of the technique. However, the power-law exponents were different for the different material functions, and were discussed in light of theoretical predictions and other available experimental results.

- The use of inclusion compounds and surfactant provides a viable approach to control the hydrophobic associations and concomitant solution rheology. The complexation of the normally associating hydrophobic macromonomer components with α - and β -cyclodextrins reduces the steady shear viscosity and dynamic moduli of the HASE solutions by several orders of magnitude. Furthermore, it is possible to reversibly recover the high viscoelastic characteristics of HASE solutions containing cyclodextrins by treatment with surfactants that compete with the hydrophobic portions of HASE for complexation with the cyclodextrins. As a consequence, cyclodextrins and surfactants in combination can be judiciously employed to lower the viscoelasticity of HASE solutions during processing, while subsequently recovering the high viscosity and viscoelastic properties that are sought in their applications.

8.2 Recommendations for Future Work

8.2.1 Tracer microrheology measurements

In chapter 6, we reached the conclusion that diffusing wave spectroscopy (DWS) is a viable technique to probe the dynamic of associative polymers at the microlevel. However, the quantitative discrepancy between DWS and mechanical rheometry could be attributed to fundamental differences between the dynamics at the micro and the macrolevel. It could also be attributed to either the presence of inhomogeneity on some length scale or to the perturbation of the medium by the probing particle. It would be of great importance to further examine these last two possibilities by using another/other microrheological techniques. In particular, there are two recent techniques that would accomplish that task. The first technique, particle tracking or two-point microrheology correlates the fluctuations of two beads, separated in space, and should give a more exact measure of the bulk rheological properties. This technique does not depend on details of the tracer's size, shape and boundary conditions within the medium and overcomes many of the limitations of conventional microrheology experiments¹⁻⁴.

The second recommended technique is the use of a two-cell DWS technique⁵, a sandwich consisting of two independent glass cells. The first cell contains the viscoelastic medium under investigation while the second is filled with a viscous liquid and scatterer particles. This technique eliminates any perturbation by the scatterer probes to the viscoelastic medium. Details of this technique and the experimental setup are discussed in reference 5.

8.2.2 Recovery of solution rheology after deactivation of the hydrophobic groups

In chapter 7, we presented an approach to modulate the hydrophobic association. The first step in that approach involves the addition of inclusion compound hosts (α - or β - cyclodextrin) to the polymer solution. The encapsulation of the hydrophobic groups leads to significant reduction in the solution viscosity and viscoelastic properties. The second step requires the addition of surfactants to reactivate the hydrophobic groups and thus recover the solution rheological properties. Although, we were able to recover the solution properties, the final viscosity *profile* was different than that of the original polymer solution. This change is attributed to the polymer-surfactant interactions. However, a more direct approach to recover the solution properties is to degrade the cyclodextrin.

A novel approach to reactivate the hydrophobic groups would be through enzymatic degradation of the cyclodextrin. Currently, there are several enzymes that are capable of degrading cyclodextrins, including Cyclodextrinase, Alpha Amylase from different sources and Glucoamylase Amylase⁶⁻¹⁷. However, it is crucial that the enzyme meets the following two criteria:

1. Thermophilic enzymes (preferably has no activity at room temperature with maximum activity at 50-60°C)
2. Stable at pH 7.0 or higher and preferably have optimum pH \gg 6.0

In the next section we discuss some preliminary results of using different enzymes to degrade cyclodextrin and recover the solution properties. The first enzyme used is cyclodextrinase enzyme from alkalophilic *Bacillus* sp. I-5 (CDase I-5) with specific activity

300 u/mg on β -cyclodextrin and optimum conditions 50°C and pH 7.5. This enzyme was kindly supplied by Professor Kwan Hwa Park, Research Center for New Bio-Materials in Agriculture, S. Korea. The second enzyme is a fungal alpha-amylase enzyme derived from a selected strain of *Aspergillus oryzae* and has the commercial name Clarase[®]. The specific activity of this enzyme is 40000 SKBU/g (one SKBU will degrade 1.0 gram of limit-dextrin substrate per hour) and optimum pH and temperature 5.6 and 50°C., respectively. This enzyme was kindly supplied by Genencor International[®].

Effect of cyclodextrinase (Cdase) enzyme

Figure 1a and b shows the effect of incubation with 300 u/g Cdase at 50°C and pH 9.0 for 24 hrs on the steady shear viscosity and elastic (G') and viscous (G'') moduli of a 3% polymer solution that has the hydrophobic groups initially encapsulated with 20 moles α -cyclodextrin per moles hydrophobes. The incubation with Cdase enzymes increased the solution viscosity and viscoelastic properties. The recovery of the solution properties could be attributed to the reactivation of the hydrophobic groups as the treated sample has steady and dynamic profile similar to the original 3% solution. No full recovery, however, was achieved even after long incubation time. This is due to the incubation pH being higher than the optimum pH for the enzyme.

To increase the activity of the Cdase enzyme, a 3% polymer solution was prepared at pH 7.5. Figure 2a and b shows the reduction of the solution pH from 9.0 to 7.5 has slight effect on the solution rheological properties. However, incubation with 300 u/g Cdase enzyme at 50° and pH 7.5 showed a near full recovery of the solution

rheological properties even after 1 hour as shown in Figures 3a and b. Incubation for longer times showed a slight increase in the rheological properties.

Effect of Clarase enzyme

Because the optimum pH for the Clarase enzyme is 5.5, we have not attempted the incubation at pH 9. Incubation at 50°C and pH 7.5 with 1200 SKBU u/g clarase enzyme for 30 hrs showed a significant increase in the rheological properties of the 3% polymer solution as shown in Figures 4a and b.

In summary, our preliminary data suggests that using enzymes to degrade cyclodextrin, as a way to reactivate the hydrophobic groups, is a promising approach. A detailed study, however, needs to fully explore the optimum use of the enzymes.

8.3 References:

1. Mukhopadhyay, A.; Granick, S. Micro- and Nanorheology, *Current Opinion in Colloid & Interface Science* **2001**, 6 (5,6), 423-429.
2. Mason, T. G.; Ganesan, K.; van Zanten, J. H.; Wirtz, D.; Kuo, S. C. Particle Tracking Microrheology of Complex Fluids, *Physical Review Letters* **1997**, 79 (17), 3282-3285.
3. Crocker, J. C.; Valentine, M. T.; Weeks, E. R.; Gisler, T.; Kaplan, P. D.; Yodh, A. G.; and Weitz, D. A. Two-Point Microrheology of Inhomogeneous Soft Materials, *Physical Review Letters* **2000**, 85 (4), 888-891.
4. Levine, A. J.; Lubensky, T. C. Two-point Microrheology and the Electrostatic Analogy, *Physical Review E: Statistical, Nonlinear, and Soft Matter Physics* **2002**, 65 (1-1), 011501/1-011501/13.
5. Scheffold, F.; Skipetrov, S. E.; Romer, S.; Schurtenberger, P. Diffusing-Wave Spectroscopy of Nonergodic Media, *Phys. Rev. E: Stat., Nonlinear, Soft Matter Phys.* **2001**, 63 (6-1), 061404/1-061404/11.
6. Saha, B. C.; Zeikus, J. G., Cyclodextrin Degrading Enzymes, *Starch/Staerke* **1992**, 44 (8), 312-15.
7. Zhong, W.; Zhang, Z. S.; and Jun, Y. S. Purification and Properties of Cyclodextrinase from *Bacillus Stearothermophilus* HY-1, *Applied Biochemistry and Biotechnology* **1996**, 59 (1), 63-75.
8. Saha, B. C.; Zeikus, J. G. Characterization of Thermostable Cyclodextrinase from *Clostridium* T 39E, *Appl. Environ. Microbiol.* **1990**, 56 (9), 2941-3.
9. Oguma, T.; Kikuchi, M.; Mizusawa, K. Cyclodextrinase of *Bacillus* for Preparation of Maltooligosaccharides, JP Patent 03087193, 1991.
10. Kwon, H.-J.; Nam, S.-W.; Kim, K.-H.; Kwak, Y.-G.; Kim, B.W. Isolation of a *Bacillus* Sp. Producing both Cyclodextrin G and Cyclodextrinase and Characterization of the Enzymes, *Sanop Misaengmul Hakhoechi* **1996**, 24 (3), 274-281.
11. Kitahata, S.; Taniguchi, M.; Beltran, S. D.; Sugimoto, T.; Okada, S. Purification and Some Properties of Cyclodextrinase from *Bacillus Coagulans*, *Agric. Biol. Chem.* **1983**, 47 (7), 1441-7.

12. Galvin, N. M.; Kelly, C. T.; Fogarty, W. M. Purification and Properties of the Cyclodextrinase of *Bacillus Sphaericus* ATCC 7055, *Applied Microbiology and Biotechnology* **1994**, (1), 46-50.
13. DePinto, J. A.; Campbell, L. L. Purification and Properties of the Cyclodextrinase of *Bacillus Macerans*, *Biochemistry* **1968**, 7 (1), 121-5.
14. DePinto, J. A.; Campbell, L. L. Pattern of Action of the Amylase and the Cyclodextrinase of *Bacillus Macerans*, *Arch. Biochem. Biophys.* **1968**, 125 (1), 253-8.
15. Bryjak, J. Enzymic Hydrolysis of Starch to Maltodextrin and Starch Syrups. Part I. Enzymes, *Biotechnologia* **1999**, (1), 180-200.
16. Antenucci, R. N.; Palmer, J. K. Enzymic Degradation of α - and β -Cyclodextrins by Bacteroides of the Human Ccolon, *J. Agric. Food Chem.* **1984**, 32 (6), 1316-21.
17. Abe, J.; Nakazono, O.; Hizukuri, S. Characterization of Cyclodextrinase from *Bacillus Stearothermophilus* K-12481, *Oyo Toshitsu Kagaku* **1996**, 43 (2), 155-159.

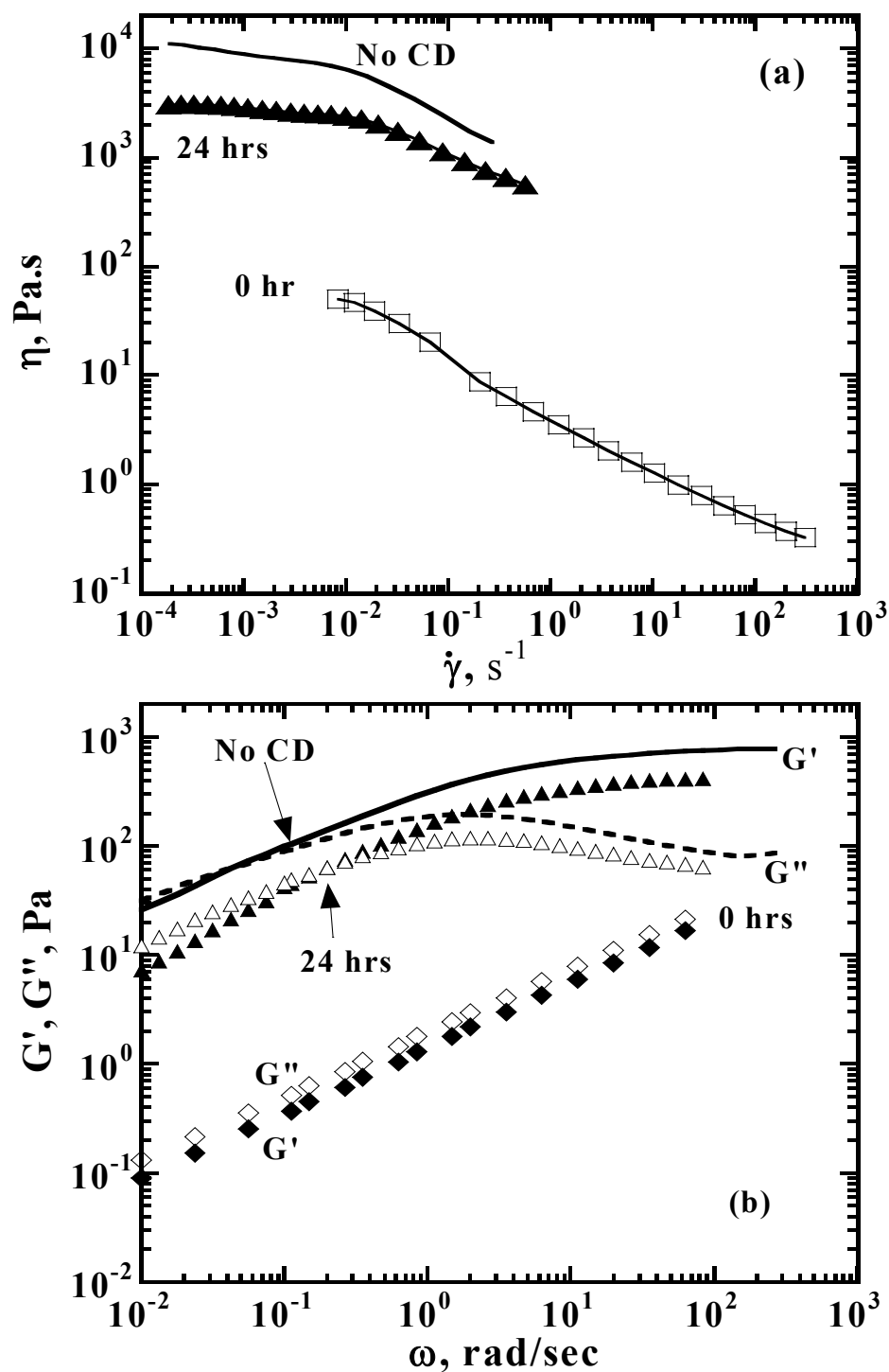


Figure 1. Effect of CDase enzyme on the (a) steady shear viscosity and (b) dynamic elastic (G') and viscous (G'') moduli of 3% polymer solution encapsulated with 20 moles α -CD/hydrophobes. pH 9, incubation temperature 50°C, incubation time 24 hrs.

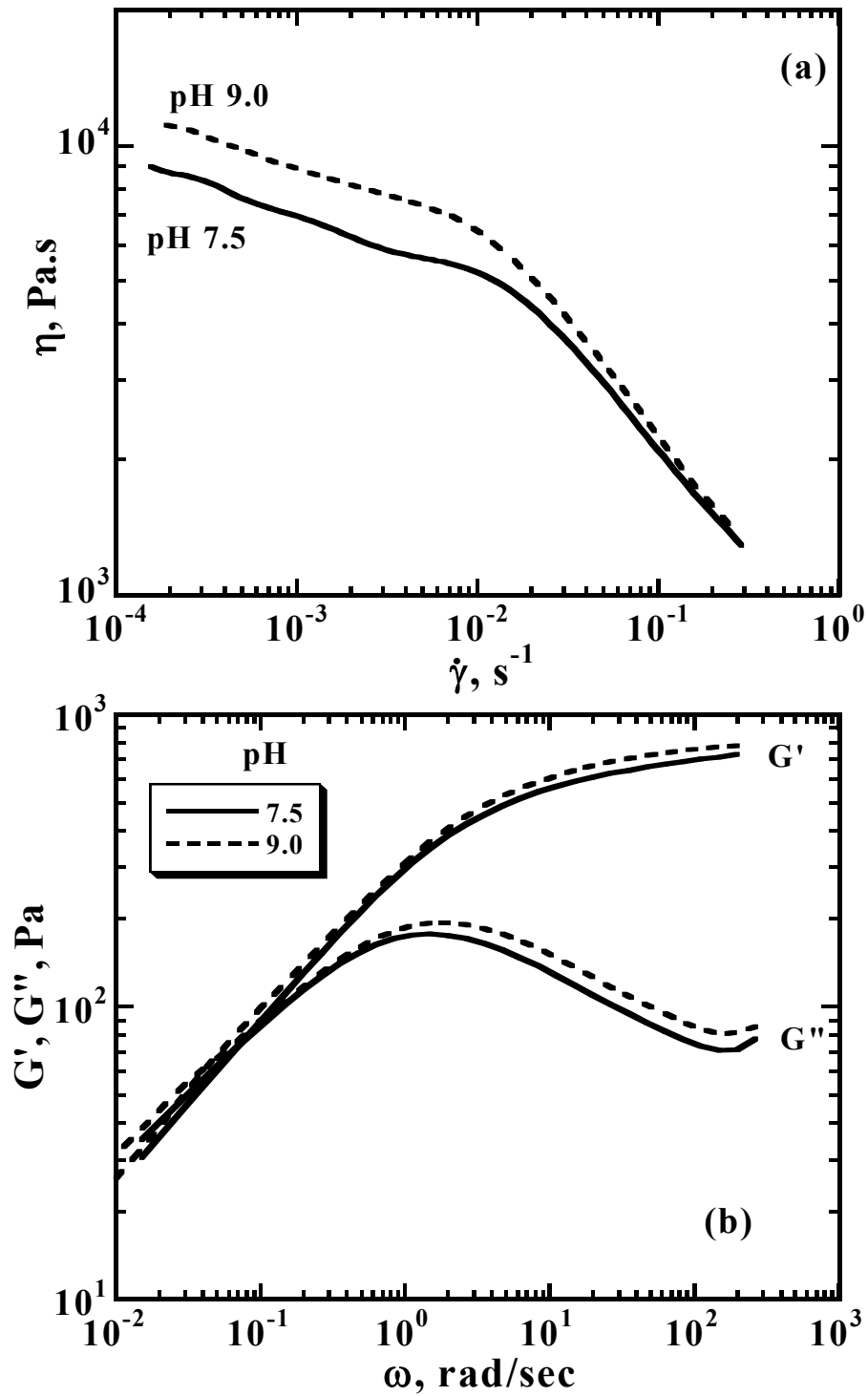


Figure 2. Effect of solution pH on the (a) steady shear viscosity and (b) dynamic elastic (G') and viscous (G'') moduli of 3% polymer solution.

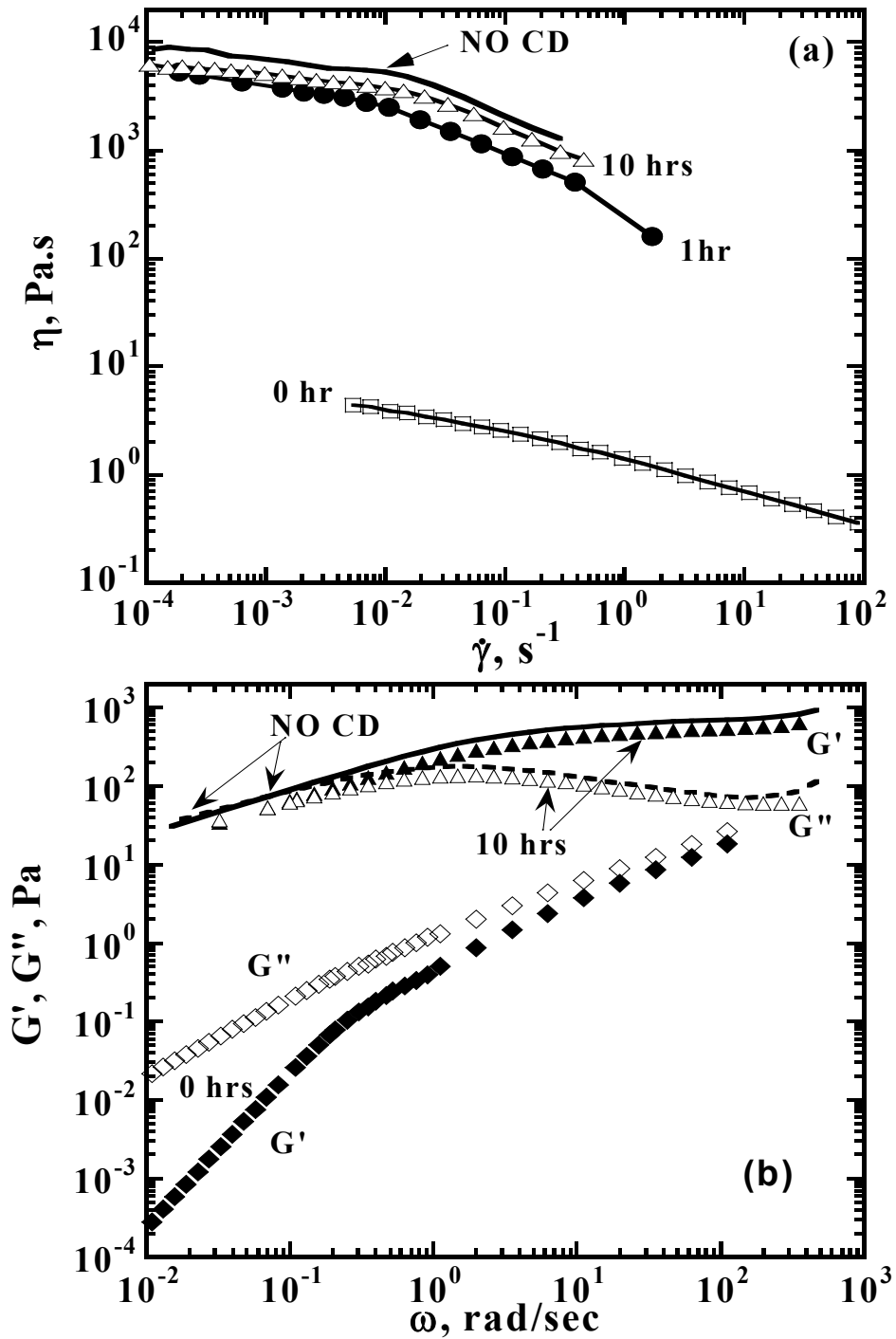


Figure 3. Effect of CDase enzyme on the (a) steady shear viscosity and (b) dynamic elastic (G') and viscous (G'') moduli of a 3% polymer solution encapsulated with 20 moles α -CD/hydrophobes. pH 7.5, incubation temperature 50°C, incubation time 1 and 10 hr.

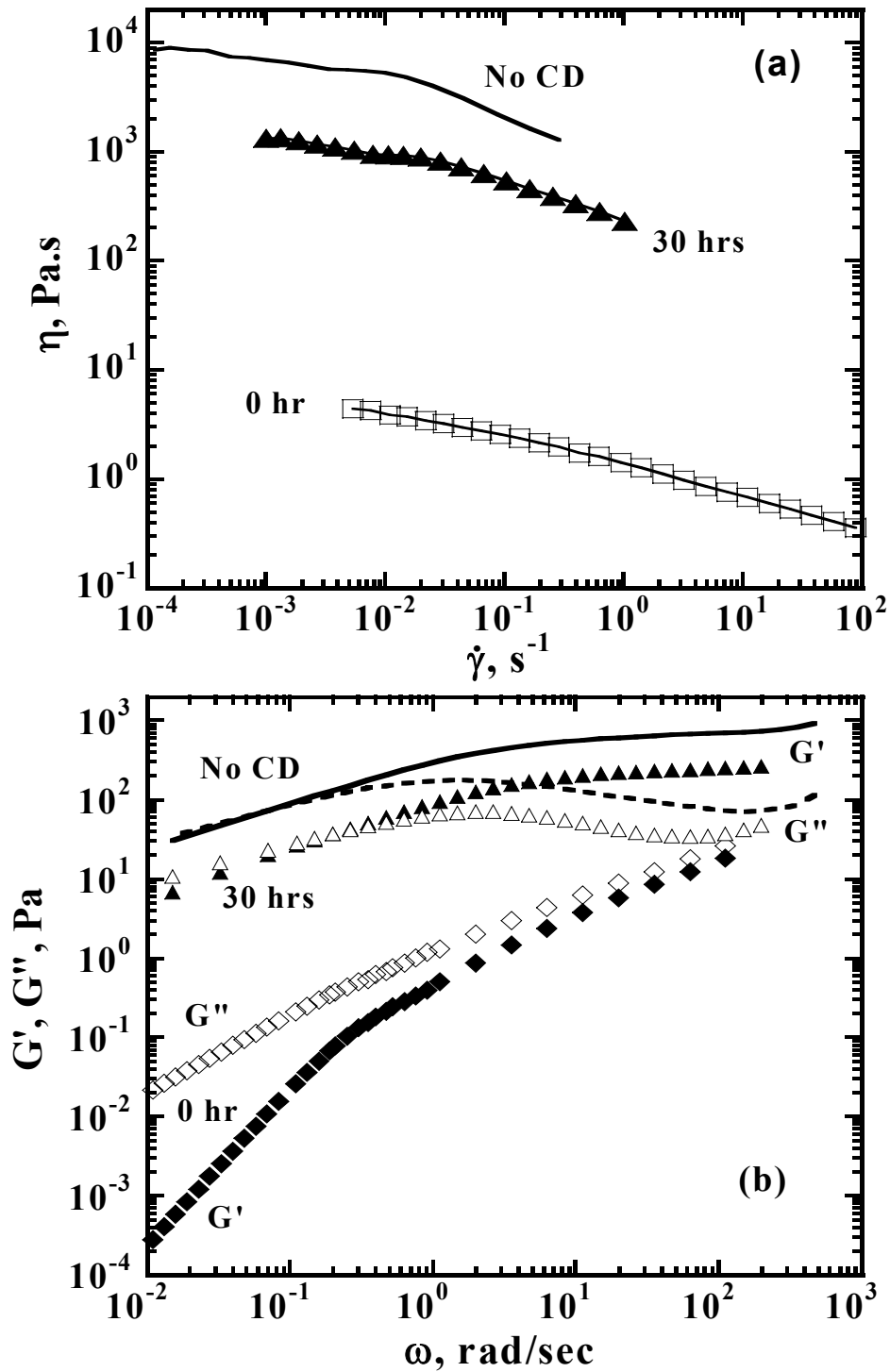


Figure 4. Effect of Clarase enzyme on the (a) steady shear viscosity and (b) dynamic elastic (G') and viscous (G'') moduli of a 3% polymer solution encapsulated with 20 moles α -CD/hydrophobes. pH 7.5, incubation temperature 50°C, incubation time 30 hrs.